

8
2 m

NATIONAL AERONAUTICS AND SPACE ADMINISTRATION

Technical Memorandum 33-591

*Mariner Mars 1971 Battery Design,
Test, and Flight Performance*

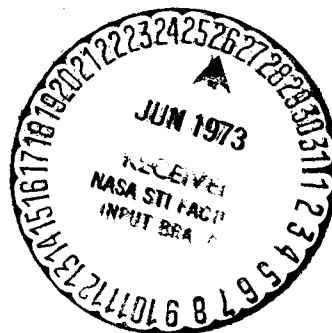
R. S. Bogner

(NASA-CR-132986) MARINER MARS 1971
BATTERY DESIGN, TEST, AND FLIGHT
PERFORMANCE (Jet Propulsion Lab.)
HC \$11.75

194 p
CSCL 10C

N73-25095

G3/03 05481
Unclas



JET PROPULSION LABORATORY
CALIFORNIA INSTITUTE OF TECHNOLOGY
PASADENA, CALIFORNIA

April 15, 1973

Reproduced by
NATIONAL TECHNICAL
INFORMATION SERVICE
US Department of Commerce
Springfield, VA. 22151

195 ps

NATIONAL AERONAUTICS AND SPACE ADMINISTRATION

Technical Memorandum 33-591

*Mariner Mars 1971 Battery Design,
Test, and Flight Performance*

R. S. Bogner

JET PROPULSION LABORATORY
CALIFORNIA INSTITUTE OF TECHNOLOGY
PASADENA, CALIFORNIA

April 15, 1973

**Prepared Under Contract No. NAS 7-100
National Aeronautics and Space Administration**

PREFACE

The work described in this report was performed by the Guidance and Control Division of the Jet Propulsion Laboratory.

CONTENTS

I.	Introduction	1
II.	Summary	2
	A. Battery Operation on the Spacecraft	4
	B. Battery Manufacture	4
	C. Battery Cells	5
	D. Battery Handling and Spacecraft Tests	5
	E. Laboratory Tests	7
	F. Flight Battery Performance	8
III.	Conclusions and Recommendations	10
IV.	Design Considerations and Reviews	12
	A. Preliminary Design Analysis and Considerations	12
	B. Design Requirements and Design Reviews	16
	C. Battery Schedule and Milestones	17
	D. Power Subsystem Battery Integration	21
V.	Battery Design, Manufacture, and Qualification	23
	A. Design Configuration and Analysis	23
	B. Battery Manufacture	29
	C. Fabrication and Qualification Tests	32
VI.	Cell Procurement, Testing, and Matching	37
	A. Cell Description	38
	B. Cell Manufacture	39
	C. Cell Receiving Tests and Matching	40
VII.	Spacecraft and Laboratory Tests	43
	A. Battery Handling and Safety	43
	B. Battery Handling for Spacecraft Systems Tests	46

Preceding page blank

CONTENTS (contd)

C.	Spacecraft Tests	48
D.	Laboratory Tests	52
VIII.	Flight Battery Performance	72
A.	Launch and Cruise	72
B.	Mars Orbit Insertion and Orbit Trims	74
C.	Sun Occultation	75

TABLES

1.	Comparison factors	77
2.	Battery/charger commands	78
3.	Synopsis of the preliminary structural analysis	79
4.	Battery TA vibration requirements	80
5.	Z-Z axis vibration summary	81
6.	Calculated steady-state temperatures	82
7.	Battery thermal property and density data	82
8.	Measured and calculated temperature gradients for various battery operational modes	83
9.	Measured and calculated temperature transients during discharge and charge	84
10.	Measured and calculated temperatures at various locations for various operating modes	85
11.	Type approval and flight acceptance battery test sequence	86
12.	Cell vendor evaluation criteria	87
13.	Test data	88
14.	Vibration test results	90
15.	PTM thermal vacuum test mode summary	91
16.	Subsystem status for different test modes.	92
17.	Parameter variation effects on temperature	93

CONTENTS (contd)

TABLES (contd)

18.	Cell history.	94
19.	Battery charge efficiency tests	95
20.	Battery/charger interface data summary	96

FIGURES

1.	Mariner Mars 1971 battery development schedule	97
2.	Mariner Mars 1971 preliminary power profile	98
3.	Mariner Mars 1971 battery system milestone schedule.	99
4.	Battery wiring layout	101
5.	Power subsystem functional block diagram	102
6.	Engineering model battery.	103
7.	Battery wiring schematic	104
8.	Typical plot of data	105
9.	Power spectral density plot	105
10.	Transient response of battery for 76-W dissipation bus temperature constant at 27°C (80°F), louver operating range	106
11.	Shear plate temperature (battery case) vs battery and power dissipations	107
12.	Thermal network for first cell	107
13.	Power dissipations	108
14.	Calculated temperature response and power dissipation event	109
15.	Calculated internal cell temperature response for continuous 74-W dissipation	110
16.	Calculated temperature response at various locations for 74-W dissipation	110
17.	Test setup, thermal vacuum	111

CONTENTS (contd)

FIGURES (contd)

18.	Temperature measurements during high-temperature thermal vacuum test.	112
19.	Temperature measurements during high-temperature thermal vacuum test.	112
20.	Temperature recorded during low-temperature thermal vacuum test.	113
21.	MM '71 battery test, EM-1 thermal-vacuum.	113
22.	Manufacturing flow diagram	114
23.	Inspection of rough-machined chassis	115
24.	Cell compression operation	116
25.	Application of RTV thermal filler before cell installation	117
26.	Cell and thermal bracket installation	118
27.	Shims and cell installation.	119
28.	Keeper angle installation with keeper bar and end plate in place	120
29.	Battery instrumentation for vibration tests	121
30.	Battery assembly sine vibration tests	121
31.	Battery random vibration test.	122
32.	Cutaway of Ni-Cd cell, 20-Ah Gulton	123
33.	Gulton ceramic-to-metal terminal seal	123
34.	Cell manufacturing flow plan	124
35.	Cell receiving and test flow	127
36.	Electronic assembly shipping container assembly	128
37.	Battery handling flow plan	129
38.	Battery operations schedule	130
39.	Battery charge voltage limits.	130

CONTENTS (contd)

FIGURES (contd)

40.	Laboratory test setup	131
41.	Mission profile test battery SN EM-1, prelaunch	132
42.	Mission profile test battery SN EM-1, launch	132
43.	Mission profile test battery SN 202, prelaunch	133
44.	Mission profile test battery SN 202, launch	133
45.	Mission profile test battery SN EM-1, first midcourse	134
46.	Mission profile test battery SN 202, first midcourse . . .	134
47.	Mission profile test battery EM-1 cruise data trickle charge at 0.65 A	135
48.	Mission simulation test battery SN 202, cruise data, trickle charge at 0.65 A	137
49.	Mission profile test battery SN EM-1 midcourse 2, discharge at 12 A	138
50.	Mission profile test battery SN 202 midcourse 2, discharge at 12 A	139
51.	Mission profile test battery SN 202 recondition discharge at 52 ohms after 6-mo trickle charge	139
52.	Mission profile test battery SN 202, orbit insertion at 9 A	140
53.	Mission profile test battery SN EM-1, orbit insertion maneuver at 9 A after 6-mo trickle charge	141
54.	Mission simulation test battery SN EM-1, first orbit trim discharge at 9 A	142
55.	Mission profile test battery SN 202, first orbit trim at 9 A	142
56.	Extended mission A discharge time vs cycle, battery SN EM-1 and 202	143
57.	Mission simulation test battery SN EM-1, end of discharge voltage vs cycle	143

CONTENTS (contd)

FIGURES (contd)

58.	Mission simulation test battery SN 202, end of discharge voltage vs cycle temperature	144
59.	Mission profile, extended mission, cycle 5	144
60.	Mission profile, extended mission, cycle 60	145
61.	Mission profile, extended mission, cycle 125	145
62.	Discharge after cycling on extended mission A, discharge rate 12.0 A	146
63.	Discharge time as a function of cycle, extended mission B	146
64.	Extended mission B, battery SN EM-1, end-of-discharge voltage and temperature profile vs cycle, discharge rate 10 A	147
65.	Extended mission B, battery SN 202, end-of-discharge voltage and temperature profile vs cycle, discharge rate 10 A	147
66.	Extended mission B, battery test, orbit 25, January 31, 1972, SN EM-1	148
67.	Extended mission B, battery test, orbit 77, February 26, 1972, SN EM-1	148
68.	Extended mission B, battery test, orbit 110, March 13, 1972, SN EM-1	149
69.	Extended mission B, battery test, orbit 15, January 26, 1972, SN 202	149
70.	Extended mission B, battery test, orbit 55, February 16, 1972, SN 202	150
71.	Extended mission B, battery test, orbit 78, February 26, 1972, SN 202	150
72.	Extended mission B, battery test, orbit 140, March 28, 1972, SN EM-1	151
73.	Extended mission B, battery test, orbit 140, March 28, 1972, SN 202	151
74.	Test setup, thermal vacuum, real-time mission test . . .	152

CONTENTS (contd)

FIGURES (contd)

75.	Test setup, thermal vacuum, real-time mission test . . .	152
76.	Real-time mission simulation launch sequence, June 14, 1971, battery SN 307	153
77.	Real-time mission simulation launch sequence, June 30, 1971, battery SN 201	154
78.	Real-time mission simulation, battery SN 307, cruise data	155
79.	Real-time mission simulation, battery SN 201, cruise data	156
80.	Predicted voltage and actual voltage, battery SN 307, simulated orbit insertion test, October 26, 1971	157
81.	Real-time mission profile test, battery SN 307, launch discharge compared to orbit insertion discharge	157
82.	Real-time mission test, battery SN 307, orbit trim 1, discharge and recharge performed prior to Mariner 9 . .	158
83.	Real-time mission test, battery SN 307, orbit trim 2 discharge and recharge	158
84.	Battery performance, battery SN 201, Mars orbit insertion	159
85.	Real-time mission test, battery SN 201, orbit trim 1 discharge and charge	159
86.	Real-time mission test, battery SN 201, orbit trim 2 discharge and recharge	160
87.	Real-time mission profile test, extended mission test, battery SN 307	160
88.	Real-time extended mission, battery SN 307	161
89.	Real-time test, battery SN 307, 4th cycle, 30 min	161
90.	Real-time test, battery SN 307, 7th cycle, 60 min	162
91.	Real-time test, battery SN 307, 27th cycle, 95 min	162
92.	Typical cell discharge after 6-months trickle charge . . .	163

CONTENTS (contd)

FIGURES (contd)

93.	Mission profile test, battery EM-1, orbit insertion and orbit trim discharge voltage comparison, both discharges at 9 A	163
94.	Mission profile test, battery SN 202, orbit insertion and orbit trim discharge voltage comparison, both discharges at 9 A	164
95.	Mission profile test comparison of orbit insertion discharges on batteries SN EM-1 and 202	164
96.	Predicted voltage and actual voltage of battery SN 307 orbit insertion test, October 26, 1971	165
97.	Real-time mission profile test battery SN 307 launch discharge compared to orbit insertion discharge	165
98.	Battery charge efficiency vs state of charge at 2-A rate	166
99.	Charge battery SN 306, current 650 A, discharge 12 A	166
100.	Charge efficiency test, battery SN 306, charge 2 A, discharge 12.09 A	167
101.	Charge efficiency test, battery SN 306, charge 3.98 A, discharge 12 A	167
102.	Charge efficiency test, battery SN 306, charge 2.0 A, discharge 12 A	168
103.	Charge efficiency test, battery SN 306, charge 650 mA, discharge 12 A	168
104.	Charge efficiency test, battery SN 306, charge 3.85 A, discharge 12.04 A	169
105.	Charge efficiency test, battery SN 306, charge 2 A, discharge 12 A	169
106.	Charge efficiency test, battery SN 306, charge 2 A, discharge 12 A	170
107.	Charge efficiency test, battery SN 306, charge 2 A, discharge 12 A	170
108.	Battery/charger interface test 9	171
109.	Battery/charger compatibility test run 3	171

CONTENTS (contd)

FIGURES (contd)

110.	Battery/charger compatibility test run 11.	172
111.	High-rate charger characteristics.	172
112.	Low-rate charge current as a function of difference between input voltage and battery voltage	173
113.	Results of JFACT discharge, battery SN 304	173
114.	Battery SN 305 performance data at launch.	174
115.	Battery SN 304 launch performance data during and after launch.	175
116.	Effect of first midcourse maneuver on battery	176
117.	Battery data, Mariner 9 cruise.	177
118.	Battery performance during MOI	178
119.	Battery performance, orbit trim 1	178
120.	Battery performance, orbit trim 2	179
121.	Battery performance, solar array test 2	179
122.	Battery performance, end of discharge voltage, capacity used, and length of occultation	180
123.	Battery discharge/recharge, revolution 298	180
124.	Battery discharge/recharge, revolution 328	181
125.	Battery performance, revolution 375	181

ABSTRACT

The design, integration, fabrication, test results, and flight performance of the battery system for the Mariner Mars spacecraft launched in May 1971 are presented.

The battery consists of 26 20-Ah hermetically sealed nickel-cadmium cells housed in a machined magnesium chassis. The battery package weighs 29.5 kg and is unique in that the chassis also serves as part of the spacecraft structure. Active thermal control is accomplished by louvers mounted to the battery baseplate.

Battery charge is accomplished by C/10 and C/30 constant current chargers. The switch from the high-rate to low-rate charge is automatic, based on terminal voltage. Additional control is possible by ground command or on-board computer.

The performance data from the flight battery is compared to the data from various battery tests in the laboratory. Flight battery data was predictable based on ground test data.

I. INTRODUCTION

This report presents the design, development, manufacture, test, and flight performance of the battery system used in the 1971 Mariner Mars (MM'71) orbiter spacecraft power subsystem. The system used was a single 20-Ah nickel-cadmium battery weighing 29.4 Kg, containing 26 cells in series and mounted in a machined magnesium chassis which also served as part of the spacecraft structure. It was capable of delivering over 800 Wh. Temperature control was effected by use of thermal control louvers mounted on the base of the battery.

Previous Mariner spacecraft had utilized silver oxide-zinc batteries partly because the missions were planet flybys and consequently were dependent on battery power for only launch and trajectory changes (mid-course maneuvers) and possible backup for the solar panels in case of emergencies. The MM'71 program, however, consisted of a planet-orbiting spacecraft which depended on battery power during all of the previous modes plus the orbit insertion maneuver, orbit trim maneuvers, and Sun occultation periods during orbital operations, which was well beyond the capability of the state-of-art silver-zinc battery and more in line with the capabilities of a nickel-cadmium battery.

This report is divided into five major sections describing, in chronological sequence, the selection, design, manufacture, cell procurement, and testing and flight performance of the battery.

II. SUMMARY

The Mariner Mars 1971 Project was the first to fly a hermetically sealed nickel-cadmium battery on a planetary mission. This report was written to document all aspects of the battery program (a major new spacecraft subsystem) from its inception, design, manufacture, and test through flight performance.

The preliminary planning effort for the battery system was inaugurated in February 1968. A silver oxide-zinc battery system was given first consideration since it was flown on past JPL missions. A review of past flight data and laboratory test data indicated the Mariner silver oxide zinc battery would not adequately support the Mariner 1971 requirements. It was recommended that an R&D program be initiated to upgrade the cycle and life capabilities of the silver oxide-zinc battery. This was done; however, the development contract was not started until January 1969.

In the interim it had been proposed that a nickel-cadmium battery be considered. A Battery Study Working Group was established in December 1968 to investigate the various aspects of utilizing the two types of batteries. The group established three baseline design approaches: (1) two silver oxide-zinc batteries, (2) two nickel-cadmium batteries, (3) a single nickel-cadmium battery. A list of items was generated to compare and evaluate which of the three approaches was best. The Battery Study Group concluded that a single 20-Ah nickel-cadmium battery was the best approach and established the basic design concepts for the battery system.

Time was of the essence, since the Project required a battery for the Proof Test Model Spacecraft in March 1970, and it was now February 1969. This required writing an RFP, evaluating proposals, and designing and qualifying a new battery design in one year. TRW was selected from three bidders as the battery contractor in April 1969, and work was initiated May 28, 1969, under letter contract.

Battery Design Review I, which was held on June 24, 1969, covered primarily the mechanical and packaging configuration concepts. This review established that (1) the chassis would serve as an integral part of the spacecraft structure in that the battery baseplate was also the shear plate of Bay VIII; (2) the cells would be laid with their edges on the base plate rather than on their bottoms to provide better heat dissipation; and

(3) the cell terminals would face out rather than in to provide easier access for soldering intercell connections.

Design Review II was held on August 15, 1969, to assess the design analysis vs requirements prior to release of the documentation for fabrication of the engineering model battery. Seven alerts and five action items resulted from the review. The most significant item flagged was the value of the yield stress used in the battery magnesium chassis design. The actual magnesium forgings differed from the materials handbook value by about 65%. Other items were concerned with temperature control, charge voltage specifications, circuitry, and cell testing.

A Power Subsystem Design Review for the Project was held on August 26, 1969, primarily as a critique of the design, test, and fabrication procedures and to assure compatibility of the subsystem with the spacecraft as a system. A total of 14 action items relating to the battery were generated. However, no significantly new action items or design changes resulted.

After assembly and test of the engineering model battery, Design Review III was held on February 4, 1970. Test results from the battery indicated that the design was adequate, and approval was granted to begin manufacture of the qualification and flight batteries.

The battery contained 26 20-Ah rectangular cells. The cells were electrically insulated from each other and the chassis by fiberglass tape. They were held in place by compressive forces in each of three perpendicular axes. The battery contained two electrical connectors: one was used strictly for ground testing to monitor cell voltages while the other was the power connector. An L-shaped metal plate was positioned between the middle cells of each cell row upon which temperature transducers and switches were mounted. The temperature switches were safety devices to be used to stop high-rate charge automatically in case of overheating. A diode was placed in the charge line for isolation from ground support equipment and a 1-A fuse was placed in the battery voltage sense line in case of shorting of the spacecraft umbilical. Bimetal controlled louvers were mounted on the battery base plate for temperature control in flight. Battery temperature control during lab testing was accomplished by mounting the battery on a heat sink.

A. Battery Operation on the Spacecraft

Battery operation on the spacecraft was automatic. The battery is isolated from the dc voltage bus via two pairs of series, paralleled diodes. When not supplying power, the battery is kept on constant charge at about 0.6 A. After a discharge, the battery is recharged at 2.0 A to 37.5 V. The high-rate charger is automatically switched off and the low-rate charger is automatically switched on. In addition to the voltage cutoff on high-rate charge, there is a safety temperature switch which automatically switches from high- to low-rate charge if the temperature of the battery exceeds 38°C.

The circuitry was designed so that the automatic features could be disabled or overridden by ground commands or programmed into the onboard CC&S. The CC&S mode of operation was used quite extensively during solar occultations. Also during certain operations where solar panel power was marginal it was sometimes necessary to command the low-rate charger off to conserve about 35 W.

B. Battery Manufacture

The battery was assembled per the top assembly drawing, following a JPL approved detailed assembly process. The FPP listed all of the applicable documents, equipment, and materials inspection and quality assurance points required for battery assembly. Before assembly, a Parts Assembly List (PAL) which kits all of the required parts was issued, thus insuring traceability of serial numbers or lot numbers. A Manufacturing Shop Order (MSO) was also issued. The MSO listed each assembly, inspection, and quality assurance operation. It also provided for signoff by personnel performing the work and listed any nonconforming material reviews (NCMR) that might have occurred. The PAL and MSO were included in the battery log book for review before the battery was accepted as flight hardware.

After the battery was assembled and all connections soldered, wire continuity and insulation tests were performed to assure proper wiring and assembly. The battery was then subjected to functional tests (three charge-discharge cycles) followed by either the type approval (TA) or flight acceptance (FA) tests.

C. Battery Cells

In essence, battery performance is dependent on the individual cells, and a great deal of effort was expended to assure that high-quality matched cells were procured and selected for each battery. In order to obtain relatively uniform performance, cells for all of the batteries except the engineering model were assembled from one lot of positive and negative plates. A total of 360 cells (including 30 for the EM) were purchased. Based on previous experience, TRW rated the cell manufacturers against a list of selection criteria and recommended that the cells be procured from Gulton Industries. JPL concurred with the decision.

The cells were purchased to a TRW specification approved by JPL. In addition, Gulton provided a Process Identification Document (PID) which identified manufacturing processes, procedures, and inspection documents used to manufacture the cells from receipt of raw material to shipment of the finished cell. The documentation and facilities were reviewed by TRW and JPL engineering and quality assurance personnel. A TRW quality assurance representative was in residence at Gulton during cell manufacture.

Upon receipt of the cells from Gulton, TRW put the cells through a 100% inspection and test program per specification. The cells were given various electrical and capacity tests and run through a 30-cycle burn in test. The data was punched on computer cards, and a listing of the data by cell SN was printed out along with the mean and standard deviation. Providing the cells met the test criteria, the prime factors in the matching of the cells for a battery were the spreads in the end-of-charge voltage and capacity output, namely, 15 mV and one Ah, respectively.

D. Battery Handling and Spacecraft Test

Since this was a new battery system for JPL, a new philosophy of battery handling, usage, and test was developed. On previous programs, the flight battery was never tested and mounted on the spacecraft until a few weeks before launch because of the limited life and cycle capability of the silver-zinc batteries. All testing at the spacecraft level utilized non-flight system-test batteries. A survey of other users of spacecraft Ni-Cd batteries was made to determine how the batteries were stored and when in the program they were mated to the spacecraft. The answers on storage were

quite varied; however, most users placed the flight battery on the spacecraft early in the program. TRW had recommended that the batteries be stored on trickle charge. JPL elected to store the batteries at room temperature discharge and shorted. At four- to six-week intervals a conditioning charge-discharge cycle was put on each battery. The data gathered from the periodic conditioning cycles was compared to determine if battery characteristics changed during storage. No significant changes were noted on any of the batteries, thus increasing the confidence level of the batteries capability.

It was recommended that the batteries be stored shorted rather than having a constant trickle charge because it was considered to be the state of least chemical activity. If stored on trickle charge, chemical activity would be continuous and the oxygen generated would tend to attack the separator material and age the battery more rapidly. If longer storage periods, greater than one year, were in the offing, the batteries would have been stored at low temperature, which would further reduce chemical activity.

A "Battery Handling and Safety Procedure For Ground Operations" and a "Cognizant Engineer Summary" were issued. These documents provided detailed safe handling methods and operational constraints for operating personnel to observe during laboratory and systems tests. Other users had reported that flight batteries were mated to the spacecraft early in the test phase. It was deemed inadvisable to do this in the MM'71 Program because there would probably be long periods of time during the 6- to 9-month test phase when the battery would sit open-circuited, which was considered detrimental to battery performance. The flight batteries were placed on the spacecraft for specific well-defined tests which assured total system compatibility. These were: (1) Free Mode, (2) Solar Thermal Vacuum, (3) Vibration and Acoustics, and (4) Final Systems Tests at ETR. A Battery Operational Log was maintained by the power operator whenever the battery was on the spacecraft. The flight batteries were removed from the spacecraft after the Final Systems Test at ETR and were given a complete inspection and test. They were returned for final mating to the spacecraft approximately one month prior to launch, during which time the spacecraft was armed, encapsulated, and mated to the launch vehicle. Also during this time, at least one simulated launch countdown was performed using battery power. This was another first for the program, and it

provided the last check of the battery before launch. Because of past practice, which dictated that little or no testing be performed on the flight battery, the test directors were somewhat hesitant to perform the test. This was the first program in which no PFR's were generated by the battery.

E. Laboratory Tests

At the beginning of the program, there were many unknowns, and accurate data was almost nonexistent in the published literature. Most of the data in the literature was based on individual cell testing and was difficult to relate to a battery because in many instances key details of the test were missing, such as prior test history or where the temperature of the cell was measured if at all. Most often temperatures reported were ambient.

A major area of concern was related to the question of how the battery would behave after six months (the cruise period from launch to Mars encounter) of trickle charge. Using results from batteries stored on trickle charge, TRW had indicated early in the program that the battery voltage would be severely degraded. The entire industry was surveyed, and the results were mixed. However, no one presented factual data to show actual results. The reason for this lack of data was that all other spacecraft were put into Earth orbit and there was no need to test for long-term trickle charge effects.

In 1970 two batteries were put on a mission simulation test to evaluate battery performance based on predicted mission requirements. One battery was operated at 13°C and one at 18°C during cruise as measured on the battery temperature transducer. Battery temperature was controlled by heat sinks. After simulating the launch discharges, midcourse correction discharges, and cruise period, one battery was given a "recondition cycle," which was a 24-h discharge through 50-ohm load followed by recharge. Both batteries were completely discharged to determine voltage and capacity characteristics. There was little difference in voltage between the two batteries. Their voltages and capacities were not severely degraded and they easily supported the mission requirements.

The final decision on whether or not to perform a reconditioning cycle was dependent on the results of batteries placed on a real-time mission test. Two batteries were placed in thermal vacuum chambers and duplicated the

use profile of the flight battery. About four weeks before the Mars orbit insertion discharge, one of the batteries was discharged. The results showed that it would not be necessary to recondition the flight battery.

Two extended mission tests (which represented the cycling regime during Sun occultation, which was to occur after about four months in Mars orbit) were run on the MST batteries. The first orbit regime of 130 cycles tested the batteries to a maximum of 50% depth of discharge (DOD), and the second (a worst case) to a maximum of 100% DOD. The results indicated there should be no problem with the battery supporting the mission.

In addition to the extensive, long-term mission tests, charge efficiency and charger/battery interface tests were run. The charger/battery interface test determined the effect of voltage input to the charger on its current output as related to the differential voltage between the input voltage and battery voltage. It was anticipated that solar panel voltage would be low near Earth and that it might prevent the battery from being fully recharged. The tests proved that the predicted low voltage would not prevent the battery from reaching full charge.

F. Flight Battery Performance

The battery performance on Mariner 9 was as predicted based on the test data bank generated from the tests described above. After launch on May 30, 1971, which only required 8.8 Ah, the battery was not discharged until Mars orbit insertion on November 13, 1971. The midcourse corrections were not of sufficient magnitude to cause loss of solar panel power. The Mars orbit insertion discharge removed only 6.34 Ah from the battery. The first orbit trim maneuver, performed on November 13, 1971, required a 4.4-Ah discharge. An additional orbit trim maneuver, performed on December 30, 1971, required only 3.94 Ah of discharge. The battery performed as predicted in each instance.

Sun occultations began on April 2, 1972, and lasted for 63 days. The orbit period was approximately 12 h; a total of 126 cycles were put on the battery. Periodic tracking and data return gave information on battery performance. A plot of the capacity discharge as a function of cycle formed a left-skewed parabola. The maximum discharge was near 45 cycles and was 14.3 Ah. The plot of the end of discharge voltage as a function of cycle was

near the predicted curve. No anomalies or surprises were observed on the battery to this time in the mission. A supplementary report will document battery performance from occultation period to the end of mission.

/

III. CONCLUSIONS AND RECOMMENDATIONS

The battery program for the Mariner Mars 1971 Mission proved to be very successful, and the battery met all mission requirements. No design weaknesses were found during the course of the program, and no major changes to the battery design were recommended.

The battery was designed, built, and qualified within the span of a year. If more time had been available, the battery chassis design might have been simplified (the present design requires intricate machining).

The decision to change from a silver-zinc to a nickel-cadmium battery made it possible to extend the mission time well beyond the capability of the previous Mariner batteries, thus providing for additional scientific data concerning the seasonal changes on Mars and the celestial mechanics experiments related to the theory of relativity.

The decision to use 26 cells in place of 24 cells proved to be a good one. The use of 26 cells allowed the battery to be discharged to nearly one volt per cell average. If only 24 cells were used, the average cell voltage discharge limit would have been about 1.14 V. The latter value is near the operating voltage level of aged cells cycled at 50 to 70% DOD. This effectively increased the energy output by 30 to 50% and made it feasible to complete the mission without attempting to "recondition" the battery in flight.

The plan for reconditioning the battery in flight was to discharge it through a 50-ohm load for 24 h. However, test data showed that it is necessary to discharge the battery completely to properly recondition it. If reconditioning is contemplated on future flights, it is recommended that a higher discharge rate (lower load) be considered as a part of the overall reconditioning. Possibly two load levels could be considered.

The safety and handling plans and procedures developed for this program were well defined and carefully followed by the operating personnel. This was attested to by the fact that there were no significant battery problems during the course of this program. The method of storing the batteries and the periodic conditioning cycles were quite stringent and could possibly be relaxed on future programs. Cold storage and less frequent conditioning cycles (three to six month intervals) are recommended.

For future missions of longer duration, it is recommended that the battery system be designed for a lower operating temperature, which will prolong the life of the battery and reduce voltage and capacity degradation.

In order to predict battery performance within the degree of accuracy expected by flight operations personnel, it is necessary to test batteries or cells in real-time to the expected use conditions since the previous history of battery use tends to be related to its future performance.

It is also recommended that information concerning the hydrogen gas-gassing potential of cells and the optimum (minimum) trickle charge rate as functions of temperature be generated. Very little data exists in the literature covering these aspects of nickel-cadmium battery operation.

Methods of bypassing shorted or weak cells for long-duration missions also need to be explored.

IV. DESIGN CONSIDERATIONS AND REVIEWS

This section discusses the historical background and analysis that led to the decision to use a single nickel-cadmium battery on the MM '71 orbiter spacecraft. The preliminary battery requirements are outlined along with a discussion and the summary of the results of the various design reviews. Battery integration and operation in the power subsystem are discussed.

A conceptual design review was held on June 24, 1969, which basically covered three alternate mechanical configurations. A second design review was held on August 15, 1969, prior to the release of drawings for the fabrication of the engineering model. A power subsystem design review was held on August 26, 1969, at JPL for the NASA/JPL MM '71 Project Office. A third battery design review was conducted February 4, 1971, covering test results on the engineering model battery prior to the release of the drawings and documentation for assembly and test of the flight batteries.

A. Preliminary Design Analysis and Considerations

A preliminary planning effort for the MM '71 orbiter spacecraft battery was inaugurated in February 1968 to determine the feasibility of utilizing the silver oxide zinc battery, which was the baseline design. The Mariner Mars 1971 Project Office initially limited the maximum allowable weight of the battery to 18.1 kgs. Three electrochemical systems were considered for the MM '71 mission. These were (1) silver-zinc (Ag-Zn), (2) nickel-cadmium (Ni-Cd), (3) silver-cadmium (Ag-Cd). Previous JPL spacecraft (Rangers, Mariners, Surveyors) utilized silver-zinc batteries because of system weight constraints. The Mariner 1969 battery weighed 15.4 kg and when new delivered a minimum of 1350 Wh. A Ni-Cd battery capable of delivering the same energy was estimated to weigh 50 kg, and an Ag-Cd battery was estimated to weigh approximately 25 kg.

Battery performance, life, and cycling data generated on previous JPL flights was reviewed. The data indicated the batteries were adequate for their particular application; however, the data also indicated that the Mariner Ag-Zn battery design was not capable of meeting the more rigorous MM '71 mission requirements. The primary mission, 90 days in orbit, required a minimum battery life of approximately nine months to one year and a minimum of nine cycles. Extended mission use was not a design

requirement, but after four months in orbit, Sun occultations would occur and battery power would be required for varying times on each orbit. The occultations were estimated to last for about two months.

Previous in-flight Mariner spacecraft battery utilization was limited to one or two discharge/charge cycles very early in flight, usually not beyond 10 days. Therefore, the effect of the space environment as compared to ground or bench tests on the long-term life and cycle life of Ag-Zn batteries was unknown. The MM '71 mission required the battery to be used for orbit insertion and orbit trims in addition to launch and midcourse maneuvers. The heaviest use of the battery subsequent to launch was expected during orbit insertion after the battery was about eight to nine months old. In reviewing life test data on the Mariner programs it was found that some of the batteries survived about 8 months in the laboratory and a couple of discharge cycles before showing signs of failure.

The flight battery on Mariner 2 (a Venus flyby) appeared to be good at 130 days of flight, which was the end of recorded data. Venus encounter occurred at about 109 days; however, the battery was not used after the midcourse correction, which occurred nine days after launch. The Mariner 4 (a Mars flyby) flight battery was not used after the midcourse correction. After 86 days, the battery terminal voltage exceeded the maximum predicted voltage of 34.9 V. It reached a high of 37.2 V at about 265 days. The reason for the anomalous performance is unknown, but it was surmised that the battery had developed a leak and would probably not have been capable of delivering useful energy. The Mariner 1969 program had not progressed enough to produce any significant life test data at this time. Based on the analysis of the performance of previous Ag-Zn batteries, it was recommended that an Ag-Zn battery development program be instituted and that the possibility of using a Ni-Cd battery be evaluated. It was decided not to initiate any effort on the Ag-Cd system because of fund limitations and the lack of good technical data for aerospace use.

A program schedule as shown in Fig. 1 was outlined in September 1968 to establish the simultaneous development approach of two different battery systems, Ag-Zn and Ni-Cd. Preliminary power profile estimates indicated that a battery capacity of 30 Ah would be sufficient to power the spacecraft. A statement of work and request for proposal were sent to

Ag-Zn battery manufacturers for the development of a 30-Ah long-life Ag-Zn battery. This resulted in JPL Contract No. 952472 with ESB, Inc., which was initiated in January 1969. In the meantime, procurements were initiated for Ni-Cd cells from different manufacturers for a cell test program. Since 30-Ah cells were not available, 20-Ah cells were procured and development contracts initiated for 30-Ah cells with General Electric Co. and Gulton Industries.

A Battery Study Working Group was established in December 1968 to examine all the ramifications of the two battery systems. The group consisted of the following:

Division 34 Project Rep.	J. L. Savino
Battery Engineer	R. S. Bogner
Power Conditioning Engineer	T. J. Williams
Power Subsystem Engineer	A. B. Krug
Thermal Control Engineer	L. N. Dumas
Mechanical Packaging Engineer	W. S. Read
Spacecraft System Engineers	E. K. Casani/A. G. Conrad

The first meeting established the three baseline design approaches to be investigated and 14 study items or action items to consider in making the selection. The group was to complete its objective by March 1, 1969.

The three design approaches were:

- (1) A dual Ag-Zn system using two 30-Ah batteries was selected. One of the batteries would be used for launch, trajectory corrections, and backup during cruise. The second battery would be stored cold, 0°C, then warmed up to operating temperature, 20°C, near the time for orbit insertion and switched by command in parallel with the other battery.
- (2) The second approach was simply to use a single 30-Ah Ni-Cd battery. This would be similar to past Mariners that used single Ag-Zn batteries, except the charging scheme would be different. There was also the possibility of a requirement to recondition the battery.

- (3) A third approach was to use redundant 15-Ah Ni-Cd batteries for reliability and the possible problem of reconditioning. Another experienced user of Ni-Cd batteries had indicated to JPL that there would be a severe loss in battery voltage following a long trickle charge period similar to the cruise period to Mars, which was about six months. To eliminate the voltage loss it was necessary to deep discharge and recharge the battery. If only one battery was available, there would be no backup during the reconditioning period if the spacecraft lost lock on the Sun.

The 14 basic action items were:

- (1) Thermal control considerations.
- (2) Packaging and cabling considerations.
- (3) Failure modes.
- (4) Sequencing and mission flexibility.
- (5) Command requirements.
- (6) Power profile effects.
- (7) Cost considerations.
- (8) Weight, battery.
- (9) PCE mechanization.
- (10) Operational effects and considerations.
- (11) Telemetry requirements.
- (12) Schedule.
- (13) Magnetic interference.
- (14) Battery performance characteristics.

By the end of January 1969, the Battery Study Group recommended that a single Ni-Cd battery system be used on the MM '71 program. Table 1 summarizes the findings of the group. It was also established that a 20-Ah cell size was adequate to perform the mission based on updated power requirements and allowing an 80 to 90% DOD.

B. Design Requirements and Design Reviews

The first battery was scheduled for delivery for the proof test model spacecraft (PTM S/C) by March 1970. This required the design, fabrication, and test of a new battery in one year, which was a very tight schedule. A statement of work and a request for proposal was sent out on February 14, 1969. TRW was selected as the battery contractor by the proposal review board April 17, 1969, and the Contract (952544) was executed August 19, 1969; however, work was started May 28, 1969, under letter contract. The basic requirements for the battery at this stage of the program were that the battery would be used for launch, midcourse maneuvers, orbit insertion and orbit trim maneuvers for a minimum period of nine months. Operational use beyond nine months had not been defined, but it was stated the battery should be capable of an additional year's use. The flight battery system (FBS) design requirements were defined as follows:

- (1) The FBS must be capable of handling the power requirements shown in the preliminary power profile (Fig. 2). The FBS shall have the capability of supplying power for either a midcourse correction or an orbit insertion maneuver after approximately six months' cruise within the operational voltage constraints of the MM '71 orbiter power conditioning equipment (PCE).
- (2) The battery must be capable of supplying the required power for an orbit trim maneuver with 10 hours of charge after the orbit insertion maneuver.
- (3) Battery charging was not completely defined, but it was estimated that a maximum current of 2.00 A would be available for high-rate charging and 0.65 A for trickle charging.
- (4) The FBS shall be configured so that it shall occupy one of the MM '71 orbiter spacecraft octagonal bays.
- (5) The FBS weight shall be 27.18 ± 2.26 kg.
- (6) Provisions shall be made for mounting FBS temperature transducers.
- (7) The battery shall be capable of performing its required functions when operated in a temperature environment from -1.11 to 32.22°C .

- (8) The battery terminal voltage shall be from 25 to 39 V over the temperature range specified in (7) above.
- (9) Provisions shall be made for monitoring individual cell voltages as well as battery terminal voltage from power operational support equipment and bench test equipment.
- (10) Provisions shall be made to facilitate a charge control method by means of temperature-compensated voltage cutoff.
- (11) Provisions shall be made for a temperature safety switch to terminate high-rate charge.
- (12) Provisions shall be made for charge-discharge bypass circuitry of individual cells.
- (13) The battery mechanical design shall be compatible with the overall spacecraft structure and thermal design.

C. Battery Schedule and Milestones

The previous discussion outlined the background that led to the decision to use a single Ni-Cd battery and the establishment of the basic design requirements. The final design requirements or specifications were developed in parallel with the battery contract. Figure 3 shows the FBS program milestone schedule. Basically the program met the major milestones. In the figure it is seen that a total of 10 batteries were to be built and delivered. During the course of the program, one type approval and one system test battery were deleted. The final report was also deleted.

The preliminary design review was held on June 24, 1969. The purpose of the review was to study three packaging concepts presented and choose the best compatible design. Prior to the design review JPL provided the contractor with the following guidelines:

- (1) The battery would contain 26 20-Ah Ni-Cd cells.
- (2) The cells would be mounted on the baseplate on their edges for better heat dissipation.
- (3) The baseplate of the battery would also be an integral part of the spacecraft structure forming the shear plate of Bay VIII.

- (4) The chassis would be machined from a billet (forging) of magnesium ZK60 A-T5.
- (5) Thermal control louvers would be mounted to the battery base-plate for temperature control.

Design Review II was held at TRW on August 15, 1969, prior to the release of drawings for the engineering model fabrication. The primary function of this review was to determine if the analytical design capabilities would meet the requirements. Table 1 lists the topics covered in the design review. The design presented was accepted by the review board; however, seven alerts and five action items were generated during the review. The major alert item was that the magnesium forgings were purchased to a $1.172 \times 10^8 \text{ N/m}^2$ yield stress whereas the stress analysis assumed a yield stress of $1.792 \times 10^8 \text{ N/m}^2$ as quoted in materials handbooks.

The five action items were as follows:

- (1) Review the cell and battery specifications to insure that the test levels meet the requirements and that the two specifications are compatible with each other.
- (2) Review the magnetic requirement of the spacecraft and define what magnetic requirement, if any, should be imposed on the battery.
- (3) (a) Determine the temperature setting for the louvers. (b) Determine the setting of the thermal switch. (c) Determine the voltage level for switching to trickle. (d) Based on expected flight temperatures, develop a mutually agreeable high-temperature limit for type acceptance testing (qualification testing).
- (4) Provide an addition to the data package covering the rationale for lack of a cell bypass system using diodes.
- (5) Provide an estimate of cost and schedule implication of X-ray examination of the cells after vibration.

Samples of the magnesium forgings were tested and records screened. It was indeed found that the forgings had stress yields as low as $1.213 \times 10^8 \text{ N/m}^2$ and resulted in a reevaluation of the battery chassis design.

Action Item 1 resulted in a few changes to the parts and equipment specification so they were compatible to one another. Action Item 2 resulted in the basic wiring layout of the battery which is shown in Fig. 4. The two rows of 13 cells on opposite sides of the batteries were wired such that the induced magnetic fields produced by the flow of current would cancel out. There were no project documents defining magnetic requirements.

Action Item 3 is too detailed to discuss in depth here. The results of the analyses were as follows:

- (1) The recommended louver setting in the closed position was 12°C .
- (2) The recommended thermal switch setting was $38.78^{\circ}\text{C} \pm 1.67^{\circ}\text{C}$ for closing on temperature rise and $35.00^{\circ}\text{C} \pm 1.67^{\circ}\text{C}$ for reopening.
- (3) The recommended voltage limit for switching to trickle charge was 37.4 V, but was later set at 37.5 ± 0.1 V.
- (4) The recommended high-temperature level for type approval testing was $43.33^{\circ}\text{C} \pm 2.78^{\circ}\text{C}$.

Only recommendation (2) remained unchanged in the final design. The louver setting was lowered to 7°C . The voltage limit for switching to trickle charge was raised to 37.5 V. After negotiations with the spacecraft environmental engineer, the TA upper temperature limit was set at 48.9°C as measured by the battery temperature transducer.

The text of Action Item 4 presented the rationale for the elimination of the requirement for cell bypass diodes in case of a cell failure. In essence it was shown that the voltage characteristics of diodes were not sufficient to prevent gassing in partially shorted cells in either the charge or discharge mode. Diodes would be useful in shunting the current around "open" cells, but this type of failure was considered to be of the same order of magnitude as the failure rate of the diode itself.

Action Item 5 indicated it would cost approximately \$4.00 per cell for X-rays after vibration tests. Later in the program it was decided not to X-ray the cells after vibration since they were X-rayed during manufacture.

The MM '71 Project Office required a detailed power subsystem review. This review was held at JPL on 26 August 1969. The objectives of the review were as follows:

- (1) To yield a critique of the design, test, fabrication, and operation procedures to assist in assuring that the best design and procedures have been achieved within program constraints
- (2) To assure compatibility of the power subsystem with the system and other systems
- (3) To evaluate the documentation for accuracy and completeness

The agenda for the battery portion of the review is shown as follows:

- (1) Design
 - (a) Description of Ni-CAD battery/cell and characteristics.
 - (b) Electrical and mechanical requirements and configuration.
 - (c) Summary results of preengineering design review and analysis.
- (2) Manufacturing
 - (a) Cell procurement.
 - (b) Battery fabrication.
 - (c) Quality assurance activities.
- (3) Test program
 - (a) Cell evaluation program.
 - (b) TA and FA test program.
 - (c) Bench test equipment.
- (4) Reliability
 - (a) MM '71 design and comparison to other flight programs.
 - (b) Failure mode analysis.
 - (c) Areas of concern and possible improvements.
 - (d) Risk items.
- (5) Safety

(6) Status

- (a) Milestone schedule.
- (b) Documentation status.
- (c) Major program problems.

A total of 14 action items relating to the battery were generated by the review board. Many of the action items were not relevant to the objectives of the review in that there was little probability that a design change was involved. Possible items that affected a design change were classified as Category I and required immediate attention.

Category II items received second priority and were items that would be closed out as a normal part of the project effort. There were only three Category I battery action items and these pertained to: (1) battery cell bypass in case of a cell failure, (2) the yield strength of magnesium forgings, and (3) apparent lack of TRW quality assurance activities at Gulton. The first two action items had been established during Battery Design Review II and were subsequently answered. It was also established that TRW would have a QA resident engineer to monitor the Gulton QA activities during cell manufacture.

Design Review III was held February 4, 1970, after assembly and test of the engineering model (EM) battery. No significant action items were generated, and no change of the battery design was indicated. The major item of concern was the resolution between JPL and TRW of the Type Approval Test Specification. JPL required that the upper TA temperature be at 49°C, whereas TRW advised not to test above 43°C. It was finally established that 49°C would be the upper temperature limit. The test results on the EM battery are presented in Section III.

D. Power Subsystem Battery Integration

A brief description of the power subsystem is given to show how the battery is integrated into the system. Figure 5 shows the functional block diagram of the system. The primary power source is four solar panels, and the battery provides backup power. Whenever the solar panel cannot provide the power demands of the spacecraft, power is automatically supplied by the battery, which is always on line but is isolated from the power bus by quad diodes which are series-paralleled. The battery may either

supply all of the power, as in the case where the solar panels are completely shaded from the Sun, or it may share the power with the solar panels if they are partially shaded.

1. Battery charger. In addition to a new battery, a new charging system was designed. The battery charger consists of independent high-rate and low-rate constant-current chargers. The high-rate charger, which provides 2A, is a pulse-width-modulated switching regulator. Constant current regulation is maintained by a duty cycle variation of the series regulator as a function of output current changes. The low-rate charger (trickle charge) is a constant-current series regulator. The fixed output of 0.65 A is controlled by the voltage developed across a resistance in series with its output.

A circuit in the battery charger automatically switches from the high-rate charger to the low-rate charger when the battery terminal voltage reaches 37.5 V. Automatic transfer from high to low rate is also made if the battery temperature reaches 38°C (100°F). The automatic function is not reversible in that once the charger is in the low-rate mode it must be manually commanded back to high rate.

2. Commands. The battery charger can be controlled by either a direct command (DC) from the ground or commands stored in the CC&S. These commands, summarized in Table 2, operate a toggle switch for on or off and high-rate or low-rate charge. The chargers can also be commanded from the ground to remain in high rate by inhibiting the automatic switch-over function. This also inhibits the high-temperature switch function and would allow the battery to be high-rate charged if it should go above the temperature limit on charge. A command is also available to switch a 50-ohm load on the battery to discharge it for reconditioning if required.

The telemetry channels and their functions are:

- Channel 205: battery voltage
- Channel 225: battery output current
- Channel 305: battery charger output current
- Channel 405: battery temperature

In addition, telemetry channel 406 monitors the position of relays that control battery charge rate, charger rate transfer, and the boost converter operation.

V. BATTERY DESIGN, MANUFACTURE, AND QUALIFICATION

As indicated in Section II, the battery design was an evolutionary process with many people participating via the design reviews. Before fabrication and assembly of the battery, the design was analyzed. To confirm the analysis, an engineering model battery was built and tested. This section will follow the design, fabrication, and testing of the engineering model battery SN EM-1. As it turned out, the initial design proved to be adequate, with one minor change.

A. Design Configuration and Analysis

Figure 6 is a photograph of the battery. The battery consists of 26 Ni-Cd cells in two rows of 13 cells. The cells are laid on edge on the baseplate of the chassis rather than on the cell bottom as had been previous battery design practice. This gives greater heat dissipation surface and consequently better temperature control. The cells are held in place by the compressive forces in each of three perpendicular axes by the keeper bars, end plates, and chassis cover (see Section V-B). The wiring schematic of the battery is shown in Fig. 7. The battery contains a diode in the charge line for isolation from support equipment (SE) during ground testing and a 1-A fuse. Two connectors are incorporated in the battery. One of the connectors is used strictly for ground testing and cell monitoring, while the larger connector J2 is the power connector for mating to the spacecraft power system. The temperature transducers for monitoring battery temperature are mounted to aluminum plates, referred to as thermal brackets. The thermal brackets are placed between the middle cells of each 13-cell row and thus measure the average temperature across the broad face of the cells. The temperature switches used as backup to stop the high-rate charge are also mounted on the aluminum plate with the temperature transducers. Temperature control is effected by thermal control louvers mounted on the outside of the battery baseplate or spacecraft shear web.

1. Mechanical design analysis and confirmation. As discussed previously, it was discovered during the second design review that the battery structural design was based on the assumption that the magnesium forgings for the chassis had a yield strength of $1.792 \times 10^8 \text{ N/m}^2$ instead of the actual value of $1.172 \times 10^8 \text{ N/m}^2$. The result of this was that the base

plate was increased in thickness from 3.42×10^{-3} to 3.81×10^{-3} m. Table 3 is a synopsis of the structural analysis.

Confirmation of the mechanical design was accomplished by subjecting the engineering model battery to the type approval environmental vibration requirements, which consisted of the sine and random levels listed in Table 4. A low-level resonance sweep was also run. Before the battery was tested, the vibration fixture was evaluated running a 1 g-rms sweep at a rate of one octave/min from 20 to 2500 Hz in all three axes. The response in the vertical direction (Z-Z axis) of the fixture was good, and only small variations in the environment were noted. In the other two directions, transmissibilities as high as 3.5 in the area of 1600 Hz were recorded. Due to the response of the test fixture, the +3.5 and -1.5 dB test tolerances could not be met. This was not considered a major problem, and the tolerances in the high-frequency range were relaxed by Project approval.

The EM-1 battery was instrumented with eight accelerometers at the positions listed in Table 5. The Z axis of the battery was perpendicular to the base plate. The Y axis was through the face of the cells; the X axis was through the length of the cells as mounted in the battery.

The data obtained from the test is too detailed to present in this report. Figure 8 shows a typical plot of the data (baseplate/control ratio) for sine vibration in the Z-Z axis; Fig. 9 shows a power spectral density plot in the Z-Z axis during random vibration.

The major mode of the battery was a disconnected single-degree-of-freedom system (nonlinear), half of which is the baseplate and the other half is the upper keeper assemblies. The major structural response occurred between 280 and 320 Hz, which is in the more benign portion of the qualification level environment. The baseplate was calculated to have a natural frequency of 260 Hz. During the resonance search the major mode of the battery was found at 320 Hz, and during the high-level sine test the major mode was 280 Hz (Fig. 8). Thus the test results were in good agreement with the analytical results. The fact that the frequency decreased as input level increased is also in agreement with the behavior of a nonlinear system.

The highest transmissibility found was 16 and was at the upper keeper bar. It occurred between 280 and 320 Hz. The transmissibility on the baseplate was 14. The structural analysis was made using an assumed transmissibility of 20; consequently there was a good safety margin. Table 5 summarizes the Z-Z axis test results.

Electrical tests performed on the battery during and after vibration testing did not indicate any abnormal behavior. It was concluded the battery design was capable of surviving the qualification level dynamic environment and approval was given to start flight battery fabrication.

2. Thermal design analysis and confirmation. Thermal design considerations required a coordinated effort because of temperature control effects on the total spacecraft. It was concluded early in the design effort that the battery should have active thermal control in order to maintain the battery in the preferred operating range of 10 to 18°C. Initial temperature calculations were made in a gross manner to determine maximum shear plate (battery baseplate) temperatures for two assumed spacecraft bus environmental temperatures, namely 18.35 and 26.67°C. The following assumptions were made:

- (1) Steady-state conditions prevail on the spacecraft bus.
- (2) View factor from shear plate to bus assumed to be 1.0.
- (3) Louver operating range was 15 to 29°C.
- (4) Bay face around louver was fully shielded.
- (5) Louvers and shields radiated to deep space.
- (6) Battery weighed 27.21 kg.
- (7) Battery specific heat was $8.52 \times 10^3 \text{ J/Kg-}^\circ\text{C}$.

Worst-case steady-state battery baseplate temperatures were calculated at estimated power dissipation levels of zero, 29 and 76 W, representing open-circuit, trickle charge, and high-rate overcharge or discharge modes respectively. The rates of temperature increase (dT/dt) were also calculated at 29- and 76-W dissipation levels. The results based on the assumptions were 4.0 and 12.0 °C/H which indicated there would be a thermal problem. Table 6 presents the results of the steady-state temperature calculations.

From these results it was evident that the louver operating range needed to be biased downwards since the actual battery cell temperature would be even higher than the shear plate temperature.

Additional analyses were performed by JPL using refined battery-louver interface data and a computerized model. The analyses were for: (1) temperature transient for a 3-h period at 76 W dissipation, (2) steady-state temperatures at various power dissipation levels at a constant bus temperature of 21.11°C, (3) steady-state temperature at 24-W dissipation (assumed during trickle charge) at a constant bus temperature of 26.67°C. In all cases the thermal model included the variation in the shear plate emissivity with temperature with a louver operating range of 12.78 - 26.67°C.

Figure 10 shows the transient temperature response of the battery shear plate at 76-W dissipation. This figure represents the estimated response of the battery shear plate during a 3-h period of high-rate over-charge at 2 A or a discharge at about 12 A.

Figure 11 shows the calculated battery shear plate steady-state temperature as a function of the battery power dissipation. Also shown in the figure is a plot of quantity of heat which is rejected through the louvers. The differences in the abscissae between the shear plate and the louvers represent the heat conduction to or from the bus and the external shield heat rejection to deep space.

The steady-state analysis for 24-W dissipation at an assumed bus temperature of 26.67°C produced a shear plate temperature of 17.78°C. From Fig. 11 it is seen that the corresponding shear plate temperature (for 24 W and bus at 21.1°C) is 16.68°C, indicating that the battery is fairly insensitive to the bus temperature. In Section V it will be seen that the actual battery temperature was more sensitive to the bus temperature than calculated. Also during testing on the thermal control model (TCM) spacecraft it was found that louver opening set point had to be lowered to 4.6°C in order to meet the preferred battery operating temperature range.

The thermal network was constructed considering one quadrant of the battery because the battery is symmetrical about two mutually perpendicular axes. Seven modes were assigned to each cell with one at the geometric center and one on each of the six surfaces of the cell as shown in Fig. 12.

One mode was assigned to the area of the battery baseplate (shear plate) under each cell. The basic assumptions used for the analysis were as follows:

- (1) The battery baseplate temperature as a function of heat out was as shown in Fig. 11.
- (2) The radiant surrounding (bus) temperature was 21.11°C.
- (3) There was no heat transfer from the baseplate to the spacecraft bus structure by conduction, and the external surface emissivity of the battery was 0.85.
- (4) The power dissipations were as shown in Fig. 13.
- (5) The thermal properties of the magnesium chassis and nickel-cadmium cell components were as listed in Table 7.
- (6) The cells were electrically insulated with 1.78×10^{-4} meters of fiberglass tape.
- (7) The area between the cells and the baseplate was filled with RTV-11. The interface conductance between the cells and the baseplate was $0.4325 \text{ W}/(\text{cm}^2)(0^\circ\text{C}/\text{cm})$.

The results of the analysis are summarized in Fig. 14, which shows cell transient internal temperatures and average baseplate temperature as a function of time during a discharge-charge cycle and the steady state on low-rate charge. Additional analyses were made to determine maximum temperatures for conditions in which the battery was completely discharged or was on continuous high-rate charge. For these conditions it was assumed that the heat generation was 74 W. The results are shown in Figs. 15 and 16. Figure 14 shows the spread of internal cell temperatures compared to top surface temperature of cell 7, where the temperature measurement was to be made. (As discussed previously the temperature transducer was mounted on an aluminum plate which was between two cells). Figure 16 shows the calculated temperatures on the top surface of the cells and the average baseplate temperature. At the end of 4.5 h there is a difference of about 16.67°C between the baseplate and the internal cell temperature. However, there was a difference of only 2.78°C between the internal and the top of the cell temperatures.

After this analysis was made a design modification was made to bring the temperature of the end cells (Nos. 1, 13, 14, and 26) of the battery closer to the inner cells. The fiberglass-epoxy board shims totaling about 6.35×10^{-3} meters thick placed between the end cells and the chassis had holes drilled in them which reduced the contact area by 50%. The reduction in contact area increased the thermal resistance by a factor of 4.

The minimum temperature that the battery could drop to with no heat output was 12.78°C as shown in Fig. 11. From these analyses it was evident that the thermal control louver closing set point would have to be lowered. The final setting was 4.45°C and was determined during spacecraft thermal vacuum tests.

Confirmation of battery thermal design analysis was accomplished by thermal vacuum tests on the engineering model. It is pointed out, however, that the thermal vacuum testing does not attempt to duplicate flight conditions. Final confirmation was the result of thermal vacuum tests on the total spacecraft system in various operational modes (see Section V-C).

Two separate thermal vacuum tests were performed on the engineering model battery; however, the initial test provided sufficient temperature data to correlate with the analytical data (electrical performance will be discussed later). Twenty-one calibrated thermocouples were mounted on the battery at various locations to obtain its temperature profile. The battery was mounted to a standard JPL thermal vacuum test fixture. Shims were utilized to assure good contact between the heat sink and the battery baseplate. The chamber pressure was maintained at 1.330×10^{-3} N/m² or less. The chamber did not contain a shroud; consequently the wall temperature was near room ambient. A photograph of the test setup is shown in Fig. 17.

During the test the heat sink was maintained nearly constant. High- and low-temperature runs were made with the heat sink maintained near 27 and 3°C respectively. Steady-state temperatures were obtained with the battery on overcharge at 0.65 A. Transient temperature measurements were made during discharge at 12.0 A for 2 h followed by a 2.0-A charge.

Figures 18 and 19 show selected thermocouple measurements obtained on the high-temperature test run; Figs. 20 and 21 show the results for the

low-temperature test. It is observed that the difference in temperature between the end cell 13 and center cell 7 is on the average about 1.0°C, whereas the analytical data indicated about a 5.5°C differential before the modification. From these results it was concluded that the design change (discussed above) corrected the situation and that the battery temperature was quite uniform. This was also confirmed by measurements made at other locations but not shown here.

Tables 8, 9, and 10 partially summarize the comparison of the analytical data and the test data. Table 8 compares the temperature differentials between the baseplate and the center cell and the end cell on trickle charge, end of discharge, and end of high-rate charge. The temperature difference between the end cell and center cell is also evident. In every case, the test results were better than the analytical results. A possible explanation for the difference is that there was an assumed gap between the plates and the cell case filled with gas. If the gap was not as big as assumed in the analysis, the thermal resistance would be smaller, thus reducing the temperature differentials.

Table 8 compares the transient temperature response of the various battery locations for the analysis and the high-temperature test. In most instances it is seen that the transient response of the battery was within about one degree. The largest difference was the end cell and the reason for the lower analytical result was discussed previously. Table 8 shows the actual temperature measurements for the high-temperature test compared to the calculated temperatures from which the data in Table 7 was obtained. The average temperature of the battery during test was approximately 11°C higher than that assumed for the analysis. It was concluded that the thermal model was consistent with the test results and that the thermal design and performance were quite good. In the actual mission, it was unlikely that the battery would be discharged at a rate of 12 A for more than 1 hour; consequently the maximum ΔT would only be about 5°C during discharge.

B. Battery Manufacture

This section outlines the major steps of battery assembly. The battery was assembled per drawing number 10028180 following step by step

instruction described in FPP 08-053B, "Assembly Process For Program MM '71 Battery." The FPP lists all of the applicable documents, equipment, materials, and material preparation necessary for battery assembly. In addition, it lists all the test, quality control, and inspection points in the manufacturing flow.

The steps in battery manufacture are described by the flow diagram shown in Fig. 22.

A major operation was the fabrication of the battery chassis. The chassis was machined from a solid magnesium alloy (ZK60A-T5) forging using numerically controlled milling machines. Figure 23 shows a rough machined chassis being inspected. Certain areas of the chassis such as the inner corners of the gussets were finish-machined by electrochemical mills. The piece parts consisting of end plates, keeper bars, keeper angles, hold down frame, and connector brackets were machined from magnesium alloy plate stock (AZ318-H24). After machining and inspection, the chassis and piece parts were given a Dow 17 treatment which chemically anodizes the surface for corrosion protection.

Before the assembly operation is initiated, a Manufacturing Shop Order (MSO) and a Parts Assembly List (PAL) are made out and issued by manufacture planning. The PAL kits all of the parts necessary for the assembly of one battery and lists the serial number or material lot number of all parts for traceability. It forms the basis for the as-built list. Basically, the MSO lists each assembly operation by number and description and the work center where the operation is performed, including inspection and quality assurance. It also indicates who performed the operation and when it was performed and provides for appropriate signoff by the operator and inspection. It also indicates if any nonconforming material reviews (NCMR) were involved during assembly. Both the PAL and MSO are included in the battery log book and are reviewed before the battery is accepted as flight hardware.

The accepted and selected battery cells (see Section V for cell selection) are wrapped for electrical insulation with fiberglass adhesive tape and numbered for placement in the battery chassis. Next, a row of 13 cells or cell half pack is placed in the compression fixture as shown in Fig. 24. The

length of the cell pack is measured, and the appropriate combination of shims is selected so the cells will receive the same compression when assembled into the battery chassis.

Rubber insulators are bonded to the center rib of the chassis, and a thin coating of thermal conducting RTV is troweled onto the baseplate of the chassis as shown in Fig. 25. The cells, shims, and thermal brackets are assembled as shown in Figs. 26 and 27. It can be seen that the thermal bracket covers almost the entire broad face of the cell and thus provides an average cell temperature measurement by the transducer which is bonded to it on top. Prior to installation each serialized cell is marked for placement in the chassis.

The end plate is assembled to the chassis followed by the keeper bar (at the lower front edge of the cells) and the keeper angle (at the upper front edge of the cells, Fig. 28). A special assembly jig was used to align and press the row of cells back while the keeper angle and bar were assembled. The top hold down frame is assembled and the assembly to this point is checked for insulation resistance to make sure none of the insulation was damaged during assembly. In a couple of instances it was found that indeed the insulation was damaged during assembly. At this stage, it is relatively easy to disassemble the battery since wiring and soldering have not been done.

The preformed cell jumper wires are installed and soldered to the negative terminals only, because the cell voltage monitoring wires which have not been assembled yet are all soldered to the positive terminals of each cell. Next the connector bracket and prewired connectors are assembled. The wires are routed per the wire list, sleeved, connected, and inspected for proper placement. The fuse and diode are installed, and all connections are soldered. A wire continuity test is performed to assure proper wiring. The battery is then subjected to a functional test and the appropriate acceptance test, depending on whether the battery is to be a type approval or flight battery. These tests are covered in Section V-C.

After final acceptance testing the battery is shorted down (each cell individually), packed and shipped to JPL, where the battery is conformal-coated and all terminals encapsulated to prevent arcing and corona. Thermal

control paint is also applied to the outside, exposed baseplate of the battery where the thermal control louvers are mounted.

C. Fabrication and Qualification Tests

The batteries were subjected to several tests during and after manufacture; some of the tests were briefly discussed in the previous sections. A total of 10 batteries were assembled and tested, and the engineering model battery was used to shake down the test procedures. Batteries were subjected to two different levels of environmental tests: Type Approval (TA) and Flight Acceptance (FA). The TA tests are performed to conditions more severe than expected during flight and are designed to determine if the test article has any design deficiency. The test levels are set and approved by the spacecraft environmental engineer as delineated in the environmental specification (two batteries and the EM battery were TA tested). The FA tests are performed to conditions and levels which are expected during flight or ground testing and are designed to prove that the test article is flightworthy. Table 11 summarizes the test sequence for both TA and FA battery testing.

1. Fabrication tests. All batteries were subjected to a set of tests called "fabrication tests" during and after assembly and all testing was performed under QA surveillance. The fabrication tests were as follows:

- (1) Insulation resistance, in process.
- (2) Wiring continuity.
- (3) Insulation resistance, complete.
- (4) Electrolyte leakage.
- (5) Dimensional workmanship and marking.
- (6) Temperature transducer and thermal switch test.

As mentioned during battery manufacture, insulation tests were performed during assembly and after assembly was complete to assure there were no shorts between the cells or between the cells and battery chassis. The resistance was measured with a megohmmeter at 500 ± 50 Vdc applied for a minimum of 10 s. Leakage resistance readings ranged from 10 to 40k megohms, with 5k megohms required to pass.

Battery assembly wiring continuity tests consisted of measuring the resistance between each connector pin and its mating connection point on the cell, terminal board, and/or component part terminal with a volt-ohmmeter. Values from 0.1 to 0.2 ohms were obtained.

The electrolyte leakage test was performed to assure the integrity of the cell terminal seals after the assembly operations. This is a repeat of the leak test performed on the cells described in Section VI-C. Electrolyte leakage tests were also performed later in the program, after the batteries were tested and delivered, but prior to conformal coating.

The thermal switches and temperature transducers were tested by subjecting the battery to a temperature cycle. The battery was not electrically operated during the test, and the temperature cycle was accomplished by using a thermal electric temperature-controlled heat sink. The battery was set on aluminum shims cut to fit the major surface area of the battery baseplate. The shims were bonded to the heat sink with thermally conducting RTV. Calibrated thermistors were bonded with RTV to the battery thermal bracket at the bases of the thermal switches. Starting at 15.56°C, battery temperature was increased at a rate of 0.3°C per min. Temperature transducer and thermistor readings were recorded at discrete steps and when the thermal switches closed. After the switches closed the temperature was reduced at 0.3°C per min, and the temperature at which the switch opened was recorded. Specifications required that the switch close at $37.78 \pm 2.22^\circ\text{C}$ and open at $35.00 \pm 2.22^\circ\text{C}$.

2. Qualification testing. After passing the fabrication tests the batteries were subjected to either TA or FA environmental level tests. Two batteries, SN 201 and 202, were TA-tested, and five batteries, SN 301 through 304, were FA-tested. Batteries SN 306 and 307 were not environmentally tested, but were subjected to Group I and II tests.

Both TA and FA tests followed the same sequence. However, TA vibration and thermal vacuum tests were at greater levels, and the Group II functional tests were run before and after environmental tests on the TA batteries as noted in Table 11, but not on the FA batteries.

3. Vibration test. Since the cells are still in the shorted state from battery assembly, the shorting wires are removed. The battery is

mounted to the thermal electric temperature controller and the temperature is adjusted to 18.33°C. The charge consists of a 2.0-A charge to 3.75 ±1.0 V and switch to trickle charge 0.65 A for a total time of 24 h. The appropriate data is recorded on a data sheet and in the laboratory notebook. The battery tester was set to automatically terminate the charge if the battery exceeded 39.0 V or 37.78°C, or if any one cell exceeded 1.50 V. (If the battery was to be a TA unit it was subjected to the Group II tests, which are discussed later.)

The battery was then mounted in the vibration fixture and subjected to sinusoidal and random vibration in each axis. During each vibration run the battery was discharged through a 3-Ω load, and the voltage, current, and thermal switches were monitored on a visicorder. A schematic of battery instrumentation is shown in Fig. 29. No battery voltage or current anomalies were observed on any of the TA or FA test runs. During sinusoidal vibration the sweep rate was logarithmic from the lowest frequency to the highest frequency and back to the lowest frequency per the sweep rate and levels shown in Fig. 30. The TA and FA random vibration levels and rates are shown in Fig. 31.

4. Thermal vacuum tests. The TA and FA thermal vacuum testing was similar to that described previously in Section V-A, under design verification on the engineering model battery. The same chamber, fixtures, equipment, and data acquisition equipment were used except that an aluminized Mylar cover was placed over the battery since the chamber wall temperature was not controllable. The FA thermal vacuum test consisted of one low-temperature cycle (1.67°C minimum) and two high-temperature cycles (39.44°C maximum) during a 96-h period. The test was initiated with the battery fully charged. The heat sink temperature was adjusted to obtain a stabilized battery temperature transducer reading of 1.67°C. The battery was then discharged at the 2.0-A rate and trickle charged at 0.65 A for approximately 14 h without adjusting the heat sink temperature. While still on trickle charge the heat sink was adjusted upward to obtain a steady-state battery temperature of 23.89°C. The two high-temperature cycles were performed without further adjustment to the heat sink. The battery was charged at 2.0 A until the battery temperature reached 32.22°C. The battery was discharged at 12 A until the battery temperature reached 39.44°C. The minimum discharge requirement was 76 min or 15.2 Ah.

The TA thermal vacuum test consisted of two low-temperature cycles and five high-temperature cycles during a minimum period of seven days. The low-temperature cycles were performed by adjusting the heat sink until the battery temperature transducer stabilized at -3.89°C with the battery on open circuit. The battery was then cycled without further adjustment of the heat sink. The TA high-temperature cycles were run by adjusting the heat sink temperature to maintain the battery at 35.00°C (measured by the transducer), with the battery on charge at 0.65 A. In order to reach the upper temperature of 48.89°C , the battery was overcharged at the 2.0-A rate until it reached approximately 43.33°C and then discharged at 12.0 A. The minimum acceptable output on any of the discharge cycles was 15.4 Ah or 1.62×10^6 J. Both TA batteries passed the thermal vacuum test.

5. Group I functional tests. Following both the vibration and thermal vacuum tests at either the TA or FA levels, the batteries were subjected to the Group I functional tests to determine if the battery sustained any damage. These tests were essentially the same as the fabrication tests and consisted of the following:

- (1) Visually examine for physical damage.
- (2) Discharge and short each cell.
- (3) Wiring continuity.
- (4) Insulation resistance.
- (5) Electrolyte leakage.

The visual examination is self-explanatory, and the battery was shorted out in order to perform the other tests safely. Tests 3, 4, and 5 were described previously.

6. Group II functional tests. As noted in Table 11, the Group II tests were performed twice on the TA batteries after the vibration and after the thermal vacuum tests to determine if any damage was sustained.

These tests consist of three charge/discharge cycles, a charge retention test, temperature transducer and thermal switch test, and the diode test. The three cycles calibrate or determine the voltage characteristics

and the capacity of the battery at a nominal operating temperature subsequent to the environmental tests. The minimum acceptable output of the battery at the end of the third cycle was 2.16×10^6 J. The charge retention test is a repeat of the test made to determine if there was any possible internal damage to the cells during environmental tests. The temperature transducer and thermal switch tests are also repeats to assure that they were not damaged.

The three charge/discharge cycles at 100% depth of discharge conditioned and determined the voltage characteristics and the capacity of the battery at a nominal operating temperature subsequent to the environmental test. The minimum acceptable output at the end of the third cycle was 2.16×10^6 J. The batteries delivered 2.7×10^6 J. The cycles were performed on a thermal electric heat sink, and battery temperature was maintained between 18.33 and 26.67°C. Battery charge on each cycle was at 2.0 A for 12 h followed by 0.65 A for 12 h. The discharge was to 27.0 V on the battery or until the first cell reached 1.0 V. In practically all instances, the discharge was limited by a cell rather than the battery terminal voltage.

The charge retention test is the same test that was performed on cells during the cell screening tests. It was performed again to determine if the cells were damaged during assembly and the subsequent battery test regime. Since the test has been described elsewhere it will not be repeated.

The temperature transducer and thermal switch test previously described was also repeated to assure that they were not damaged during environmental testing.

A test is performed on the diode in the battery charge line from the umbilical line for ground support equipment to assure that the reverse leakage current is within specification. With the battery charged, a 1-M Ω resistor is placed across pins L and U of the J2 power connector through a breakout box. This short-circuits the battery through the diode. The voltage drop across the resistor is measured and must be below 10.0 V which is equivalent to 10 μ A.

VI. CELL PROCUREMENT, TESTING, AND MATCHING

Since the heart of the battery is the individual cells that comprise the battery, this report would not be complete without some discussion covering the procurement and screening of the cells. In essence, battery performance is no better than the weakest cell in the battery; therefore, considerable effort was expended to assure that cells of top quality were obtained and selected for each battery.

Early in the program JPL was deeply concerned about the advisability of procuring cells from one manufacturer. It was thought that cells should be obtained from at least two sources in case problems were encountered similar to those that befell the Orbiting Astronomical Observatory (OAO) battery as noted in the Transcript of Proceedings of the Conference on OAO Battery Trouble Shooting, October 30, 1968, at NASA/Goddard. The major problem encountered was that the cell voltage characteristics on charge were increasing with age. The specific cause of the problem was never pinpointed, but indications were that the problem was due primarily to a bad lot of separator material.

TRW proposed that all cells be purchased from one manufacturer and that the cells be made from one lot of plate stock and one lot of separator material. The cells would be built under rigid and improved control procedures. This it was reasoned should produce uniform batteries. Also the cells from different manufacturers were somewhat different in size and would cause design and assembly problems. TRW's proposal was accepted. Based on the evaluation criteria listed in Table 12, TRW proposed to procure the cells from Gulton Industries, and JPL approved the decision.

Prior to the selection of the cell manufacturer, JPL purchased 30 20-Ah cells each from three manufacturers for in-house evaluation and testing. At the time of TRW's selection, early test data indicated there was little difference in the performance between General Electric Co. (GE) and Gulton Industries (GI) cells. More recent data, contained in JPL Report 610-200, "Mariner Mars 1971 Extended Mission Nickel Cadmium Cell Test," July 15, 1971 (an internal report), finds that subtle differences begin to show up. The GI cells tend to have a slightly higher charge voltage and generate slightly more heat.

A. Cell Description

The nickel-cadmium cell is so called because its active material which provides the electrochemical energy is nickelic hydroxide (positive plate) and cadmium (negative plate). Both the positive and negative plate supporting structures are the same. The supporting structure is sintered nickel that is about 80% porous. The nickel is sintered onto a perforated, nickel-plated iron grid. The plate plaques are impregnated with solutions of $\text{Ni}(\text{NO}_3)_2$ and $\text{Cd}(\text{NO}_3)_2$, which are subsequently electrochemically formed to the active materials. The GI plate stock for the Mariner 1971 battery cells was procured from SAFT of France.

The positive and negative plates are separated by a continuous strip of a single layer of nonwoven nylon, Pellon 2505. The positive and negative plate tabs are heliarc-welded to steel combs, which in turn are heliarc-welded to the respective positive and negative terminals of the preassembled cell cover or header. A polyethylene bag separates the plate stack (element) from the cell case. The cell case is made from 304 L stainless steel 7.62×10^{-4} m thick. The cover is heliarc-welded to the case. The electrolyte is a 30% solution of potassium hydroxide, and each cell contains approximately 88 g (66 cc). There is no free or excess electrolyte in the cell, as it is all contained within the plates and separator material. The total cell weight was 890 g. Figure 32 shows a partially dismantled cell.

Terminal seals originally consisted of a silver braze joining the terminal to the ceramic insulator, and many of the early cells contained only one insulated terminal. This type of seal was susceptible to migration of the silver across the ceramic insulator, producing a short-circuit path. In order to reduce the migration of silver, two terminals were put on the cell. By using two terminals, the potential driving force across the insulator was reduced. In addition, the silver braze was replaced by a silver-copper alloy braze. These changes eliminated this failure mode. A problem was also encountered with electrolyte leakage at the ceramic-to-metal seals which was traced to three major causes: (1) differential thermal expansion between the ceramic insulator and metal cover, (2) chloride contamination after nickel plating, and (3) corrosion from water and solder flux. Changes were made to correct for these deficiencies: (1) a stress relief collar was added between the insulator and the cover; (2) chlorine contamination was

prevented by a temporary rubber seal during plating, and a chemical analysis was made to check for residual chloride; and (3) corrosion from water and solder flux was stopped by using alcohol and filling the void between the terminal post and ceramic with epoxy. Figure 33 shows a sketch of the Gulton terminal seal.

B. Cell Manufacture

The cells were purchased to TRW specification PT 3-1047, approved by JPL. The specification required that Gulton furnish a Process Identification Document (PID), which identified the manufacturing processes, procedures, and inspection documents used to manufacture the cells from receipt of raw material to shipment of the finished cell. Both TRW and JPL engineering and quality control personnel reviewed the documents. In addition, these personnel also inspected the manufacturer's facilities. After approval of the PID, no changes were allowed without approval by TRW. A TRW resident inspector was stationed at Gulton for certain mandatory customer inspection points. Complete traceability of raw material to the completed cell was also required. Figure 34 is the flow plan and summary of the PID for cell manufacture.

It is noted that there are several tests listed at the end of the flow chart which are worthy of comment. The proprietary electrical process is where the adjustment of the state of charge of negative electrodes in relation to the positive electrodes is made. Specification PT 3-1047 required that the cells contain a minimum of 5.0 Ah of uncharged active negative material and 1.7 Ah of charged active material, sometimes referred to as "pre-charge." The excess uncharged material is to prevent the cell from gassing hydrogen on overcharge; the excess charged material supposedly reduces the loss of capacity (fading) with cycling. Problems were encountered with the process and changes were incorporated with the approval of TRW. The next electrical process is a series of cycles which measure cell capacity, pressure, and voltage characteristics. The next test is destructive and measures the negative to positive material ratios noted above. A random number of cells per Mil Std 414 (Table D-1 for an AQL of 1.00) are selected and flooded with electrolyte, shorted for a minimum of 16 h, and discharged at 12 A to -1.0 V. This measures the excess negative plate capacity or precharge. The cell is overcharged in the flooded and open condition to

charge the positive and negative electrodes to their maximum capacity. The cell is again discharged at 12 A to -1.0 V. The capacity to 0.50 V is subtracted from the capacity to -1.0 V, which gives the total excess capacity available in the cell. Subtracting the value obtained in the first discharge from the value obtained in the second discharge yields the quantity of uncharged active negative material.

The remaining cells from the formation lot that passed the material ratio requirement are backfilled with a mixture of 5% helium and 95% oxygen to atmospheric pressure, and the fill tube is pinched off and welded. A Veeco mass spectrometer leak detector is used to determine the helium leak rate, which must be less than 1×10^{-7} standard cc/s. The final acceptance test is a charge retention or short test. All cells are then radiographed to show the plate alignment and detect loose particles in the free space of the cell. The major drawback to the process is that loose particles between the plates cannot be seen. The cells are dead-shortened and shipped via common carrier air freight.

C. Cell Receiving Tests and Matching

In addition to the tests performed on the cells by GI, TRW subjected the cells to a series of tests to assure proper performance and obtain data for matching the cells in a battery. Figure 35 shows the flow of the cells at TRW and lists the major operations or tests. As noted from Fig. 35, most of the operations are performed in the battery laboratory, where the cells are subjected to a series of nine tests. The leak test is performed during the condition charge, which consisted of a 1.0-A charge for 48 to 64 h on a heat sink at $23.89 \pm 1.67^\circ\text{C}$. Near the end of the charge period a phenolphthalein solution is sprayed around each cell terminal and along the cover to case welds. If a pink color is observed it is an indication of electrolyte leakage and the cell is rejected. The conditioning cycle discharge is at 12 A to 1.0 V to measure cell capacity.

Three "calibration" charge/discharge cycles are performed with the heat sink set at 18.33°C . The charge consists of a 2.40-A charge to 1.46 V, followed by a 0.65-A charge for a total of 22 ± 1 h. Any cell exceeding 1.46 V is removed from the test. The discharge is at 12 A to 1.0 V. The cells are required to deliver a minimum of 24 Ah on the first cycle and to

be within ± 1.7 Ah of the mean. The cells are required to deliver a minimum of 22 Ah to 1.10 V on the third cycle. The data is recorded on the appropriate data sheets.

The cells are shorted down and prepared for sinusoidal vibration. Up to 30 cells are vibrated at one time in each of three orthogonal axes. This was the first JPL or TRW program in which cells were vibration-tested before assembly into a battery. The vibration was as follows:

<u>Frequency, Hz</u>	<u>Level, g</u>
5 - 250	3.5
250 - 400	6.5
400 - 2000	13.0

The sweep rate is logarithmic at 1.0 octave/min, and the sweep is from low frequency to high frequency and back down to low frequency.

Following the vibration test the cells were again assembled into 6-cell packs and mounted on heat sinks set at $15.56 \pm 1.67^\circ\text{C}$ in preparation for the 30-cycle burn in test. The 30 cycles consist of the following regime: Charge at 4.80 A for 3 h; discharge at 12 A for 1 h. The voltage at the end of every fifth charge and discharge cycle is recorded on a data sheet for analysis.

The postcycle test measures the cell capacity to 1.16 V. Capacity must be above 14.6 Ah or the cell is rejected. The criteria for this test were established on other TRW programs and do not really apply to Mariner 1971 since the spacecraft is capable of operating to about 1 V per cell on the battery.

Three calibration charge/discharge cycles are run on the cells the same as before, and the cells must meet the same limits as noted on the previous calibration cycle test. The ac impedance of each cell is measured with 60 Hz current through the cell. Any cell exceeding $0.010\ \Omega$ is rejected. Electrical leakage is measured by shorting each terminal of the cell (charged) to the case through a milliammeter. The cell is rejected if any measurement greater than 0.005 A is obtained.

The charge retention test attempts to measure or determine if the cell contains internal short circuit paths between any of the plates. The

discharged cell is dead-shortened with a wire across the terminals for 8 to 16 h. The shorting wire is removed and the cell charged at 2.40 A for 6 min (0.24 Ah input). After 24 h of open-circuit stand, the cell voltage is recorded. If the measured voltage is less than 1.16 V, the cell is rejected. Cells that have passed the tests are discharged, shorted, and placed in storage for kitting and battery assembly.

Following the completion of the electrical tests, the data is accumulated and analyzed by the battery engineer to select and match the cells for each battery. All cells which have passed inspection and test criteria are candidates for assembly into batteries. All of the data is reviewed; however, the prime data used in selecting the cells is obtained from the end of the 30 cycle test and the last two calibration charge/discharge cycles. The data is punched on computer cards, and a listing of the data by cell SN is printed out as are the mean values and the standard deviation. A typical set of data for a group of cells is shown in Table 13. In addition, the computer is programmed to provide various plots of the data such as Ah in on Cycle 2 vs Cycle 3, Ah out on Cycle 2 vs Cycle 3, end-of-charge voltage on Cycle 2 vs Cycle 3, a histogram of capacity input to 1.46 V on Cycle 3, end-of-charge voltage on Cycle 3, capacity out to 1.0 V on Cycle 3, Ah out vs Ah in on Cycle 3, and Ah out vs end-of-charge voltage on Cycle 3. The prime factors in the final selection and matching of the cells for a given battery were the spread in end of charge voltage, the spread in capacity and the correlation of input to output on Cycle 3. The cells were matched to within 15 mV at end of charge and within 1 Ah on discharge.

VII. SPACECRAFT AND LABORATORY TESTS

Several tests in addition to the "routine" conditioning cycles were performed on different batteries throughout the course of the MM'71 program and are summarized herein. A Mission Simulation Test was run on two batteries (SN EM-1 and 202) in the battery lab. A Real-Time Mission Test was performed on two batteries (SN 201 and 307) in thermal vacuum chambers in the environmental laboratory. These last two batteries lag behind the flight spacecraft by two and four weeks and are duplicating the conditions on the spacecraft as nearly as possible. Special "reconditioning" tests were performed on some of the batteries to determine if it was necessary to recondition the battery before orbit insertion. Charge efficiency tests were performed within limited conditions and a flight charger/battery compatibility test was made. In addition to battery tests, a series of tests was performed on cells early in the program. Voluminous data from these tests is contained in a series of engineering memos and will not be discussed in this report.

The flight batteries were on the spacecraft for free mode test, solar thermal vacuum (STV), vibration and final systems tests. The results of these tests are discussed here.

A. Battery Handling and Safety

Early in the program there was considerable concern for safety in handling the battery from the standpoint of both hardware and personnel. An internal JPL report, Document 610-117, titled "Mariner Mars 1971 Battery Handling and Safety Procedure for Ground Operations," was prepared and issued. This document presented battery pressure limits, failure modes and their detection, charge/discharge voltage and temperature constraints, and the safety features of the spacecraft system test equipment (STE) and Launch Complex Equipment (LCE).

In addition to the handling and safety procedure, a "Cognizant Engineer Summary" accompanied each battery that was delivered to the spacecraft. The major topics covered were:

- (1) Summary of deviations from flight design.
- (2) Constraints on interface testing.

- (3) Constraints to be observed during systems tests to assure safe handling.
 - (a) Shipping-handling-storage.
 - (b) Operational constraints.
- (4) Final cleanup/fabrication work.
- (5) Special recalibration plans or efforts.
- (6) Final preparations/test before launch.

The major item in the summary was (3), which summarized the information from the handling and safety procedure and is discussed herein.

Batteries were always transported and handled according to standard JPL procedures, using an inner and outer carrying case with the battery mounted in its handling fixture. A drawing of the carrying cases and handling fixture is shown in Figure 36. The handling frame contains two shock indicators set at 35 g. A red indicator shows if the shock limit is exceeded. To prevent damage from moisture, desiccant bags are packed in the lid of the container, and a humidity indicator which turns color is an integral part of the container. Every time a battery was placed in or removed from the containers, a cognizant JPL inspector was present and verified the packing process on the equipment traveler. The inspector also sealed the outer container with a lock wire and stamp.

The battery was always stored and tested in the handling frame, and about the only time it was removed from the frame was when it was mated to the spacecraft. When not in use, the system test and flight batteries were stored in locked steel cabinets in an air conditioned room maintained below 21.1°C. The batteries were stored completely shorted. Each cell was individually shorted by means of a shorting connector attached to the cell monitoring connector, J1.

The batteries were stored shorted because (1) it is the state in which the least chemical activity occurs; (2) it reduces migration of the silver alloy braze at the terminals; and (3) it keeps the electrodes (plates) at the same relative state of charge.

Connector savers were kept on the batteries at times to prevent damage to the connectors and a mate/demate record was kept. A record was also kept of each time the battery was moved.

At four- to six-week intervals, all batteries not in use were removed from storage and given a conditioning charge-discharge cycle, shorted, and placed back in storage. These cycles reconditioned the battery by preventing morphological changes in the active material and maintained the battery in top condition. The data obtained from these periodic cycles was useful for performance analysis and provided added confidence in battery performance. The cycles were performed under uniform conditions on a temperature-controlled heat sink with the battery in its handling fixture. The tests were performed under the control of the bench test equipment discussed in Section VI. The charge consisted of a 2.0-A charge to 37.5 V then switch to trickle charge at 0.65 A for a total of 24 h, thus simulating the charge sequence on the spacecraft. The battery voltage and temperature profile was recorded along with cell voltages and the time to 37.5 V. High and low cell voltages were listed at the end of high- and low-rate charges. If battery or cell voltages and time to 37.5 V varied significantly it would provide an indication of impending problems. None were observed and battery performance was consistent.

The batteries were discharged at a constant 12-A rate until the first cell went to 1.0 V. Data similar to that of the charge cycle was recorded, and battery capacity in Ah was noted. There was no significant change in battery capacity.

Figure 37 summarizes the battery handling flow plan from the time batteries were received from the manufacturer until launch. Figure 38 shows the battery operations schedule. From Fig. 37 it can be seen that there was considerable handling of the batteries. The batteries were received at the JPL battery laboratory for receiving inspection and log book review. They were then shipped to the plastics laboratory, where they were given a final test for electrolyte leakage and cleaned. The exposed metal cell ends were conformal-coated and all terminals were encapsulated. They were then shipped to the paint laboratory for application of the temperature control paint and returned to the battery laboratory for charge/discharge calibration cycles, storage, or shipment to the spacecraft assembly facility (SAF) for mating to the spacecraft.

On previous flight programs, the flight batteries, which were silver oxide-zinc, were never placed on the spacecraft until launch operations at

the Eastern Test Range (ETR). On the MM'71 program the flight battery was placed on the spacecraft for specific system test phases to assure total system compatibility. It was felt that it was not advisable to place the flight battery on the spacecraft for all of the systems tests, since the test time was a period of about six months. The battery was placed on the spacecraft for the following test phases:

- (1) Free mode test.
- (2) Solar thermal vacuum.
- (3) Vibration and acoustics.
- (4) Final systems test at ETR.

The first three tests were run in succession and required only one mate-demate on the spacecraft.

The batteries were shipped to ETR in their containers on the same van with the spacecraft and a battery laboratory was set up at ETR. After the final systems test on the spacecraft at ETR, the batteries were returned to the laboratory for final inspection and checkout, which consisted of:

- (1) Standard 12-A discharge.
- (2) Charge retention test to assure there were no internal cell shorts.
- (3) Diode leak test.
- (4) Case leakage.
- (5) Wiring continuity.
- (6) Insulation resistance.
- (7) Visual inspection for damage and electrolyte leaks.
- (8) Charge/discharge/charge to recondition and determine if battery characteristics had changed.

The battery was returned for final mating to the spacecraft approximately one month prior to launch.

B. Battery Handling for Spacecraft Systems Tests

The use of the nickel-cadmium battery on the Mariner 1971 program placed greater demands on the spacecraft power test teams than previous programs because of the required surveillance and the extended use of the flight battery on the spacecraft. Initially, it had been planned to keep the battery on trickle charge when the spacecraft was undergoing systems test. This became impractical because it required an operator present any time

power was on. The requirements were changed and charging was required every other day. The charge scheme was to charge at high rate (2A) to the switch point and trickle charge until the battery voltage stabilized or started to drop because of battery temperature increase. Typically the charge required 3 to 4 h.

A battery operations log was maintained by the power operator whenever a battery was on the spacecraft. This log (JPL Form No. 4069 and 4070) listed the battery SN, terminal voltage, temperature, time on discharge, discharge current, charge time and current and periodic cell voltages.

Operational guidelines were provided to the personnel responsible for operation of the spacecraft to provide a reference for making decisions should battery anomalies occur and to assure the condition and safety of the battery. By following the limits established, cognizant personnel could take corrective action before an impending or existing anomaly caused catastrophic failure. Figure 39 shows battery charge voltage limits as a function as applied to the trickle charge mode since the high-rate charge was not in operation above 37.5 V. The curve also shows that the battery will not reach 37.5 V if the temperature exceeds about 25.0°C. If this occurred the operators were required to manually switch the charger to low rate when 100 ±10% of the capacity removed was restored. All charging was stopped if the temperature exceeded 32.22°C or if any cell was over 1.50 V.

The normal, alarm, and stop discharge limits were as follows:

	<u>Normal</u>	<u>Alarm</u>	<u>Stop</u>
Battery voltage	35.0 - 31.0	30.0	28.5
Cell voltage	1.35 - 1.20	1.15	1.10
Current, A	0 - 15	20	30
Temperature, °C	10 - 26.67	32.22	37.78

Since there was little or no temperature control during systems test it was requested that the battery not be discharged greater than 12 Ah.

Battery life is a function of the temperature to which it is exposed; therefore, the battery was subject to rejection for flight use if the following temperature limits were exceeded:

<u>Temperature, °C</u>	<u>Time, h</u>
43.33	Never
37.78 - 43.33	24 cumulative
32.22 - 37.78	72 cumulative
26.67 - 32.22	168 cumulative
< 26.67	∞

These temperature limits were established by engineering judgment since exact data was not available to define life as a function of temperature.

The safety guidelines established were rigidly followed by the operating personnel. Consequently, there were no batteries damaged during the extensive systems tests and no battery PFRs were generated.

C. Spacecraft Tests

Power to operate the spacecraft during test evaluation comes from three sources: (1) external power supplies, (2) solar panel simulators, and (3) battery. During a considerable portion of spacecraft systems tests power was supplied by external or solar panel simulators. Battery power was used for very limited test modes; consequently, there was not a significant amount of data generated on the battery as most of the time it was merely on trickle charge. In most instances when the battery was used, the DOD was only about 10% and did not attempt to duplicate flight conditions.

1. Free mode test. The Free Mode Test was a significant milestone for JPL/NASA and evaluated the operation of a flight-configured spacecraft similar to flight conditions. The spacecraft is powered by either the battery or solar panels exposed to the Sun. The major portion of the test was performed on solar panel power. The battery was used to supply power for only about 20 min total at the start and end of the test, and performed as expected.

2. Vibration tests. For the first time in Mariner programs, the MM'71 flight battery was included in the equipment complement of each spacecraft for the FA level vibration tests. There was some concern about this test because there was no data which indicated how much vibration the cells could withstand. It was felt that each vibration run or test would degrade the cells. (There is really no way to measure the degradation until

the cell shows signs of shorting.) The cells had already been vibrated during cell tests and the battery level FA tested. The FA vibration test on the spacecraft and the actual launch meant that the cells would be subjected to four separate vibration sequences.

A triaxial accelerometer was attached to the spacecraft structure where the battery was mounted to record as accurately as feasible the vibrational stresses imparted to the battery by the spacecraft structure. The "g" output of each axis of the accelerometer was recorded on a strip chart for the sinusoidal vibration. Random vibration test runs were not recorded. Battery terminal voltage was recorded on the same strip chart as the accelerometer readings with a common time base. All but 1.0 V of the battery voltage was bucked out on the recording equipment, and the battery voltage measuring scale was 1.0 V per 1.27 cm.

Flight spacecraft 1 (M71-1) vibration data was limited because of difficulties with facility vibration equipment. Data was obtained only for the low-frequency run, which peaks at 120 Hz. Flight spacecraft 2 (M71-2) vibration data was complete and the data from both spacecraft is shown in Table 14. There was no measurable fluctuation in battery voltage recorded during any of the vibration sweeps; however, instrument null varied ± 125 mV. The peak g levels listed in Table 14 were recorded on the spacecraft structure where the battery was mounted and occurred in the Z or thrust axis of the battery. This then meant that the greatest stress on the cells was orthogonal to the plane of the plates and would not be as damaging as if the peak g levels occurred in either of the axes parallel to the plane of the plates. It is also noted that the peak g rms output at the battery was greater than the input levels for the TA tests on the batteries; consequently, the spacecraft level vibration tests were apparently more severe than the battery level tests.

A total of nine discharge/charge cycles were put on battery SN 305 on 71-1 ranging from 0.9 to 2.4 Ah, and 16 cycles ranging from 0.8 to 4.1 Ah were put on battery SN 304 on 71-2 during vibration tests. No adverse effects were detected in battery performance.

3. Solar thermal vacuum test. The Mariner 1971 Proof Test Model (PTM or M'71-3) underwent system level testing in the JPL 25-ft (7.6-m) Space Simulator during the period of July 26 through August 8, 1970. The flight spacecraft M71-1 and M71-2 underwent system level testing in the Space Simulator in December 1970 and January 1971, respectively. The primary objectives of the tests from temperature-control point of view were:

- (1) Verify the capability of the thermal design and the flight temperature control hardware to maintain acceptable temperatures when exposed to flight environmental conditions and flight operating modes.
- (2) Obtain comparison of thermal characteristics of flight-type spacecraft.
- (3) Obtain detailed information on thermal characteristics of design to assist in temperature predictions for flight operations.
- (4) Identify design problems on PTM and verify adequacy of design modifications implemented on flight spacecraft.

Specific details of the STV test are contained in JPL Report 610-177, "Mariner Mars 1971 PTM and Flight Spacecraft Space Simulator Tests, Temperature Control Report," June 15, 1971 (an internal report). Most of the data contained herein was extracted from the temperature control report.

Table 15 is a summary of the test mode performed on the PTM spacecraft. Only modes significant for thermal data are listed, and no attempt is made to describe the various system functional verification and characterization tests performed. The two test phases were similar as far as the battery data is concerned but did affect other spacecraft components. Temperature data from bays 1 and 7 located on either side of the battery (bay 8) is shown along with the average spacecraft bay temperature to indicate effects on the battery temperature. Except as noted, the spacecraft was at thermal equilibrium at the times indicated. From the results of the PTM tests, it was concluded that thermal control of the battery was adequate, as most of the battery temperatures obtained were in the preferred operating range of 10.00 to 18.33°C.

Table 16 lists the different test modes and subsystem status along with the pertinent temperature data for the two flight spacecraft. It is noted that

in addition to monitoring the battery temperature transducer, a thermocouple was mounted at the center of the battery shear plate for additional data. (Thermocouples were also mounted adjacent to the transducers, but the data is not reported here since there was little difference in the temperatures). From the tables it is seen that the results were similar for all three spacecraft. It is seen that there was a fair amount of thermal conduction between Bays VII and VIII in that when Bay VII went from 12.78 to 20.00°C, the battery temperature increased 3.33°C. It is also noted that the ΔT between the battery transducer and the battery shearplate was 2.22 to 3.33°C, which is similar to the results obtained on batteries in the laboratory when the batteries were tested on heat sinks.

A significant item that affected battery temperature which is not shown by the tables was the interrelationship of the power source logic (PSL) voltage output (raw bus stage) and the charger output current. During the earth cruise mode tests, the PSL was set at about 39.2 V, and the low-rate charger output was only 0.1 to 0.2 A instead of about 0.615 A, which was obtained when the PSL exceeded about 44 V. This increase in charge rate increased battery heat output by about 19 W, which resulted in a battery temperature increase of about 2.78°C. Had this fact been understood early in the design phase, it would have been requested that the thermal control louvers be biased down an additional 2.78°C in order to keep the battery cooler during the greater portion of the mission. The lower temperature which would have occurred only during about the first 30 days of the mission could have been easily tolerated.

Table 17 summarizes the temperature deltas due to different test modes and power levels. The deltas are the results of one test mode subtracted from the other test mode. The sources are listed in the Mode Δ 's row. The launch transients shown in columns 1 and 2 came directly from the test data. The difference in battery temperature change during the launch transient between the spacecraft was due to the fact that M'71-1 was on internal power for 12 min, whereas M'71-2 was on internal power for an hour at an average current drain of 8.25 A. The M'71-2 battery temperature increased from 25 to 28.89°C. Under actual launch conditions, battery temperature would be lower because of the air conditioning and shroud used on the launch pad.

D. Laboratory Tests

1. Mission profile test. Battery SNs EM-1 and 202 were placed on a "Mission Profile Test" in October of 1970. The intent of the test was to evaluate battery performance by subjecting the battery to the predicted use regime of the actual MM '71 mission. Both batteries had seen considerable use in various tests in the laboratory and system tests on the spacecraft prior to the initiation of the Mission Profile Test. A test procedure was written, and the batteries were given three calibration charge/discharge cycles at 100% DOD to recondition the batteries before starting the test.

The test was performed with the computer-controlled test console. Battery temperature was controlled by mounting the batteries on thermal electric heat sinks. The thermal vacuum mounting fixtures and thermal shims were used to assure good thermal conduction between the battery and the heat sink. The test was performed in the battery laboratory in ambient air; however, the batteries were covered with lucite boxes. The thermal electric heat sinks were adjusted to obtain temperatures (measured on the battery transducer) of 12.78°C on SN EM-1 and 18.33°C on SN 202 while on trickle charge at 0.65 A. Figure 40 is a photograph of the test setup.

Both batteries were put through a prelaunch simulation of charge/discharge/charge before the launch discharge which was at 12.0 A for a total discharge of 1.490×10^6 J (13.1 Ah). Figures 41 through 44 show the voltage and temperature profiles of both batteries for the prelaunch and launch sequence. After 51 h from the start of the test, a midcourse correction discharge/recharge was performed at 12 A for a 9.3-Ah discharge. The battery voltage and temperature profiles for both batteries are shown in Figs. 45 and 46.

Figures 47 and 48 summarize battery performance throughout the test by showing periodic plots of the temperatures and terminal voltages of each battery. The events or cycles performed on each battery are noted as are test interruptions due to equipment malfunction or power outages.

It is interesting to note that the batteries performed differently during the low-rate sequences. Some of the variations in the trickle charge voltage of each of the batteries are probably due to slight changes in the trickle charge current and slight temperature variations. The major variation between the batteries is that after a discharge, battery SN EM-1 immediately

started out at a high trickle charge voltage and gradually dropped over a period of several days, whereas SN 202 did just the opposite. It started out at a low voltage and gradually increased in voltage; however, it reached a maximum voltage near 38 V at a temperature of 13°C.

After about 6 months (148 days) of trickle charge the batteries were discharged at 12 A for 1 h, simulating a second midcourse maneuver (trajectory correction). Figures 49 and 50 show the voltage and temperature profiles of each battery. There is no significant difference between the discharge curves of the batteries, but SN EM-1 is approximately 0.10 V lower than SN 202. In comparing this discharge with the previous discharges on the batteries, it is noted that the voltage drops more rapidly and is generally about 0.2 to 0.3 V lower on the second maneuver discharge than the previous discharges. This voltage degradation was the result of the 5-month trickle charge.

The orbit insertion (OI) discharge was performed following an additional month of trickle charge. However, it was decided to perform a reconditioning discharge on one of the batteries. (A discussion covering reconditioning is covered in Section VII-D-5.) The reconditioning cycle was performed on SN 202 and consisted of a 24-h discharge through a 52-Ω load followed by a standard recharge. Battery temperature and voltage for the cycle are shown in Fig. 51. The orbit insertion (OI) discharge was performed on the battery 48 h after the initiation of the reconditioning cycle. The OI discharge was at 9.0 A until the first cell in the battery dropped to 1.0 V. The 100% DOD was performed on the battery to determine if its characteristics were degraded. Figure 52 shows the discharge/recharge data. The battery yielded 28.8 Ah (3.225×10^6 J) and showed a slight voltage degradation.

Battery SN EM-1, which did not receive a recondition cycle, was discharged the same as SN 202 for the OI discharge to determine its characteristics. The data is shown in Fig. 53, and it can be seen that there was little apparent degradation.

Following the OI discharges the batteries were subjected to a series of orbit trim maneuver (OTM) discharge/recharge cycles. The first OTM cycle was performed 24 h after the OI cycle and consisted of a 9.0 A discharge to 100% DOD. During the actual mission the OTM was expected to require only 1 h, but the laboratory test was made to determine the effect

of the OI discharge on the OTM discharge. The results of the OTM cycles for both batteries are shown in Figs. 54 and 55, and it can be seen that the discharge voltage characteristics improved. Three more OTM cycles were performed on the batteries at approximately 30-day intervals. These three cycles were at 9.0 A for 1 h followed by the standard recharge, and no significant differences in battery characteristics were noted.

a. Extended Mission A. The mission design, as noted previously, was for 90 days in orbit to map Mars. There was, however, the possibility that the mission would be extended to obtain additional science data; therefore, testing was continued. At the end of approximately 140 days in orbit, the spacecraft would be occulted from the Sun by Mars, and power would be required from the battery on every orbit for approximately 135 orbits. Based on early estimations of occultation periods and spacecraft power requirements, a simulated extended mission test was performed on batteries SNs EM-1 and 202.

After 134 days from the OT discharge the batteries began the 12-h cycle regime which was the period for one revolution around Mars by the spacecraft. Figure 56 shows how the length of discharge time (occultation period) was varied with cycle. In the actual mission, the occultation period will follow a smooth curve, but for test convenience the periods were stair-stepped. The capacities removed from the batteries at each cycle interval are also shown. The batteries were discharged at 7.0 A on each cycle based on an estimated load of 180 W; therefore, the test was set up to slightly overtest the batteries. Battery SN 202 was recharged in the standard mode following each discharge, but SN EM-1 was charged only at the 2-A rate to 37.5 V and left on open circuit until the next discharge cycles.

Figures 57 and 58 show plots of the end of discharge voltage and temperature as a function of cycle for each battery. It is noted that SN 202 dropped to 31.1 V at the maximum DOD of 11.7 Ah, whereas SN EM-1 dropped to about 30.1 V. Figures 59, 60, and 61 show discharge/recharge plots of the battery data for cycles at the start, middle, and end of the test. The effect of no trickle charge on battery SN EM-1 is clearly evident in that its voltage degradation is greater than SN 202.

After the last cycle, both batteries were discharged at 12 A to 100% DOD until the first cell reached 1.0 V. The results are shown in Fig. 62

and were quite surprising in that SN EM-1 yielded only 12.75 Ah while SN 202 yielded 28.4 Ah. Also the discharge curve of SN 202 had a partial second plateau during about the last 25 min (5 Ah) of discharge. It is also noted that the cells were evenly matched since the "cutoff" occurred at 26.3 V, which is when the first cell reached 1.0 V. It is difficult to account for the "tailoff" of the discharge curve. It can hardly be attributed to a "memory effect" because the depth of discharge varied from only 3.5 to 11.8 Ah while the tailoff occurred beyond 23 Ah. It is interesting to note that the 5 Ah obtained during the tailoff is about equivalent to the quantity of low-rate charge. As previously seen, discharges after long periods of continuous trickle charge did not produce such a deviation in the discharge curve. It is therefore concluded that the effect was the result of recharge scheme during the cycle regime. The battery is never fully recharged at the high rate and is dependent on low-rate charge for full recharge. This is evident from the results obtained on SN EM-1, which was never trickle charged. It is theorized that the repetitive "topping off" of the battery in low rate without deep discharges produces crystalline changes in the electrodes which essentially result in a net increase of the internal electrochemical impedance of the cell. This effect is also evident from the end of charge voltages shown in Figs. 59, 60, and 61, where the voltage increased from 37.20 at cycle 5 to 38.25 V at cycle 125. It is further theorized that the effect might be negated if the battery was overcharged slightly in high rate before switching to trickle charge.

In reviewing the cycle data of the batteries, it was found that after the first few cycles the capacity returned at 2.0 A was relatively consistent but different for each battery. Battery SN 202 recharge was approximately 0.2 to 0.4 Ah less than discharge capacity removed, while SN EM-1 was 0.8 to 1.0 Ah more than the discharge capacity removed. The difference probably represents the capacity lost by SN EM-1 while on open circuit between the end of charge and start of discharge.

b. Extended Mission B. After completing the Extended Mission A test, the batteries were left on trickle charge for 71 days before initiation of Extended Mission B test. By this time the spacecraft power system engineers had better estimates on the required spacecraft power level during the Sun occultation, and the revised estimated power requirement was 300 W or approximately 120 W greater than estimated for Extended Mission A

test. This difference was considered significant enough to retest the extended mission phase of the test. Consequently, Extended Mission B test was set up. It was decided that the B test should be a worst case test which would test the batteries to near their maximum capabilities. The cycling regime simulating the occultation was similar to the first test. However, the batteries were discharged at a constant current of 10 A, and the maximum discharge time went to 120 min. The standard charge procedure of high-rate charge to 37.5 V followed by low rate until the start of discharge was used on both batteries. The batteries were not given a conditioning cycle prior to start of cycling.

Figure 63 shows the step-wise discharges as a function of the cycle and the capacity removed for each cycle. Figures 64 and 65 show plots of the end of discharge voltage and the minimum and maximum temperatures during cycling for each battery. No problems were encountered with battery SN 202. It went through the five 20-Ah discharge cycles even though the maximum possible recharge was 20 Ah. The recharge, of course, is not 100% efficient; therefore, the battery had enough reserve capacity to survive the five deep cycles without fully recharging.

Battery SN EM-1 performed fairly well up through cycle 60. However, when the discharge time was increased from 90 to 100 min, the end of discharge voltage dropped about 1.2 V to 28.5 V and remained near that level. On cycle 66 the battery temperature was lowered about 5.5°C to determine if this would improve battery performance, but there was no improvement. On cycle 71 the discharge time was increased to 110 min, and the battery was automatically taken off of discharge at 105 min when its voltage dropped to 27.0 and one cell was at 0.978 V. (The battery safety stop device had been set at 26.0 V on the battery and 1.0 V on any cell). The safety stop settings were readjusted to 23.0 V on the battery and 0.5 V on any cell. The test was continued. In addition, the 37.5-V setting for switching to low-rate charge was negated on battery SN EM-1 so it would stay in continuous high-rate charge. This improved battery performance and its end-of-discharge voltage increased from 28.03 V on cycle 72 to 29.0 V on cycle 75.

The discharge time was increased to 120 min on cycle 76 and end-of-discharge voltage dropped to 26.86 V. On cycle 78 the battery was automatically removed from discharge at 119 min due to low voltage. Battery

voltage was 24.77 V and the lowest cell was 0.65 V. The highest cell was 1.04 V, and the average cell voltage was 0.955 V. On cycles 79 and 80 the battery discharge was stopped at 115 and 111 min respectively. The discharge time was dropped to 110 min at cycle 81. From this point on, battery SN EM-1 was able to support the discharge, and by cycle 83 the end-of-discharge voltage rose to 29.98 V. At the start of cycle 84, SN EM-1 was placed back on the standard charge regime. However, end-of-discharge voltages began to drop and the battery was put back on continuous high-rate charge for cycles 87 through 91. As can be noted in Fig. 65, the end-of-discharge voltage improved and no further problems were encountered.

Before the start of the test it was thought the gradually increasing depth of discharge on SN EM-1 would recondition it. This in fact did occur. However, the test was quite severe since it required reserve capacity during the 20-Ah discharge cycles. If the step function of the discharges had been smoother (as in the actual mission) it is possible SN EM-1 might have passed the test.

One might have expected that the continuous low rate charge between Extended Mission Tests A and B would have also increased the capacity of the battery. This apparently was not the case and the reason for not doing so is not obvious. Many people would refer to this apparent loss of capacity (or lack of understanding) as the "memory effect." The tests do point out that it is important how the battery is managed, as this condition was apparently caused by not low-rate-charging during the previous cycling test.

Figures 66 through 71 show computer plots of the data for various discharge/charge cycles during the test. The center plot of each figure shows the spread in voltage between the highest and the lowest cell in the battery. It is pointed out, however, that each plot does not necessarily represent the same cells each time. Also, due to the wiring of SN EM-1 there is IR drop on cell 13 of approximately 0.003 - 0.010 V on low- and high-rate charge and 0.070 V on discharge, which accounts for the large spread in the high and low cells.

At the end of the cycling regime, both batteries were discharged completely to measure the available capacity and observe the voltage characteristics. Figures 72 and 73 show the data. SN EM-1 delivered 23.5 Ah, and SN 202 delivered 28.9 Ah to a cutoff of 25 V. The voltages of both batteries

were similar and somewhat degraded from a "fresh" battery. It is also noted that about the last 25% of the voltage curve tails off rather slowly; whereas on a fresh or reconditioned battery the voltage drops more abruptly. The capacities of the batteries were nearly the same as when they were new.

The tailoff of the discharge voltage points out an important factor to keep in mind when designing a battery. If possible, the battery and power system should be designed to operate down to an average of at least 1.0 V per cell. This allows one to operate deeper into the battery and effectively increases the energy density of the battery. Many satellite power systems are designed to operate down to an average of only 1.15 V per cell. If this were the situation in this instance it would reduce the available battery capacity to 16.6 and 18.2 Ah on SNs EM-1 and 202, respectively, or a loss of approximately 25%, which is a considerable price to pay for not adding two additional cells.

The batteries were recharged and placed back on low rate (trickle) charge for continued life tests.

2. Real-time mission tests. In addition to the mission profile tests in the battery lab, it was decided that two batteries should be subjected to test in thermal vacuum chambers. This test was to simulate the operation of the Mariner 9 flight battery as nearly as possible; hence the name Real-Time Mission Test. Batteries SNs 202 and 307 were selected for the test. Battery SN 202 was a qualification battery that was subjected to TA testing, whereas SN 307 was similar to the flight battery but had not been FA-tested.

A new test system that was semiautomatic was assembled at JPL to control and monitor the batteries. The system contained safety stop devices for battery and cell undervoltage and overvoltage limits and battery temperature limits. Voltage, current, and temperature measurements were made with a DVM and outputted on paper tape under control of a programmable digital clock. The system was capable of automatically switching the battery from high-rate charge to low rate but could not automatically switch from low to high, which became a problem during cycling. The system also contained a constant power discharge unit which more closely simulated

battery discharge on the spacecraft; however, it was programmable only in steps of 25 W.

Test Procedure MPT-342-M71 presents the details of the test. Each battery was mounted on a heat sink like that used for TA and FA testing, instrumented, and placed in a separate vacuum chamber in the JPL Environmental Sciences Laboratory. Figures 74 and 75 show the test setup. Before closing the vacuum chambers, the batteries were charged for 3 h at $18.35 \pm 2.78^\circ\text{C}$ and discharged for 1 h at about 290 W and recharged. The chamber was closed and evacuated to 10^{-4} mm Hg or less. During the pumpdown, the same launch sequence as performed on the spacecraft was initiated. Battery SN 201 was placed on test approximately two weeks after launch and SN 307 was four weeks behind the spacecraft.

Figures 76 and 77 show battery voltage, temperature, and loads during the simulated launch sequence for each of the batteries. In general, the performances of both batteries compare quite well with each other and with the flight battery. The voltage of SN 201 was about 1 V higher during the initial charge and from 0.2 to 0.3 V higher during the launch discharge. The discharge of the flight battery was nearly identical to that of SN 307. The largest discrepancy was the temperature rise during discharge. The rise in temperature of the flight battery was about one-half that of the test batteries. A possible explanation for the difference is that the spacecraft cooled down much more rapidly in space than the response time of the test setup.

Figures 78 and 79 show the battery voltage, current, and temperature of the test batteries during the simulated cruise period. Also noted in the figures are events where problems such as power failures occurred. In general, the data is comparable to the flight battery. The voltage of SN 307 was very close to that of the flight battery. However, the voltage of SN 201 gradually decayed to about 1 V below the flight battery. It is also noted that each time the test was interrupted the voltage rose and gradually decayed. A similar occurrence was noted on one of the mission profile test batteries. The reason for this phenomenon is not known and should be investigated.

Shortly before Mariner 9 was scheduled to be placed in Mars orbit, a simulated orbit insertion (OI) discharge was performed on SN 307 to determine if the flight battery should be reconditioned. Reconditioning is discussed

in Section VII-D-3. All previous testing had included discharges during the cruise period simulating trajectory correction maneuvers (TCM). However, Mariner 9 TCMs did not require battery power. It was thought that these TCM discharges might have "reconditioned" the battery. The worst case OI discharge was estimated to be 335 W for 1 h. Figure 80 shows the results of the OI discharge on SN 307 along with the predicted voltage band based on prior tests. Figure 81 compares the OI and launch discharge voltages of SN 307. The voltage difference was considered insignificant, taking the difference in loads into account. Considering the facts that the battery voltage was in the middle predicted voltage band and that OI discharge was close to the launch discharge, it was concluded that it was not necessary to attempt to recondition the flight battery.

From this time on, tests on SN 307 preceded the spacecraft battery operation. However, SN 201 continued to follow the flight battery in near-real-time.

Figures 82 and 83 show the results of the simulated orbit trim discharges on battery SN 307. It is noted that the test system failed to switch the battery from high- to low-rate charge. Voltage levels (considering differences between the test load and the actual) and temperature responses were similar on both SN 307 and the flight battery. The results obtained on SN 201 were also in fair agreement, as can be noted in Figs. 84, 85, and 86. After 36 days from OI, the sun occultation phase or cycling regime was initiated on SN 307. Figure 87 shows the predicted occultation time as a function of calendar day and cycle number. The dashed line shows the actual test time on discharge as a function of the cycle number and was a step function rather than the smooth curve. The discharge cycles were at a constant power load of 290 W. The charge regime was changed to more nearly match that of the spacecraft in that the battery was initially charged for 41 min at low rate then switched to high rate. This mode of operation was required on the spacecraft because of power limitations of the solar panels.

Figure 88 summarizes the results of the Sun occultation test by showing battery end-of-discharge voltage and the temperature of the battery as a function of cycle. This data is very close to the data obtained on the flight battery, particularly the temperature performance during maximum discharge times. There was less than 1°C difference. Figures 89, 90, and 91

show the battery data for three randomly selected discharge/charge cycles during the test. It can be noted that as the battery was cycled there was a gradual improvement in battery discharge voltage.

The average discharge current was about 9.5 A during the constant power discharge. Therefore, one can calculate the Ah removed each cycle. The maximum discharge was 15.1 Ah or 77.5% depth of discharge (DOD) based on the rated capacity of the battery. The battery is presently on test, simulating a possible postoccultation operation. It is being discharged at 2.0 A for 9 h twice a week. This simulates a possible solar panel/battery share mode during data playback maneuvers. This test will continue for about two months.

Battery SN 201 is presently in the middle of its occultation test and the data has not been reduced at present. A cursory look at the raw data indicates that the battery is performing normally.

3. Reconditioning tests. The results of tests performed to determine the need for reconditioning the Mariner 9 battery are summarized here. The possibility of the need for reconditioning resulted from preliminary design consideration discussions with TRW. TRW indicated it would be necessary to recondition the battery before the orbit insertion (OI) discharge after about six months of trickle charge. Their recommendation was based on internal data which showed that a second voltage plateau of about 1.0 V per cell would appear during discharge. Several other battery users, manufacturers, and NASA Goddard were questioned. None of them had factual data to support TRW's position. Four separate tests were performed to determine the necessity for reconditioning the battery.

a. Cell tests. The initial test was performed by TRW under a separate contract early in the battery design phase of the MM '71 program. Gulton Industries and General Electric Co. 15 Ah-cells were tested, seven from each supplier. The cells were relatively new and the only tests reported performed on the cells prior to the test for JPL were those listed in Table 18, which was taken from the TRW report. It is noted in the table that the cells were placed directly on trickle charge from the shorted state at ambient room temperature. The trickle charge rate was not reported, but in private communications with Dr. W. Scott and Mr. C. Bancroft of

TRW it was stated that the rate was probably C/40. It was further stated that TRW usually recharged the cells before placing them on trickle charge storage. At room ambient it is possible that cell temperatures of 30°C were obtained.

The cells were discharged at 10 A to 0.8 V on a heat sink set at 23.9°C after approximately six months' trickle charge, recharged, and given a second discharge. Typical results on the cells are shown in Fig. 92, which was taken from TRW's report. The second voltage plateau is seen at about 1.03 V per cell (equivalent to 26.8 V on the Mariner 1971 battery). On the following discharge cycle it is seen that the second voltage plateau is not present and the cell voltage is about 0.025 V higher than the initial discharge voltage, or equivalent to 0.65 V on the Mariner 1971 battery. It is also noted that the initial discharge yielded greater capacity than the second discharge. As will be seen later, a second plateau has not been observed on any JPL trickle charge test, but voltage degradation equivalent to about 0.65 V was observed.

Mission simulation tests were run on 5-cell packs of 20-Ah cells. The detailed results of the tests are documented in JPL Engineering Memo 342-106, February 25, 1970 (a JPL internal document). Basically, the results showed that if the cells are operated within the temperature range of 10 to 21°C (measured between cells) it was not necessary to recondition them. No indication of a second voltage plateau was seen in a 70% DOD (14 Ah) of the cells simulating the orbit insertion discharge. The discharge represented an equivalent 1.62×10^6 J on the Mariner 1971 battery, which was greater than the expected energy requirement for orbit insertion.

Cells operated continuously in a temperature range of 24 to 35°C began to show degradation and the beginning of a very slight second voltage plateau when discharged to 70% DOD. There was, however, sufficient capacity available to meet the requirements for the OI discharge and the following OT discharges. In retrospect, it would have been interesting if the cells had been discharged completely to determine the extent of the lower voltage plateau. However, the object of the test, which was to determine if the mission simulation test could be performed without reconditioning, was realized.

b. Mission Profile Test. Two Mariner 1971 batteries, SN EM-1 and 202, were subjected to a test profile predicted for the mission. The test regime and results for these batteries were discussed previously. In summary, both batteries were subjected to prelaunch, launch, and two mid-course correction discharges varying from 46 to 65% DOD before the insertion discharge. Battery SN EM-1 was discharged completely for the OI discharge, whereas SN 202 was given a "recondition" discharge by discharging it through a 52- Ω load for 24 h, which removed 13.6 Ah. SN 202 was given the standard recharge for 24 h, then discharged completely for the OI simulation. Within 24 h of OI, both batteries were again completely discharged, simulating the first orbit trim. The results of the reconditioning, OT, and OI discharges are compared in Figs. 93, 94, and 95.

Figure 96 compares the OI discharge voltages of both batteries, and it is seen that there is no appreciable difference in their performance. The voltage of SN EM-1 is about 0.25 V lower than SN 202 and is due primarily to the difference in the original characteristics of the batteries. It is noted, however, that there is a slight change in the slopes of the voltage curves after 1.5 h. This slight change was probably the result of the previous cycles on the batteries. However, there is no significant second plateau suggested by the TRW cell tests.

Figures 94 and 95 compare the OI and OT discharges of each battery. The effect of the "reconditioning" cycle on SN 202 is discernible but insignificant. Reconditioning decreased the voltage degradation of the battery by about only 0.25 V during the first 40% of the discharge. It is evident from the figures that the OI discharge "reconditioned" the batteries for the OT discharges and that the OT voltages were about 0.5 to 0.6 V higher than the OI voltages. It is interesting to note that in both instances the batteries delivered about one Ah more capacity on the OI discharge than the OT discharge, and as a result also delivered more energy despite the voltage loss.

It was concluded from this test that it was not necessary to recondition the flight battery since the slight voltage degradation was well within the system capability. However, the final decision was based on the results of the Real-Time Mission Test batteries. On the actual mission the battery was not used for the trajectory corrections because they were so slight. Consequently, the previous test results did not duplicate the real mission.

c. Real-time mission test. Batteries SN 201 and 307 were put on test following the launch of the Mariner 9 spacecraft. Flight conditions were simulated as nearly as possible by testing the batteries in thermal vacuum chambers and subjecting them to the same discharge/charge regimes as expected on the spacecraft. Previous batteries were discharged at constant current while these batteries were discharged at constant power loads similar to the spacecraft.

Approximately two weeks before the OI of Mariner 9, Battery SN 307 was discharged at a power level of 346 W. This battery was on continuous trickle charge at 0.615 A for 5 months, whereas the flight battery was on trickle charge for 6 months. The 1-month difference was not considered significant. Before the test was run, a predicted voltage band was established based on the results of the Mission Profile Test. The discharge voltage of SN 307 was in the middle of the predicted voltage band, as shown in Fig. 97. Also shown is that near the end of discharge the load was reduced in incremental steps from 346 to 265 W. This was done to obtain some measure of voltage characteristics of a function of load. The 265-W load represents a load similar to that of the upper voltage band (approx. 280 W), which was a 9.0-A constant-current discharge on SN EM-1.

If the discharge would have been continued at 265 W it appears that the battery voltage would have crossed over the top of the predicted voltage band, indicating that the 5 months' continuous trickle charge produced very little voltage degradation in battery SN 307. Figure 97 compares the launch discharge to OI discharge voltages of SN 307. Even though the two discharges were at different power levels, the data provides a means of making a rough estimate of the voltage degradation due to the trickle charge period. From the curves it is seen that OI voltage is approximately 0.55 V lower than the launch voltage, but the power Δ is 58 W. By dividing the voltage Δ s by the power Δ s obtained from the discharge curves, the following values are obtained:

From 346 to 322 W	$\frac{0.15 \Delta V}{24 \Delta W} = 0.006 \text{ V/W}$
From 322 to 265 W	$\frac{0.30 \Delta V}{43 \Delta W} = 0.007 \text{ V/W}$
From 288 to 230 W	$\frac{0.30 \Delta V}{58 \Delta W} = 0.005 \text{ V/W}$

The average change in voltage with power is then 0.006 V/W.
Therefore,

$$(346 \text{ W} - 288 \text{ W}) 0.057 \text{ V/W} = 0.348 \text{ V}$$

gives the expected voltage difference between the launch discharge (288 W) and the OI discharge (346 W). However, the actual difference was 0.55 V. Therefore,

$$0.55 \text{ V} - 0.35 \text{ V} = 0.20 \text{ V}$$

which gives the value of the voltage degradation due to the trickle charge period.

From the results of this final test, it was concluded that it was not necessary to perform a recondition cycle on the flight battery before OI.

4. Charge efficiency tests. A total of 19 cycles were put on battery SN 306 to characterize the charge efficiency of the MM 1971 battery. To completely characterize battery charge efficiency would require several more cycles, but the data generated was sufficient to estimate the charge efficiency of the Mariner 9 battery over its expected operating temperature range. The term percent charge efficiency as used herein is the quantity removed (Ah or Wh), divided by the quantity put in times 100, or

$$\frac{\text{Ah out}}{\text{Ah in}} \times 100 = \text{percent charge efficiency}$$

The state of charge affects the charge efficiency; i.e., as the state of charge approaches 100%, the charge efficiency drops off rapidly to near zero. This sounds simple enough. However, the terminology "100% state of charge," as generally used is a variable because the capacity of the battery is variable with charge temperature and charge current. Therefore, for this discussion "100% state of charge" shall be defined as 20 Ah, which is the manufacturer's rated capacity of the cells in the battery. Under optimum conditions the MM '71 battery is capable of yielding a capacity of 25 to 27 Ah at a 12-A discharge rate.

The computer-controlled battery bench test set was used for these tests. All tests were performed on battery SN 306. The calculated energy input and output on each test run were from the output of the test system. All charges were at constant current, using rates of approximately 0.65, 2.0, and 4.0 A. Battery temperature was controlled via a water-cooled baseplate upon which the battery was placed. The battery was covered with aluminum foil and enclosed with a plexiglass cover. Temperature measurements were made using the battery temperature transducers. All discharges of the battery were at a constant current of approximately 12 A. The discharge was terminated when one cell reached 1.0 V.

Table 19 lists the results of each test run and the date each test was started. The three test runs at the bottom of Table 19 were not part of the charge efficiency tests but are listed to show the results of a standard charge procedure used on the MM '71 program. The charge performed on July 12, 1971, was after the battery had been completely shorted to zero volts. The charge consisted of a 2.0-A charge to 37.4 V, then a switch to 0.65 A for a total charge time of 24 h. It is seen that the following discharge yields 27.4 Ah, which is about the maximum capacity ever obtained from this battery. The two cycles performed on August 15 and 16, 1971, show the results of similar charges after the charge efficiency tests were run, except that the battery had not been shorted to zero volts. These two cycles show the battery to have a maximum capacity of about 25 Ah, or the battery lost 2 Ah during this test regime. If the battery had been shorted and given a standard recondition cycle it would recover to 27+ Ah. This points out another fact that makes charge efficiency data difficult to reproduce and predict with exactness. That is, the age and prior use of the battery affect the charge efficiency. This effect can be seen by scanning the data in Table 19. For example, the 2.0-A charge performed on July 15, 1971, at about 10°C with an input of 27.3 Ah produced a charge efficiency of 95.3%; whereas on August 10, 1971, after 12 cycles, a 2.0-A charge at about the same temperatures to only a 14.1-Ah input gave a charge efficiency of only 93%. Other anomalies such as this can be noted in the table.

Figure 98 shows the estimated charge efficiency as a function of the state of charge for the C/10 charge rate at 10 and 25°C. These curves were interpolated from the data in Table 19. The data is insufficient for plots at

other charge rates and temperatures. As far as the MM '71 battery is concerned, the charge efficiency data is somewhat academic because of the charge scheme used. The MM '71 charge consists of a 2.0-A charge to 37.4 ± 0.1 V, then a switch to trickle charge or 0.65 A; and in most instances the battery is only discharged 50% or less. Experience has shown that, in general, the Ah input before the switchpoint is about equal to the Ah removed during the discharge. One can, therefore, estimate the time on high-rate charge by dividing Ah out by 2 A to obtain the time of high-rate charge. The charge efficiency to the switchpoint is estimated to be about 95% in a temperature range of 10 to 25°C, and the battery can be considered to be fully charged at this time. It will be recalled that full charge was defined as 20 Ah. This, of course, only holds true over a few cycles, as repetitive cycling would gradually run the battery down. In the standard mode of operation the battery will be on low-rate charge for several hours before the next discharge, and the battery capacity will be at least 25 Ah or at 125% state of charge. Figures 99 through 107 show plots of the battery voltage and temperature for most of the test runs. Further tests are required to estimate the instantaneous charge efficiency at the 0.065-A charge rate and at other temperatures.

5. Charger interface tests. A series of tests were performed to evaluate the battery and the chargers as a system to determine if there would be a problem of charging the battery near Earth after launch when solar panel voltage is low. The MM '71 charge scheme consisted of two separate chargers in one module that were designed to charge the battery at two different constant current rates: a high rate of 2.0 ± 0.1 A and a low rate of 0.65 ± 0.15 A. The charge system was designed to switch from the high-rate charger to the low-rate charger when the battery terminal voltage reached 37.5 ± 0.3 V.

The high-rate charger specification called for a 4.0-V minimum differential between the PSL voltage output and the battery terminal voltage in order to obtain the maximum output of 2.0 ± 0.1 A. A minimum differential of 5.0 V was required to obtain the maximum low-rate charge current of 0.65 ± 0.15 A.

Battery SN 202, which was a type approval test battery, was used for all charge tests. The 4A12 charger used was the engineering breadboard

unit. The engineering model 4A16 inverter was used to supply the 2.4 KHz to the charger. The PSL or raw power was simulated with a 0 to 160 V NJE Model SS1603 constant voltage power supply. A support equipment command switch box was used to simulate commands to the charger. The 2.4 KHz was driven by a Lambda LH128AFM power supply. The +30-V power to the charger/command and overvoltage sense circuit was supplied by a Harrison Laboratory 814A regulated power supply.

Three voltage levels (39.2, 40.2, and 41.2 V) simulating the PSL output voltage to the charger were investigated. The pertinent data was recorded on the NLS MM '71 bench test system. Connections to the battery from the charger were made through a battery breakout box. A 2.5-A, 50-mV shunt was placed in the charge line to record the charger output current.

The charger was operated in ambient air in the battery lab. The temperature of the battery was controlled and maintained by a temperature-controlled heat sink. The temperature of the battery was recorded on the NLS system as measured by the battery temperature transducers MT-1 and MT-2.

For most of the test runs, launch conditions were simulated in that the battery was discharged at 9.5 A for 1 h, and the charge was initiated at the low rate for 20 min before switching to the high-rate mode. This procedure was followed because it is necessary to launch in the low-rate mode, and 20 min is the expected maximum time after Sun acquisition before the charger can be commanded to high rate.

A total of 12 charge/discharge cycles were put on the battery during this series of tests. The battery was reconditioned before initiating the tests. Table 20 summarizes the data obtained from the test. The first four test runs are not included because they involved charger command problems and experimentation with the test setup.

From Table 20 it is seen that test runs 2, 7, and 10 were performed with a 41.2 V input to the charger. The battery temperatures were 12.78, 20.56, and 8.33°C during each of the respective runs. In all instances the maximum high-rate charge current was obtained as was the maximum low rate current of 0.50 A. It is also interesting to note that the Ah input at

high-rate charge was 8.39, 8.74, and 10.34 Ah at 8.33, 12.78 and 20.56° C, respectively. Since 9.5 Ah was removed on the discharges preceding the charges it was evident that the battery was capable of accepting near full charge at the high rate.

Test runs 1, 5, 6, 9, and 12 were performed with an input of 40.2 V. In all instances, the high-rate charge current remained near the maximum 2-A level. However, the low-rate charge current varied from a low of 0.35 A to the maximum of 0.50 A. Figure 108 shows a plot of the battery data obtained on test run 9. The variation in the low-rate charger output was due to the change in counter EMF of the battery at the different test temperatures. On test runs 6 and 9 it is seen that the Ah input to the switchpoint agrees with the test data at the 41.2-V input level at 21.11 and 8.33° C. The reason for the differences on runs 1 and 12 is that the battery was discharged at greater depths. Prior to run 12, the battery was discharged completely (until the first cell reached 1.0 V), and the battery delivered 27.8 Ah.

From Table 20 it is seen that 26.8 Ah was returned at the high rate, which indicates the battery was nearly fully charged at high rate even at a low temperature of 7.22° C.

On run 9 the switchpoint from high to low rate was not obtained because the temperature was approximately 23.89 to 26.67° C at the time the battery was approaching full charge. In this temperature the terminal voltage of the battery will not rise above 37.5 V. When it was observed that the 37.5 V switchpoint was not reached due to the battery temperature, the charge was commanded to low rate.

Test runs 3, 4, 8, and 11 were made with the charger input voltage set at 39.2 V and the battery temperature ranging from 8.33 to 21.11° C. As noted in Table 20, the automatic switch from high- to low-rate charge occurred during only one of the four test runs. The switchover occurred only when the battery was charged at the low temperature. At the time of the switchover, the charge rate had declined to 0.75 A because the ΔV between the battery and the charger input voltage was insufficient to yield full-high-rate charge. In effect, then, if the ΔV is not great enough the battery is "taper charged," or as the battery voltage increases the charge current decreases.

At higher temperatures the charge current decreases more rapidly than the battery voltage increases. Consequently, the 37.5-V switchpoint is not reached. This is to the system's advantage (in a low-input voltage situation) in that a higher charge current is available because the ΔV required to drive the high-rate charger is less than the ΔV required to drive the low-rate charger. It is, therefore, better to stay in the high-rate charge mode. Figures 109 and 110 show plots of the battery voltage, temperature, and charge current for test runs 3 and 11, and illustrate the taper charge effect. Figure 110 shows the case where the switch voltage was reached when the battery temperature was at near 11.11°C.

Figure 109 shows a case in which the charger did not have the capability of driving the battery voltage high enough to reach the switchpoint with the battery temperature near 13.89°C. The effect of the rising battery voltage on the charger output current can also be seen in the figures. The data from these runs enabled one to determine the high-rate charger current characteristics as a function of the ΔV between the battery and the input voltage, which is shown in Figure 111. It is seen that 90% of the maximum charge output, 1.8 A, is obtained at a differential voltage of only 2.5 V. However, the output current drops off rapidly and is zero at about 1.3 V. Sufficient data was not obtained at the voltage input levels tested to plot the low-rate charger characteristics. Therefore, after the last test run, the input voltage to the low-rate charger was incrementally increased to determine the maximum ΔV required to drive the charger to its maximum output. The results are shown in Fig. 112. It is seen that the maximum charger output was about 0.55 A, which was obtained near the differential of 5 V. It is also seen that the knee of the curve is near 3 V differential and that sufficient low-rate charge current, approximately 0.45 A, can be obtained 2.0 V below the charger specification.

From these tests it was concluded that there should not be any problem in fully charging the battery after launch even with the worst case PSL voltage of 39.2 V. Since each charger was apt to have different characteristics, it was recommended that the characteristic of each flight charger be determined by the power conditioning group. As will be seen in Section VIII, there was not sufficient input voltage to the Mariner 9 low-rate charger near Earth for maximum output.

It is interesting to note during this series of tests, which consisted of only 12 cycles, that the battery discharge voltage gradually degraded. The degradation from the first to the twelfth cycle was about 1 V. However, there was no appreciable change in capacity, 27.8 vs 27.4 Ah. Owing to the differing charge conditions it was not possible to determine if the charge voltage characteristics changed.

VIII. FLIGHT BATTERY PERFORMANCE

This section discusses the flight performance of the Mariner 9 battery and compares the flight data with the test data. As of this report, Mariner 9 has just completed the Sun occultation phase of the extended mission, and plans for additional science data measurements are being made to continue until February, 1973. Owing to decreased solar panel power and the need to point the antenna back to Earth for data playback, there will be periodic share modes with the battery. These playback share modes are expected to draw 18 Ah out of the battery. The continued use and performance of the battery will be covered in a supplemental report.

A. Launch and Cruise

The initial design requirements required that the battery supply spacecraft power during launch and for two possible trajectory corrections during cruise to Mars. As it turned out, the trajectory corrections or midcourse trims did not require the orientation of the spacecraft to turn the solar panels off the Sun line; consequently, battery power was not required.

At least two relatively deep discharges (8 Ah) were performed on the battery prior to launch. These were performed during the Joint Flight Acceptance Composite Test (JFACT) and the Precountdown Test. These discharges simulated the launch discharge on the battery and also tended to recondition the battery. Figure 113 shows the results of the JFACT discharges of the batteries on the MM'71-1 and MM'71-2 spacecraft.

Spacecraft MM'71-1 was launched on May 8, 1971; however, at about 7 min into the launch, data from the spacecraft was lost because the launch vehicle went out of control. The failure was traced to the failure of the guidance control system in the Centaur stage of the Atlas/Centaur launch vehicle. Figure 114 shows the battery performance data up to the time of data outage.

Spacecraft MM'71-2 was successfully launched on May 30, 1971. Figure 115 shows the battery performance data for the launch. There was a 6-min hold, and the total battery capacity used for launch was 8.76 Ah. The Sun was acquired so rapidly that there was no evidence of the solar panel and battery share. The data that was obtained for both launch sequences compares

quite favorably. No unusual occurrences or anomalies were observed in the battery data.

Temperature control was excellent and was near prediction. Prior to switching to internal power at T-9, the temperature was 18.3°C (65°F) and rose to a maximum of only 19.6°C (67.7°F) during the 1 h and 4 min of launch discharge. Since no heat is evolved during recharge, the battery temperature dropped to 10.8°C (51.5°F) in 3.5 h and remained there until it was near full charge. From Fig. 115 it is noted that no heat was generated by the battery until Day 15 at about 06:00, when the temperature started to rise. At this time the battery had received about 103% recharge (8.98 Ah). It is estimated that the Ah charge efficiency was near 97%. The inflection of the temperature at 06:00 indicated that a portion of the charge energy was then going into heat and the battery was being overcharged. By Day 152 the temperature stabilized at 12.5°C (54.5°F), and it was estimated that the heat generated by the battery was about 11 W.

It is also noted that as the battery approached full charge the low-rate charge current gradually diminished to near 0.3 A. The PSL voltage was varying -1 DN (0.24 V) from 39.88 V due to the switching on and off of heater loads. This in turn caused the charge current to fluctuate -1 DN from 0.31 to 0.28 A because of the IV characteristics of the charger as discussed in Section VII. It is also noted that the high-rate charge current remained constant at 2.01 A even though the ΔV between the battery and the charger input was only 2.38 V at the end of high-rate charge.

The first midcourse maneuver was performed on Day 156. Figure 116 shows the effect of the maneuver on the battery. The maneuver did not require battery power, but solar panel temperature dropped, causing the PSL voltage to rise, which in turn produced the charge current and voltage transients shown.

Figure 117 shows the PSL voltage, battery data and notations of major events during the cruise period to Mars. As the PSL voltage increased, charge current increased and caused the battery temperature to rise, as can be seen in Fig. 118. The charger reached its maximum output of 0.614 A on Day 230 at a differential voltage of 5.76 V.

The turnon of the science instruments produced a significant effect on battery temperature in that the temperature increased about 4°C. The science electronics were in Bay 7 adjacent to the battery bay. The increase in temperature caused the battery voltage to decrease by 0.4 V from 37.5 to 37.1 V.

B. Mars Orbit Insertion and Orbit Trims

After 168 days from launch (November 13, 1971) Mariner 9 was placed into a 12.567-h orbit period around Mars with a periapsis of 1398 km. This was the first time that battery power was required since launch and there was concern about how the battery would perform as was discussed in Section VII. The battery was not reconditioned prior to orbit insertion. Figure 118 shows the battery performance during MOI. Also shown in the figure is the predicted discharge voltage at a constant 346-W load. Considering the difference in the actual load and the worst-case predicted load, the battery discharge voltage was very close to the predicted voltage and was within 1%. The 40-min discharge removed only 6.34 Ah or 204 Wh of energy. The battery accepted 5.4 Ah of charge at high rate before switching to low rate. It is also confirmed that the battery was near full charge (95%) at the switch-point because battery temperature started to increase shortly after the low-rate charge was initiated.

Figures 119 and 120 give the discharge and recharge battery performance data for Mars orbit trims (MOT). The MOTs were performed on November 15 and December 30, 1971. The first MOT required approximately 4.4 Ah (143 Wh) and the second MOT required 3.94 Ah (128 Wh). It can be noted that the MOT battery voltage was slightly higher than the MOI discharge. The discharge during MOI partially reconditioned the battery for the MOT discharge. Again it is noted that the battery switched from high- to low-rate charge approximately 1 Ah short of replacing the capacity removed during the discharge. Also in each instance of recharge the battery temperature was $13 \pm 0.5^\circ\text{C}$. This was considered to be very consistent performance and was also consistent with the test batteries previously discussed in Section VII. The final orbit trim put Mariner 9 into an 11.99-h orbit period.

C. Sun Occultation

After the primary mission was completed, Mariner 9 was still performing well and NASA/JPL decided to continue the mission. A Sun occultation period of approximately 63 days beginning on April 2, 1972, was predicted. On March 29, 1972, a solar array test was performed to measure the maximum power of the panels. Various loads were turned on until the solar panels and the battery shared the load. Figure 121 shows the battery performance data during the share period. It is noted that the battery temperature decreased during the discharge. This occurred because the battery heat dissipation decreased from about 24 W on low-rate charge to about 8 W during the low-rate discharge. The average load on the battery was 51 W, and the energy removed was about 107 Wh.

The first indication of Sun occultation of Mariner 9 by Mars occurred on April 2, 1972, when the spacecraft entered a penumbra for a few minutes on revolution 282 and there was a 17-min share period with the solar panels that only discharged the battery 0.5 Ah. By revolution 284, Mariner 9 entered the umbra for 35 min and the battery was discharged 4.8 Ah. The occultation periods increased rapidly and by revolution 325, or cycle 45 on the battery, the maximum time on the battery of 97 min was reached. The maximum discharge removed 14.3 Ah from the battery, which was equivalent to a 72% DOD. Figure 122 shows the battery end-of-discharge voltage, capacity removed, and the length of the occultation periods as a function of the orbit number. It is noted that the end-of-discharge battery voltage decreased rapidly, plateaued at 30.7 V, and then gradually rose as the depth of discharge decreased. It might be expected that battery voltage curve would be the inverse of the capacity curve. The reason for the battery voltage plateau is that the early discharge cycles tended to recondition the battery. Further proof of this can be seen in Fig. 120 where on the decreasing side of the occultation curve the end-of-battery voltage at an equivalent DOD is higher than on the increasing side of the occultation curve.

The fact that early discharge cycles tended to recondition is again seen by inspection of the battery voltage discharge curves. The battery temperature profile is also shown in Figs. 123 and 124. During the maximum occultation period of 97 min, shown in Fig. 123, the maximum temperature swing was 11°C, between 8°C at the end of high-rate charge to 19°C at the

end of discharge. The temperature profile of the flight battery was within a few degrees of the real-time test on battery SN 307 (discussed in Section VII). From the data in Fig. 123 it is seen that the battery cooled down rapidly during high-rate charge to the minimum and remained there until the switch from high- to low-rate charge. The temperature then began to climb, indicating the battery was being overcharged. The switch from high- to low-rate charge was quite consistent, and occurred when the Ah input was within 1 Ah of that removed on the discharge.

Daily monitoring of the spacecraft by the Goldstone 64-m antenna was not possible because the cost was prohibitive and the antenna was needed to support other missions. Since the charger was not mechanized to automatically switch back to the high-rate charge after a discharge, the switching function was programmed into the CC&S, which issued a 4-A command to the charger on a fixed time sequence. This resulted in the battery going into a low-rate charge immediately after the occultation for periods varying from about 30 to 75 min before the high-rate charge was commanded on. The low-rate charge before high rate is also shown in Figs. 123, 124, and 125.

Up to this time in the mission, battery performance was quite predictably excellent. The battery has 12.5 months of service in flight. About 10.5 months of the flight time on the battery was basically at a C/30 trickle charge with no detrimental effects noted. The remainder of the mission and battery performance will be covered in a supplemental report. Present plans indicate the mission will be terminated about February 1973.

Table 1. Comparison factors

Battery System	Packaging	Thermal Control	Weight (Including Structure)	Power Conditioning Equipment	Failure Modes	Power Profile	Telemetry and Command Requirements
<u>Dual Silver-Zinc</u> (Ag-Zn)	1) Requires one total bay. 2) Battery internal packaging easier. 3) <u>Does not</u> meet overall packaging, cabling, structures desires. 4) More complex structurally.	1) Requires development of new device for isolation and thermal control. 2) Confidence in meeting thermal control requirements lower. 3) Requires more interfaces for thermal shutter mechanization. 4) Structure related thermal isolation problem.	55# Batteries (w/cases) 5# Structure and other 60# Maximum	1) Twice complexity to P.S.L. module. 2) Adds 60% (5#) more weight to P.S.L. (Total wt = 13#). 3) Add 2# for charger increases. 4) Requires cabling additions between power cases and case to spacecraft.	1) Provides protection for single battery failure in first 6 mos of mission. 2) Complex peripheral circuitry adds potential failure modes (including command). <u>Examples</u> CC&S or command to: a) Pyro for thermal shutters. b) Power for switching on 2nd battery. c) Power for charger control and sensing.	1) Full charge: 35 watts @ 1 amp into battery $\left(\begin{array}{l} \text{Raw Power} \\ \text{Required} \\ = 43 \text{ watts} \end{array} \right)$ 2) No trickle charge.	1) <u>Telemetry</u> a) Battery 1 and 2 volt. b) Battery 1 and 2 discharge I. c) Battery charge I. d) Battery 1 and 2 temperature. 2) <u>Command</u> a) Battery charger On-Off. b) Charge Battery #1 or #2. c) Battery #2 On and warmup battery #2. d) Battery test #1 On-Off. e) Battery test #2 On-Off.
<u>Single Nickel-Cadmium</u> (Ni-Cd)	1) Requires only one-half bay (30 A-H cells). 2) Overall preferred packaging approach. 3) <u>Does</u> meet overall packaging, cabling, structures desires.	1) Possible problem in removing heat from inker cells.	69# Battery (w/case) 1# Structure and other 70# Maximum	1) Same as M'69 configuration, except: a) Add 2# for charger increases. b) Total PCE weight approximately same as M'69. 2) Overall <u>far</u> simpler PCE mechanization.	1) Dependent on charger and cycling throughout mission (charge retentivity). a) No capacity with charger failed. b) Low terminal voltage possible with no cycling.	1) Full charge: 52 watts @ 1.5 amp into battery. $\left(\begin{array}{l} \text{Raw Power} \\ \text{Required} \\ = 62.5 \text{ watts} \end{array} \right)$ 2) Trickle charge: 0.75 amp into battery. $\left(\begin{array}{l} \text{Raw Power} \\ \text{Required} \\ = 33 \text{ watts} \end{array} \right)$	1) <u>Telemetry</u> a) Battery voltage. b) Battery discharge I. c) Battery charge I. d) Battery temperature. 2) <u>Command</u> a) Battery charger On-Off. b) Battery test On-Off. c) Select charge rate. Note: Requires 3 less TLM channels and 2 less CMD's than 2 Ag-Zn.
<u>Dual Nickel-Cadmium</u> (Ni-Cd)	1) Requires more than one-half bay. 2) Cabling more difficult. 3) Temperature sensing for charging more difficult (may require two chargers).	1) Same as single Ni-Cd above. 2) Low gain ant #2 interferes with mounting of second half louver set.	76# Batteries (w/cases) 4# Structure and other 80# Maximum	1) Same as dual Ag-Zn comments 1, 2 and 4 above, <u>Except:</u> a) Probably two chargers. b) <u>Does not</u> require switching for load application to 2nd battery. 2) Add 6# for chargers (4# + 2#).	1) Same as single Ni-Cd above. 2) Provides protection for single battery failure if one battery large enough for orbit insertion. 3) Independent cycling achievable with battery always available.	1) Full charge: (Same as single Ni-Cd). 2) Trickle charge: ≈ 0.4 amp per battery. $\left(\begin{array}{l} \text{Raw Power} \\ \text{Required} \\ = 33 \text{ watts for Both Batteries} \end{array} \right)$	1) <u>Telemetry</u> (Same as dual Ag-Zn). 2) <u>Command</u> a) Battery charger On-Off. b) Charge Battery #1 or #2. c) Battery test #1 On-Off. d) Battery test #2 On-Off. (Might require an additional command to trickle charge one battery while hi-rate charging other.)

Table 2. Battery/charger commands

Toggle function	DC	CC&S
Battery test load on/off	50	-
Charger switchover on/off	74	-
Battery charger on/off	38	4B
Select charge rate high/low	81	4A

Table 3. Synopsis of the preliminary structural analysis

Component	Results	
Base plate		
Dynamic stress		20,050 psi
Natural frequency		260 Hz
Yield stress		26,000 psi
Margin of safety		0.235
Upper keeper plate		
Outside lengthwise	<u>Method I</u>	<u>Method II</u>
Dynamic stress	10,800 psi	9,600 psi
Yield stress	26,000 psi	26,000 psi
Margin of safety	1.4	1.7
Outside crosswise		
Dynamic stress	14,200 psi	12,500 psi
Yield stress	26,000 psi	26,000 psi
Margin of safety	0.83	1.04
Inside lengthwise		
Dynamic stress	14,200 psi	12,500 psi
Yield stress	26,000 psi	26,000 psi
Margin of safety	0.83	1.08
Structure from battery to inner king gusset ^a		
Dynamic stress		12,300 psi
Yield stress		26,000 psi
Margin of safety		1.1
Bending mount on keeper fastener		
Dynamic stress		73,500 psi
Yield stress		100,000 psi
Margin of safety		0.36

^aMaximum dynamic loading assumed (upper bound to actual).

Table 4. Battery TA vibration requirements

(Vibration: Low level resonance sweep. 1 g rms sweep up at a 1 oct/min rate from 20 to 2500 Hz - in all three axes - 0.4 in. D. A. displacement limit)

Equipment (random) qualification levels (1 min in each of 3 axes)	
Random response frequency, Hz	Level, g^2/Hz
20 ^a - 50	Roll up at a rate of 25 dB/oct to 0.28 g^2/Hz
50 - 200	Constant at 0.28 g^2/Hz
200 - 250	Roll off to 0.063 g^2/Hz
250 - 750	Constant at 0.063 g^2/Hz
750 - 2500	Roll off at a rate of 12 dB/oct
Equipment (sine) qualification levels (Sweep at a rate of 1 oct/min from 5 - 2000 Hz)	
Response frequency, Hz	Level (g rms)
5 - 35	0.75
35 - 250	6
250 - 600	4.5
600 - 2000	9
^a Approximately.	

Table 5. Z-Z axis vibration summary

Qualification (TA) sine level							
Accelerometer and location	Measured direction	f_n , Hz	Q	f_n , Hz	Q	f_n , Hz	Q
1 Test fixture (control)	Z-Z						
2 Top of cell 3	Z-Z	290	11.0				
3 Edge of hold down	Z-Z	290	7.0	750	3.5	1500	9
4 Top of hold down	Z-Z	290	11.0	750	2.5	1500	4.5
5 Next to gusset	Z-Z	280	2.5				
6 Baseplate	Z-Z	280	11.0				
9 Keeper angle	X-X	280	2.4				
11 Top keeper	Z-Z	280	4.0				
1 g rms test							
1 Test fixture (control)							
2 Top of cell 3	Z-Z	320	13	650	1.6	900	2.0
3 Edge of hold down	Z-Z	320	11	900	11.0	1550	11.0
4 Top of hold down	Z-Z	320	16	900	3.2	1550	6.5
5 Next to gusset	Z-Z	320	5.5	650	1.8		
6 Baseplate	Z-Z	320	15.0	900	2.1		
9 Keeper angle	X-X	320	2.4	650	2.8		
11 Top keeper	Z-Z	320	6.8	650	2.1	900	1.4
f_n = response frequency.							
Q = transmissibility = response accelerometer/input accelerometer.							

Table 6. Calculated steady-state temperatures

Battery dissipation, W	Spacecraft average bus temperature, °C	Shear plate temperature, °C
76	18.35	29.45
29	18.35	19.45
0	18.35	11.11
76	26.67	35.00
29	26.67	21.1
0	26.67	16.11

Table 7. Battery thermal property and density data

Components	Thermal conductivity, $W/(cm^2)(C^{\circ}/cm)$	Specific heat, $J/kg-^{\circ}C$	Density, g/cm^3
Positive plates		447	3.16
Perpendicular ^a	0.00667		
Parallel ^a	0.126		
Negative plates		447	3.74
Perpendicular ^a	0.00776		
Parallel ^a	0.126		
Separator	0.00478	1705	3.21
Electrolyte	—	3475	1.30
Lining	0.00251	1533	1.27
Stainless steel case	0.1635	512	8.04
Magnesium ZK60A-T5 Structure	1.177	1044	1.83
^a Direction of heat flow with respect to the plate stack.			

Table 8. Measured and calculated temperature gradients ($^{\circ}\text{C}$) for various battery operational modes

Temperature location	Battery operating mode					
	Stabilized trickle charge		End of discharge		End of charge	
	Test	Analytical	Test	Analytical	Test	Analytical
Δ between top surface and baseplate						
Center cell	2.8	5.6	6.1	10.0	0.6	3.3
End cell	2.2	3.3		5.6	0	2.2
Δ between vertical surface and baseplate						
Center cell	3.3	6.1	7.2	11.1	0.6	2.8
End cell	2.2	1.1	5.0	1.1	0.6	1.1

Table 9. Measured and calculated temperature transients ($^{\circ}\text{C}$)
during discharge and charge

Temperature location	Temperature change			
	Increase during discharge phase		Decrease during charge phase	
	Test ΔT	Analytical ΔT	Test ΔT	Analytical ΔT
Cell top surface				
Center cell	9.4	9.4	15.6	13.9
End cell	8.3	7.2	14.4	10.6
Cell vertical surface				
Center cell	10.0	10.0	16.7	15.6
End cell	8.9	5.0	14.4	7.2
Average baseplate	6.1	5.0	10.0	7.2

Table 10. Measured and calculated temperatures ($^{\circ}\text{C}$) at various locations for various operating modes

(High-temperature cycle test and analytical temperatures)

Temperature location	Battery operating mode					
	Stabilized trickle charge		End of discharge		End of high-rate charge	
	Test	Analytical	Test	Analytical	Test	Analytical
Cell top surface						
Center cell	34.4	22.8	45.0	32.2	28.3	18.3
End cell	33.9	20.6	43.3	27.8	27.8	17.2
Cell vertical surface						
Center cell	35.0	23.3	45.0	33.2	28.3	17.8
End cell	33.9	18.3	42.8	23.2	28.3	16.1
Average baseplate	31.7	17.2	37.8	22.2	27.8	15.0
Ambient (chamber wall)	25.6	21.1	26.1	21.1	25.6	21.1

Table 11. Type approval and flight acceptance battery test sequence^{a, b}

Test name	TA batteries	FA batteries
Fabrication test	X ^c	X ^c
Group II functional test	X ^c	—
Vibration	X	X
Group I functional test	X	X
Thermal vacuum	X	X
Group I functional test	X	X
Group II functional test	X	X
^a Vibration levels higher for TA than FA as shown in Figs. 2 and 3. ^b TA thermal vacuum: 3.89 to 48.89°C for 7 days minimum. FA thermal vacuum: 1.11 to 39.44°C for 3 days minimum. ^c These tests were not a formal part of the TA and FA tests.		

Table 12. Cell vendor evaluation criteria

Characteristics	Information sources
Product characteristics	
Performance	Test results, crane data
Quality	Contacts and rejections
Delivery	Receiving records
Price	Vendor quotations
Company characteristics	
Management	Prior contact, responsiveness
Technical capability	Prior contact, personal evaluations
Manufacturing capability	Prior surveys
Test facilities	Prior contacts
Quality organization	Prior contacts, responsiveness
Continuity	Vendor responses, business data

Table 13. Test data

Serial Number	AH IN Cycle 2	EOCV Cycle 2	AH Out Cycle 2	AH In Cycle 3	EOCV Cycle 3	AH Out Cycle 3	EODV Cycle 30	AH 1.16V Cycle 31	AH 0.50V Cycle 31
1257	28.320	1.436	27.600	28.000	1.437	27.200	1.192	22.600	29.400
1260	27.920	1.435	27.200	27.560	1.435	27.000	1.190	22.600	29.200
1261	27.920	1.437	27.200	27.680	1.438	27.000	1.190	22.600	29.200
1262	28.200	1.437	27.600	28.000	1.437	27.400	1.191	23.600	29.400
1263	27.720	1.435	27.200	27.600	1.436	27.400	1.191	22.800	29.000
1264	27.800	1.435	27.000	27.520	1.435	26.800	1.190	22.600	29.200
1265	28.520	1.435	27.800	28.320	1.436	27.600	1.188	23.600	29.600
1271	27.160	1.432	26.200	26.720	1.431	25.600	1.187	21.000	28.400
1272	27.760	1.436	27.000	27.520	1.436	26.800	1.188	23.000	29.200
1273	28.440	1.435	27.800	27.160	1.436	27.400	1.190	23.400	29.600
1275	27.920	1.438	27.200	28.640	1.438	27.000	1.188	23.000	29.200
1277	26.920	1.435	26.200	26.600	1.436	26.000	1.186	21.600	28.400
1280	27.760	1.436	27.200	27.640	1.436	27.200	1.188	22.600	29.000
1283	28.000	1.435	27.000	27.600	1.437	26.800	1.186	22.400	29.200
1285	28.400	1.438	27.800	27.120	1.436	27.600	1.185	22.400	29.600
1289	27.560	1.435	27.000	27.560	1.436	26.600	1.184	21.800	28.800
1292	26.920	1.436	26.200	26.680	1.437	25.800	1.183	21.000	28.400
1293	26.480	1.434	26.000	27.560	1.435	25.800	1.184	20.200	27.800
1303	27.520	1.443	27.200	27.440	1.444	27.200	1.180	21.000	29.000
1308	28.560	1.444	28.200	28.400	1.446	28.000	1.186	24.000	29.600
1309	26.200	1.439	26.000	26.200	1.441	25.800	1.178	20.600	27.600
1319	28.160	1.437	27.800	27.960	1.439	27.600	1.184	22.200	29.200
1326	27.200	1.443	27.200	27.080	1.444	27.600	1.181	20.600	28.400
1335	26.520	1.439	26.400	26.480	1.441	26.000	1.180	20.200	27.400
974	26.520	1.441	26.200	26.440	1.440	25.800	1.184	21.600	28.000
1070	29.600	1.436	29.400	29.720	1.441	29.400	1.196	26.600	30.400
1076	26.280	1.438	25.600	26.160	1.433	26.600	1.191	22.000	28.200
1083	26.440	1.435	25.600	26.120	1.434	26.600	1.184	20.600	28.200
1098	26.360	1.441	26.000	26.280	1.441	25.600	1.186	21.400	27.800
1130	26.400	1.439	26.000	26.120	1.438	25.400	1.183	20.400	28.200
1132	27.360	1.441	27.400	27.400	1.442	28.000	1.185	22.000	29.000
1143	28.560	1.438	28.000	28.560	1.438	27.200	1.181	22.000	29.600
1152	27.320	1.436	26.800	27.400	1.435	26.600	1.182	20.200	28.400
1156	26.440	1.436	25.800	26.320	1.435	25.800	1.180	19.400	28.600
1157	26.840	1.438	26.400	27.800	1.438	26.200	1.181	20.200	28.400
1169	26.600	1.443	26.600	26.680	1.444	26.400	1.187	21.400	28.200
1173	27.880	1.451	28.000	28.000	1.451	27.600	1.185	23.600	29.400
1220	28.240	1.448	28.200	28.400	1.446	28.000	1.189	22.200	27.400
1221	27.400	1.438	27.000	27.040	1.438	26.800	1.187	21.200	29.800
1222	27.120	1.440	26.600	26.880	1.441	26.400	1.186	21.200	28.600
1223	28.440	1.459	28.600	28.760	1.456	28.400	1.189	22.200	28.000
1224	28.200	1.441	27.600	27.959	1.441	27.600	1.187	21.600	29.400
1226	28.080	1.442	27.800	27.920	1.443	27.600	1.187	21.600	29.600
1227	27.320	1.439	27.000	27.200	1.440	26.400	1.187	21.400	28.400
1228	27.360	1.438	27.000	27.200	1.438	26.400	1.187	21.400	28.800
1234	27.600	1.439	27.200	27.520	1.440	26.400	1.187	21.400	29.000
1240	27.920	1.445	27.600	27.840	1.445	27.600	1.187	22.000	27.600
1242	28.080	1.443	27.600	27.840	1.443	27.600	1.188	22.000	29.600
1244	27.400	1.441	27.000	27.120	1.441	26.400	1.188	22.000	28.800
1249	27.120	1.451	27.200	27.240	1.450	26.400	1.187	21.800	27.600

Table 13 (contd)

Serial Number	AH In Cycle 2	EOCV Cycle 2	AH Out Cycle 2	AH In Cycle 3	EOCV Cycle 3	AH Out Cycle 3	EODV Cycle 30	AH 1.16V Cycle 31	AH 0.50V Cycle 31
1252	26.720	1.437	26.440	26.560	1.438	25.800	1.185	19.800	28.000
1254	27.040	1.441	26.800	26.800	1.443	26.200	1.184	20.800	28.400
1255	27.280	1.442	27.000	27.160	1.443	26.400	1.185	20.000	28.600
1317	26.200	1.439	26.000	25.959	1.439	25.400	1.183	18.000	27.600
1338	26.920	1.439	26.800	26.680	1.440	26.200	1.181	20.000	28.400
1339	25.720	1.437	25.800	25.600	1.438	26.800	1.185	18.000	27.200
1341	26.720	1.440	26.400	26.400	1.440	26.200	1.183	19.000	28.200
1342	26.200	1.439	26.000	25.959	1.440	25.800	1.184	18.200	27.600
1345	27.360	1.440	27.200	27.280	1.440	27.200	1.182	21.000	28.800
1346	27.000	1.438	26.800	26.760	1.440	26.600	1.185	19.400	28.400
1360	26.320	1.437	26.000	26.120	1.437	26.000	1.184	19.400	27.800
1361	27.720	1.442	27.000	27.560	1.442	26.800	1.185	22.600	29.000
1362	26.600	1.438	25.800	26.439	1.438	25.600	1.184	21.200	28.000
1363	26.000	1.440	25.600	26.080	1.439	25.600	1.185	21.200	27.600
1364	26.720	1.440	26.400	26.800	1.441	26.200	1.185	21.400	28.000
1365	25.720	1.440	25.200	25.800	1.440	25.200	1.181	21.400	27.200
1366	26.200	1.438	25.600	26.080	1.439	25.400	1.182	20.600	27.200
1367	27.000	1.438	26.600	27.040	1.439	26.400	1.186	22.200	28.200
1369	27.000	1.439	25.600	26.959	1.439	26.000	1.185	21.600	24.200
1370	26.840	1.436	26.000	26.800	1.436	25.800	1.181	20.600	28.200
1371	27.120	1.441	26.800	27.160	1.442	26.800	1.184	21.400	28.400
1372	27.600	1.438	27.000	27.520	1.439	26.800	1.187	22.400	29.000
1373	26.480	1.438	26.000	26.600	1.439	25.600	1.184	21.600	28.000
1374	25.960	1.437	25.200	26.000	1.438	25.200	1.182	20.800	27.400
1375	27.320	1.440	27.000	27.439	1.441	26.800	1.183	21.600	28.600
1377	27.640	1.447	27.400	27.760	1.447	27.400	1.184	22.000	27.200
1378	27.960	1.446	27.800	28.080	1.447	27.600	1.185	22.400	27.400
1379	27.520	1.441	27.000	27.560	1.442	27.000	1.183	21.800	28.400
1380	26.320	1.441	25.800	26.400	1.442	25.600	1.182	20.800	27.600
1381	27.960	1.444	28.000	28.000	1.445	27.600	1.184	21.000	28.000
1382	27.920	1.447	28.000	27.959	1.448	27.600	1.186	21.000	27.600
1383	26.600	1.441	26.400	26.479	1.442	26.200	1.183	21.000	27.800
1385	26.720	1.441	26.200	26.400	1.442	25.800	1.181	21.000	28.000
1390	27.760	1.449	27.600	27.760	1.439	27.200	1.186	22.000	28.400
1391	26.680	1.456	26.200	26.479	1.438	26.000	1.185	21.600	27.800
1392	27.720	1.440	27.600	27.640	1.441	27.000	1.185	22.000	24.600
1393	27.240	1.434	27.000	27.160	1.439	26.600	1.188	22.200	28.200
1394	28.080	1.442	27.800	27.920	1.442	27.200	1.186	23.400	29.000
1397	26.760	1.437	26.800	27.000	1.437	26.600	1.182	20.000	28.200
1399	27.520	1.440	27.400	27.439	1.440	27.000	1.185	20.800	28.600
1401	27.160	1.441	27.000	27.040	1.442	26.600	1.186	21.400	28.200
1402	27.800	1.446	27.800	27.760	1.447	27.400	1.184	21.600	27.400
1405	27.520	1.442	27.400	27.360	1.442	27.000	1.183	21.600	28.800
1406	26.920	1.442	26.800	26.760	1.442	26.400	1.184	21.400	28.000
MEAN VALUES									
	27.279	1.439	26.885	27.185	1.440	26.670	1.185	21.468	28.361
STANDARD DEVIATION VALUES									
	0.75277	0.00454	0.80615	0.76241	0.00400	0.79552	0.00304	1.29234	0.92667

Table 14. Vibration test results

Input to spacecraft		Output at battery/structure	
Frequency, Hz	g rms	Peak g rms	
Sweep		71-1	71-2
8 - 120 - 8	0.5	1.9	1.9
120 - 250 - 120	2.15	a	1.6
250 - 400 - 250	1.2 - 4.4	b	9.4
400 - 1900 - 400	5.5	b	7.5
^a Facility equipment malfunctioned. ^b Test waived.			

Table 15. PTM thermal vacuum test mode summary

M71-3 (PTM) subsystem status	Phase I						Phase II							
	Mode													
	FA cold	TA cold	Mars orbit ²	Mars orbit ³	FA hot	TA hot	Mars cruise	Mars orbit	Mars orbit	Mars orbit	Earth cruise	Earth cruise	Prop heater off	FA hot
	Date, 1970													
	July 27	July 27	July 28	July 28	July 30	July 31	Aug 3	Aug 4	Aug 4	Aug 4	Aug 5	Aug 6	Aug 6	Aug 7
	PDT													
	0700	1115	1015	1600	0300	0830	1830	1030	1630	2300	2000	0900	1200	1200
	GMT													
	208, 1400	208, 1815	209, 1715	209, 2300	211, 1000	212, 1530	216, 0130	216, 1730	216, 2330	217, 0600	218, 0300	218, 1600	218, 1900	219, 1900
TWT	#2 Low	Off	#2 High	Off	#2 High	#1 High	#1 High	#2 High	#2 High	#2 Low	#1 Low	#2 Low	#2 Low	#2 High
Science/DAS	Off	Off	On	On	On	On	Off	On	On	On	Off	Off	Off	On
Scan	Off	Off	Off	Off	On	On	Off	On	On	Off	Off	Off	Off	On
DSS	Off	Off	On	On	On	On	Off	On	On	Off	Off	Off	Off	On
Gyros	Off	Off	Off	Off	3 On	3 On	Off	Off	3 On	3 On	Off	Off	Off	3 On
Prop heater	On	Off	Off	On	Off	Off	On	Off	Off	On	Off	On	Off	Off
Batt charger	High ¹	Off	Low	Low ⁴	Low	Low	Low	Low	Low	Low	Low	Low	Low	Low
Power source	S/P	Battery	Simulated S/P	Simulated S/P	Simulated S/P	Simulated S/P	Simulated S/P	Simulated S/P	Simulated S/P	Simulated S/P	Simulated S/P	Simulated S/P	Simulated S/P	Simulated S/P
PS/L, V	39.4	33.8	43.5-45	45.6	45.6	45.6	44.1	44.4	41.1	37.9	38.9	39.1	39.1	45.6
Spacecraft power, W	238-247	159-168	355-364	301-311	379-380	376-378	285-294	347-358	376-387	338-343	229-240	242-252	231-240	372-381
Solar intensity w/m ²	5.02	0	5.76	5.85	11.52	13.75	5.67	5.67	5.76	14.12	11.61	11.43	11.43	11.43
Science stimuli	Off	Off	On	Off	On	On	-	-	-	-	-	-	-	-
Temp measurement location														
Bay I flight transducer, °C	13.3	12.8	18.9	20.5	22.2	28.3	17.2	20.0	20.5	-	17.8	18.3	18.3	22.2
Bay VII flight transducer, °C	1.1	-3.8	20.5	18.3	22.8	27.8	11.7	21.1	21.1	-	9.5	9.5	9.5	25.6
Bay VIII flight transducer, °C	5.0	11.7	15.0	12.8	19.5	25.6	14.5	17.8	17.8	-	11.7	11.7	11.7	20.0
Average bus bays, °C	10.0	8.3	19.5	18.3	24.5	30.0	16.1	20.5	21.7	20.5	15.6	15.6	15.6	24.5

1. Not fully charged for occultation to follow.

2. Not completely at equilibrium.

3. Bus and prop module not at equilibrium.

4. Batt. test load also on: 40.5 W.

Table 16. Subsystem status for different test modes

Flight spacecraft subsystem status	M71-1 (Flight No. 1)					M71=2 (Flight No. 2)					M71-2 phase 2
	Mode, GMT day, GMT										
	FA cold, 348, 0300	Mars cruise, 349, 1200	Mars orbit, 350, bus and propulsion, 2300, platform, 1700, without stimuli	Earth cruise, 351, bus and propulsion, 2100	FA hot, 353, platform, 0300, bus and propulsion, 0600	FA cold, 0900	Mars cruise, 1545	Mars orbit, 2000, IRIS off	Earth cruise, bus and propulsion, 1430	FA hot, 0000	Mars orbit, 2130, IRIS on
Solar intensity, W/m ²	5.02	5.76	5.76	11.52	11.52	5.02	5.76	5.76	11.52	11.52	5.76
PSL, V	39.3	44.2	44.4	39.2	46.1 bus and propulsion 45.6 platform	39.2	44.5	44.5	39.2	45.6	44.2
Total spacecraft power, W	238	292	341	212-228	400-412	241	276-296	343-356	236	404	340-367
Battery charge rate	Low	Low	Low	Low	Low	Low	Low	Low	Low	Low	Low
Exciter 1	2	1	1	2	1	1	2	2	1	1	2
TWT 1	1	2	1	1	1	1	1	1	1	2	2
TWT power	Low	High	High	Low	High	Low	High	High	Low	High	High
Gyros	Off	Off	Off	Off	3 axis	Off	Off	Off	Off	3 axis	Off
Prop heater	On	On	Off	Off	Off	On	On	Off	Off	Off	Off
Science stimuli	Off	Off	On bus and propulsion Off platform	Off	On	Off	Off	Off	Off	On	Off
Science and DAS	Off	Off	On	Off	On	Off	Off	On	Off	On	On
DSS	Off	Off	Ready	Off	Play-back	Off	Off	Play-back	Off	Play-back	Ready
Scan	Off	Off	On	Off	On	Off	Off	On	Off	On	On
Temperature measurement											
Bay I at flight transducer, °C	12.8	16.7	18.9	16.1	22.2	12.5	17.8	18.9	16.7	22.5	19.5
Bay VII flight transducer, °C	3.9	12.8	21.1	10.0	23.3	2.5	12.8	20.0	9.5	22.2	20.0
Bay VIII battery transducer, °C	6.8	15.6	17.8	10.0	21.7	5.6	15.6	18.9	11.1	21.7	18.9
Bay VIII shear-plate, °C	6.8	13.9	15.6	9.4	17.8	6.1	13.3	16.1	10.6	18.3	16.1
Average bus bays, °C	11.1	17.2	20.6	15.6	26.1	10.6	17.2	20.0	15.6	26.1	21.1

Table 17. Parameter variation effects on temperature

Description	Flight transducer IO	Launch transient (1)	Launch transient (2)	Mars to Earth (3)	Mars to Earth (4)	Mars to Earth (5)	Mars to Earth (6)	Mars to Earth (7)	Mars to Earth Δ TWT (8)	Mars to Earth Δ TWT (9)	TWT Low/high (10)	TWT Low/high (11)	Gyros off/on (12)	Gyros off/on (13)	Gyros off/on (14)	Science off/on (15)	Science off/on (16)	Science off/on (17)
Spacecraft phase		M71-1	M71-2	M71-1	M71-2	M71-1	M71-2, I	M71-2, II	M71-1	M71-2	M71-1	M71-2	M71-1	M71-2, I	M71-2, II	M71-1	M71-2, I	M71-2, II
Mode Δ s		Pumpdown T = 0 to T + 1 hr		FA cold to Earth cruise Δ solar = 6.5 W/m ²		Mars orbit to FA hot Δ solar = 5.76 W/m ²			Mars cruise to Earth cruise TWT power High/low		FA cold to Mars cruise TWT 1 to 2 TWT 1		(5)-(3)	(6)-(4)	(7)-(4)	Mars cruise to Mars orbit IRIS off		
Other Δ s		Δ P Δ T		Propulsion heater	On/off	Gyros off/on Science stimuli off/on TWT 1 to 2			Propulsion heater TWT 2 to 1	On/off	Exciter 2 to 1 Solar 5.01 to 5.76	Exciter 1 to 2	Propulsion heater on/off Δ solar 5.76 to 6.5 W/m ² TWT 1 to 2			TWT 2 to 1 DSS ready science stim	DSS ready No science stimuli	TWT 1 to 2 DSS ready
Bay 1 power requirement, °C	411	1.1	1.1	3.3	3.9	3.3	3.9	3.3	-0.6	-1.1	3.9	5	0	0	-0.6	2.2	-1.1	2.2
Bay 7 DAS/TV, °C	414	-1.1	1.1	6.1	6.7	2.2	2.2	2.2	-2.8	-3.3	8.9	10.0	-3.9	-4.4	-4.4	8.3	7.2	7.2
Bay 8 battery, °C	405	1.1	3.9	3.3	5.6	3.9	2.8	2.8	-5.6	-4.4	8.9	10.0	0.6	-2.8	-2.8	2.2	3.3	3.3
Battery shearplate, °C		0.6	2.8	2.8	4.4	2.2	2.2	2.2	-4.4	-2.8	7.2	7.2	-0.6	-2.2	-2.2	1.7	2.8	2.8
Bus average, °C		0.6	1.7	4.4	5	5	6.1	5	-2.2	-1.7	6.1	6.7	0.6	1.1	0	3.3	2.8	3.9

Table 18. Cell history

Cell-level testing	Date, 1968	
	Gulton SN 202, 203, 204, 207, 208, 209, 213	General Electric SN 001-01, 003-01, 004-01, 005-01, 010-01, 036-01, 047-01
750-mA conditioning charge for 48 hr	6/19	6/25
Electrolyte leak test	6/19	6/25
7.5-A discharge to 1.16 V	6/21	6/27
Electrolyte leak test	-	6/27
Applied 1-ohm resistors	6/21	6/27
Applied shorts	6/22	6/28
Removed shorts and charge at 1.5 A for 5 min	6/22	6/28
Take charge retention readings after 24-hr stand	6/23	6/29
Apply 1-ohm resistors	6/23	6/29
Remove resistors	6/24	6/30
<u>Three cycles (charge/discharge)</u>		
1.5/.375-A charge for 24 hr	6/24	6/30
7.5-A discharge to 1.16 V		
Apply 1-ohm resistors	6/27	7/3
1.5-A charge for 24 hr	7/2	-
0.375-A charge for 12 days	7/3	-
Place on trickle storage	7/15	-
Apply 1-ohm resistors for 6 days	10/4	-
Place on trickle storage	10/10	-
1.5/0.375-A charge for 24 hr	-	7/8 (SN 047-01 only)
Place on trickle storage	-	7/9 (SN 047-01 only)

Table 19. Battery charge efficiency tests

S/N 306									
Date, 1971	Charge I, A	Ah in	Joule in, $\times 10^6$	Temperature start, °C	Temperature finish, °C	Ah out	Joule out, $\times 10^6$	Percent efficiency, Ah	Percent efficiency, energy
7/16	0.65	26.8	3.47	12	10	25.2	2.88	94.1	83.0
7/15	2.00	27.3	3.59	9	10	26.0	2.98	95.3	83.0
7/19	3.85	25.0	3.30	10	9	24.6	2.69	98.5	85.9
7/20	0.65	23.1	-	26	30.5	16.1	1.80	69.7	-
7/24	0.65	27.3	3.50	25	34	14.7	1.68	53.9	48.1
7/28	2.00	24.6	3.21	25	27	20.8	2.38	84.6	74.2
7/29	3.98	24.8	3.27	25	29	22.6	2.60	91.2	79.5
8/01	2.00	26.8	3.58	9	14	24.7	2.83	92.1	79.0
8/03	2.00	22.3	2.92	11	8	20.8	2.39	93.3	81.9
8/05	2.00	18.2	2.37	11	10	17.6	2.03	96.8	85.3
8/09	2.00	14.1	1.81	25	25.5	13.4	1.66	95.0	84.7
8/10	2.00	14.1	1.81	8.3	9.4	13.1	1.52	93.0	84.0
2/04	2.00	25.1	3.27	28	16.1	24.6	1.83	98	86.2
2/05	0.65	25.7	3.32	15.5	13.3	23.9	2.73	93	82.2
2/08	2.00	25.1	3.27	17.8	16.7	24.4	2.80	97.2	85.5
2/09	0.65	25.7	3.31	17.8	19.9	22.9	2.61	89	78.9
7/12	2.00/ 0.65	29.7	N/A	17.2	20.0	27.4	3.13	N/A	
8/15 ^a	2.00/ 0.65	22.2	N/A	16.0/ 12.8	21.7	25.2	2.89	N/A	
8/16 ^a	2.00/ 0.65	23.7	N/A	36/ 13.9	22.8	25.6	2.93	N/A	
^a Standard charges of 2.00 A to switch point, then 0.65 A for a total of 24-h charge. ^b Ah input to switch point. The July 12, 1971, charge was from shorted state, while the August 15 and 16, 1971, charges were from discharged state.									

Table 20. Battery/charger interface data summary

Test run	Charger input voltage, V	Switch voltage, V	Temperature °C		Ah input		Low-rate current, A	End of charge, V
			Low	Switchpoint	High rate	Low rate		
1	40.21	37.53	12.22	12.78	12.09	6.71	0.40	37.31
2	41.19	37.53	12.78	12.78	8.74	9.61	0.50	37.40
3	39.2	37.50 ^(a)	12.22	15.00	22.15			37.41
4	39.2	37.40 ^(a)	15.00	17.78	29.95			37.10
5	40.2	37.33 ^(b)	17.78	27.78	12.09	8.5	0.50	36.58
6	40.2	37.53	17.22	21.11	10.53	9.1	0.50	36.61
7	41.2	37.53	17.78	20.56	10.34	9.00	0.50	36.65
8	39.2	37.23 ^(a)	18.89	23.06	36.53			36.86
9	40.22	37.53	7.22	8.33	8.58	8.00	0.40	37.35
10	41.2	37.53	8.33	8.33	8.39	9.26	0.50	36.88
11	39.2	37.54	8.33	11.11	13.3	3.2	0.2	36.75
12	40.2	37.53	6.67	7.50	26.8	4.07	0.35	37.49
(a) Charger did not switch to low rate; remained on high rate. Voltage shown is maximum obtained.								
(b) Charge commanded from high to low rate.								

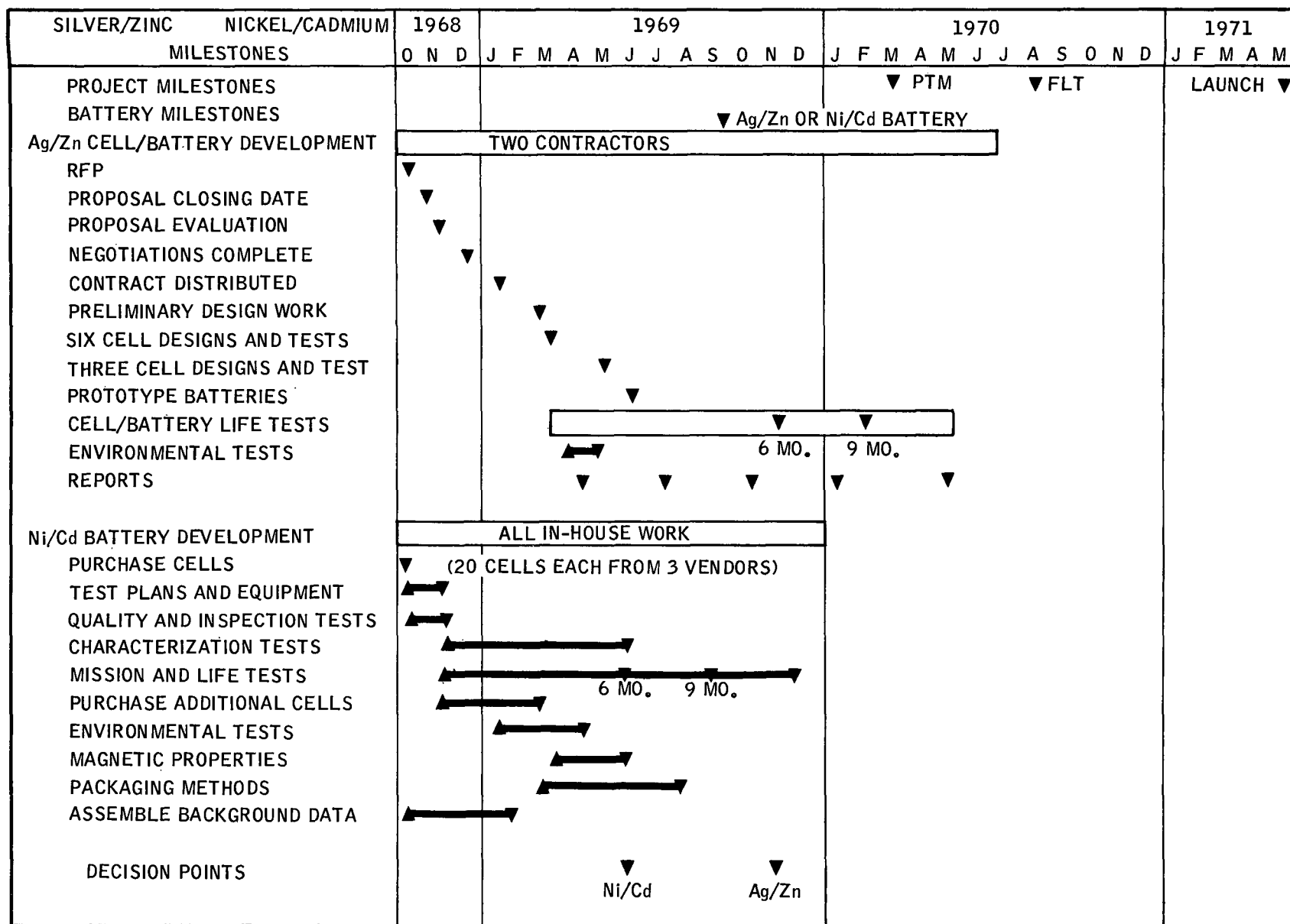


Fig. 1. Mariner Mars 1971 battery development schedule

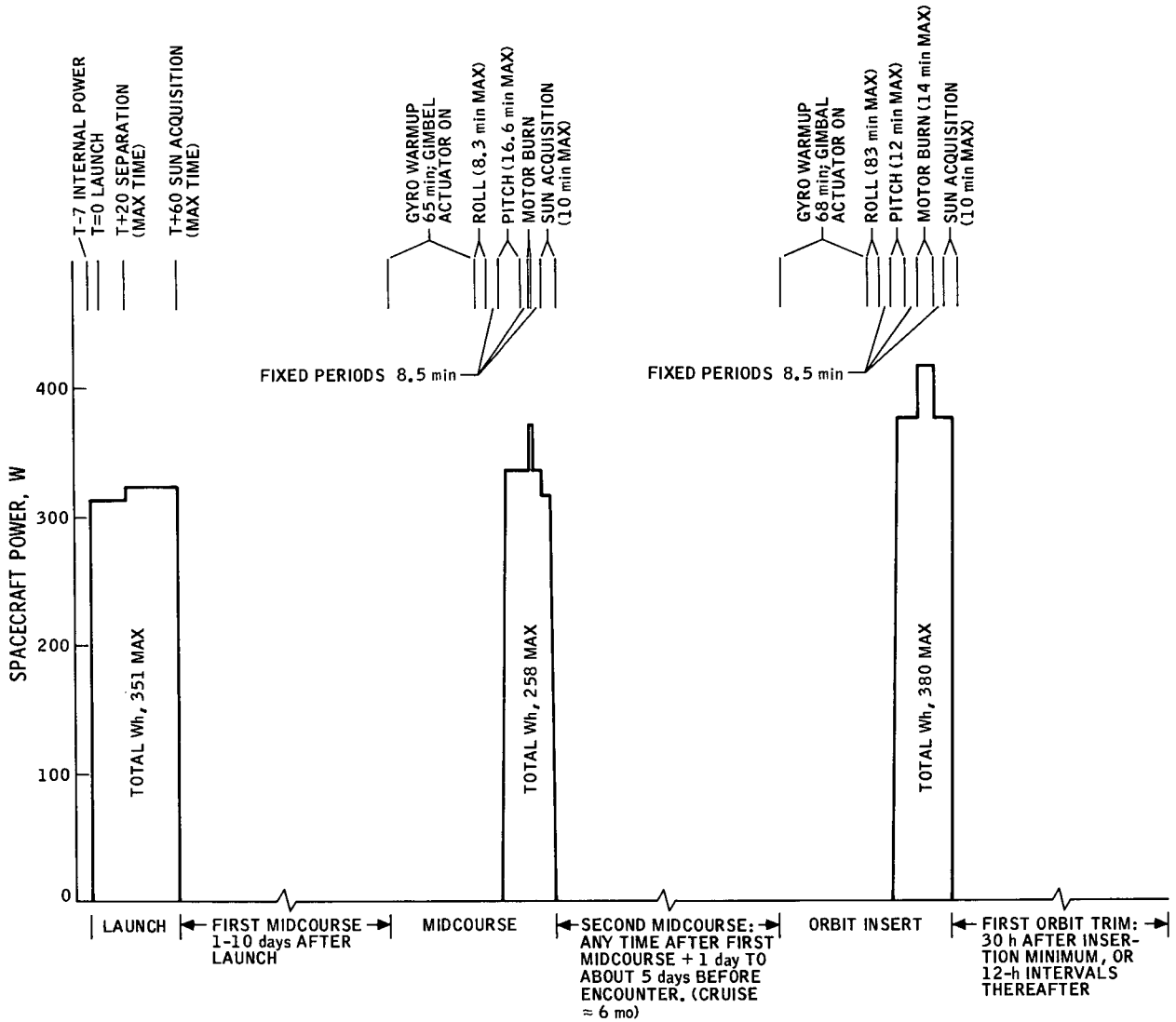
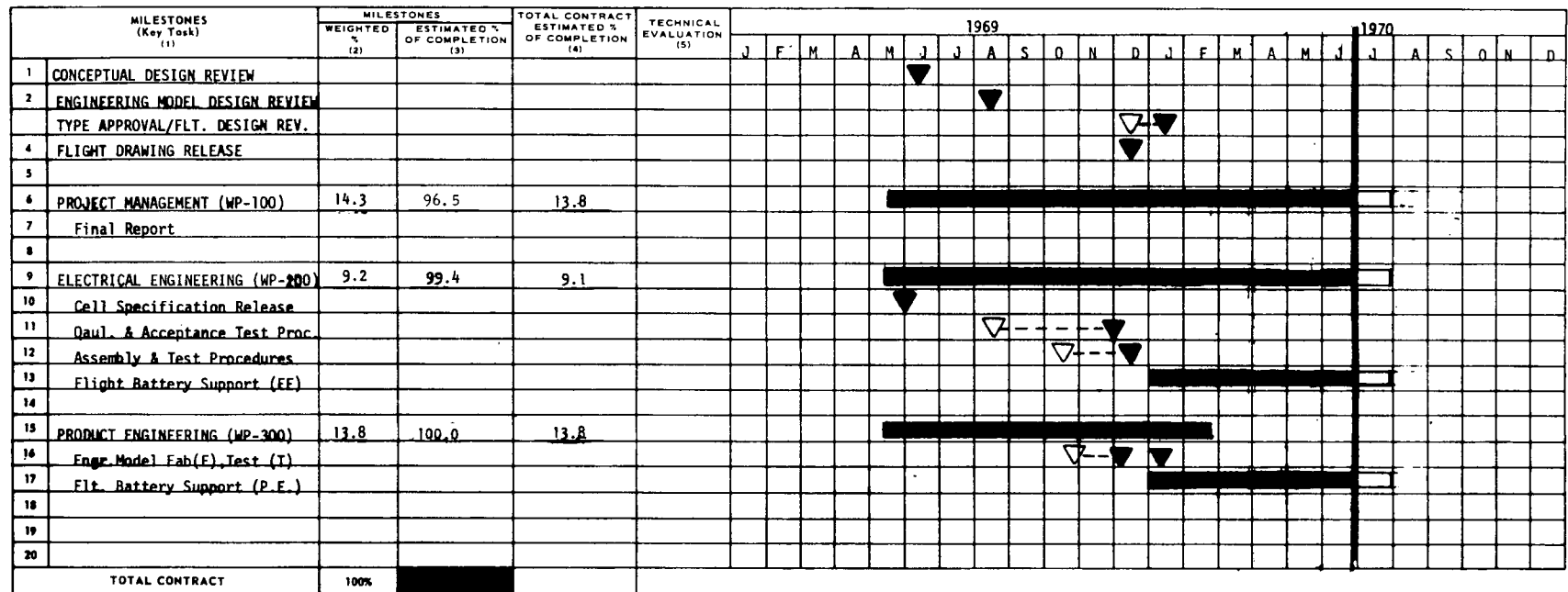


Fig. 2. Mariner Mars 1971 preliminary power profile










DELIVERIES	DATE	STATUS	SCHEDULE LEGEND:
Engineering Model	3/12	Delivered	SPAN TIME 
			STATUS 
T.A. #1 (201)	5/15	Delivered	SCHEDULED 
T.A. #2 (202)	6/5	Delivered	COMPLETED 
PTM (301)	5/22	Delivered	RESCHEDULED 
Sys. Test #1 (302)	7/3		SLIPPAGE ANTICIPATED 
Sys. Test #2 (303)	7/3		ACTUAL SLIPPAGE 
Flt. #1 (304)	7/14		
Flt. #2 (305)	7/14		
Flt. #3 (306)	6/30		
Flt. #4 (307)	6/30		

Fig. 3. Mariner Mars 1971 battery system milestone schedule

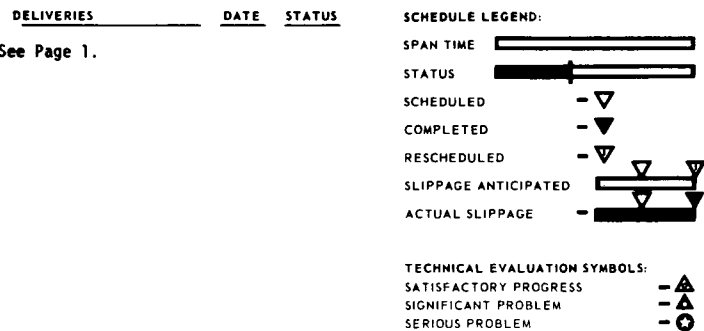


Fig. 3 (contd)

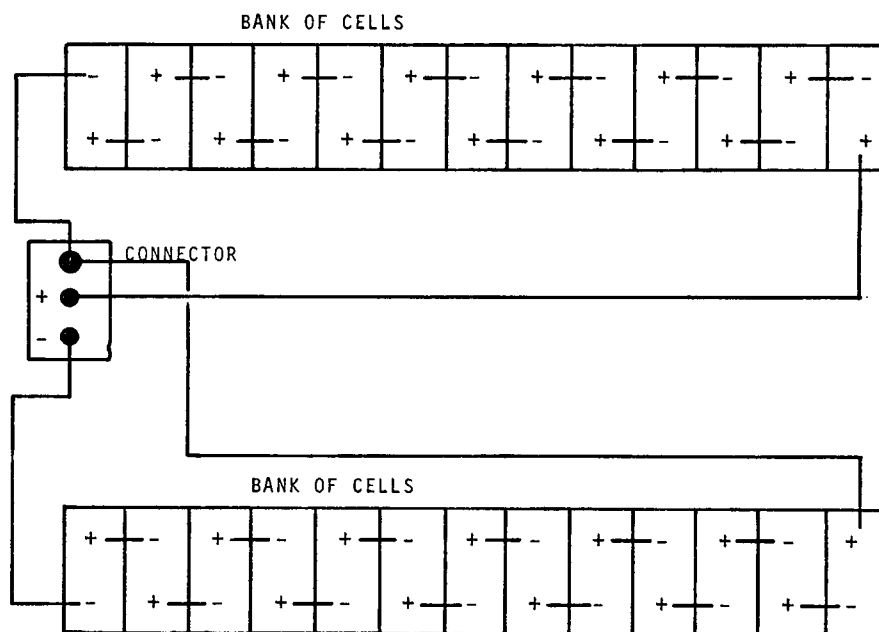


Fig. 4. Battery wiring layout

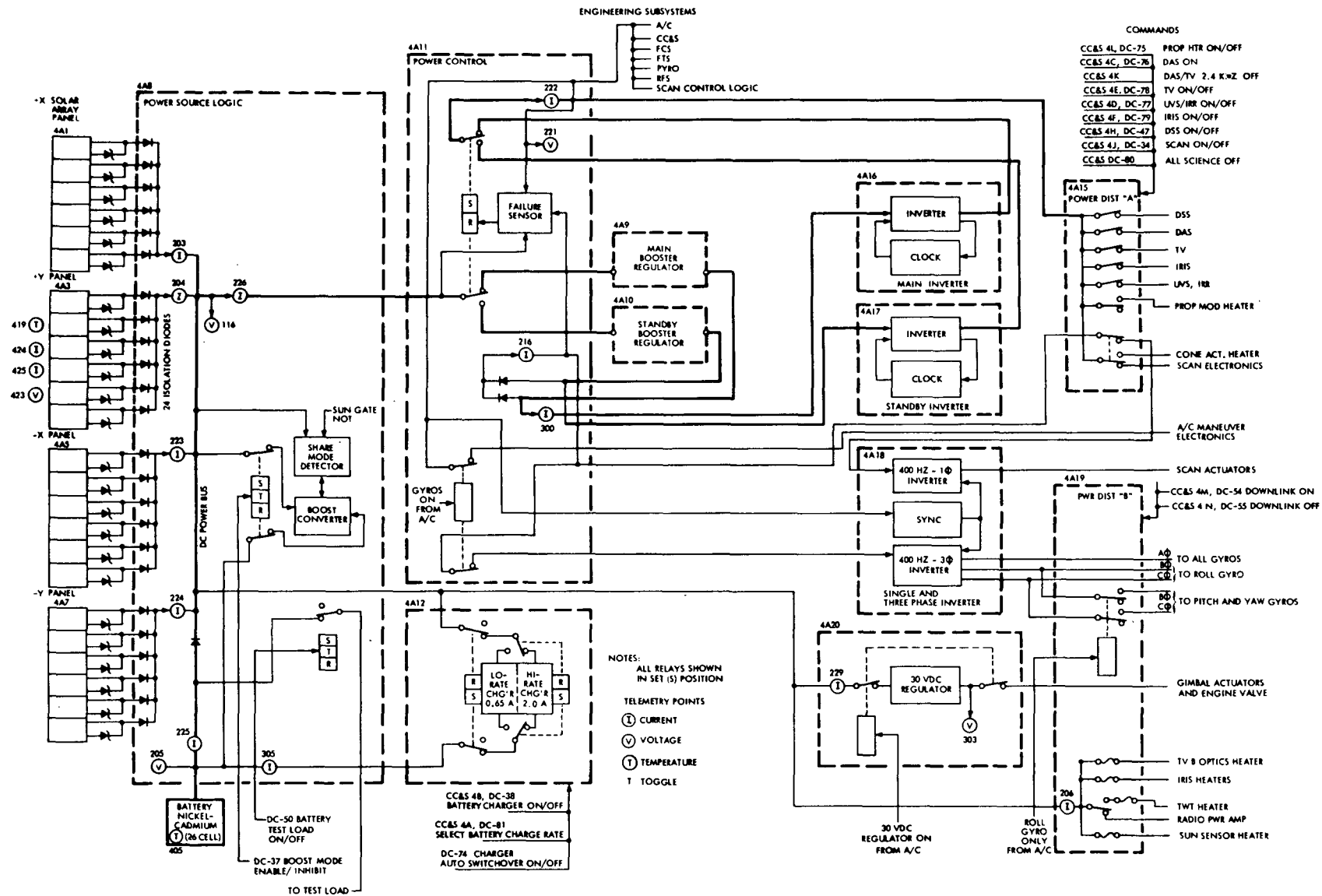


Fig. 5. Power subsystem functional block diagram

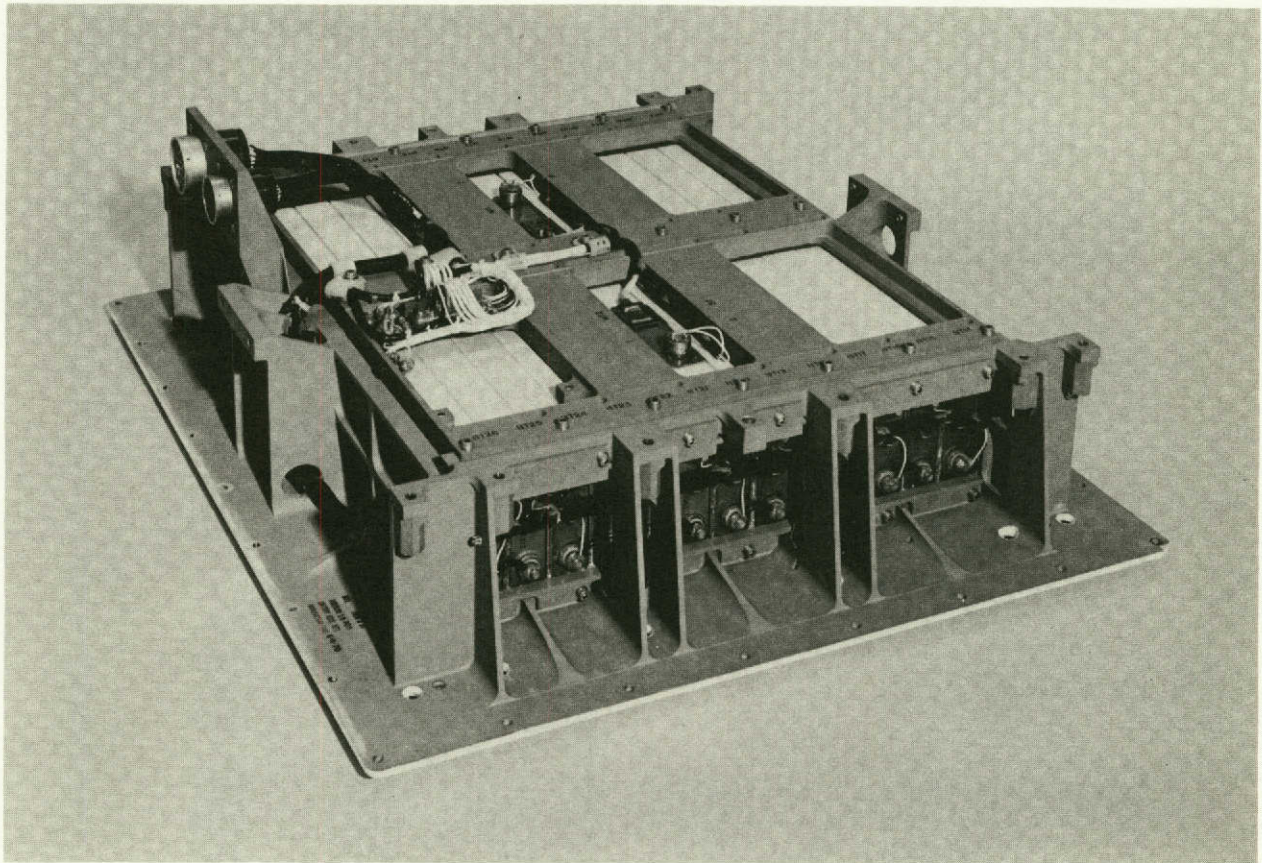


Fig. 6. Engineering model battery

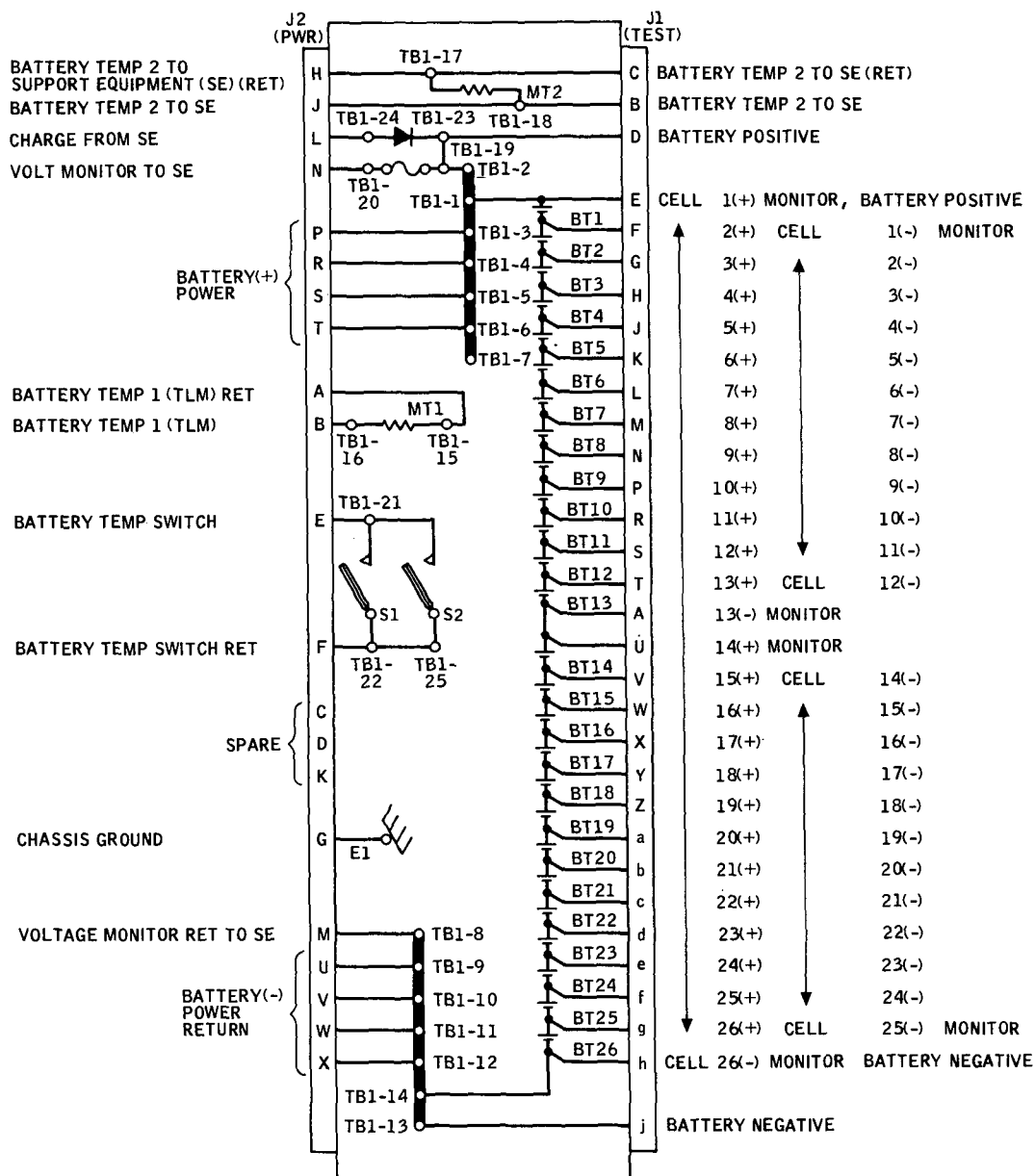


Fig. 7. Battery wiring schematic

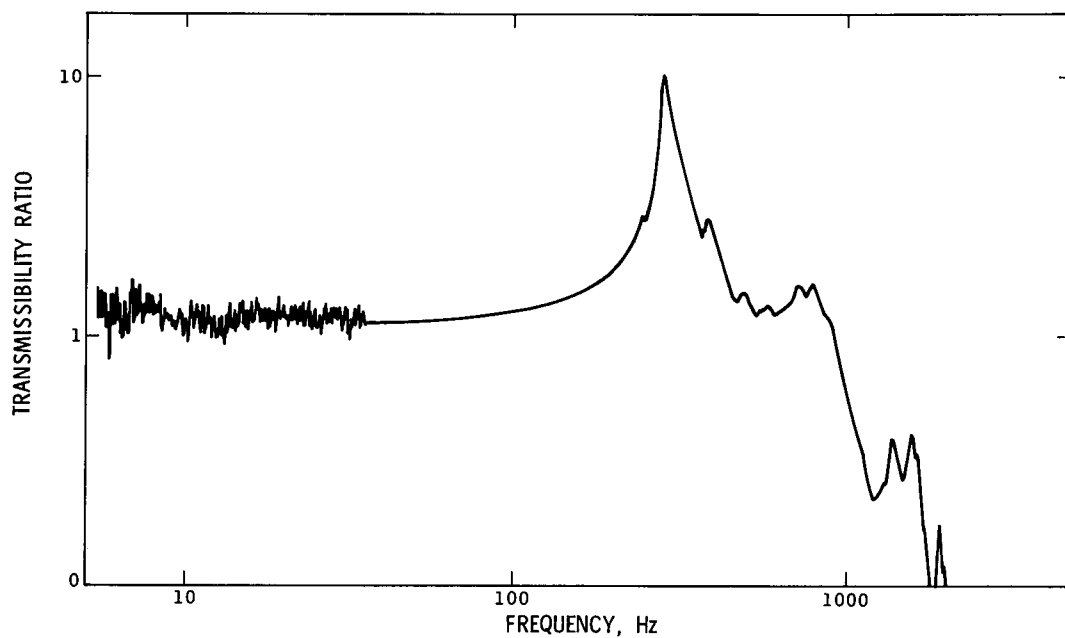


Fig. 8. Typical plot of data

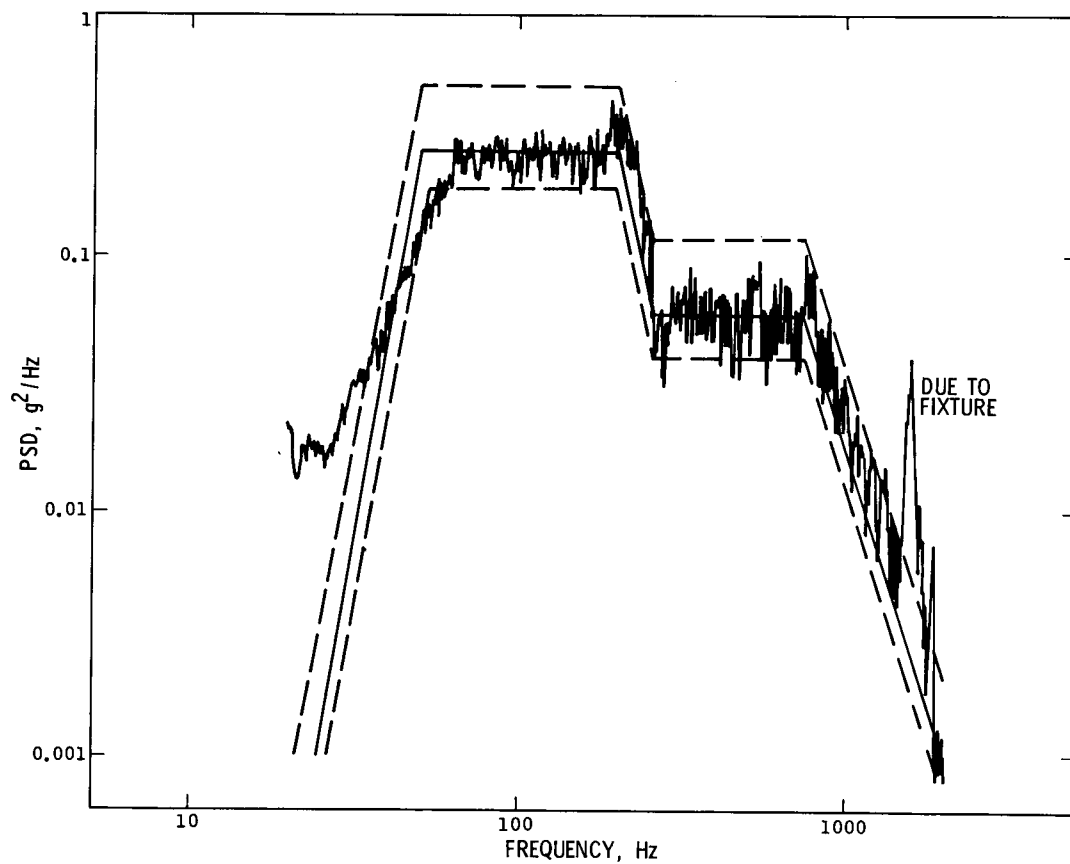


Fig. 9. Power spectral density plot

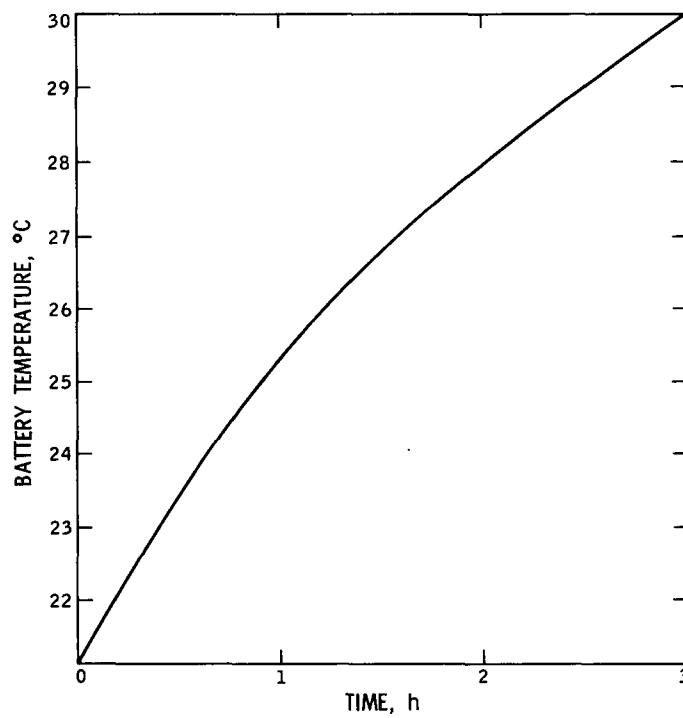
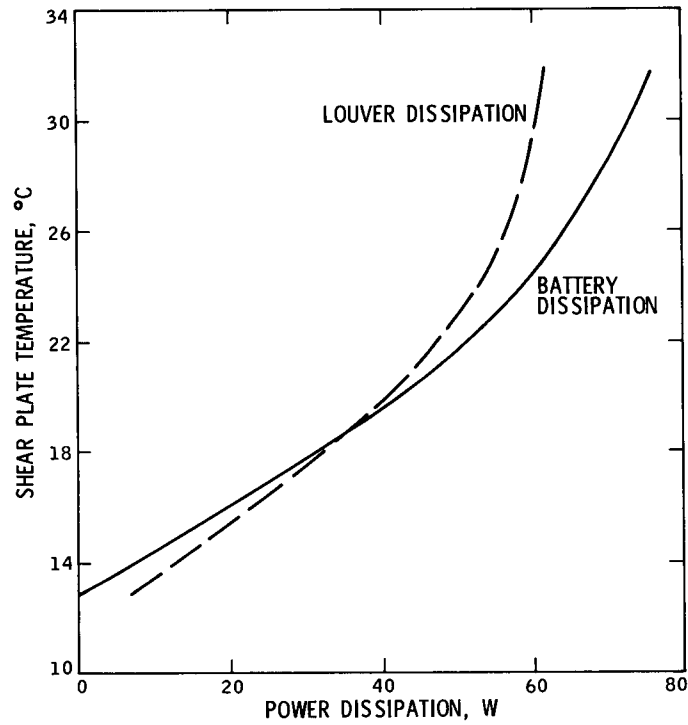


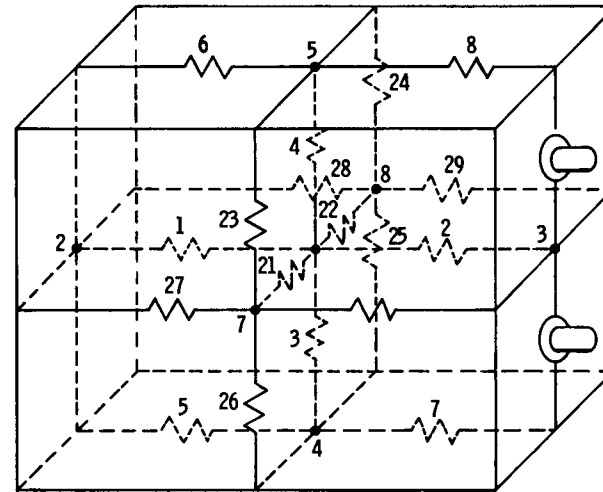
Fig. 10. Transient response of battery for 76-W dissipation bus temperature constant at 27°C (80°F), louver operating range



RUN TEMPERATURE 21°C (70°F) (CONSTANT)
LOUVER OPERATING RANGE 13-27°C (55-80°F)

Fig. 11. Shear plate temperature (battery case) vs battery and power dissipations

ALL OTHER CELLS ARE IDENTICAL WITH THE DRAWING BELOW EXCEPT FOR MODE AND RESISTANCE NUMBERS WHICH CHANGE BY 10 AND 40 RESPECTIVELY FOR EACH CELL



R_{18} CONNECTS THE FACE OF ONE CELL TO THE NEXT

Fig. 12. Thermal network for first cell

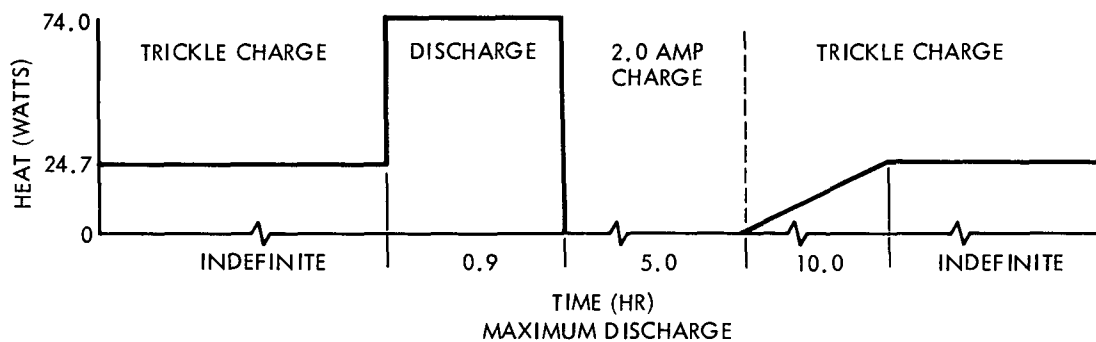
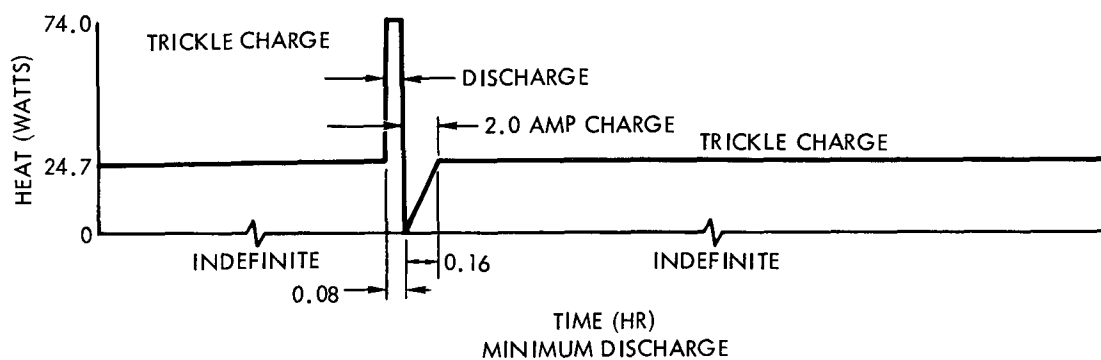
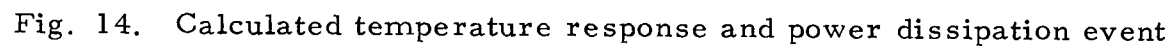


Fig. 13. Power dissipations



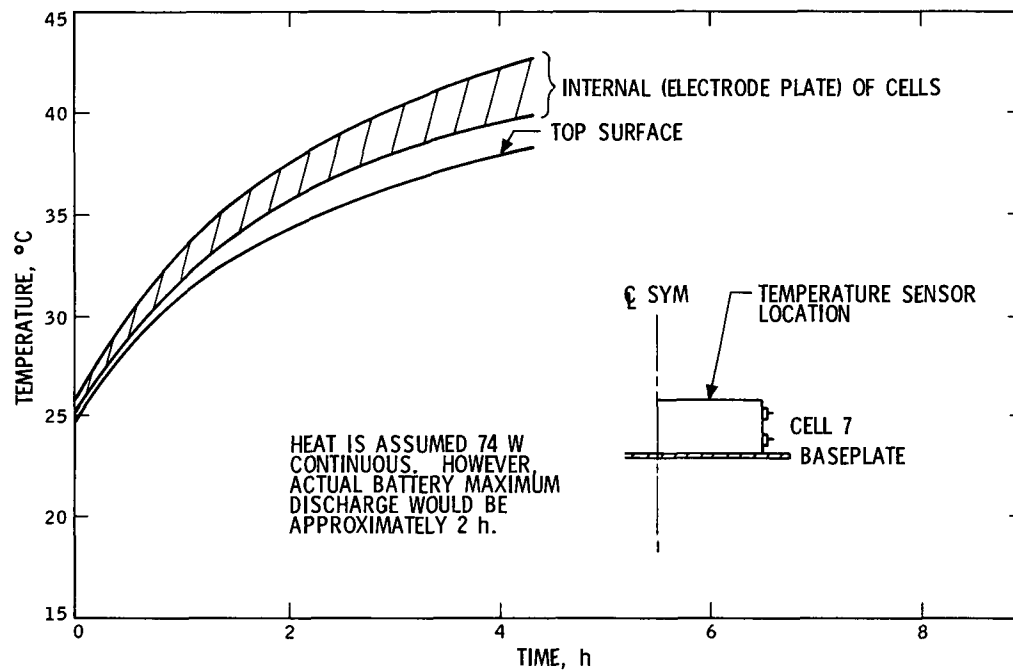


Fig. 15. Calculated internal cell temperature response for continuous 74-W dissipation

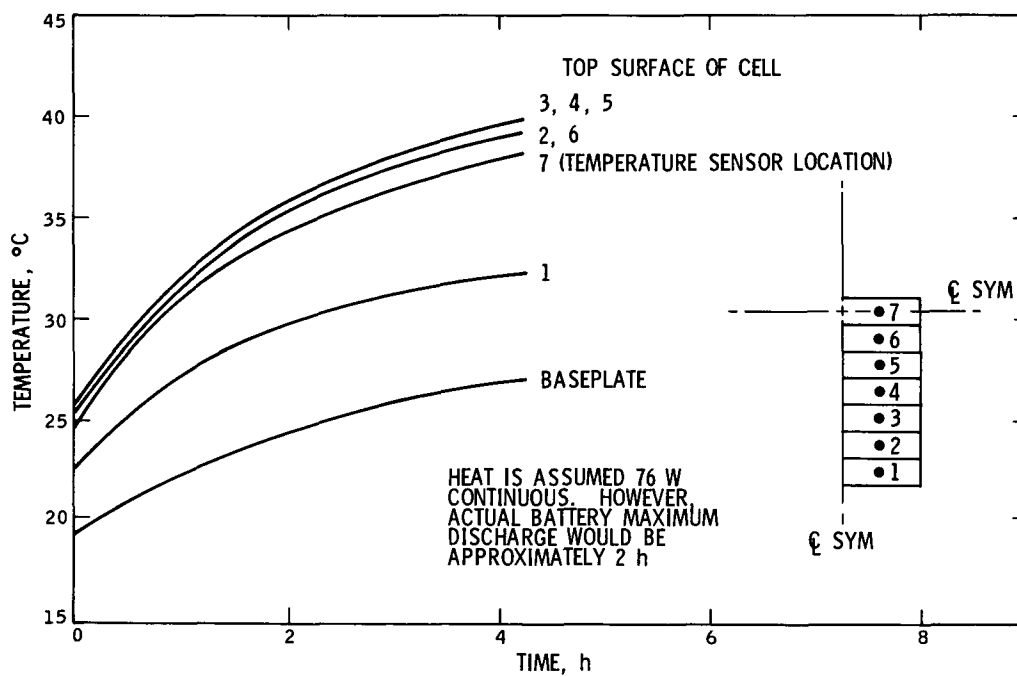


Fig. 16. Calculated temperature response at various locations for 74-W dissipation

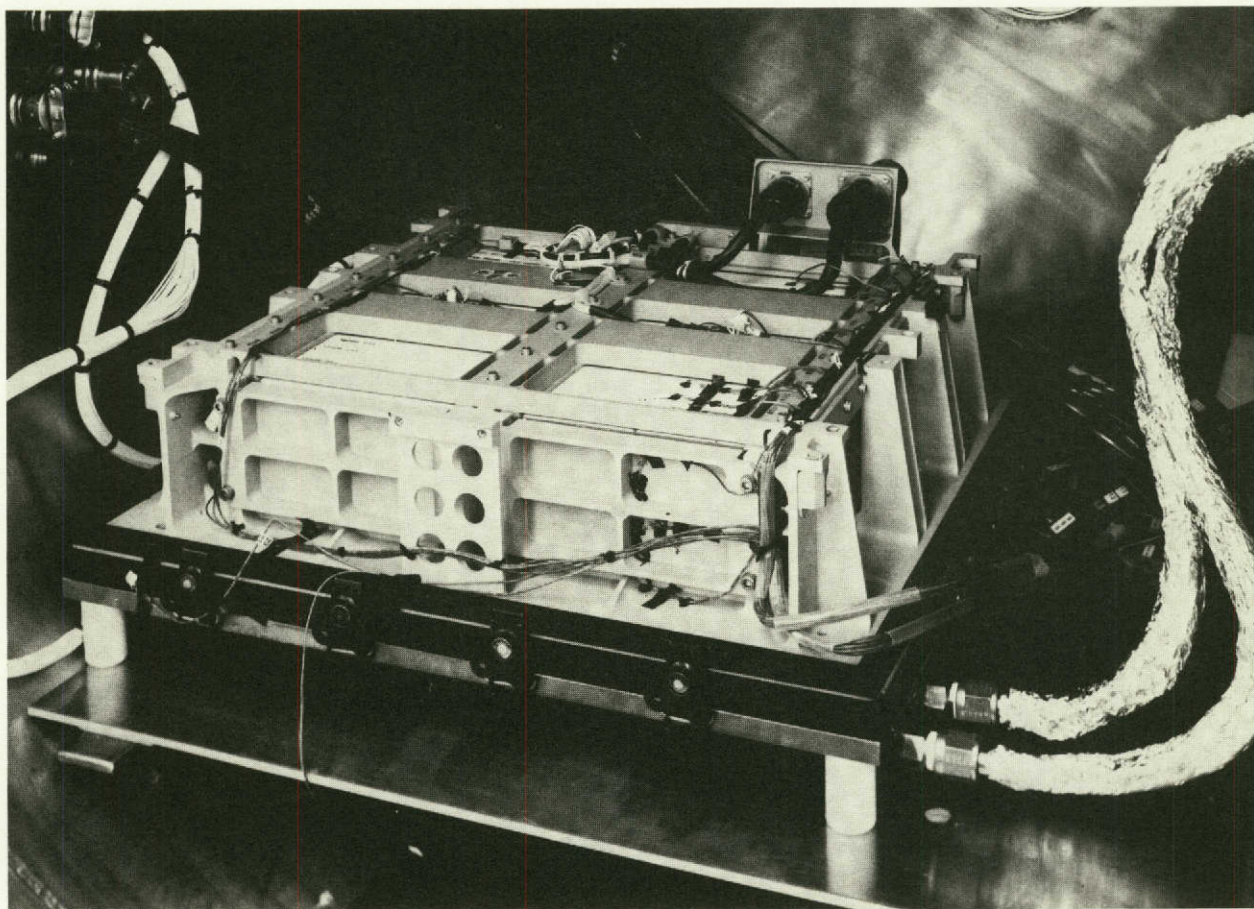


Fig. 17. Test setup, thermal vacuum

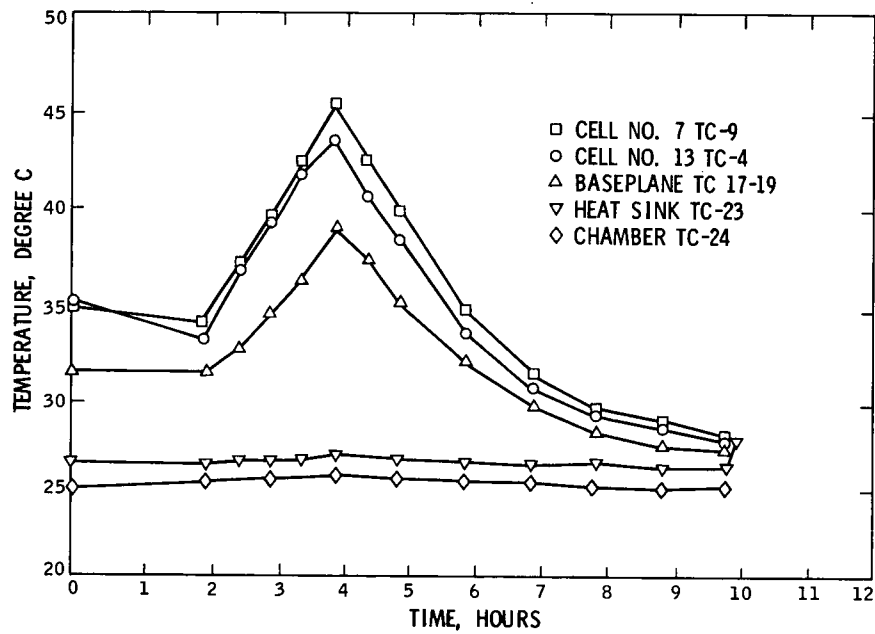


Fig. 18. Temperature measurements during high-temperature thermal vacuum test

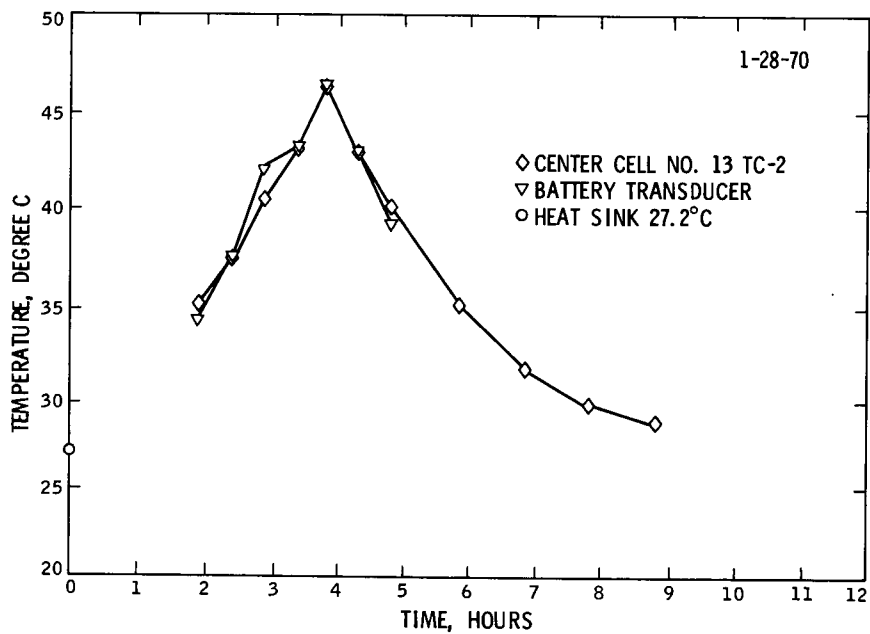


Fig. 19. Temperature measurements during high-temperature thermal vacuum test

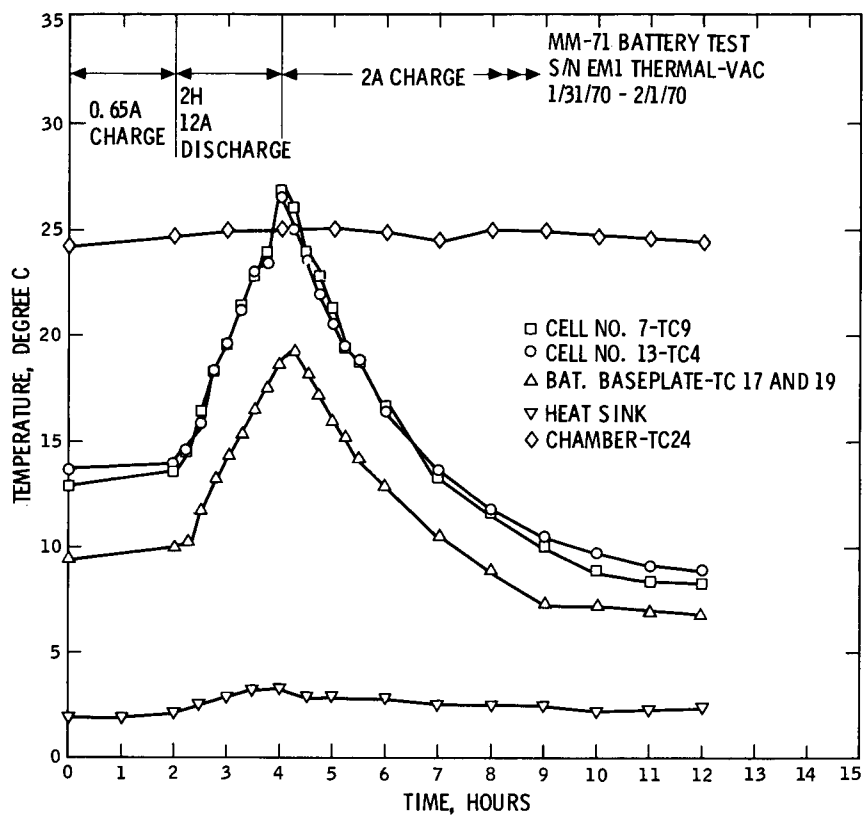


Fig. 20. Temperature recorded during low-temperature thermal vacuum test

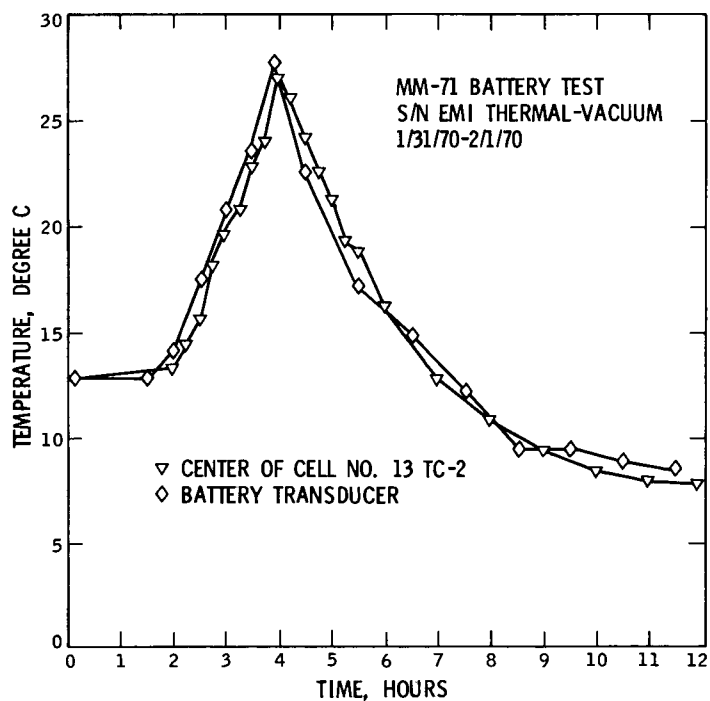


Fig. 21. MM '71 battery test, EM-1 thermal-vacuum

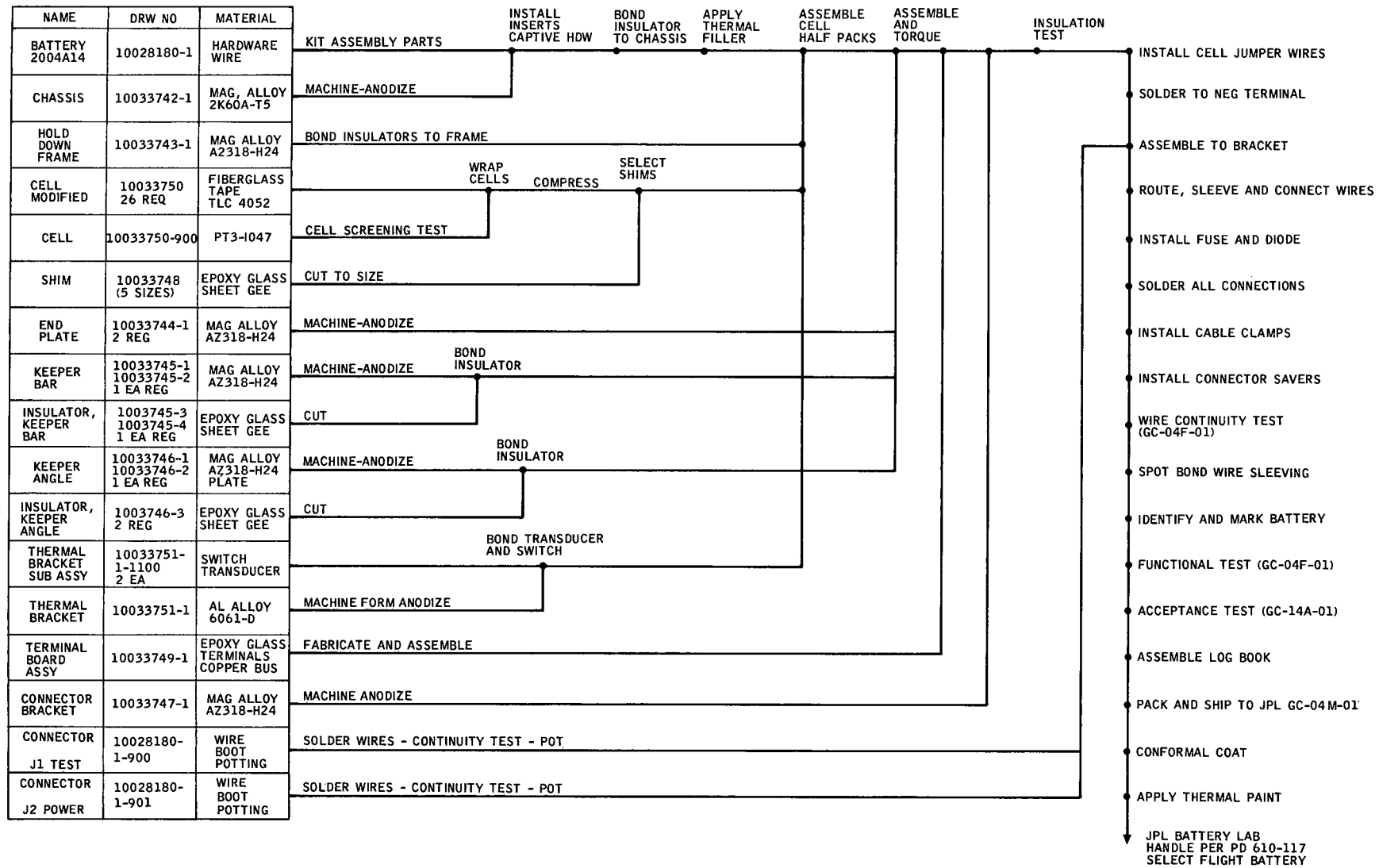


Fig. 22. Manufacturing flow diagram

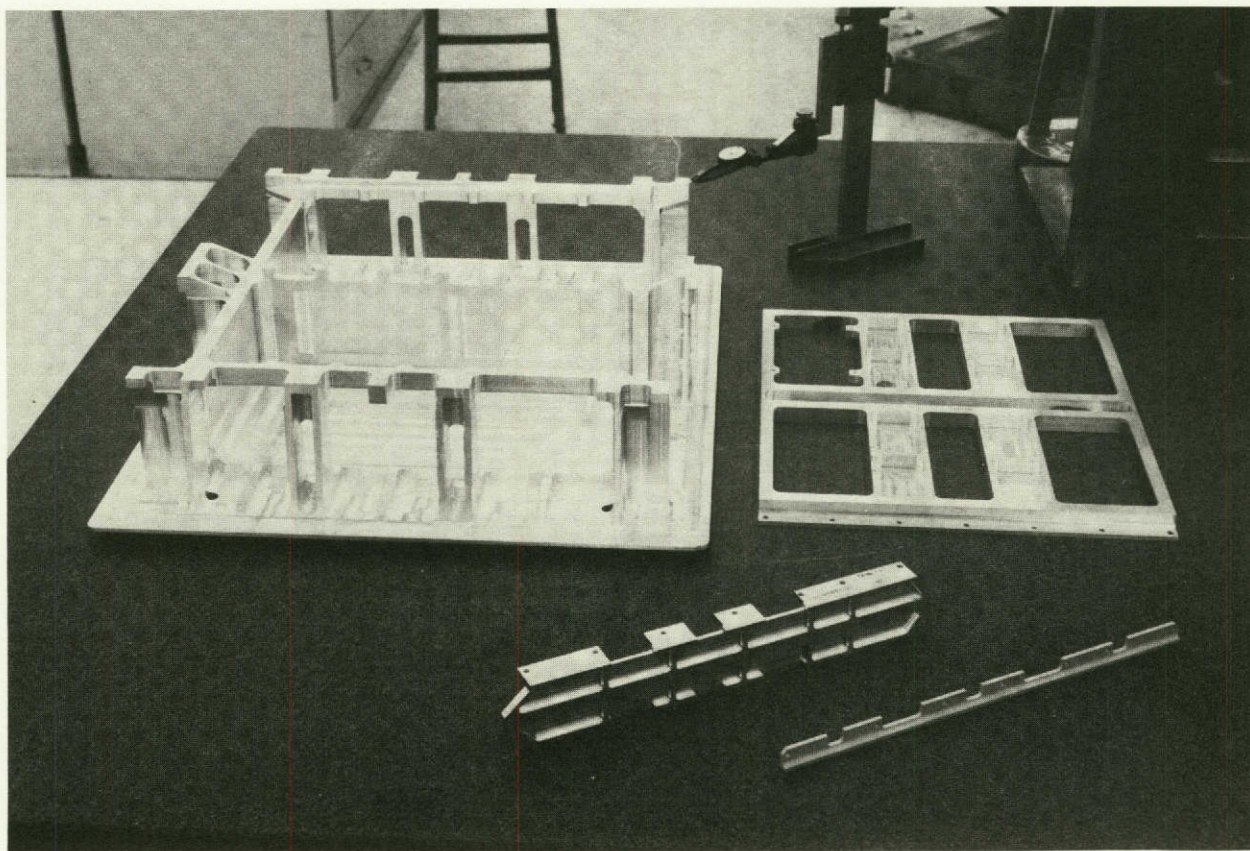


Fig. 23. Inspection of rough-machined chassis

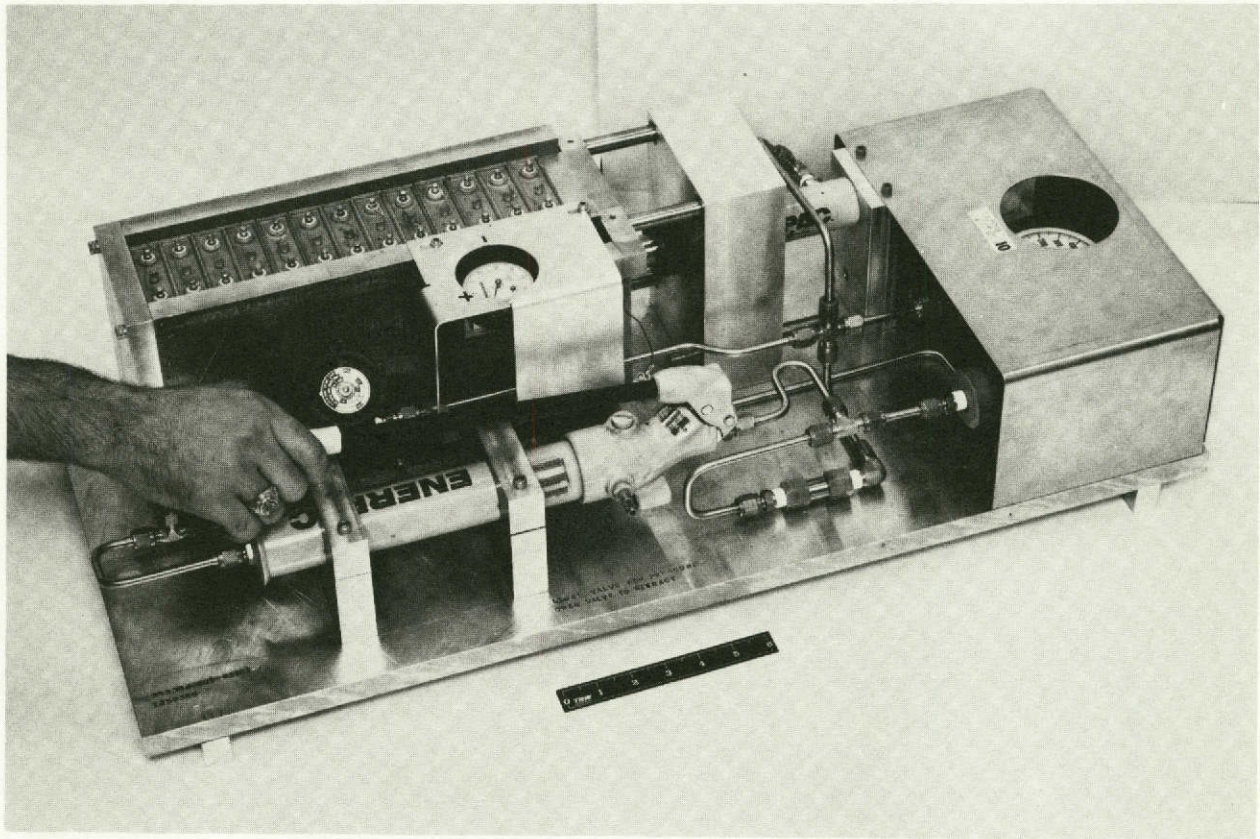


Fig. 24. Cell compression operation

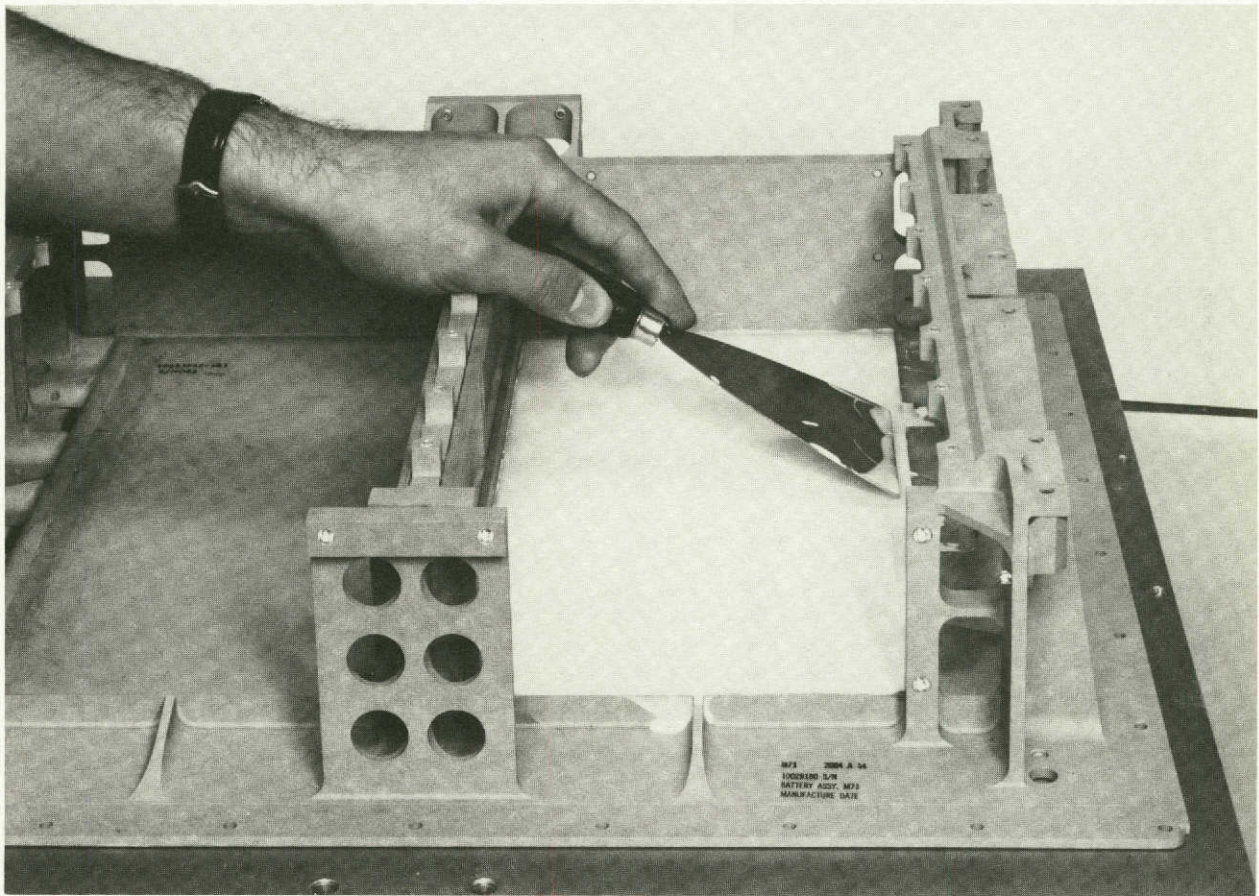


Fig. 25. Application of RTV thermal filler before cell installation

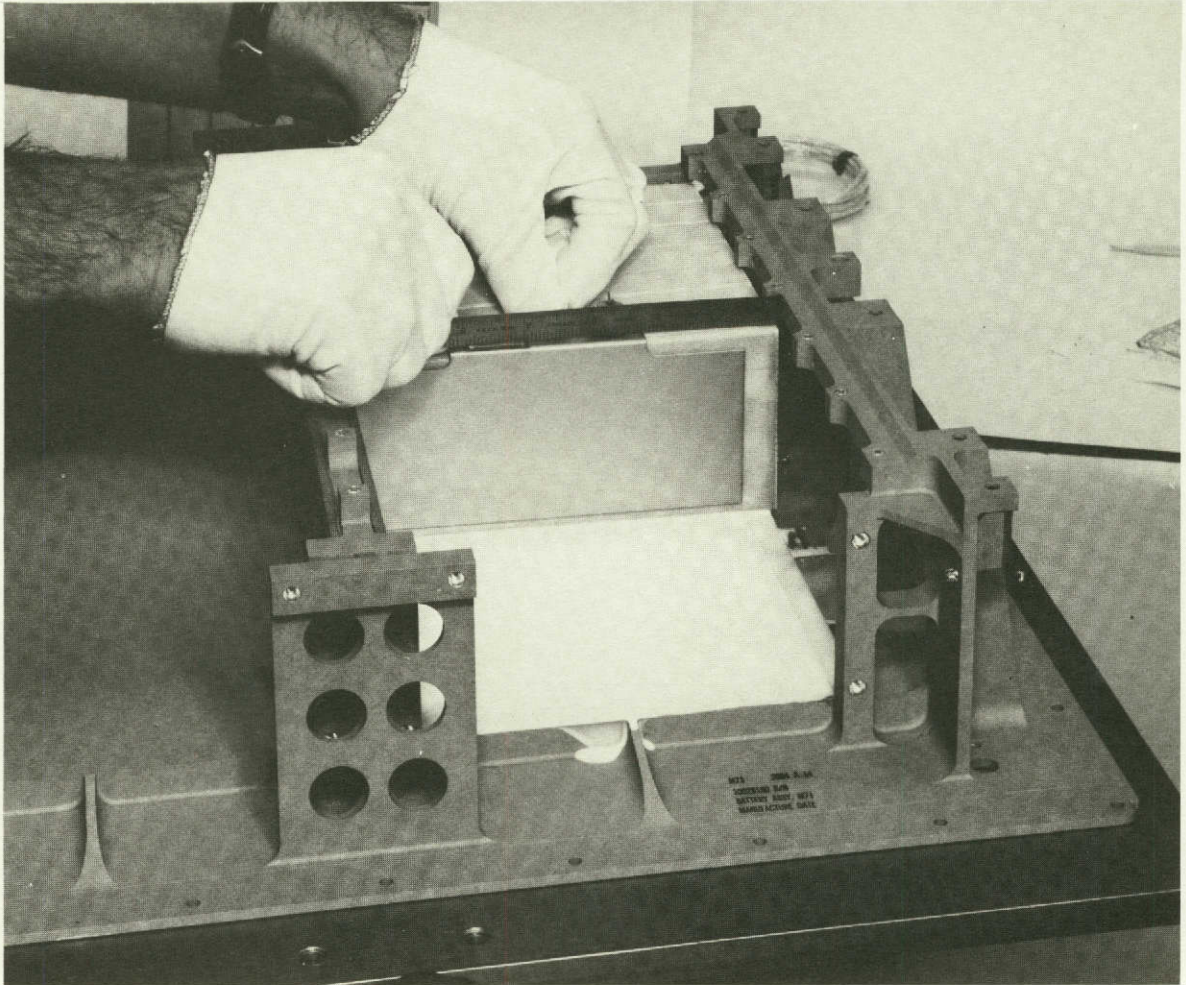


Fig. 26. Cell and thermal bracket installation

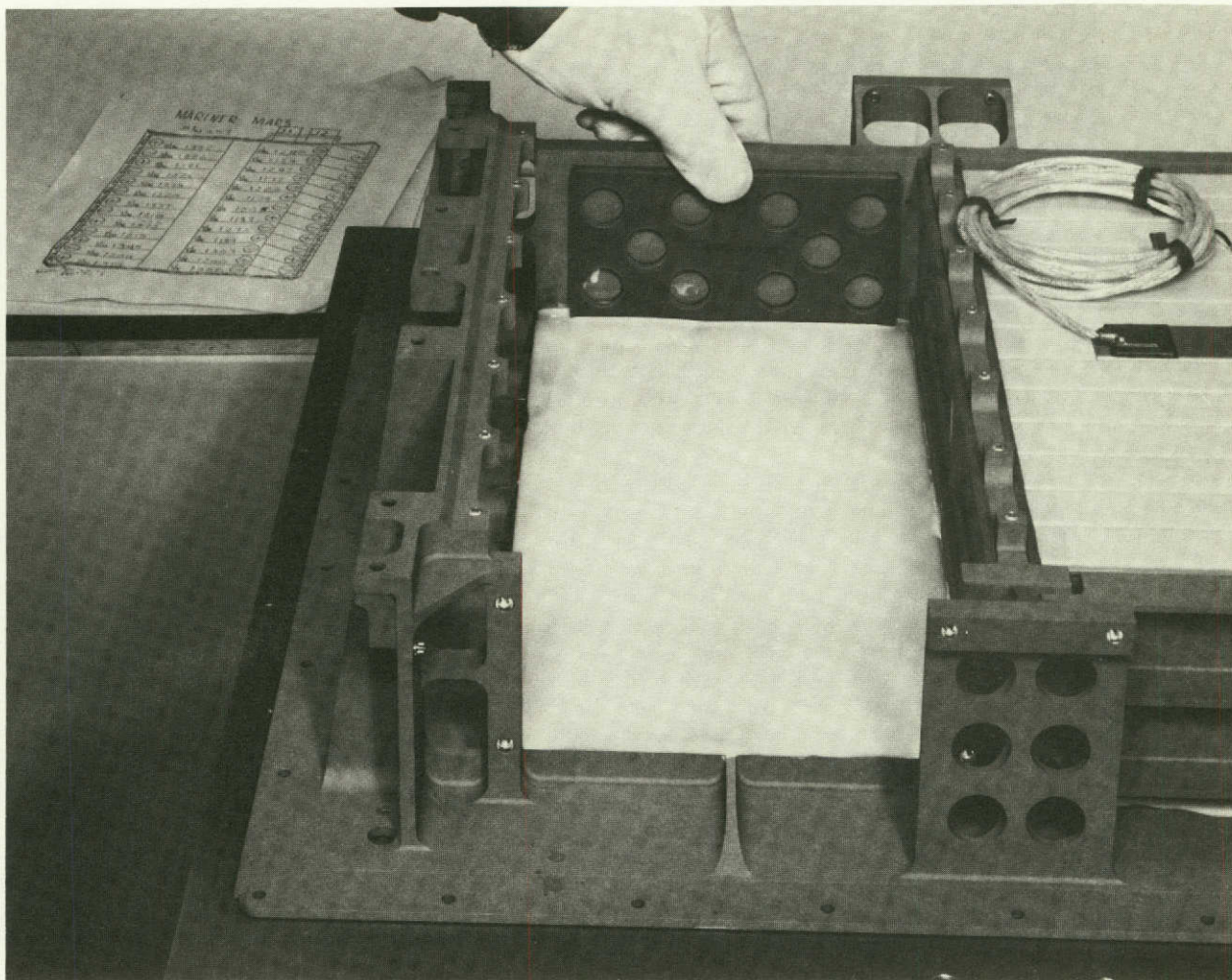


Fig. 27. Shims and cell installation

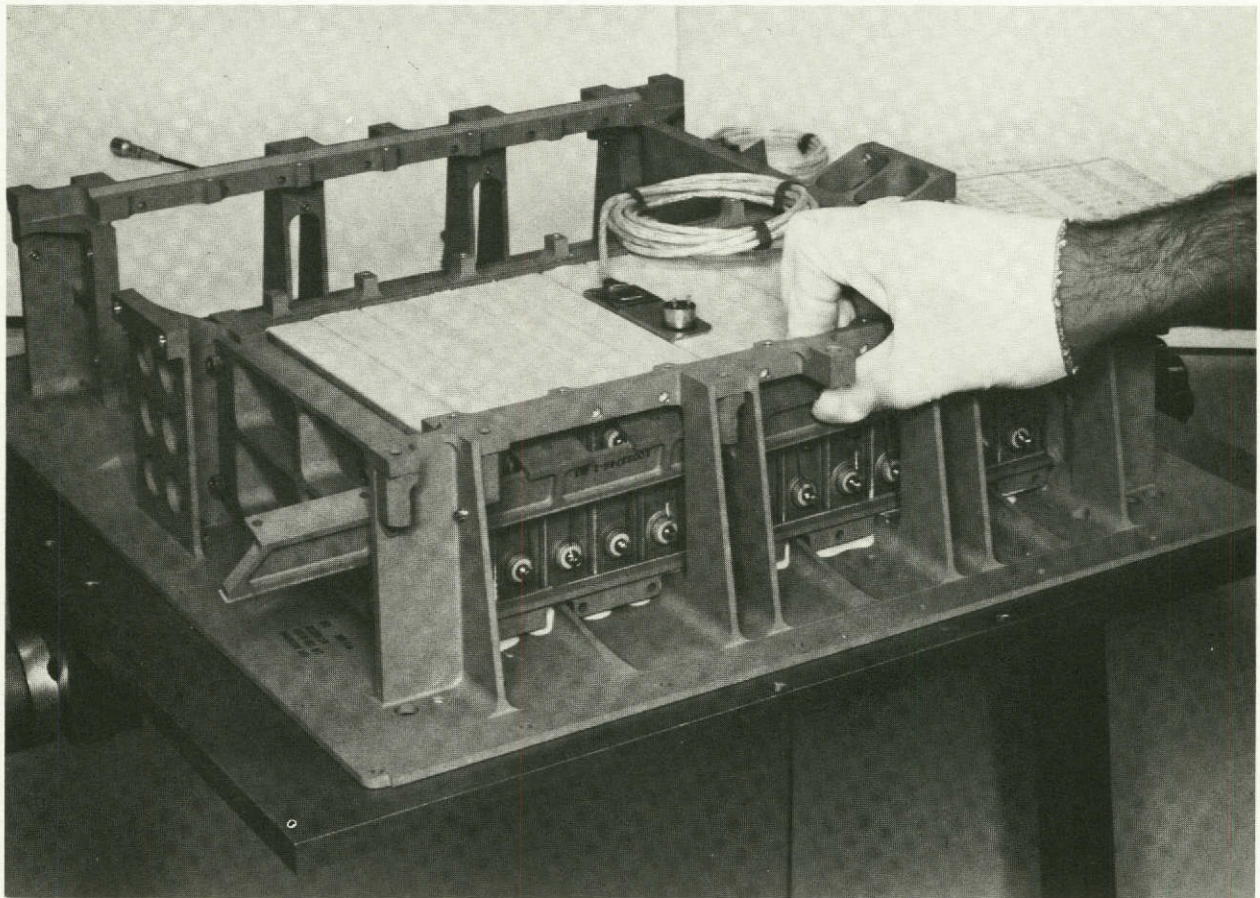


Fig. 28. Keeper angle installation with keeper bar and end plate in place

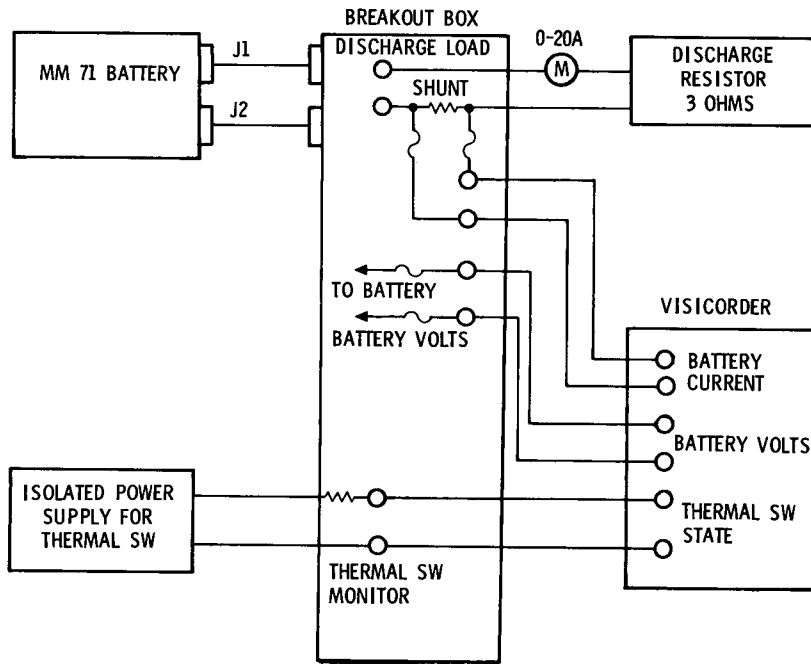


Fig. 29. Battery instrumentation for vibration tests

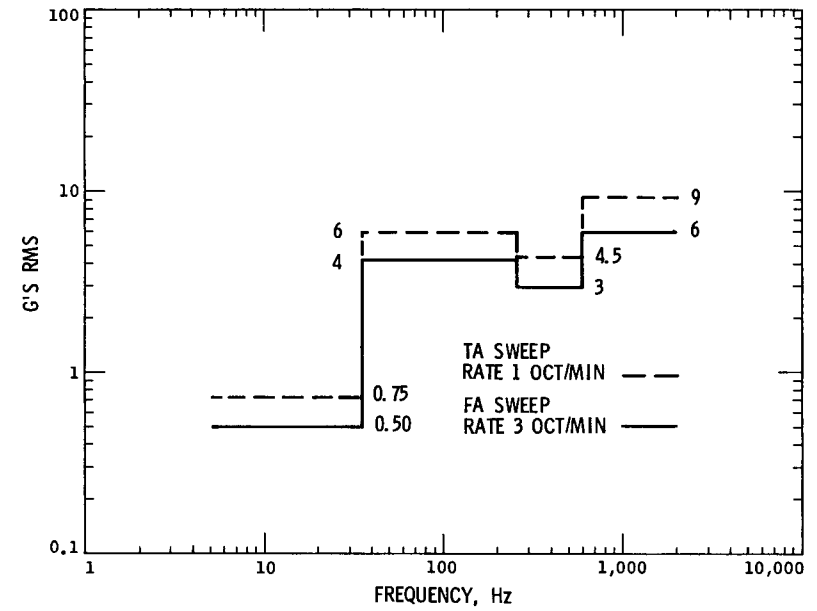


Fig. 30. Battery assembly sine vibration tests

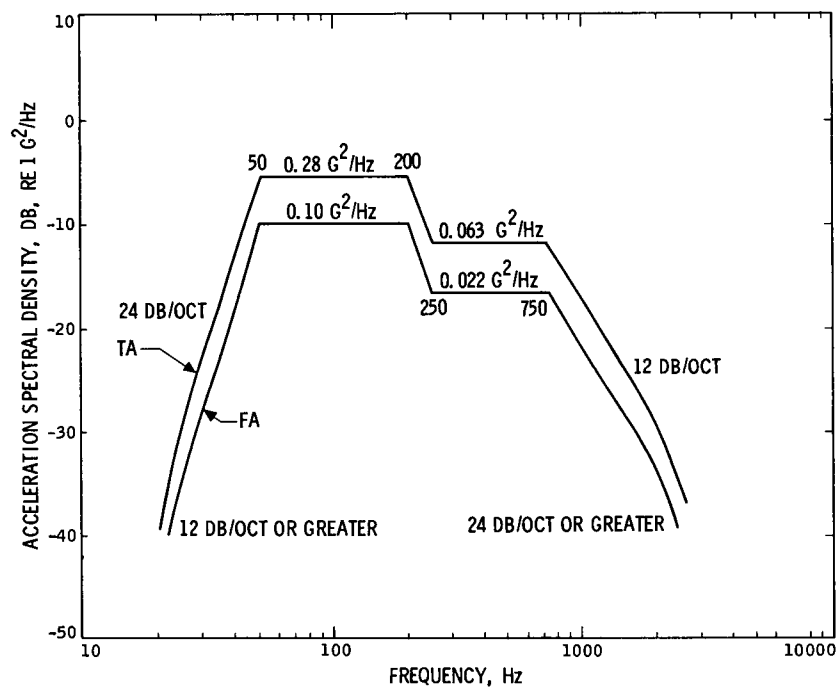


Fig. 31. Battery random vibration test

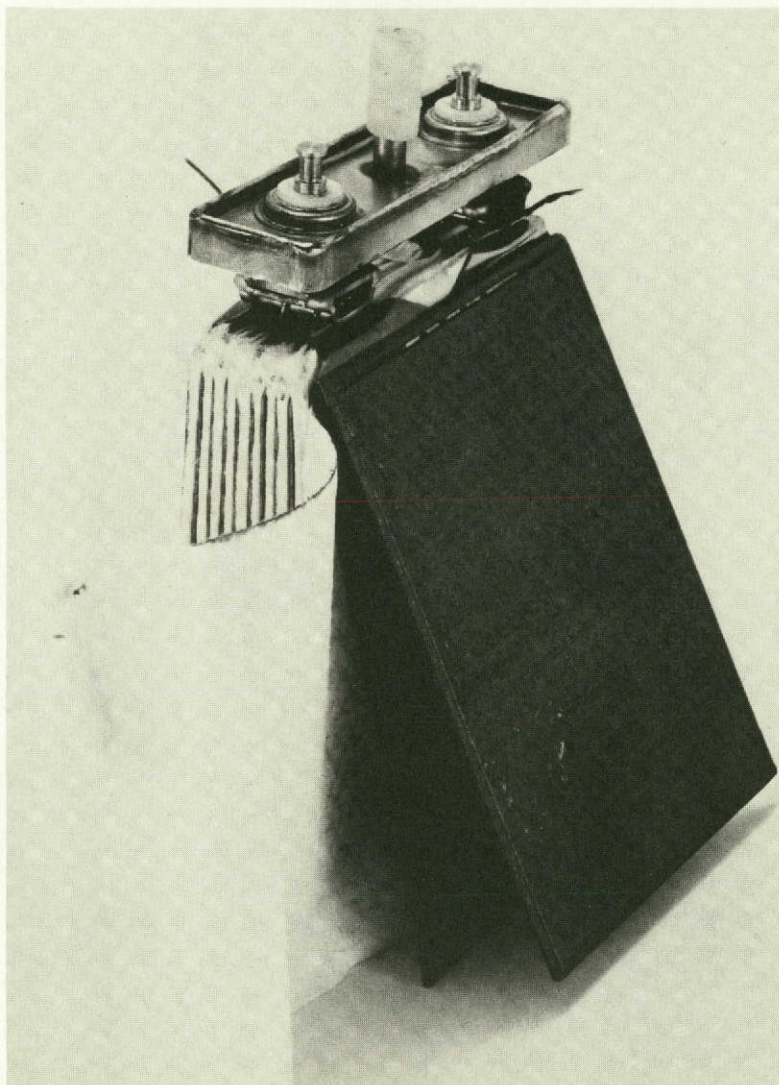


Fig. 32. Cutaway of Ni-Cd cell, 20-Ah Gulton

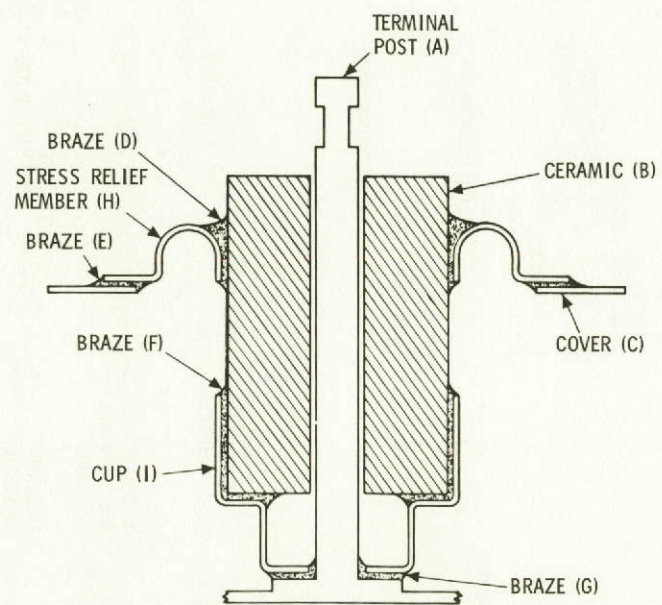


Fig. 33. Gulton ceramic-to-metal terminal seal

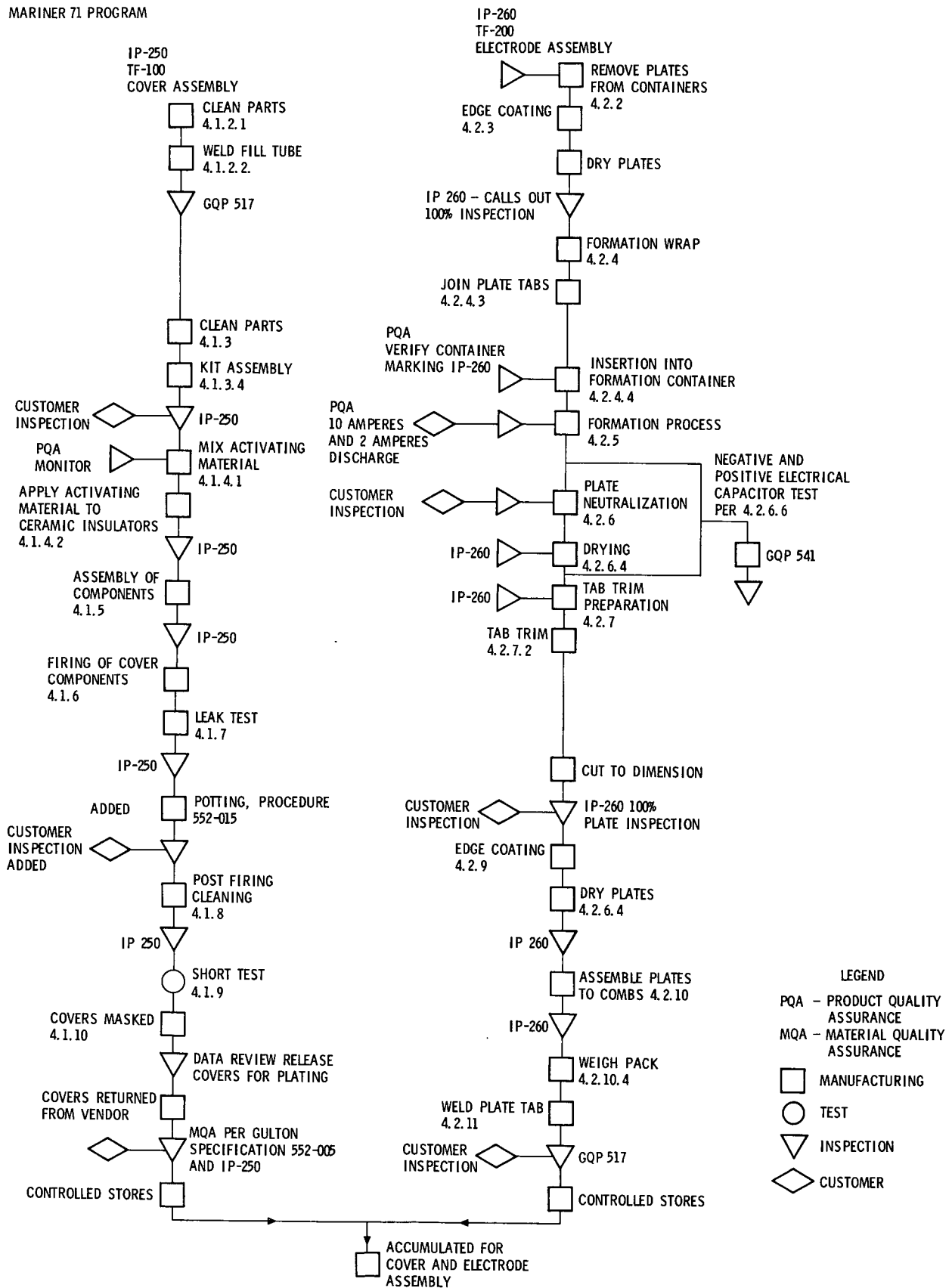


Fig. 34. Cell manufacturing flow plan

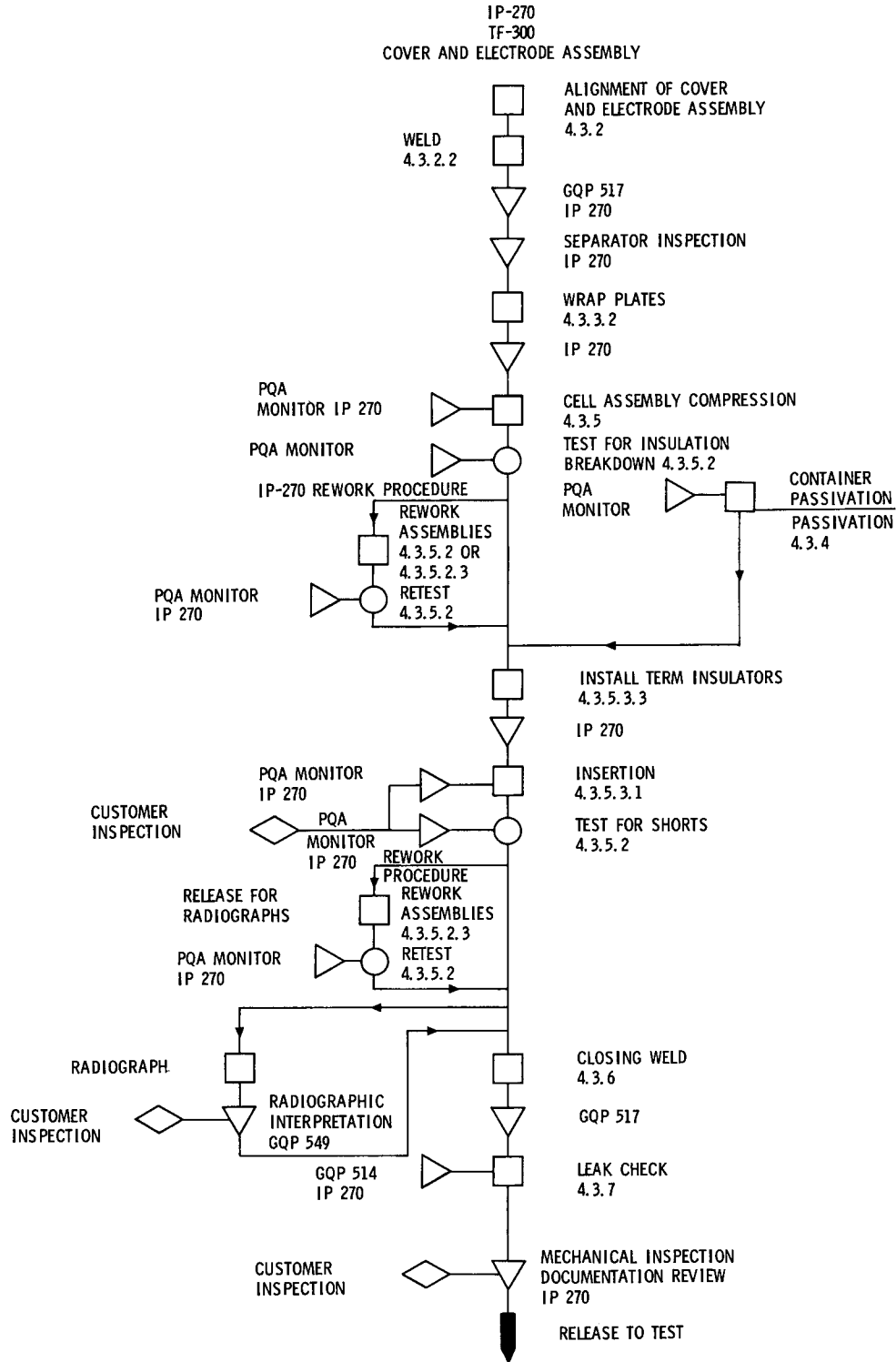


Fig. 34 (contd)

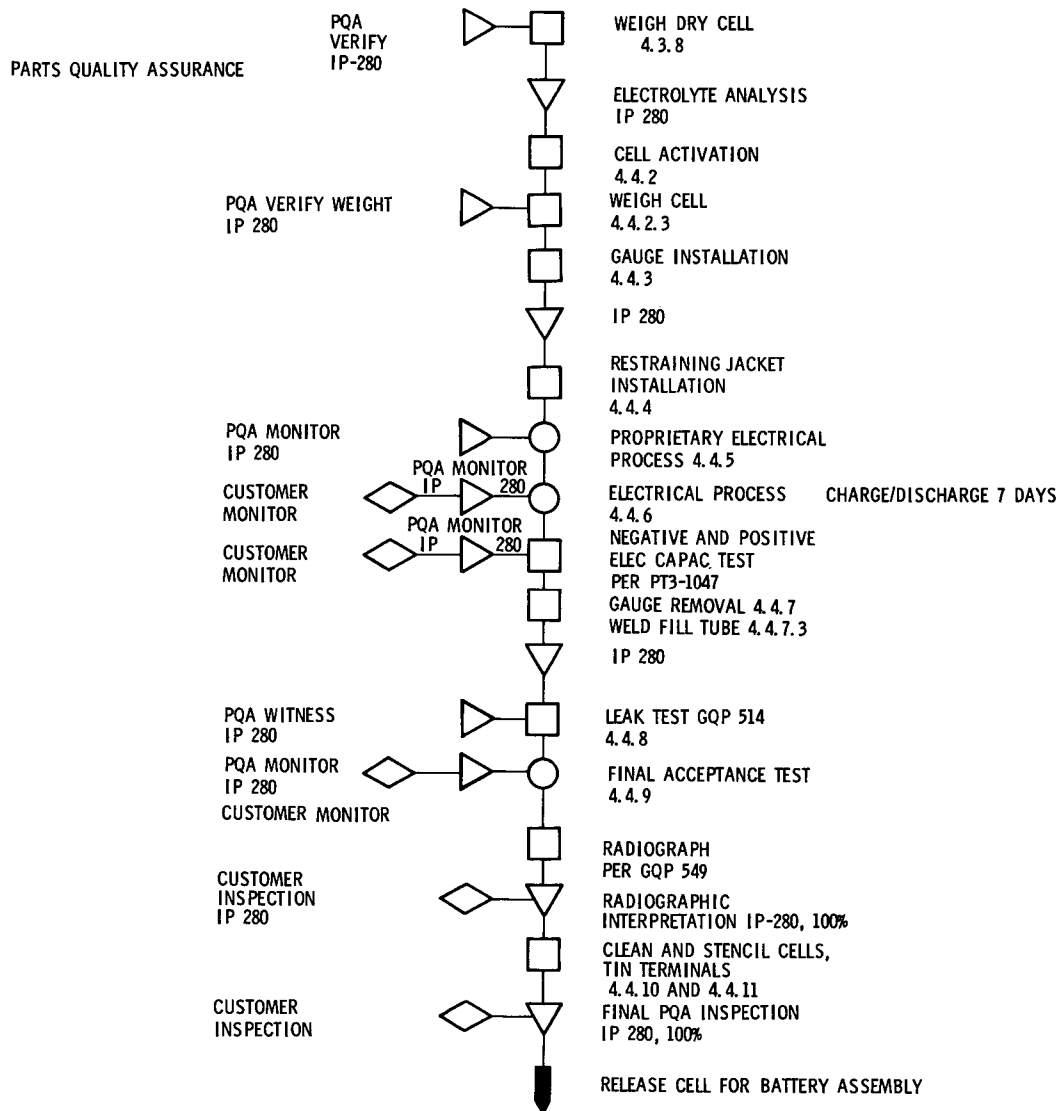


Fig. 34 (contd)

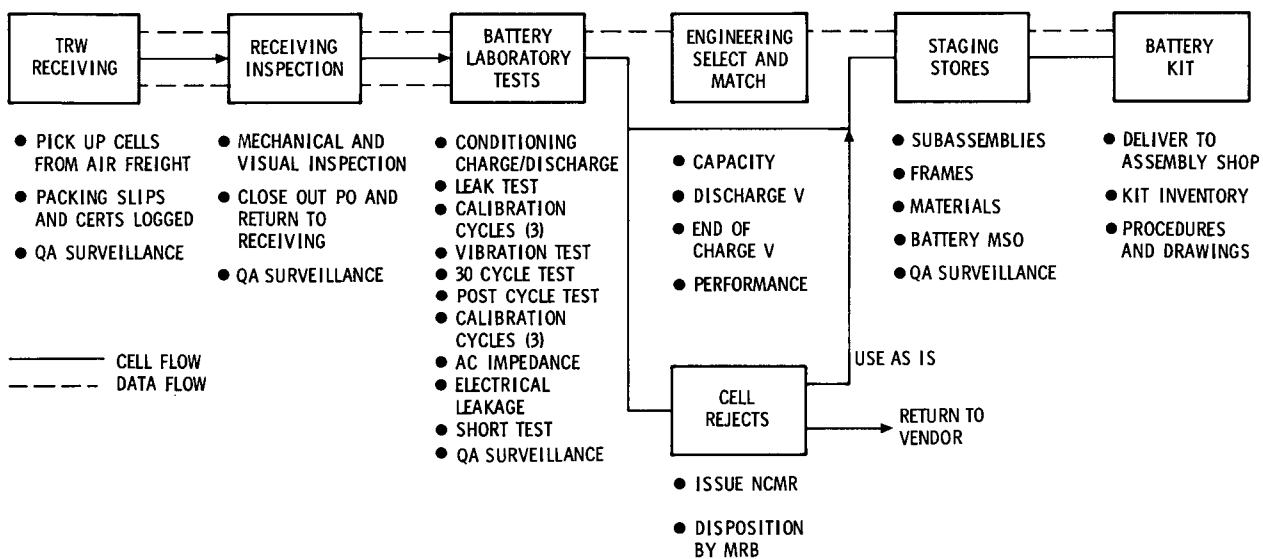


Fig. 35. Cell receiving and test flow

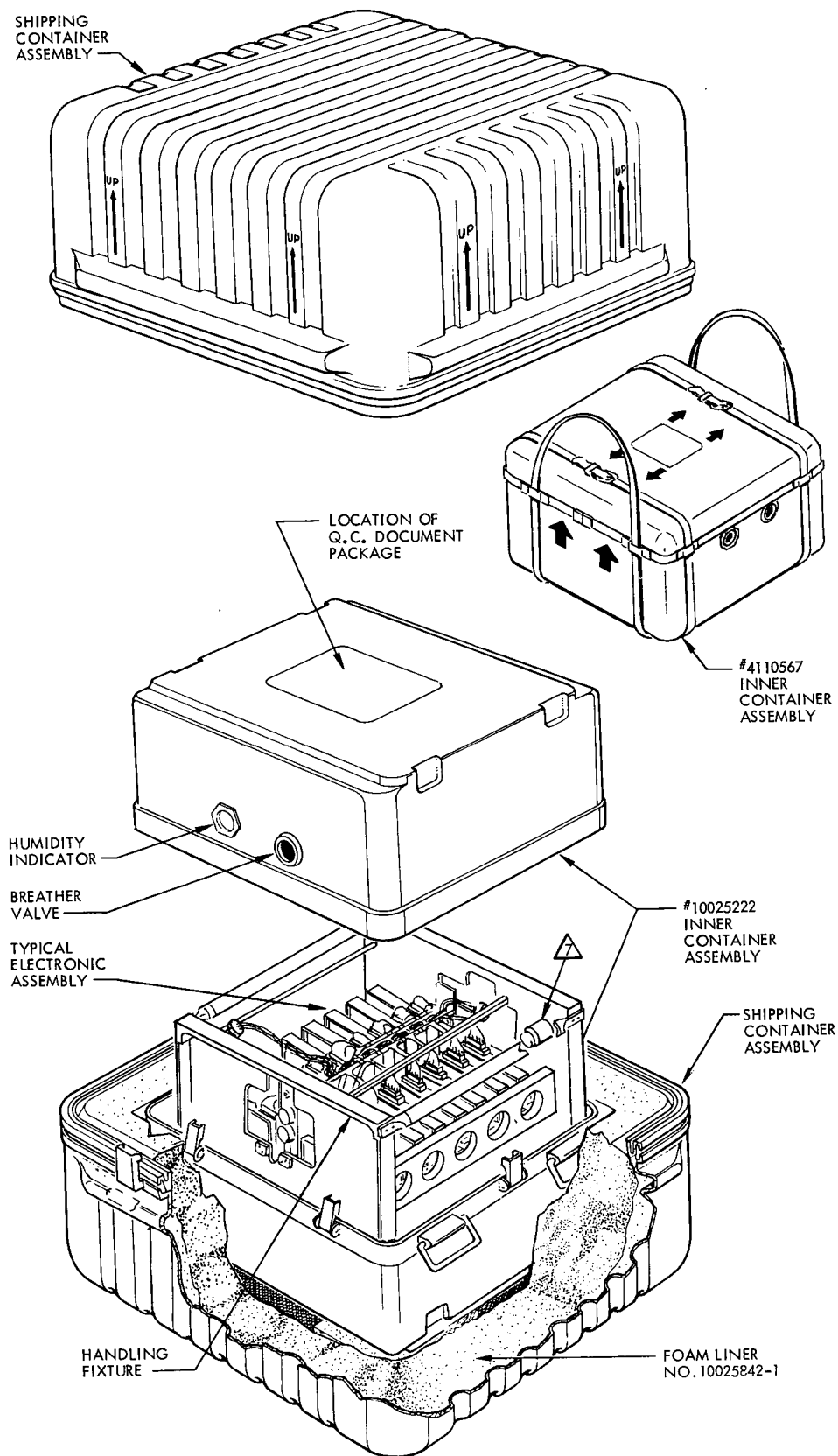


Fig. 36. Electronic assembly shipping container assembly

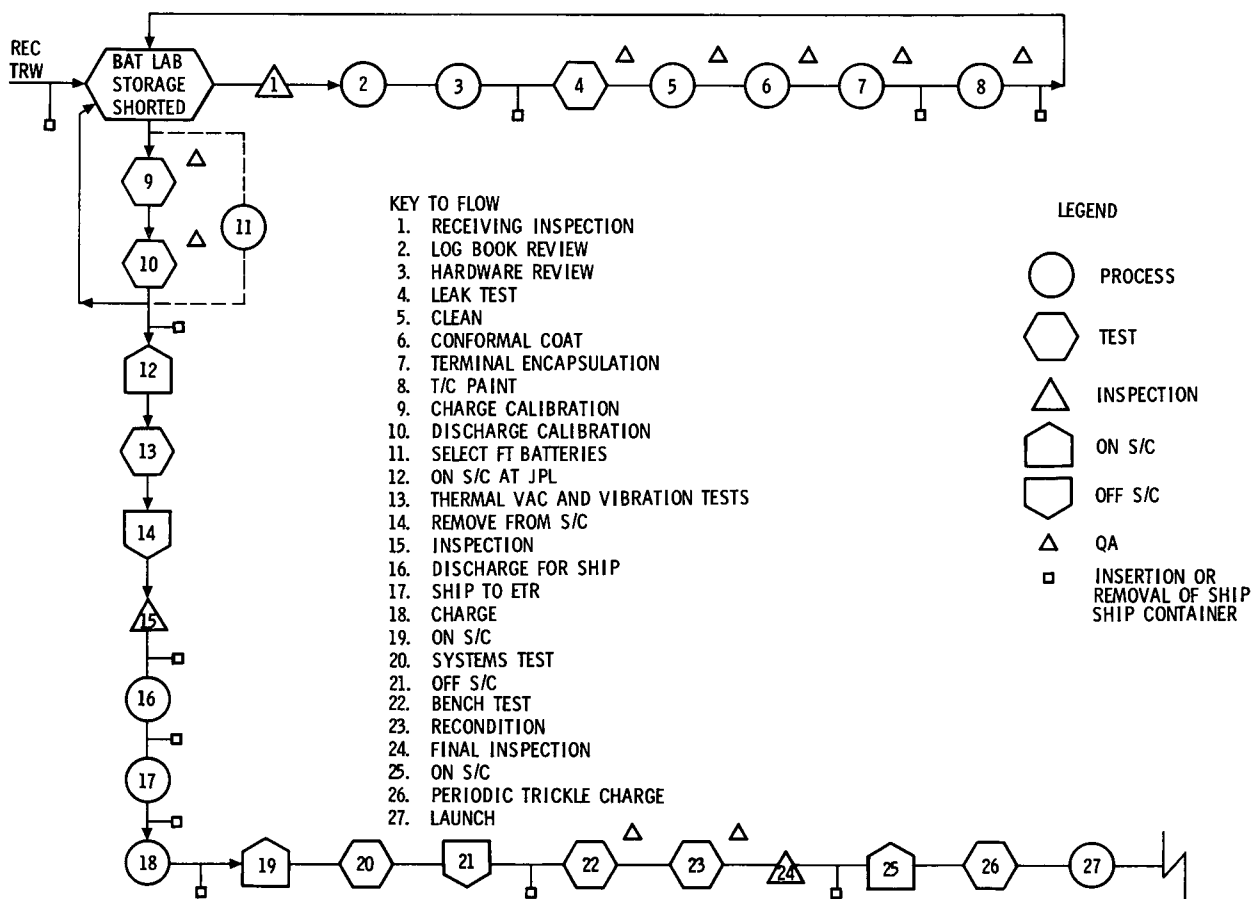


Fig. 37. Battery handling flow plan

EVENT	OCT	NOV	DEC	JAN	FEB	MARCH	APR	MAY
	4 11 18 25	1 8 15 22 29	6 13 20 27	3 10 17 24 31	7 14 21 28	7 14 21 28	4 11 18 25	2 9 16 23
CYCLE BATS ^(a)	■	■	■	■	■	■	■	
RECEIVING INSPECTION	■	■						
LEAK TEST INSPECTION	■	■						
CLEAN AND INSPECTION	■	■						
CONF COAT AND ENCAP	■	■						
PAINT	■	■						
PHOTO AND SELECT FLT BAT		■						
DELIVER TO SAF FOR STV AND VIB		▲	▲					
SHIP TO CAPE FLT AND SPARE ^(b)				▲	▲	▲		
BENCH TEST AND INSPECT				PTM				
BACK ON FLT S/C							■	
SHIP SUPPORT EQUIPMENT				▲			▲	

NOTES: (a) BATTERIES ARE STORED AND PERIODICALLY CYCLED FOR PERFORMANCE CHECK
(b) SPARES STORED SHORTED - REQUIRES 24 HOURS FOR DELIVERY TO S/C

Fig. 38. Battery operations schedule

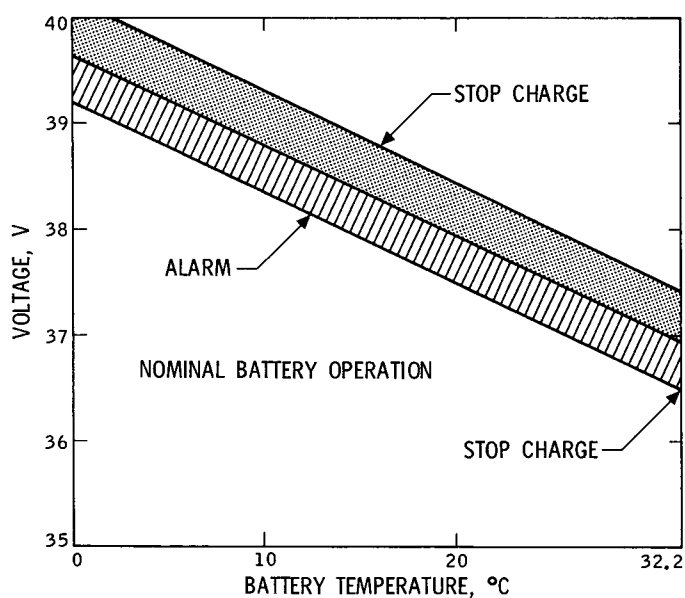


Fig. 39. Battery charge voltage limits

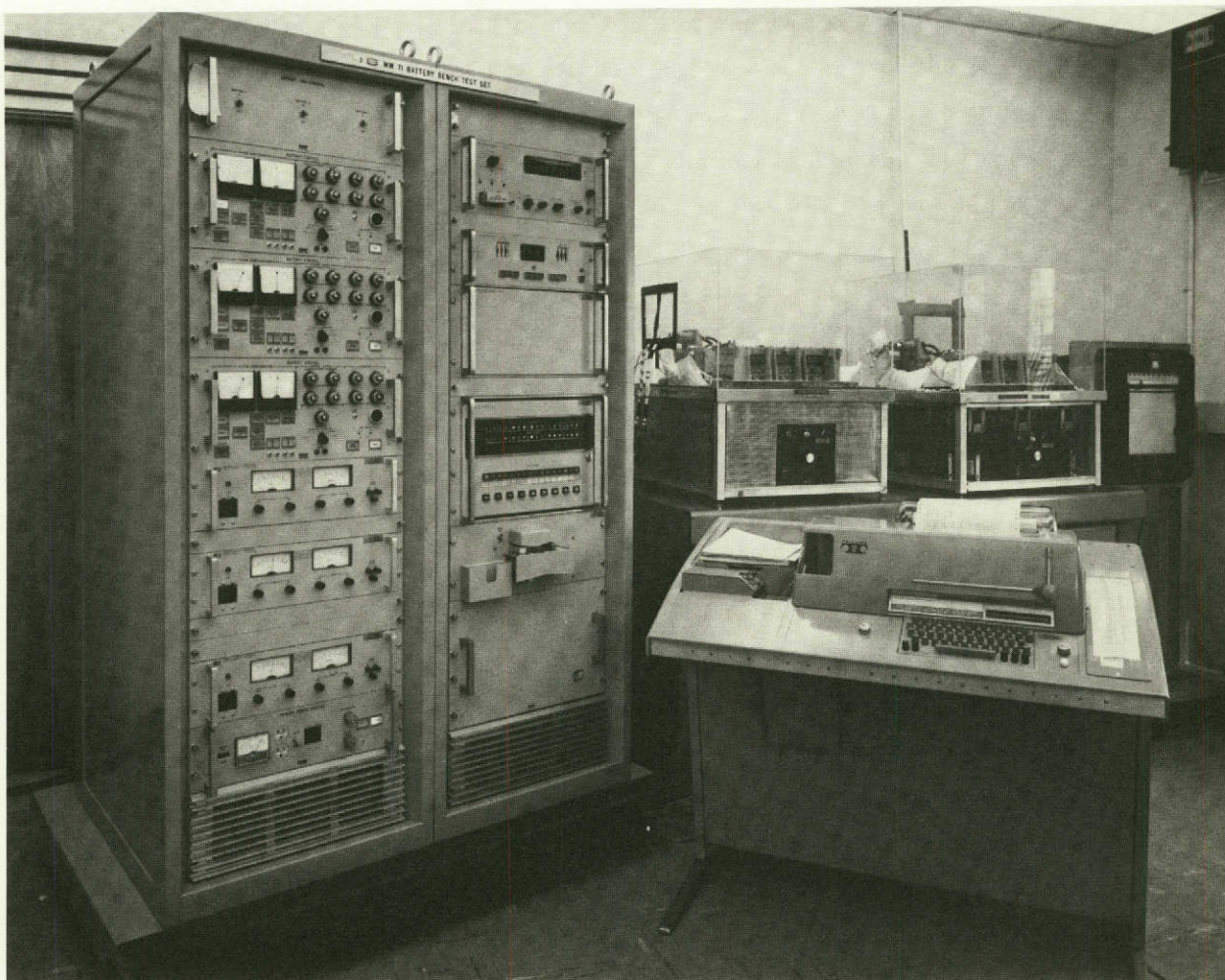


Fig. 40. Laboratory test setup

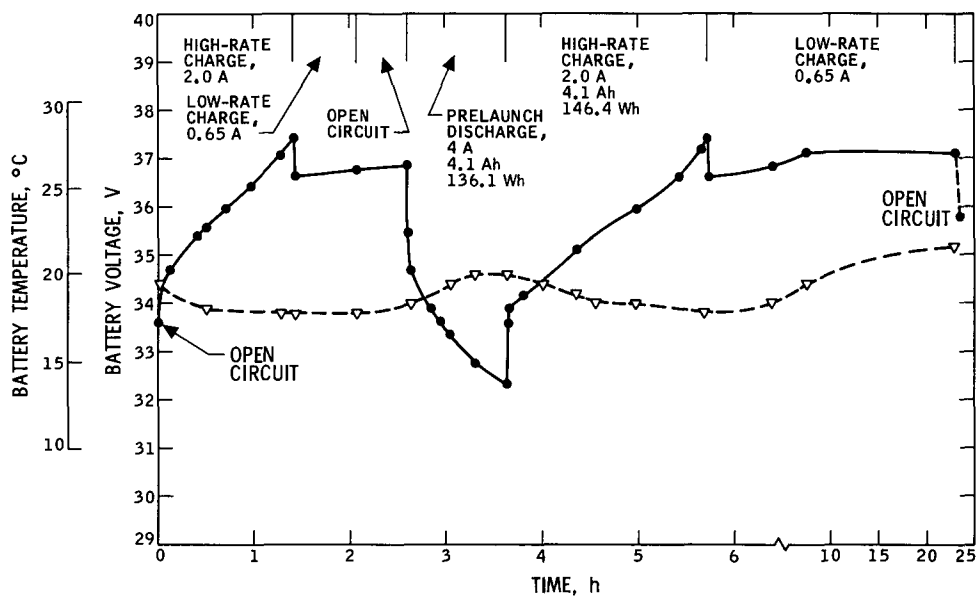


Fig. 41. Mission profile test battery SN EM-1, prelaunch

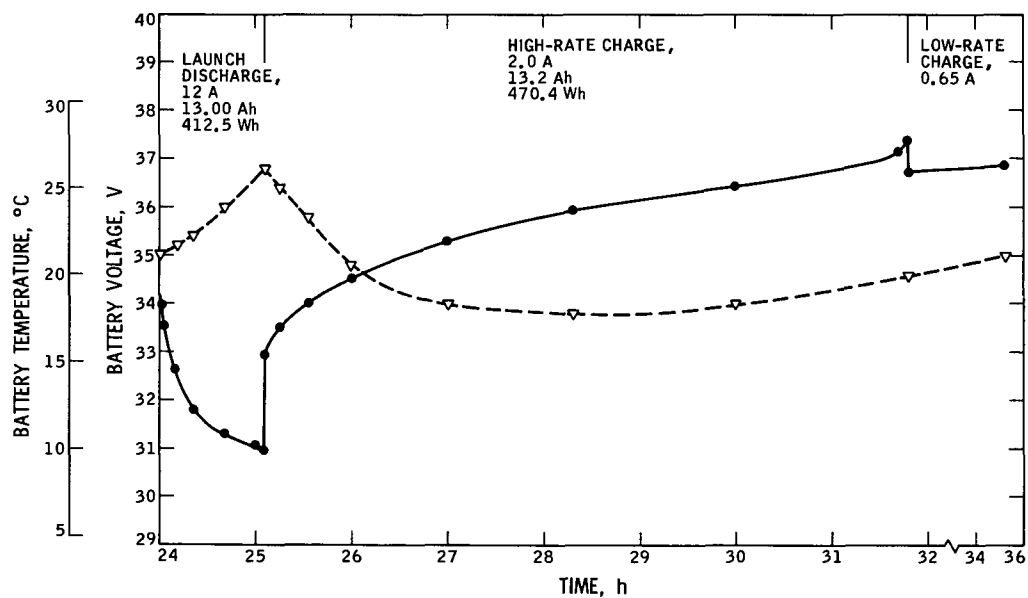


Fig. 42. Mission profile test battery SN EM-1, launch

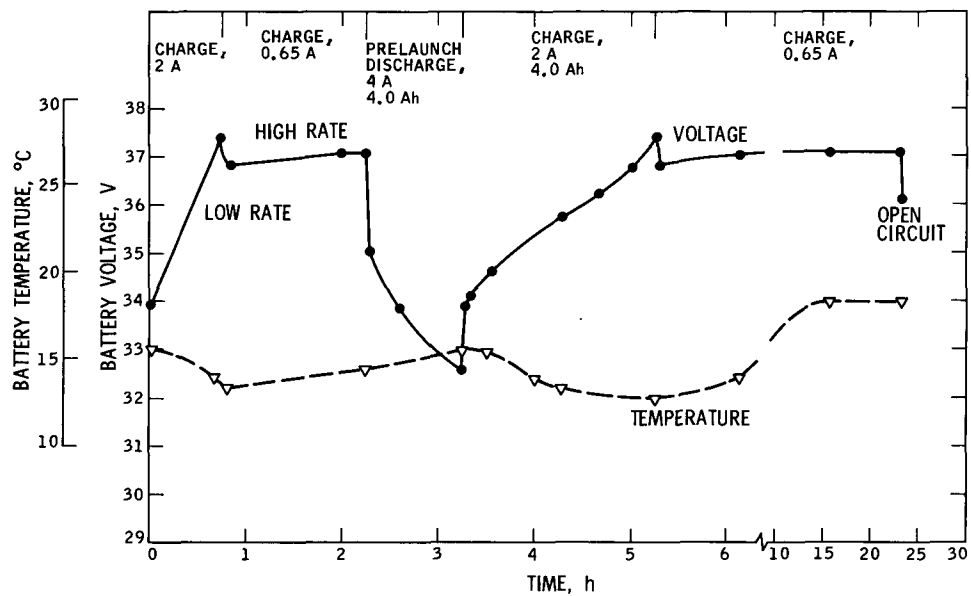


Fig. 43. Mission profile test battery SN 202, prelaunch

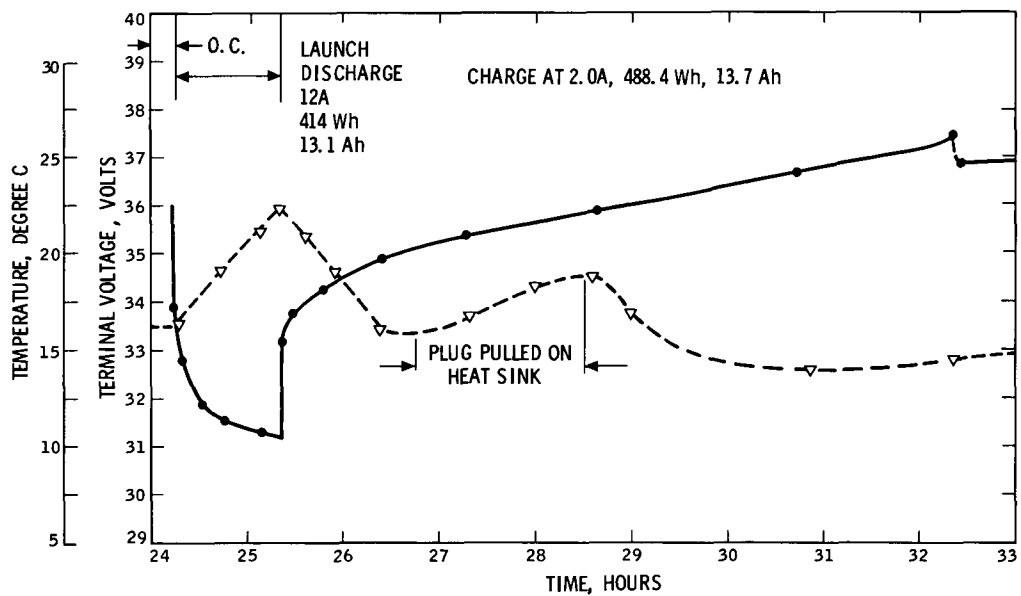


Fig. 44. Mission profile test battery SN 202, launch

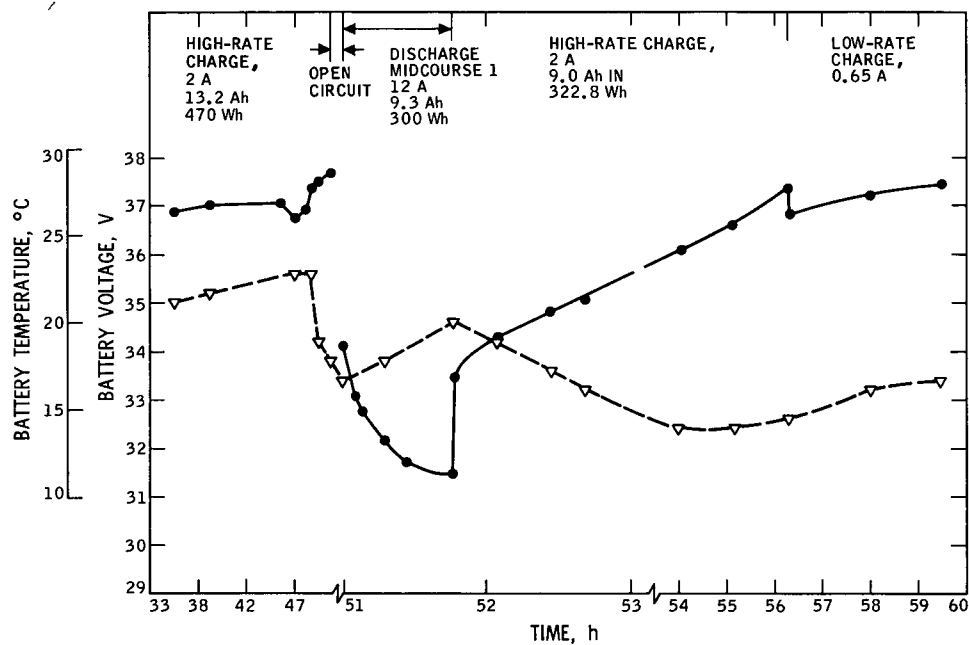


Fig. 45. Mission profile test battery SN EM-1, first midcourse

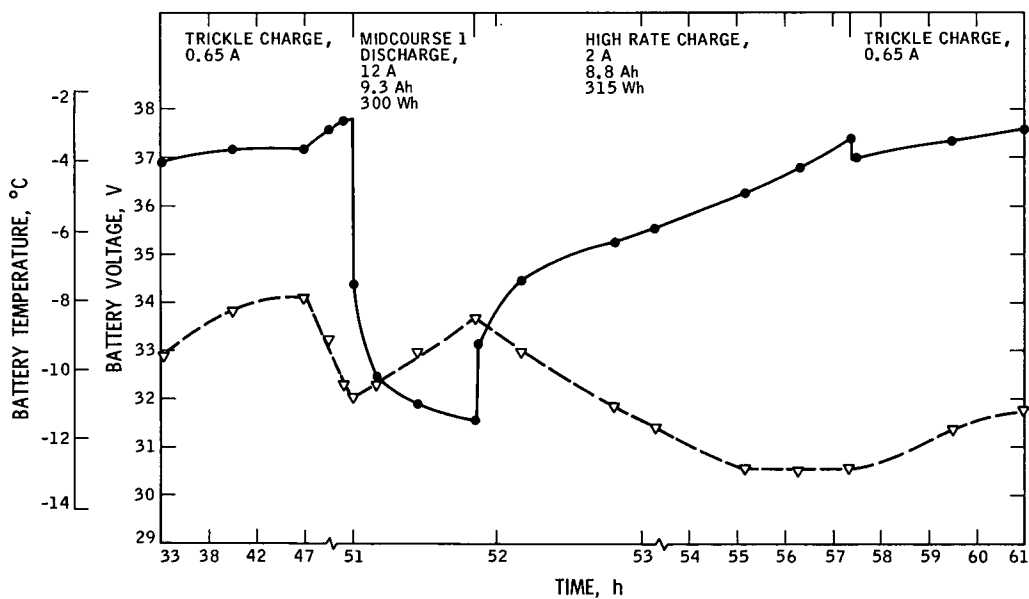


Fig. 46. Mission profile test battery SN 202, first midcourse

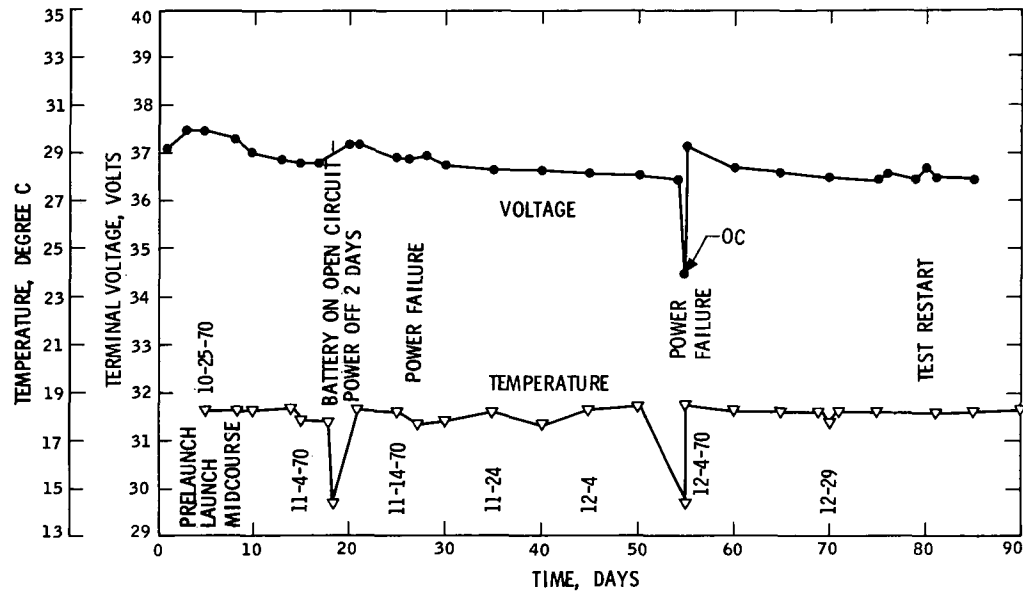


Fig. 47. Mission profile test battery EM-1 cruise data trickle charge at 0.65 A

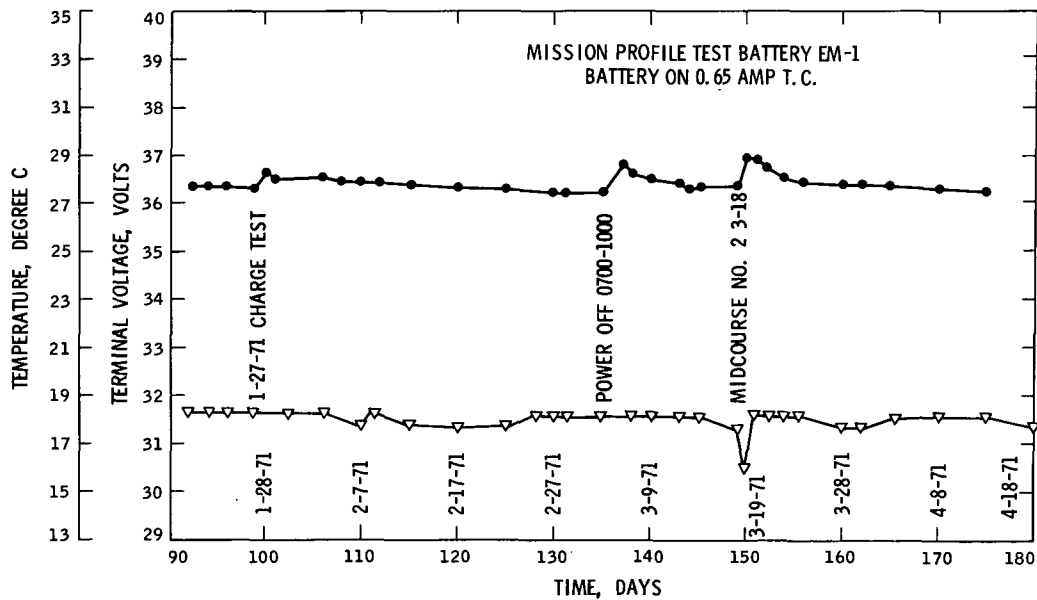


Fig. 47 (contd)

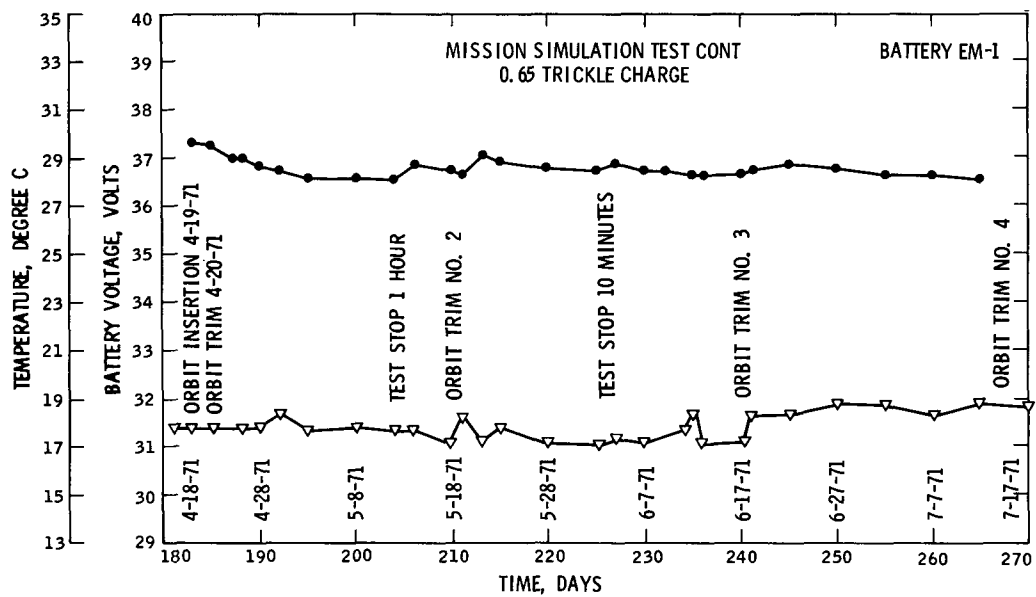


Fig. 47 (contd)

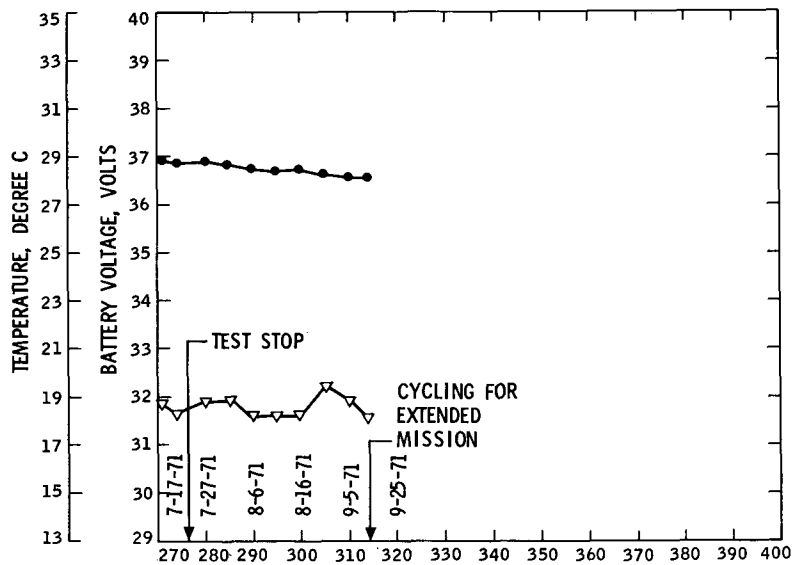


Fig. 47 (contd)

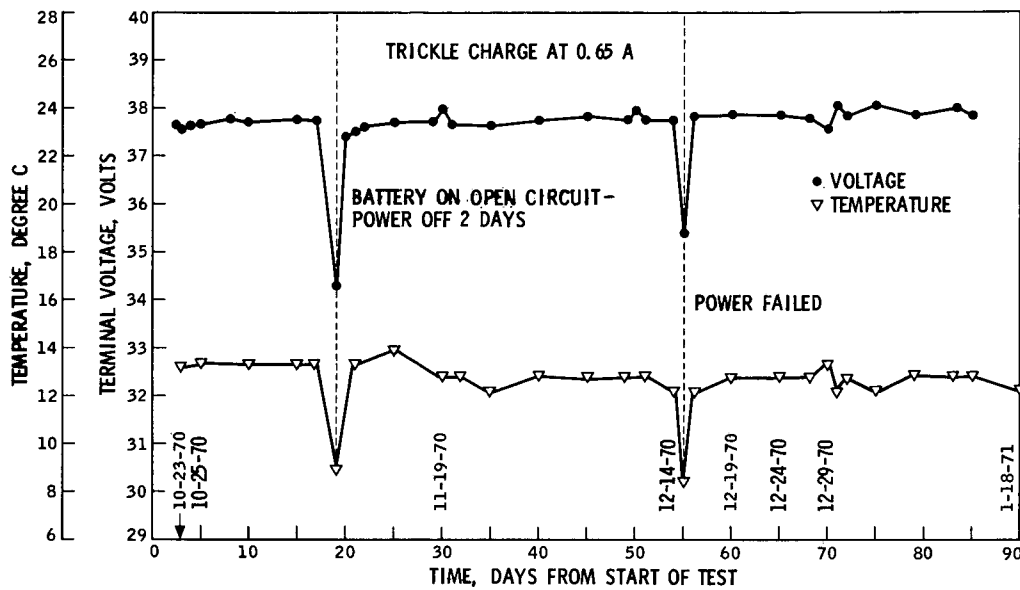


Fig. 48. Mission simulation test battery SN 202, cruise data, trickle charge at 0.65 A

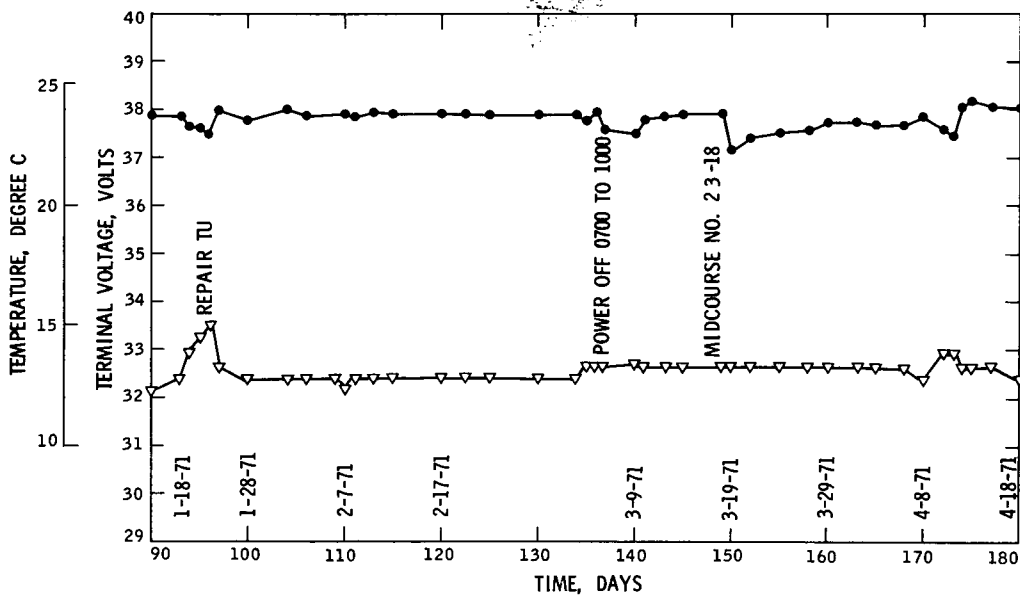


Fig. 48 (contd)

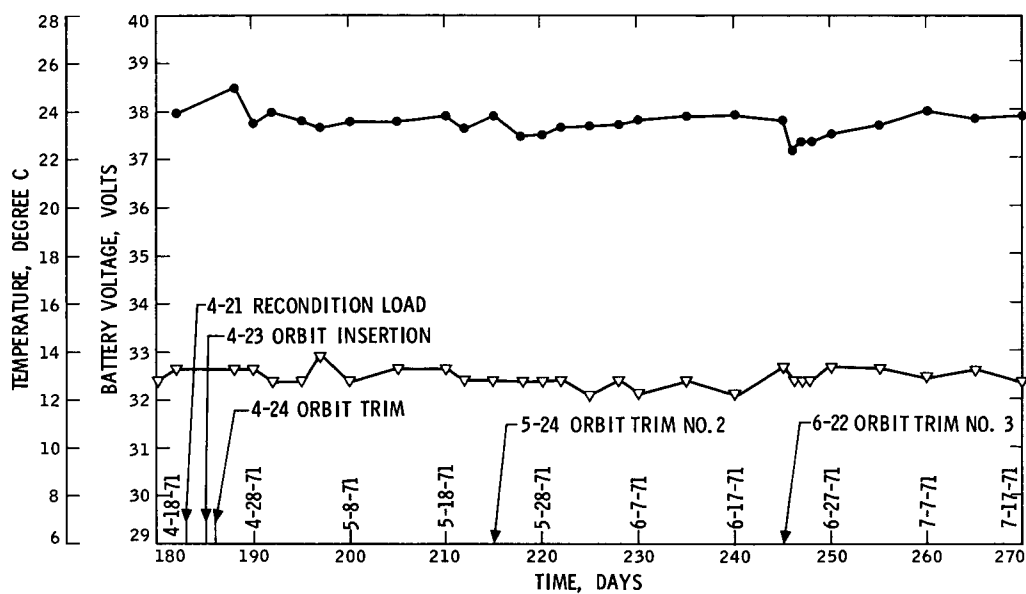


Fig. 48 (contd)

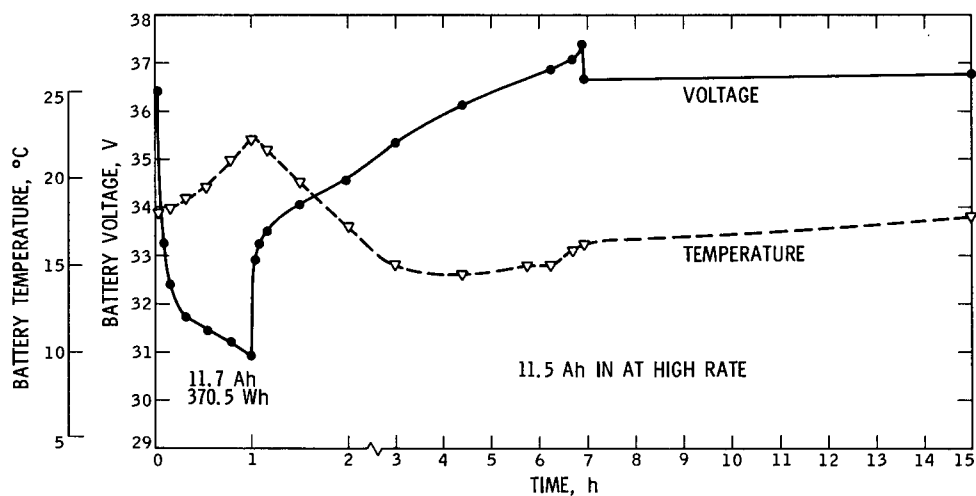


Fig. 49. Mission profile test battery SN EM-1 mid-course 2, discharge at 12 A

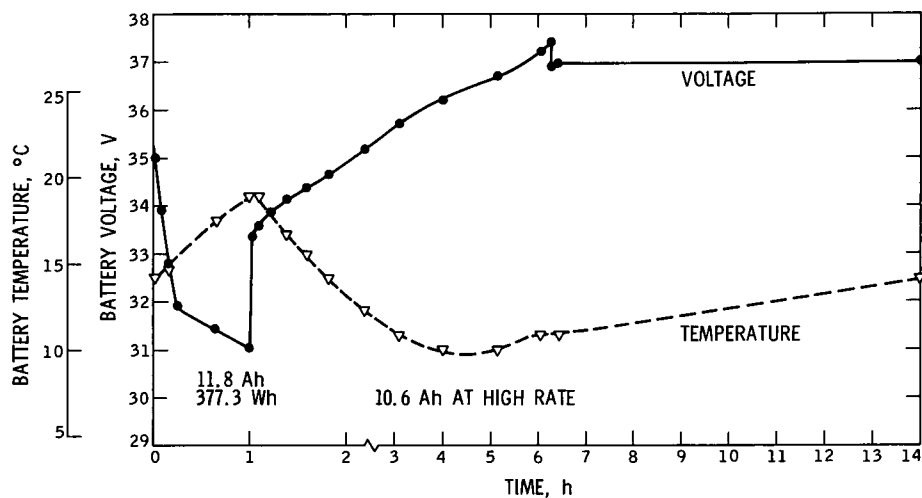


Fig. 50. Mission profile test battery SN 202 mid-course 2, discharge at 12 A

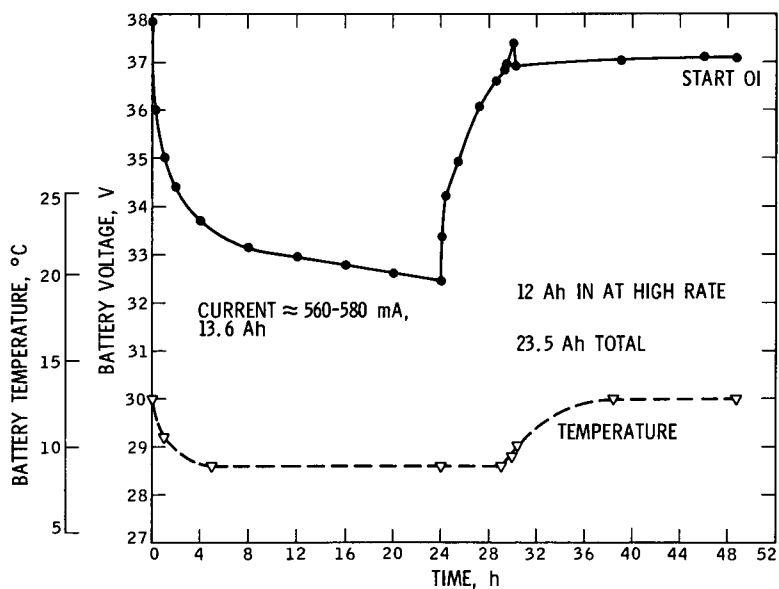


Fig. 51. Mission profile test battery SN 202 recondition discharge at 52 ohms after 6-mo trickle charge

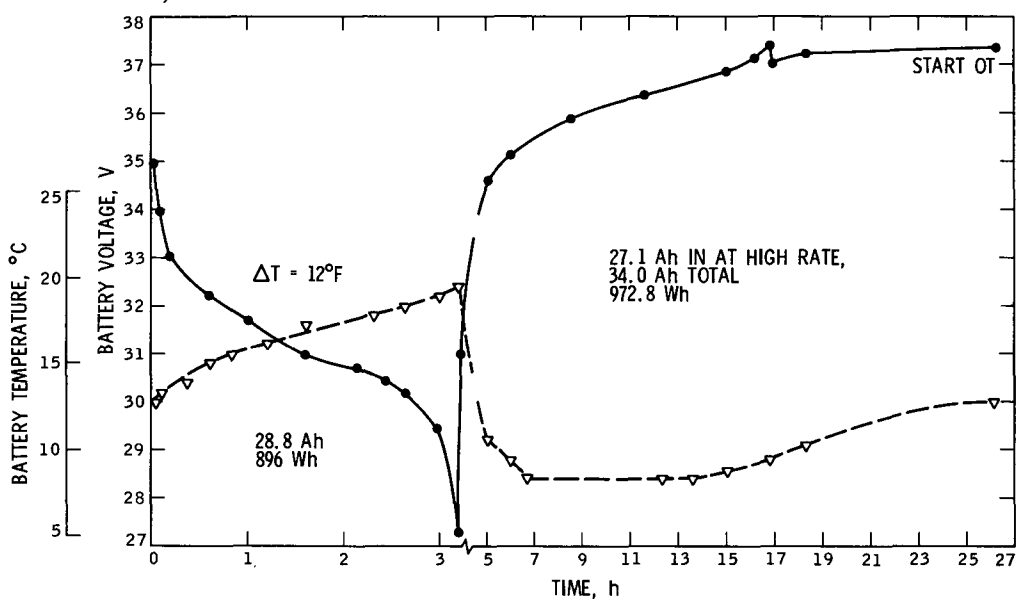


Fig. 52. Mission profile test battery SN 202, orbit insertion at 9 A

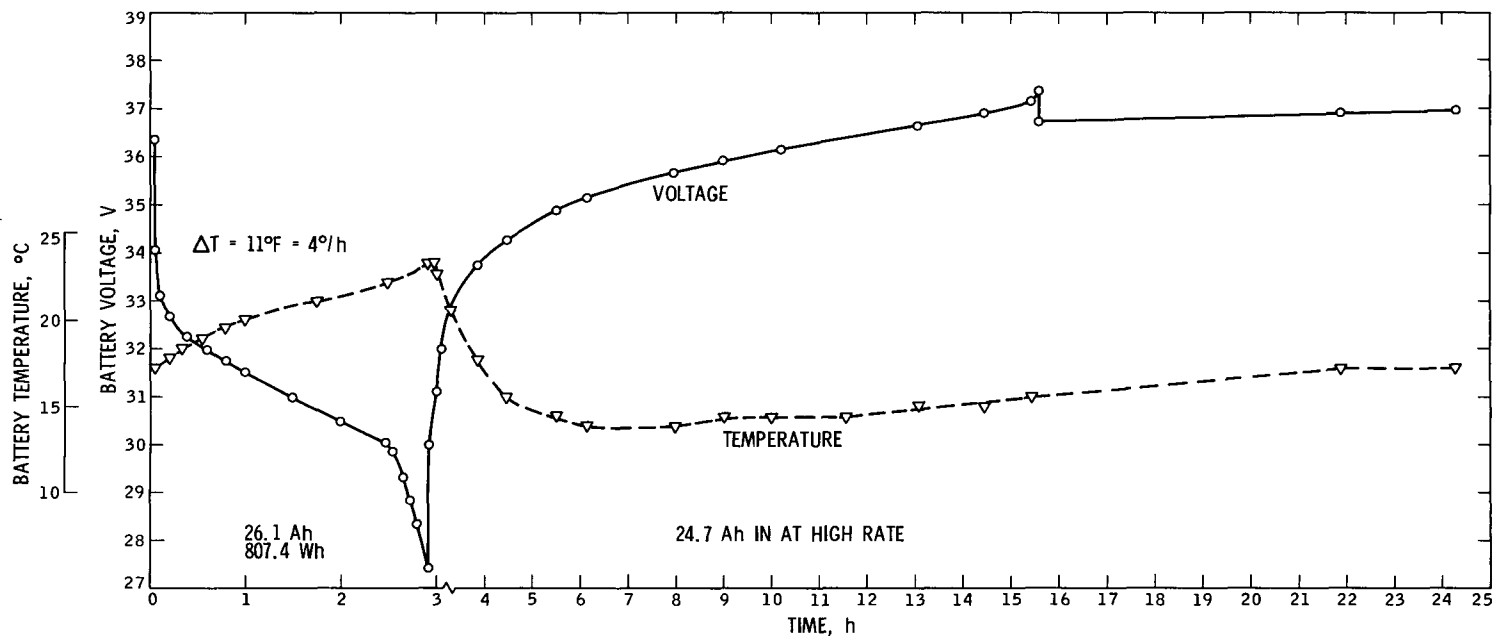


Fig. 53. Mission profile test battery SN EM-1, orbit insertion maneuver at 9 A after 6-mo trickle charge

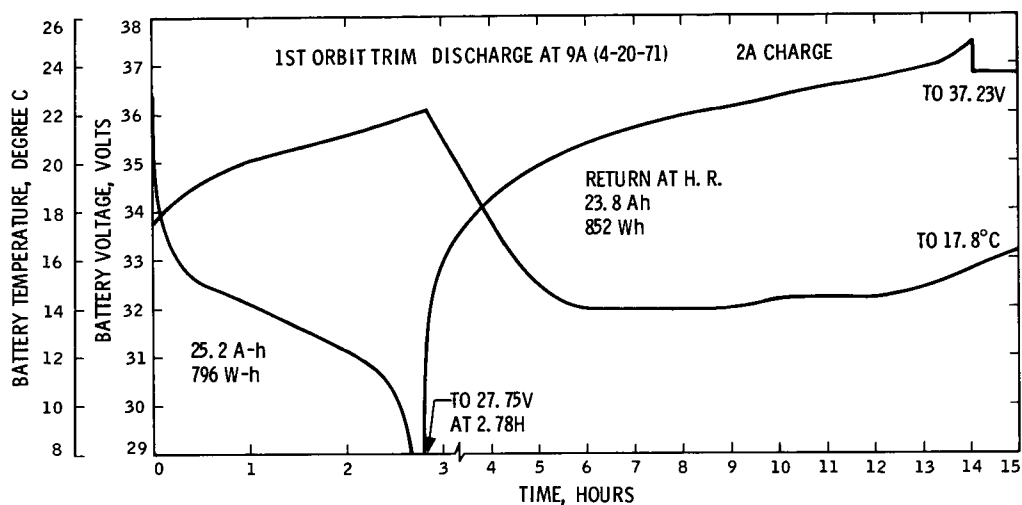


Fig. 54. Mission simulation test battery SN EM-1, first orbit trim discharge at 9 A

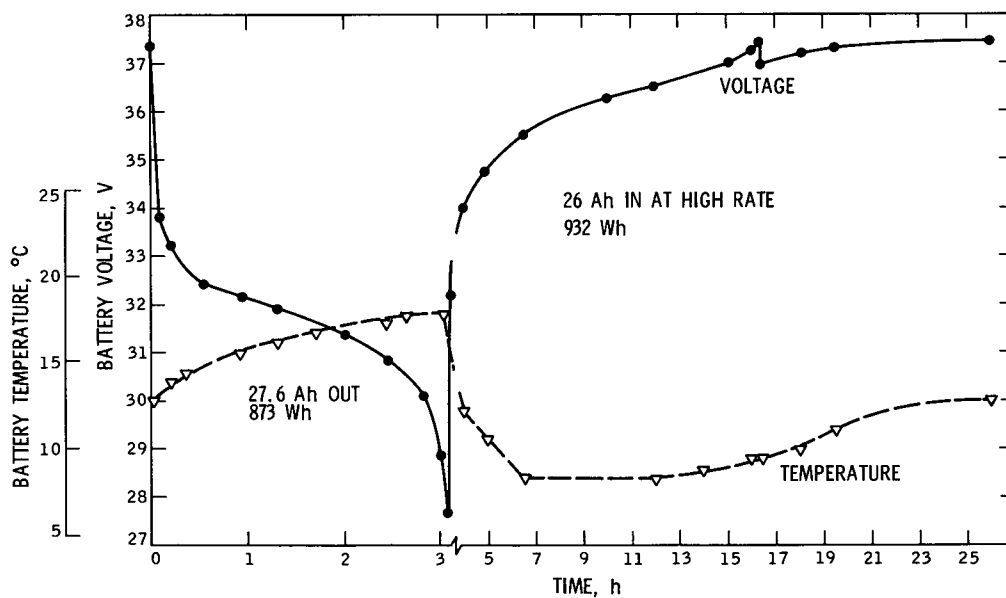


Fig. 55. Mission profile test battery SN 202, first orbit trim at 9 A

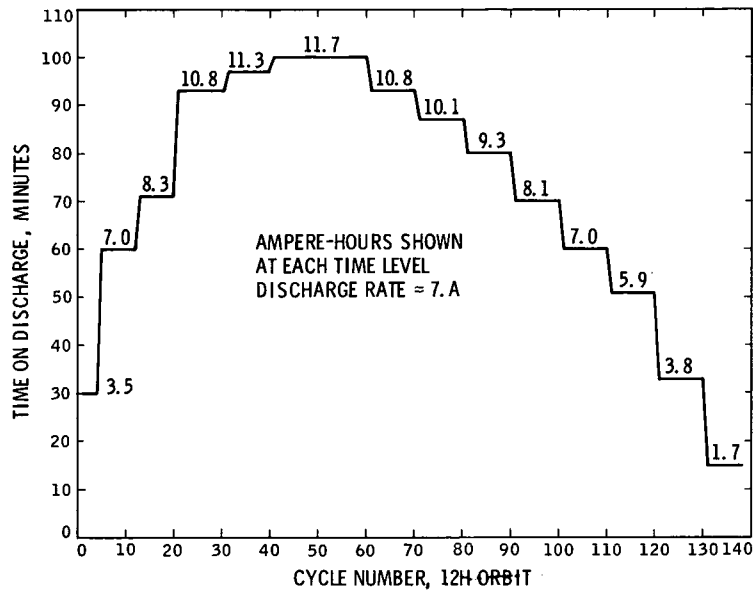


Fig. 56. Extended mission A discharge time vs cycle, battery SN EM-1 and 202

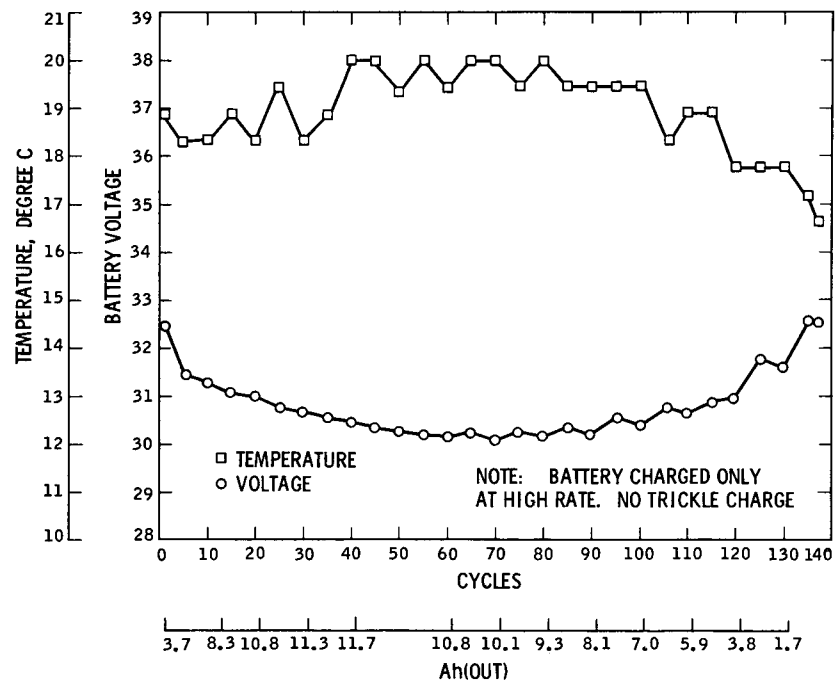


Fig. 57. Mission simulation test battery SN EM-1, end of discharge voltage vs cycle

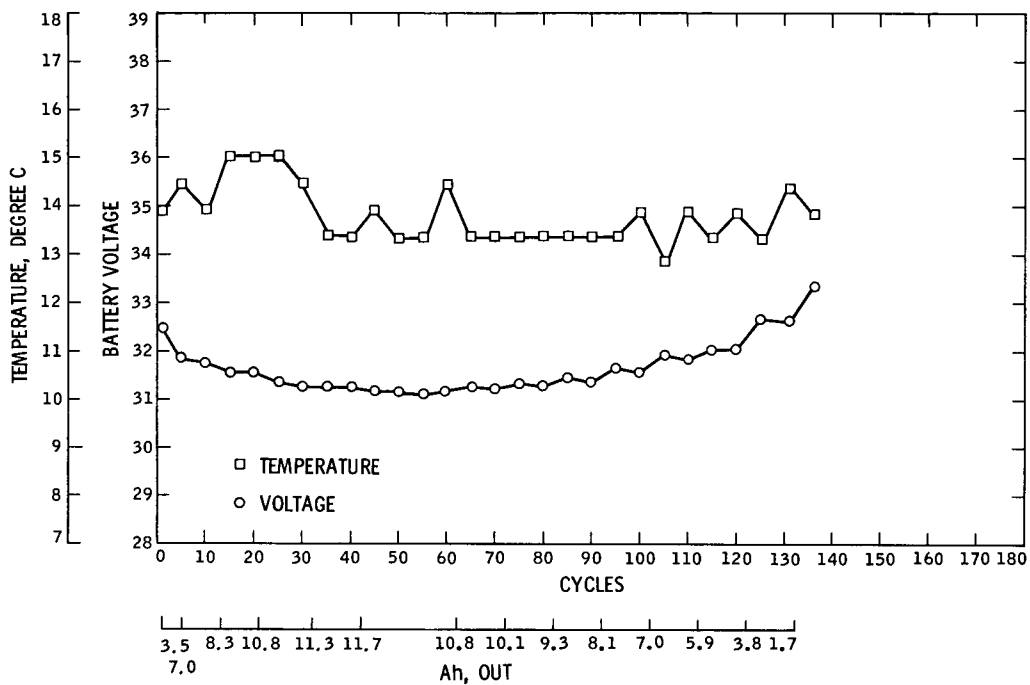


Fig. 58. Mission simulation test battery SN 202, end of discharge voltage vs cycle temperature

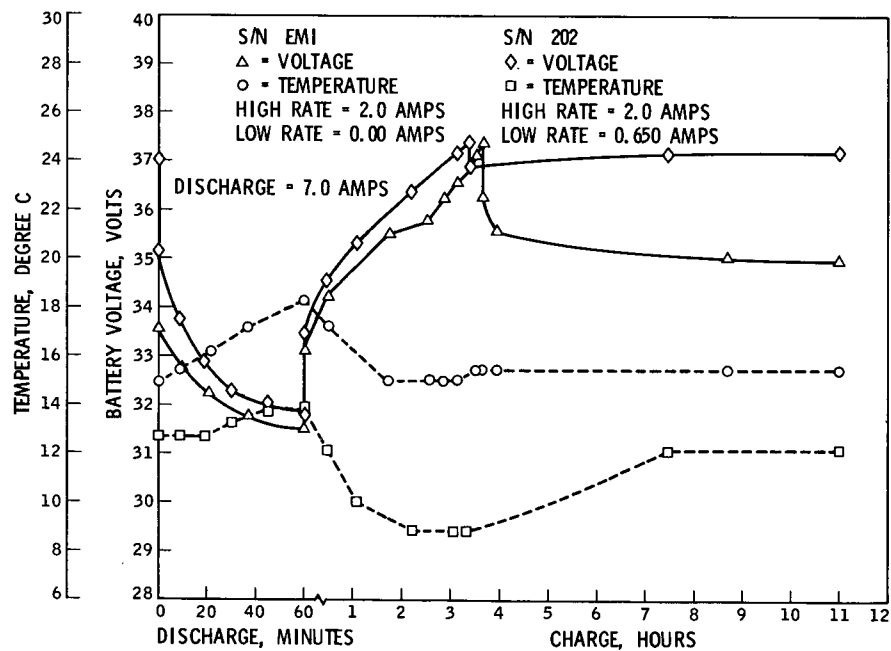


Fig. 59. Mission profile, extended mission, cycle 5

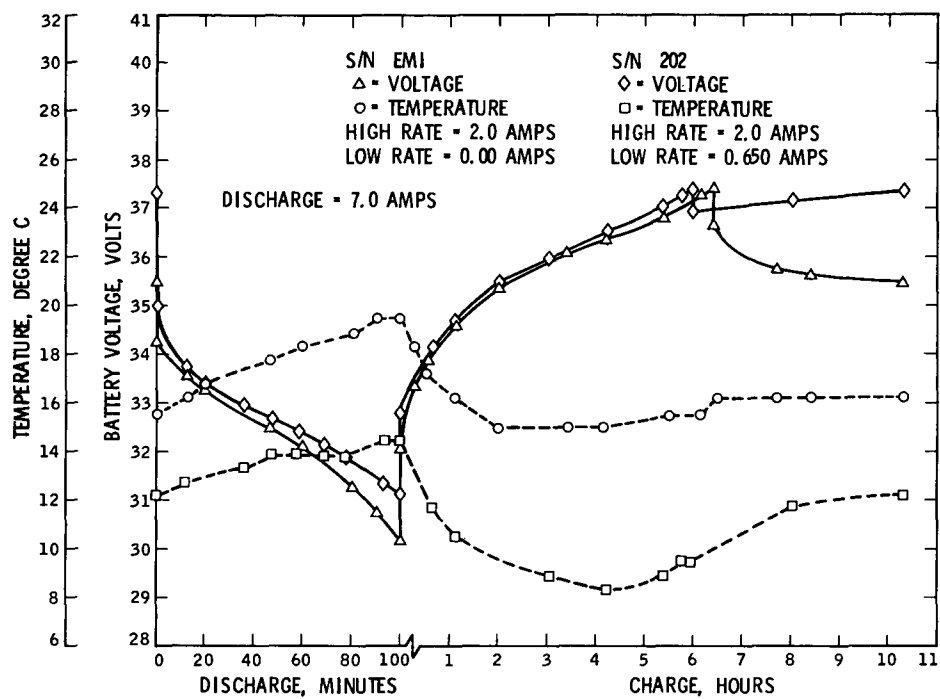


Fig. 60. Mission profile, extended mission, cycle 60

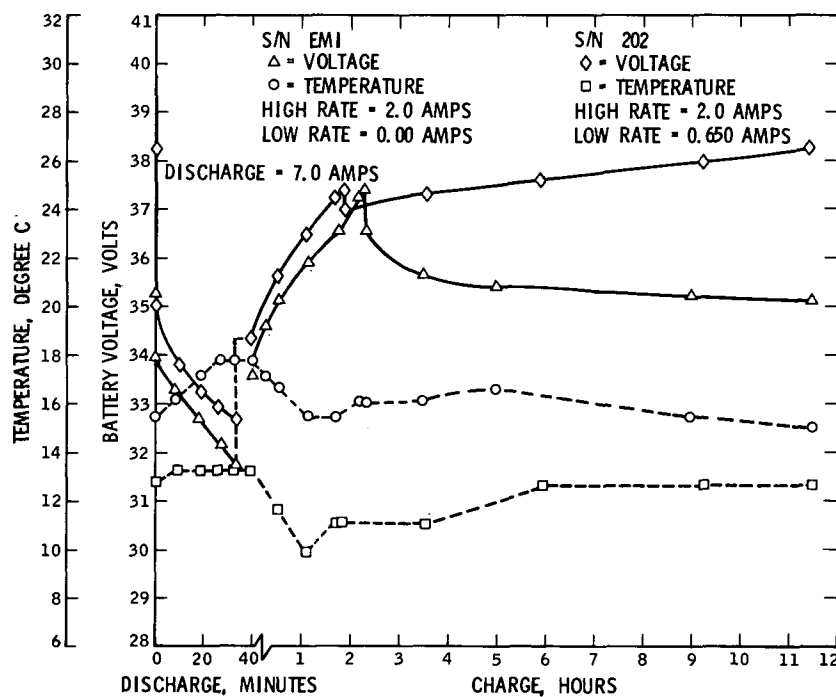


Fig. 61. Mission profile, extended mission, cycle 125

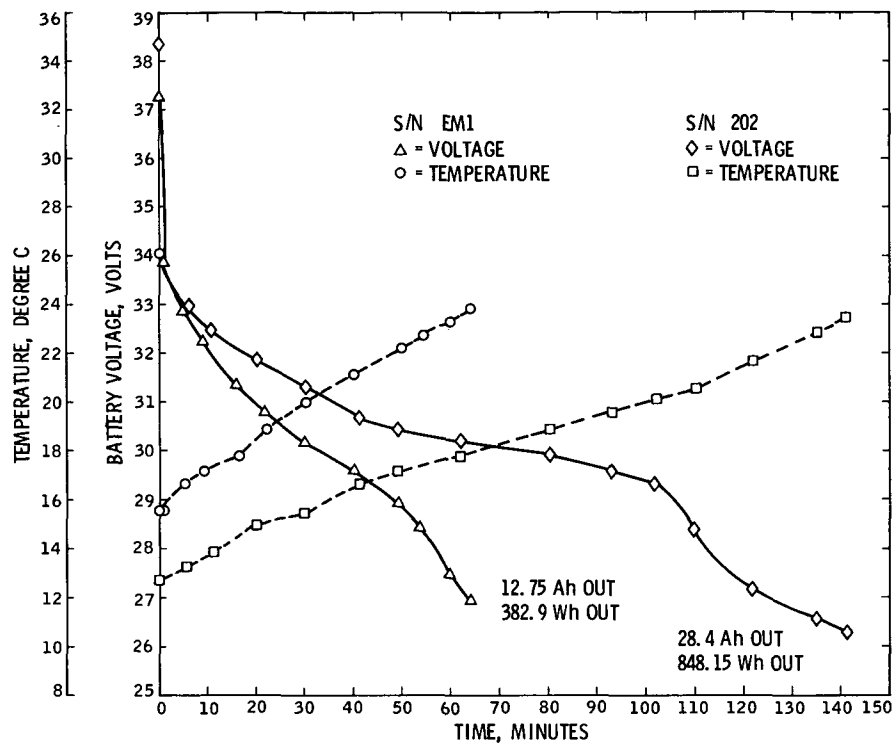


Fig. 62. Discharge after cycling on extended mission A, discharge rate 12.0 A

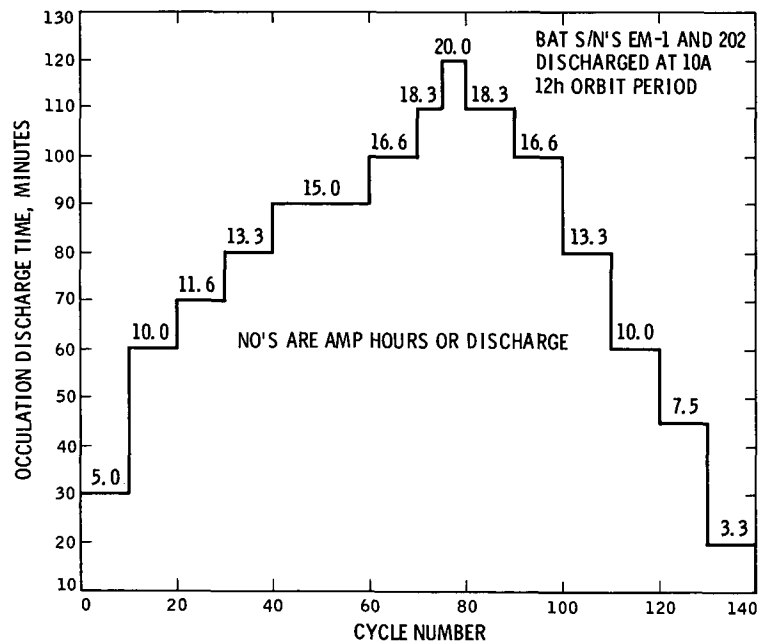


Fig. 63. Discharge time as a function of cycle, extended mission B

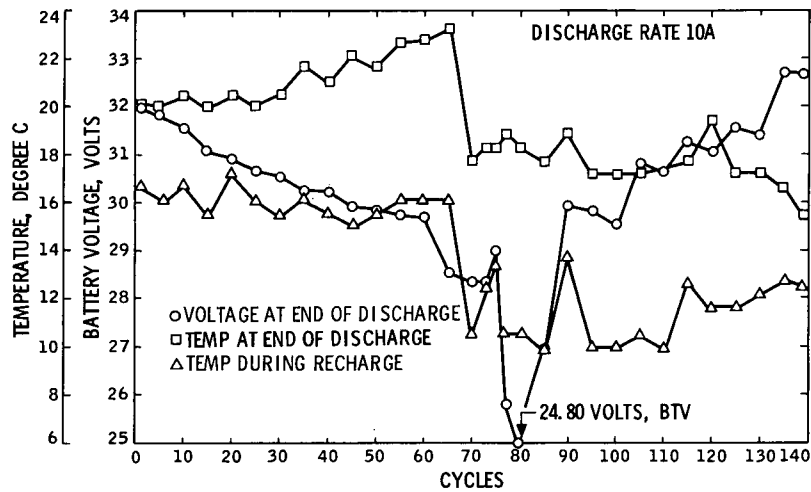


Fig. 64. Extended mission B, battery SN EM-1, end-of-discharge voltage and temperature profile vs cycle, discharge rate 10 A

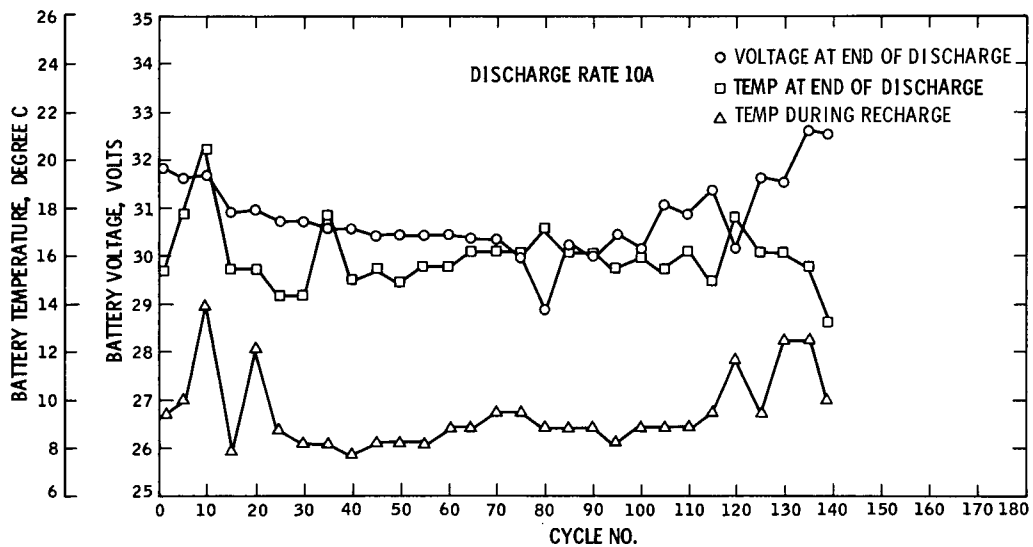


Fig. 65. Extended mission B, battery SN 202, end-of-discharge voltage and temperature profile vs cycle, discharge rate 10 A

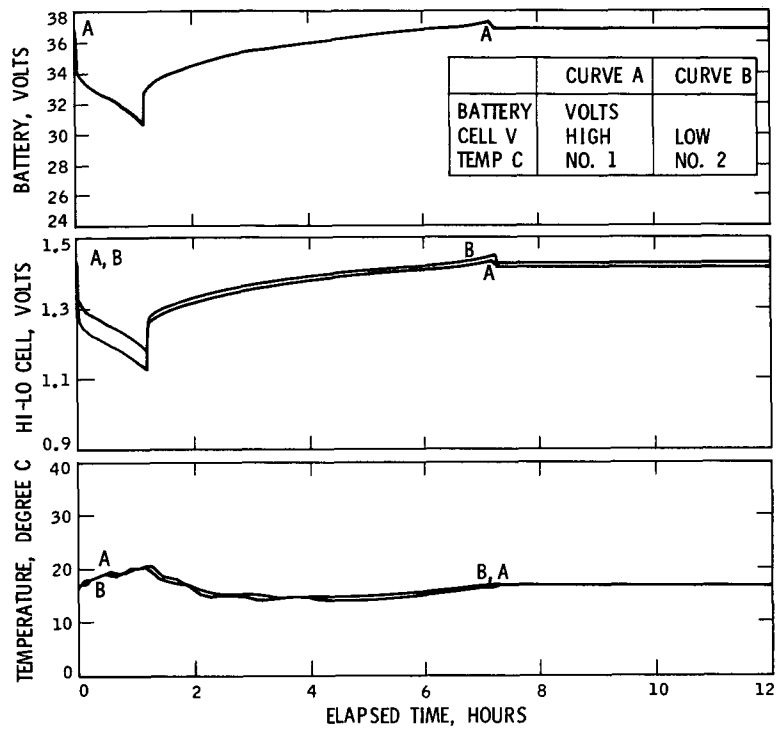


Fig. 66. Extended mission B, battery test,
orbit 25, January 31, 1972,
SN EM-1

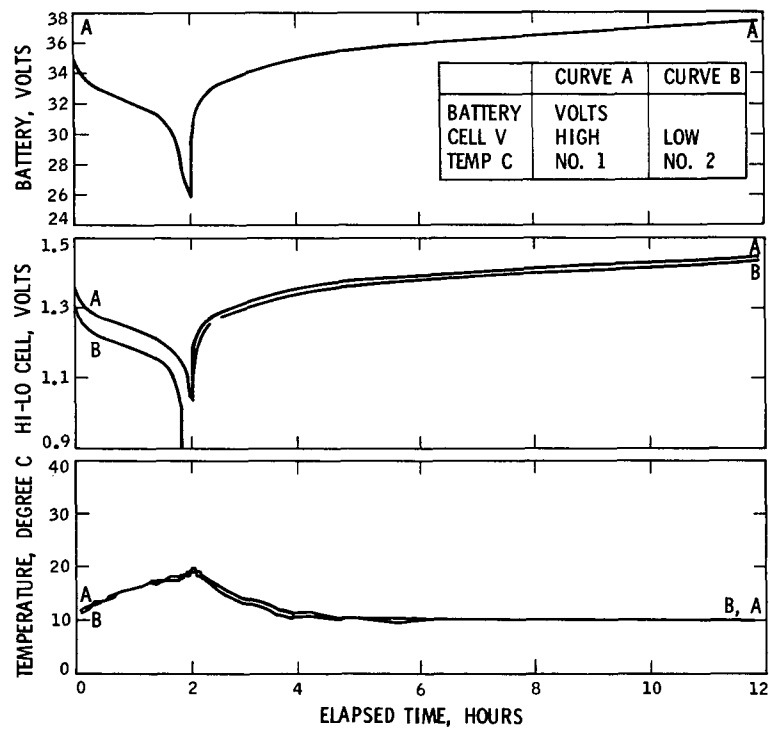


Fig. 67. Extended mission B, battery test,
orbit 77, February 26, 1972,
SN EM-1

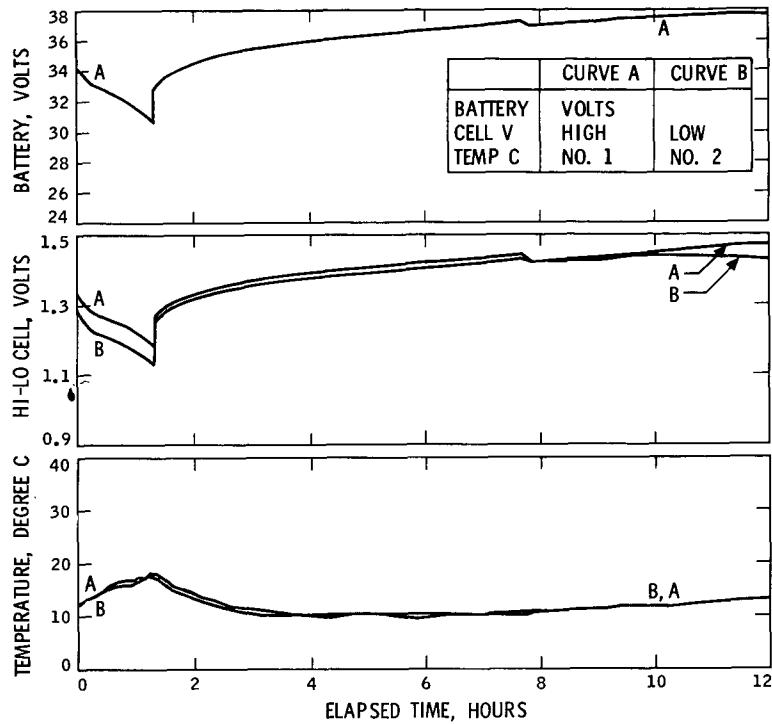


Fig. 68. Extended mission B, battery test, orbit 110, March 13, 1972, SN EM-1

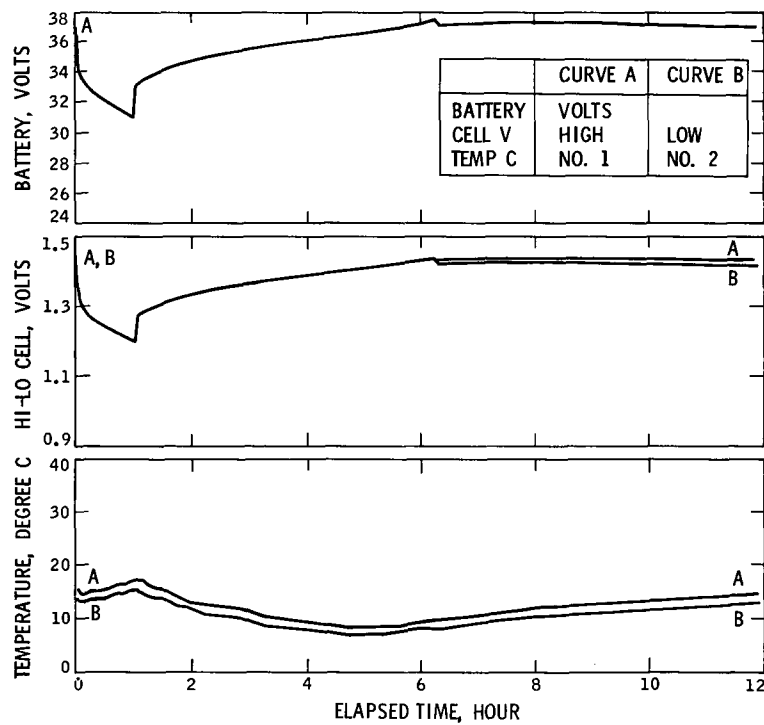


Fig. 69. Extended mission B, battery test, orbit 15, January 26, 1972, SN 202

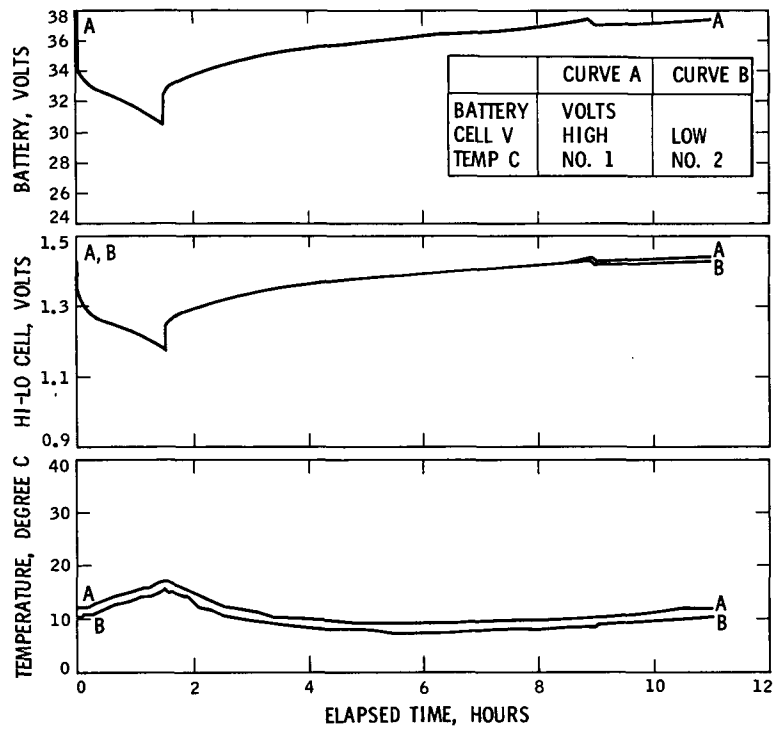


Fig. 70. Extended mission B, battery test,
orbit 55, February 16, 1972,
SN 202

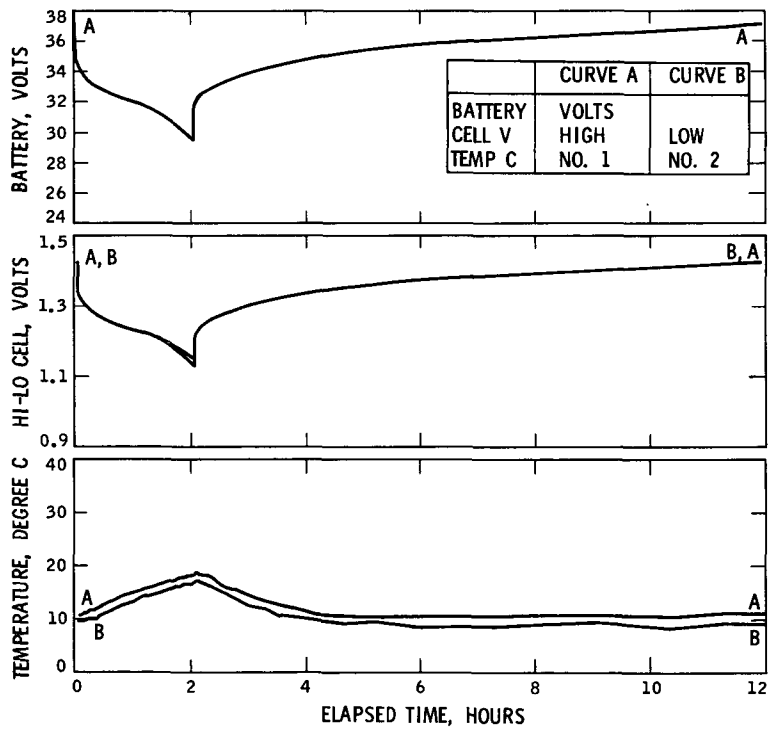


Fig. 71. Extended mission B, battery test,
orbit 78, February 26, 1972,
SN 202

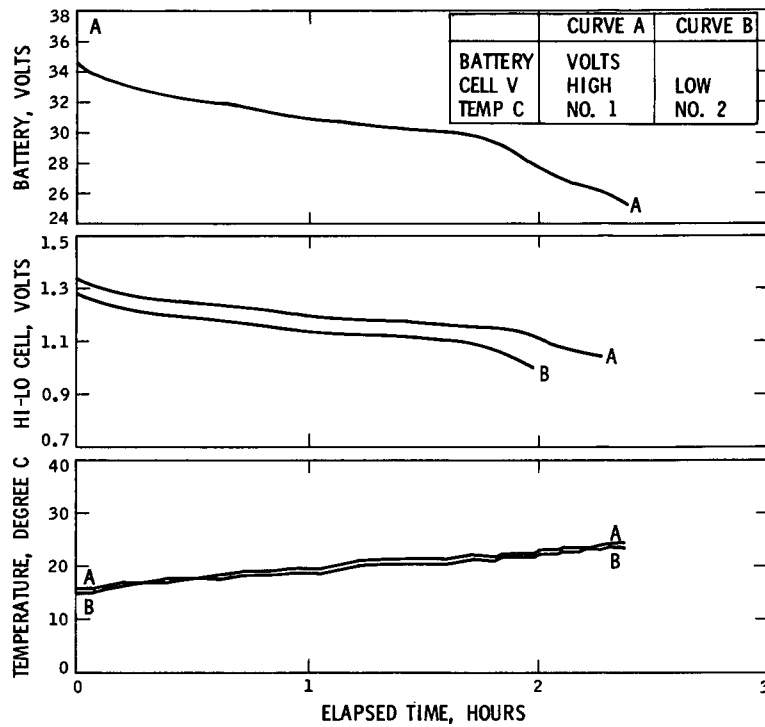


Fig. 72. Extended mission B, battery test,
orbit 140, March 28, 1972,
SN EM-1

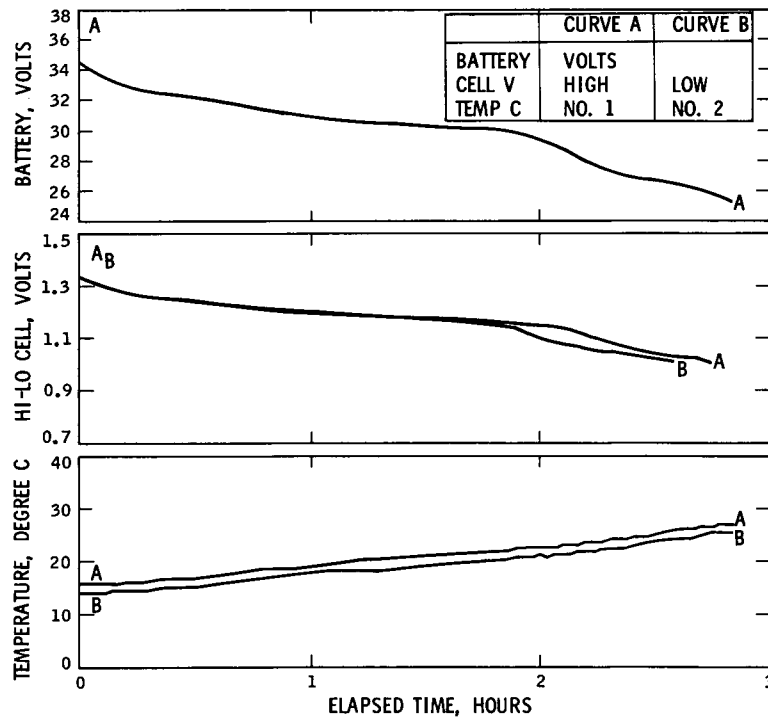


Fig. 73. Extended mission B, battery test,
orbit 140, March 28, 1972,
SN 202

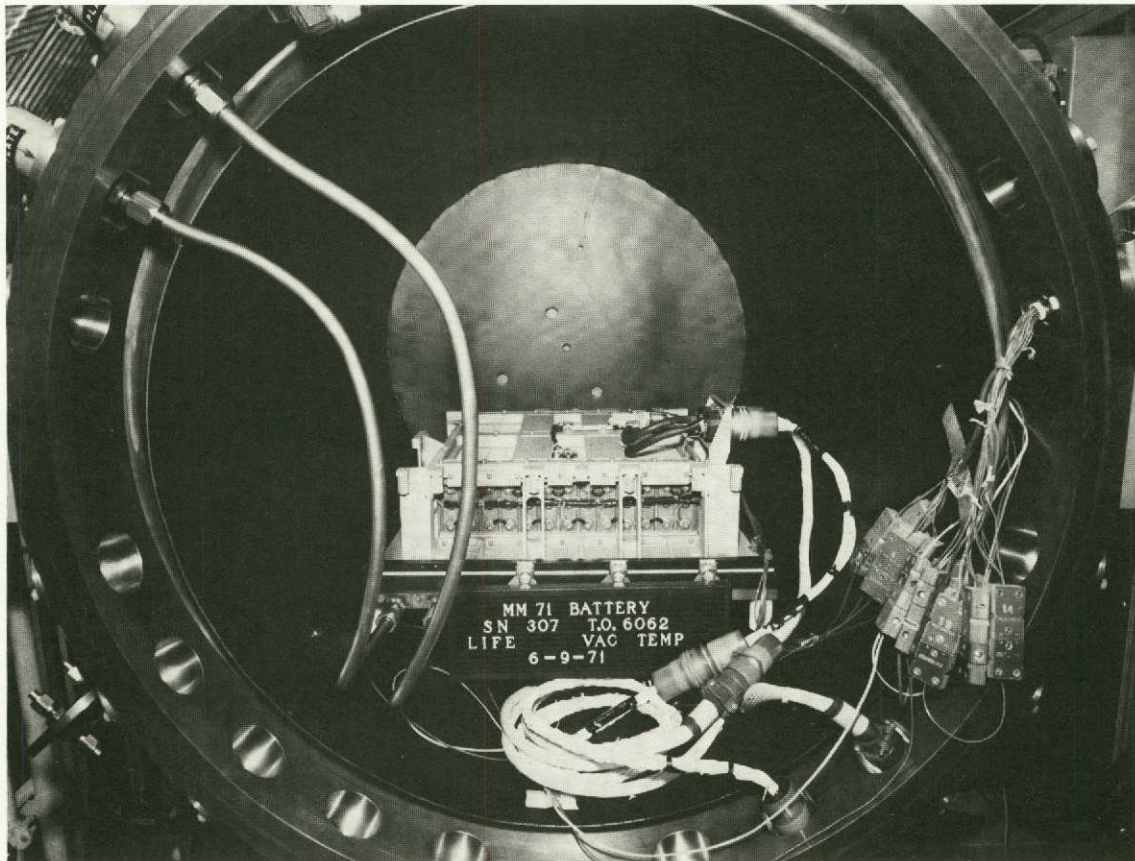


Fig. 74. Test setup, thermal vacuum, real-time mission test

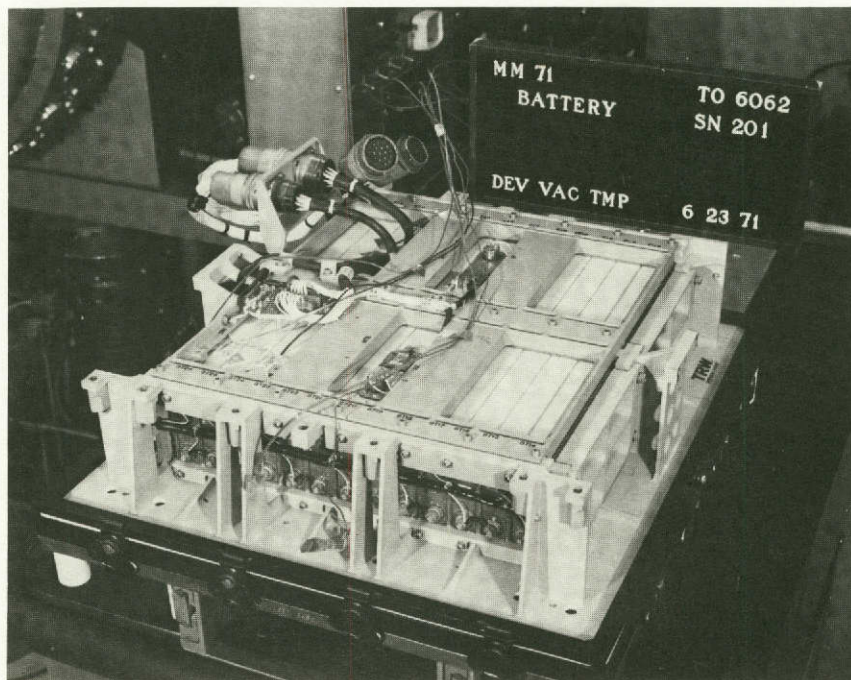


Fig. 75. Test setup, thermal vacuum, real-time mission test

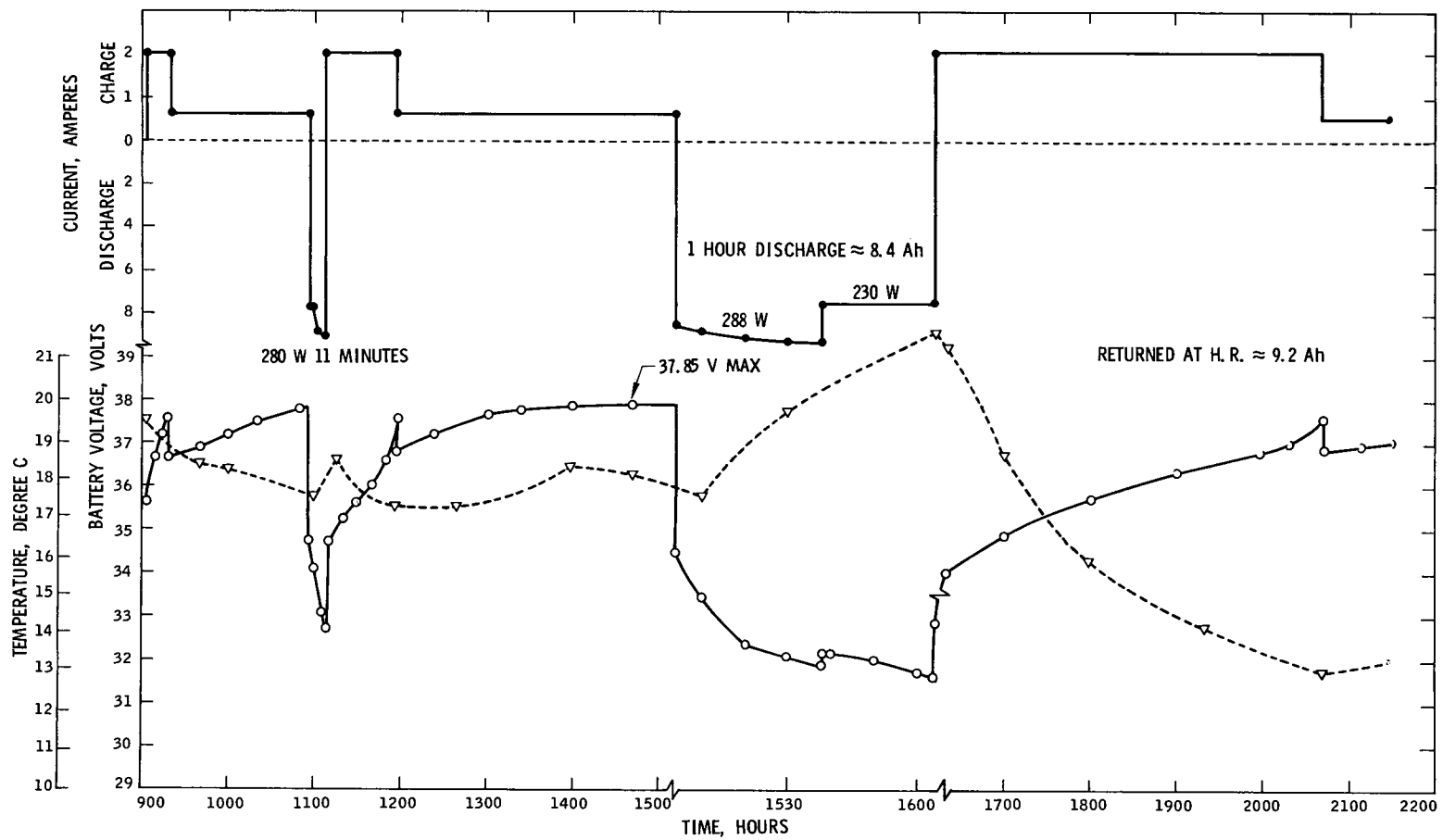


Fig. 76. Real-time mission simulation launch sequence, June 14, 1971, battery SN 307

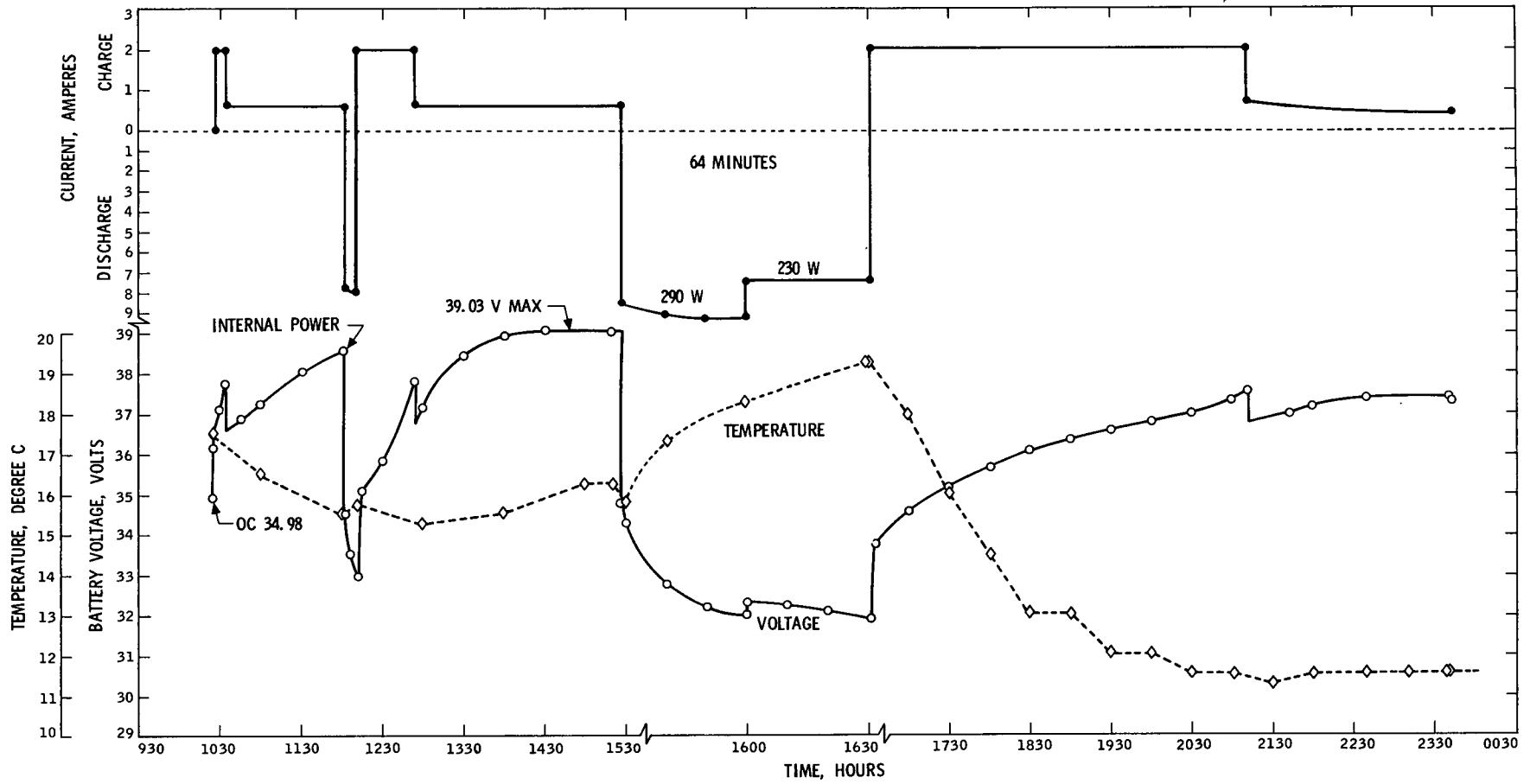


Fig. 77. Real-time mission simulation launch sequence, June 30, 1971, battery SN 201

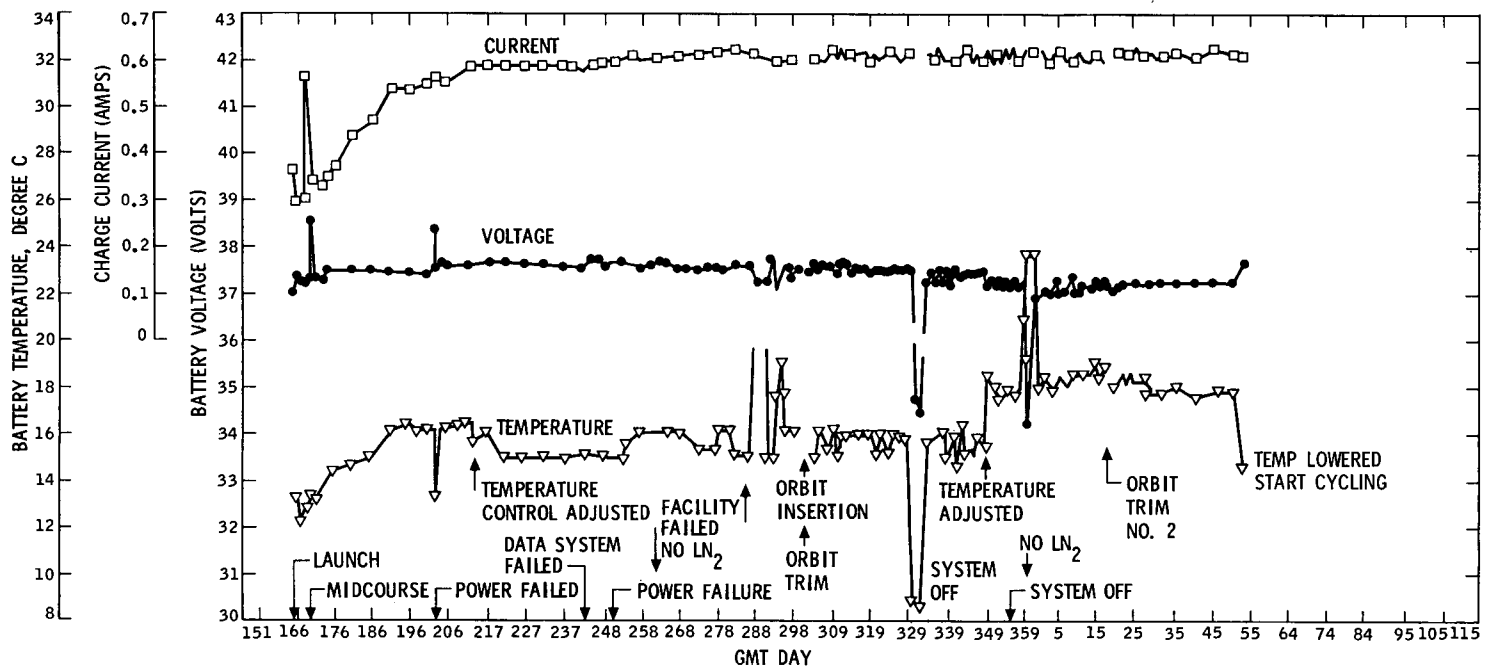


Fig. 78. Real-time mission simulation, battery SN 307, cruise data

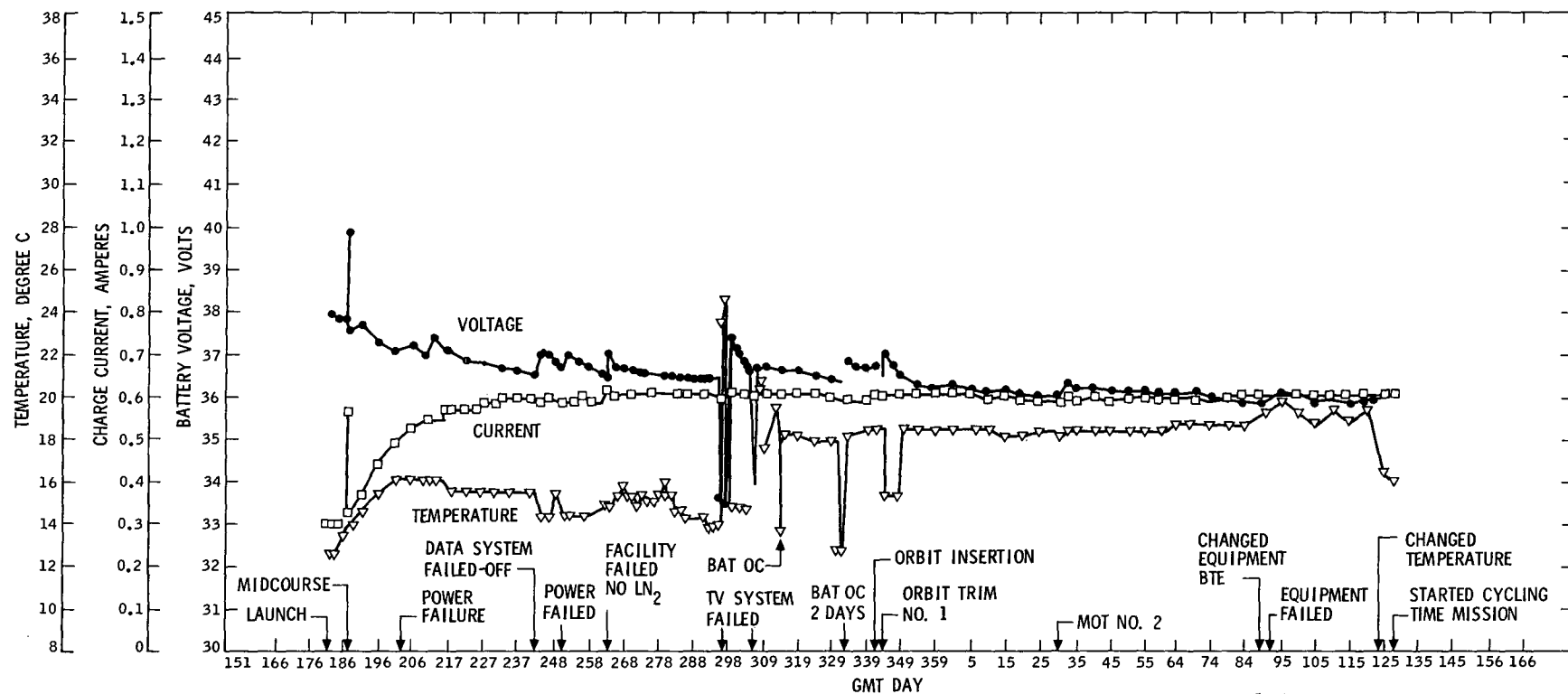


Fig. 79. Real-time mission simulation, battery SN 201, cruise data

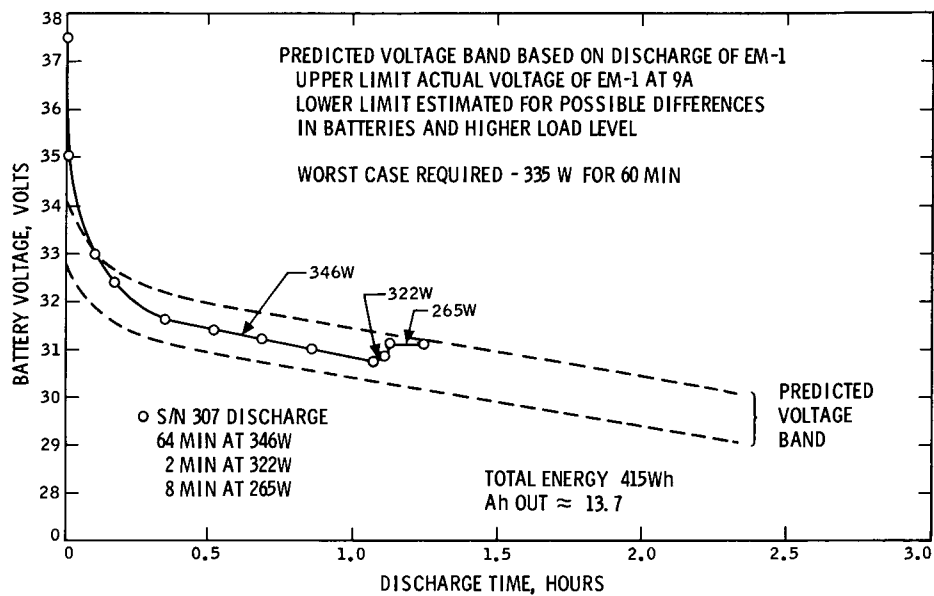


Fig. 80. Predicted voltage and actual voltage, battery SN 307, simulated orbit insertion test, October 26, 1971

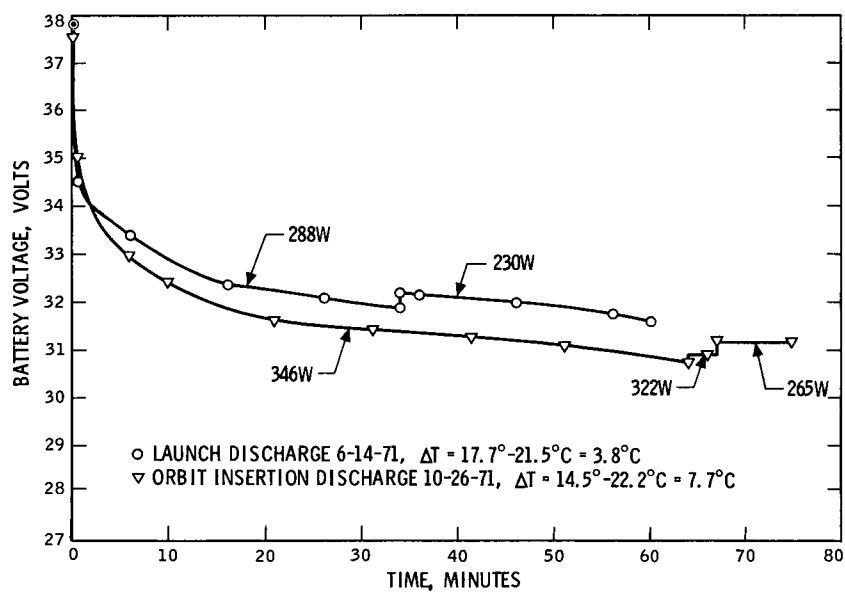


Fig. 81. Real-time mission profile test, battery SN 307, launch discharge compared to orbit insertion discharge

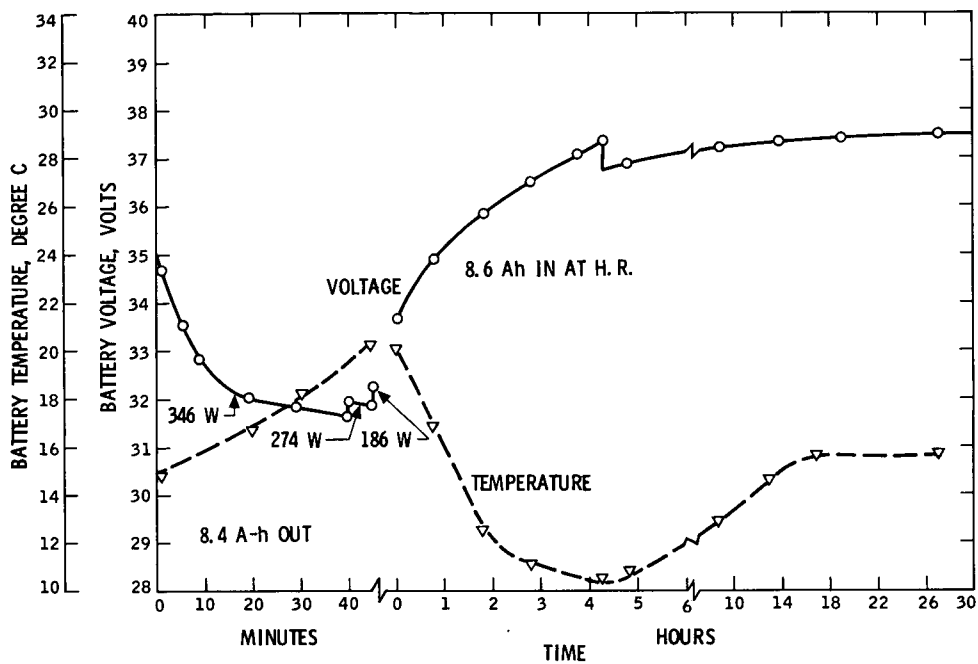


Fig. 82. Real-time mission test, battery SN 307, orbit trim 1, discharge and recharge performed prior to Mariner 9

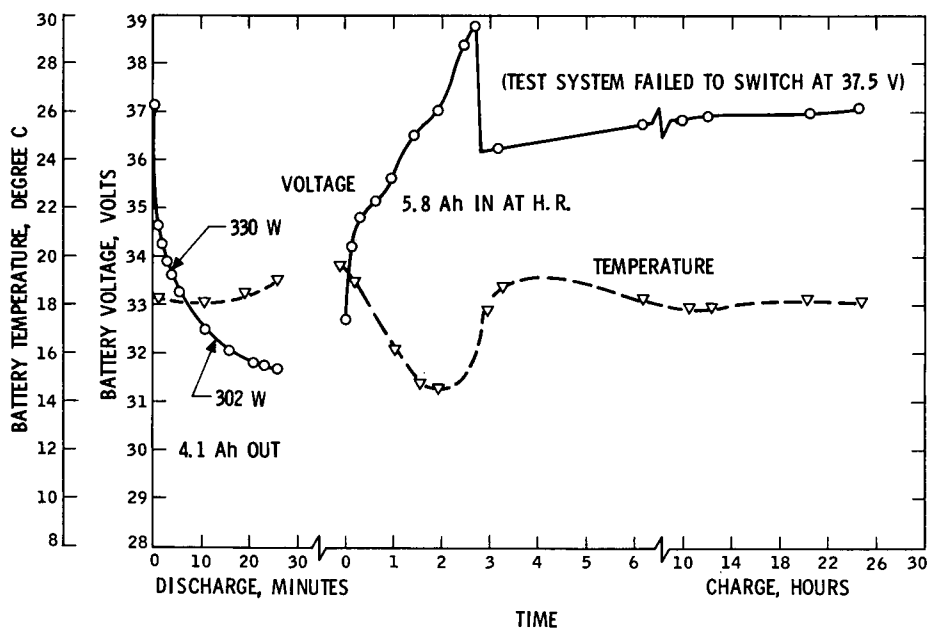


Fig. 83. Real-time mission test, battery SN 307, orbit trim 2 discharge and recharge

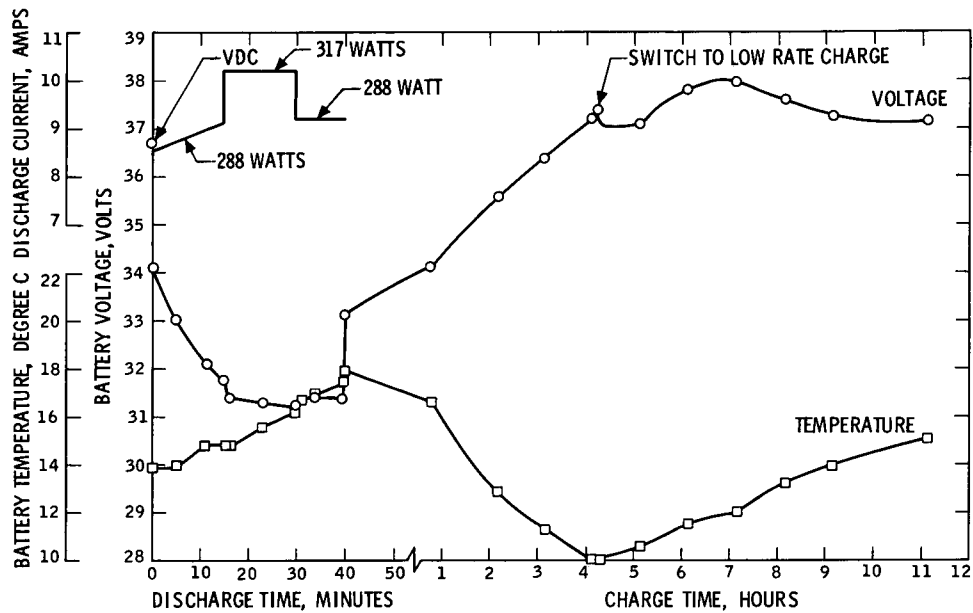


Fig. 84. Battery performance, battery SN 201, Mars orbit insertion

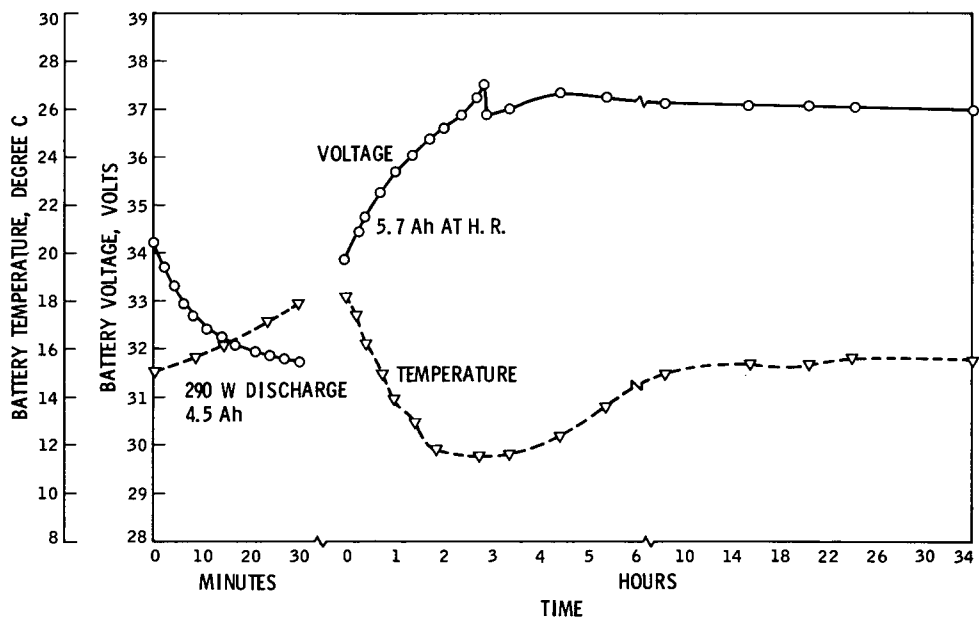


Fig. 85. Real-time mission test, battery SN 201, orbit trim 1 discharge and charge

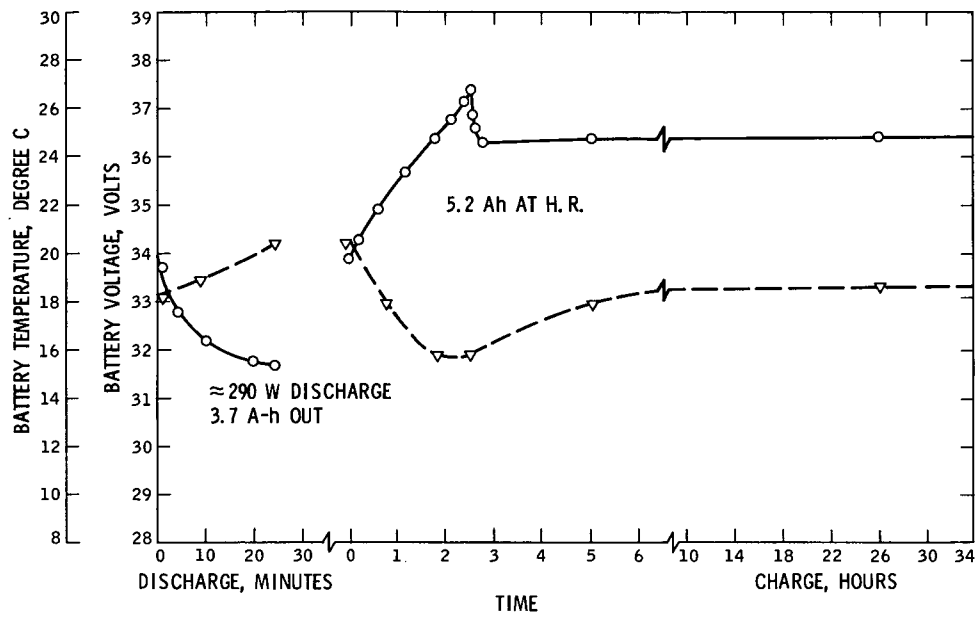


Fig. 86. Real-time mission test, battery SN 201, orbit trim 2 discharge and recharge

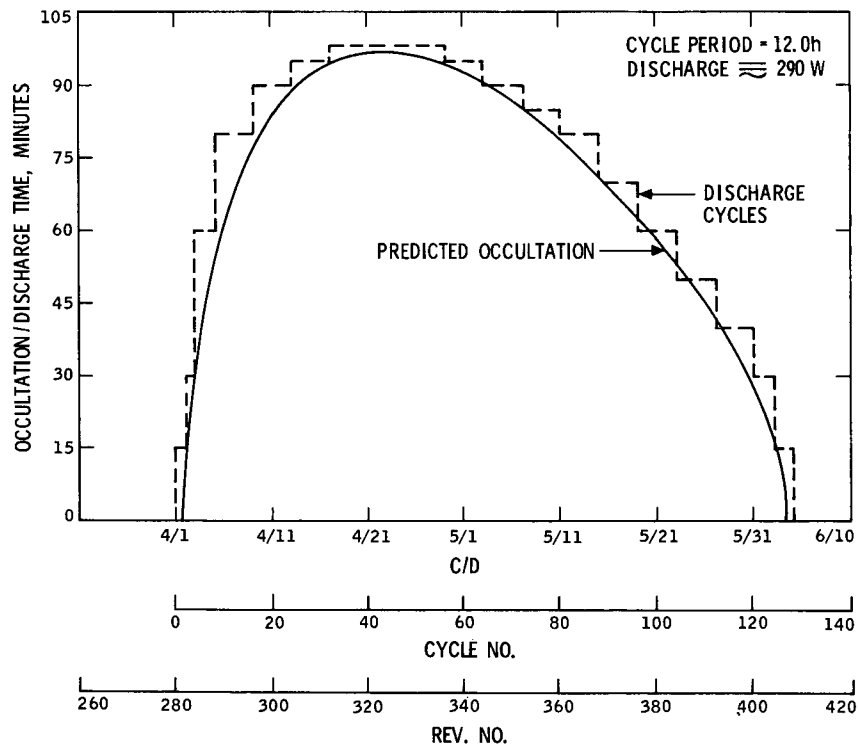


Fig. 87. Real-time mission profile test, extended mission test, battery SN 307

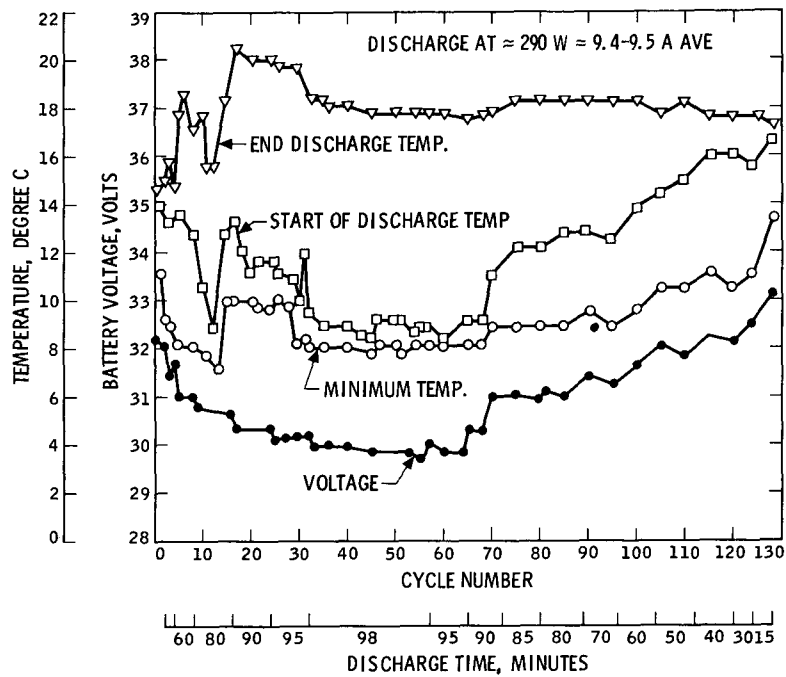


Fig. 88. Real-time extended mission, battery SN 307

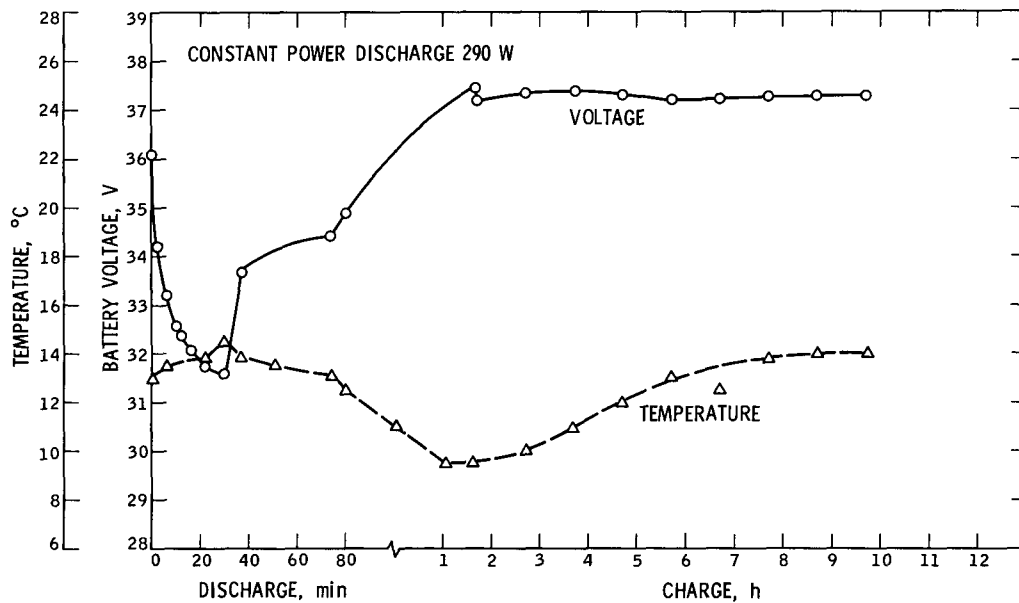


Fig. 89. Real-time test, battery SN 307, 4th cycle, 30 min

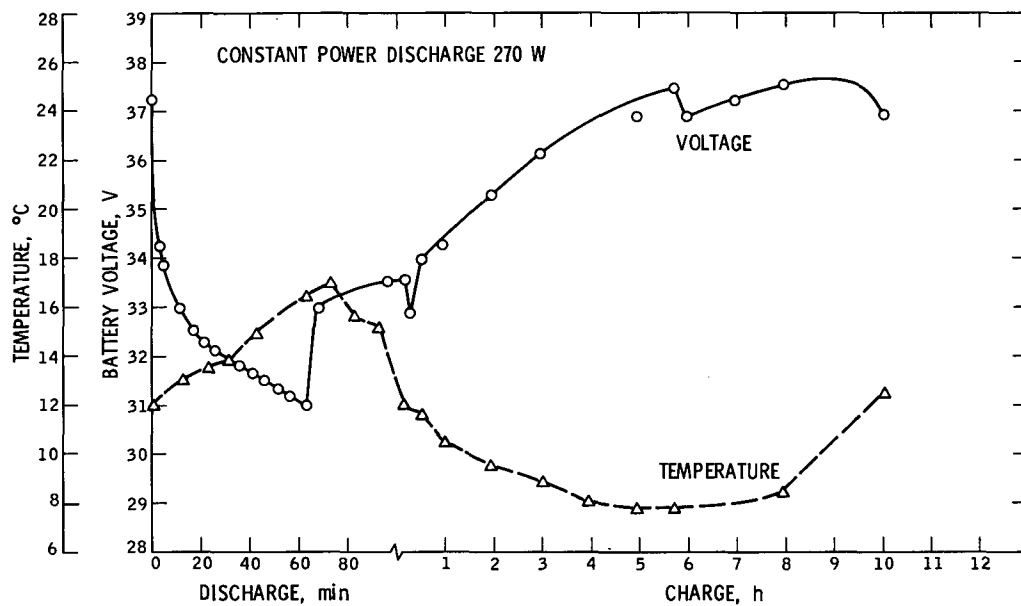


Fig. 90. Real-time test, battery SN 307, 7th cycle, 60 min

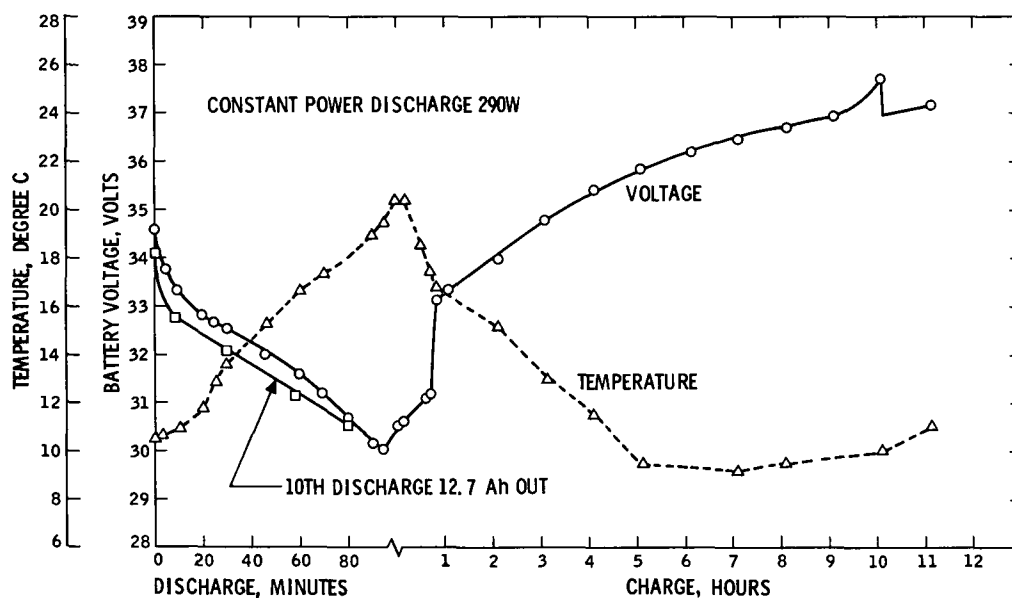


Fig. 91. Real-time test, battery SN 307, 27th cycle, 95 min

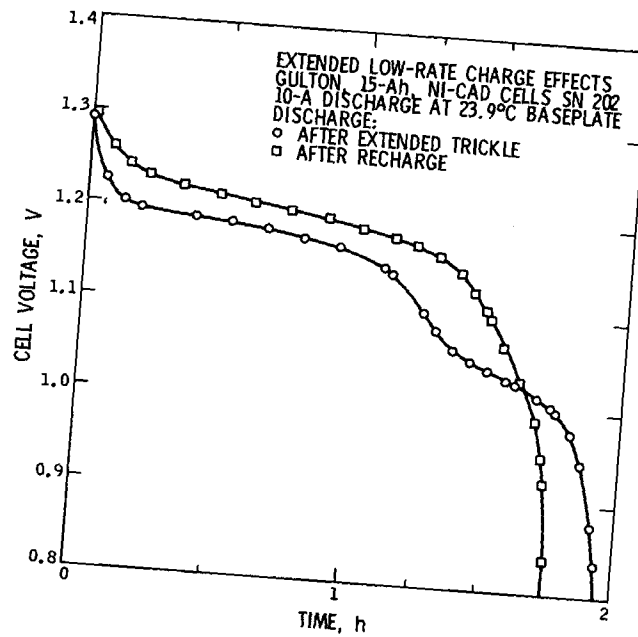


Fig. 92. Typical cell discharge after 6-months trickle charge

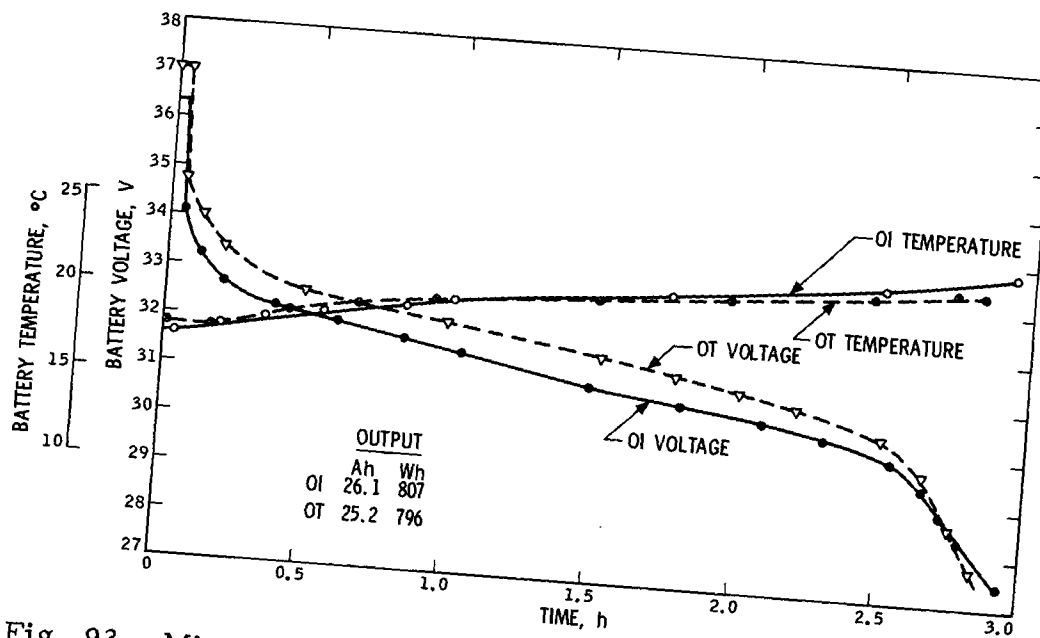


Fig. 93. Mission profile test, battery EM-1, orbit insertion and orbit trim discharge voltage comparison, both discharges at 9 A

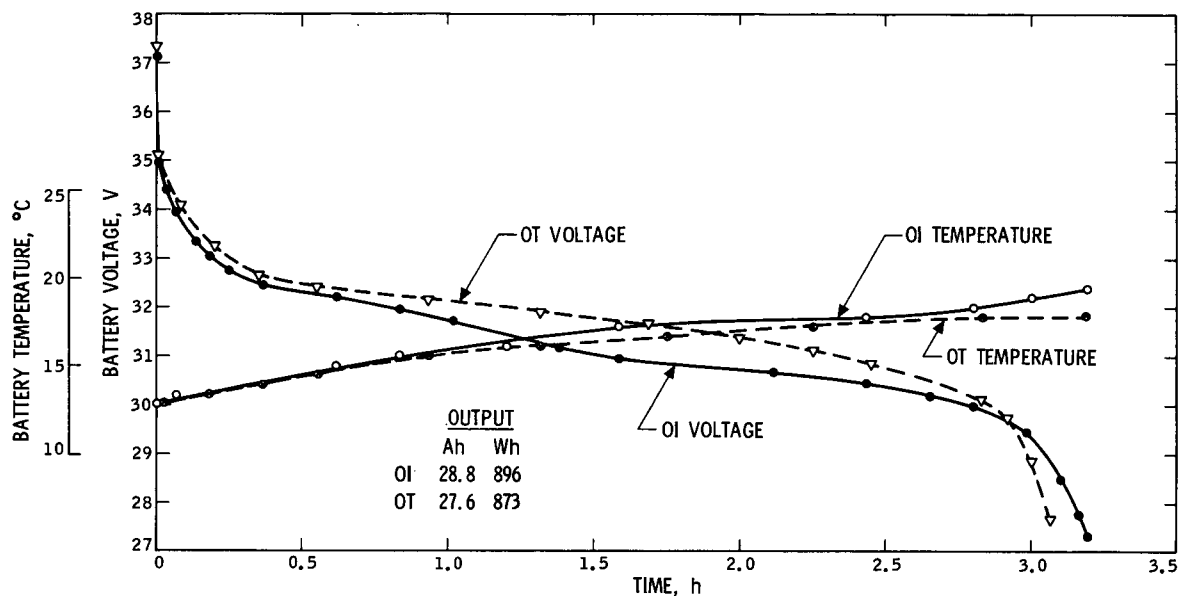


Fig. 94. Mission profile test, battery SN 202, orbit insertion and orbit trim discharge voltage comparison, both discharges at 9 A

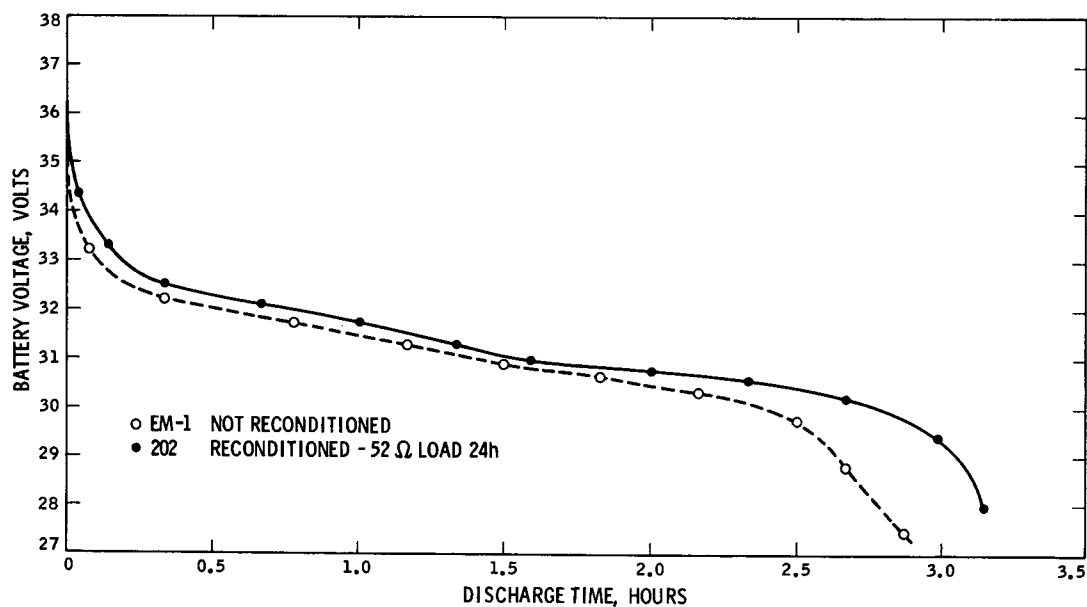


Fig. 95. Mission profile test comparison of orbit insertion discharges on batteries SN EM-1 and 202

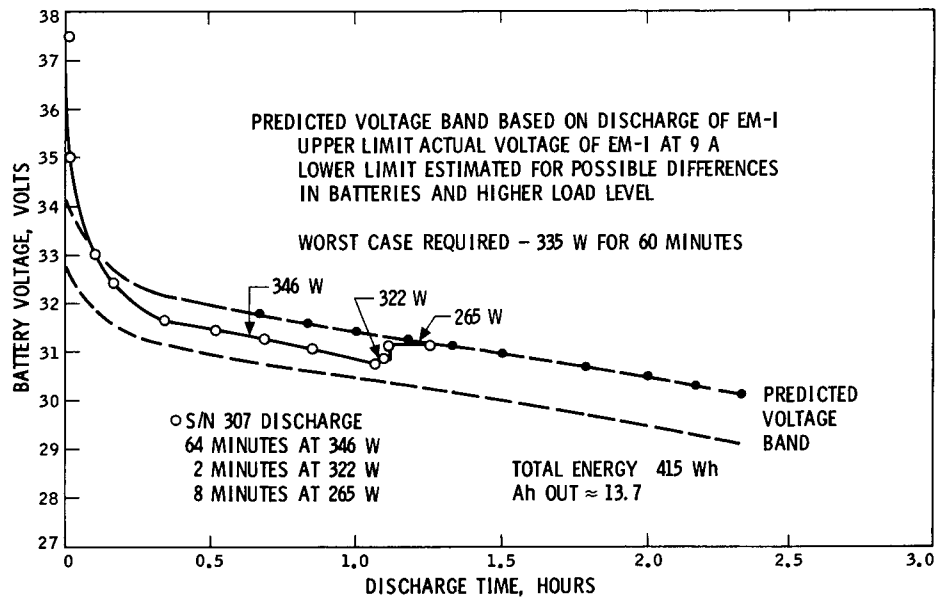


Fig. 96. Predicted voltage and actual voltage of battery SN 307 orbit insertion test, October 26, 1971

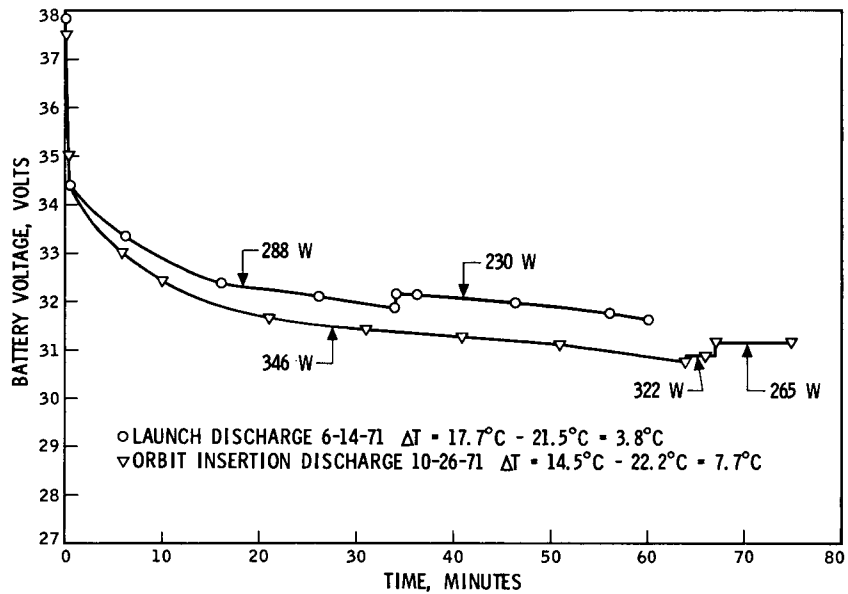


Fig. 97. Real-time mission profile test battery SN 307 launch discharge compared to orbit insertion discharge

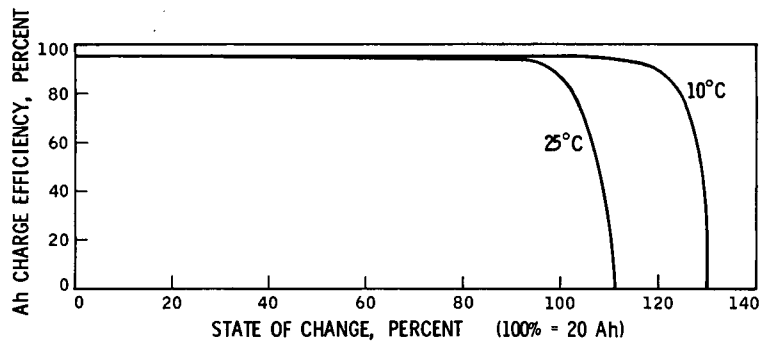


Fig. 98. Battery charge efficiency vs state of charge at 2-A rate

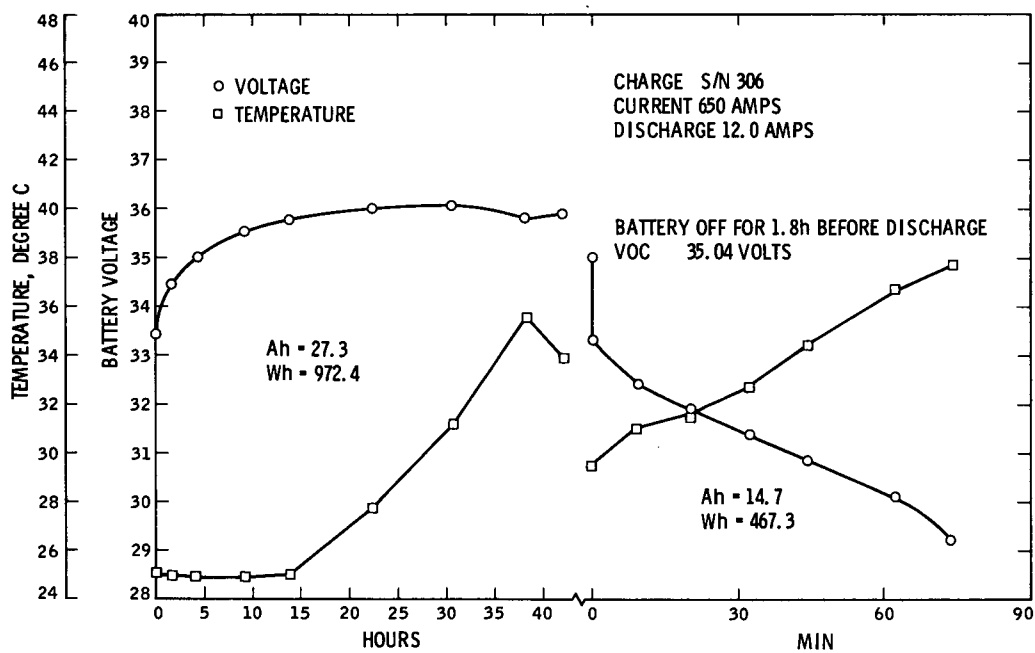


Fig. 99. Charge battery SN 306, current 650 A, discharge 12 A

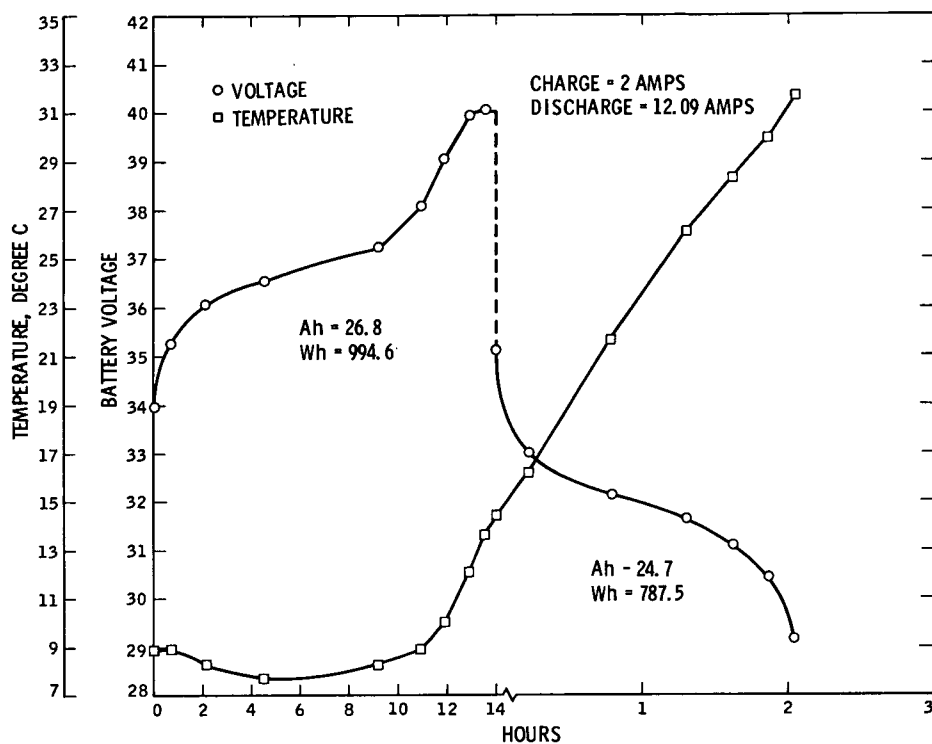


Fig. 100. Charge efficiency test, battery SN 306,
charge 2 A, discharge 12.09 A

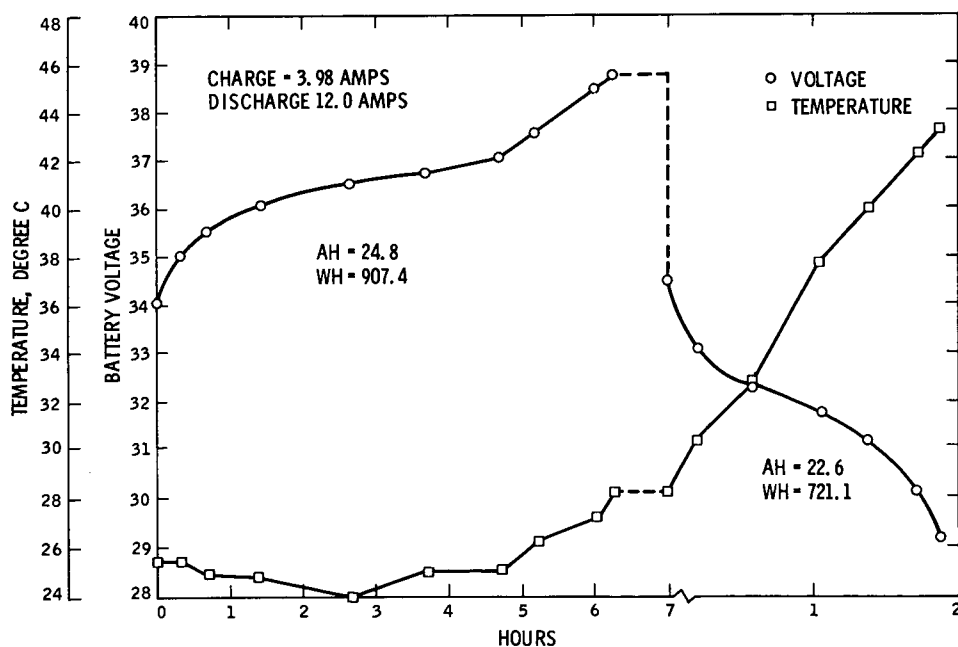


Fig. 101. Charge efficiency test, battery SN 306,
charge 3.98 A, discharge 12 A

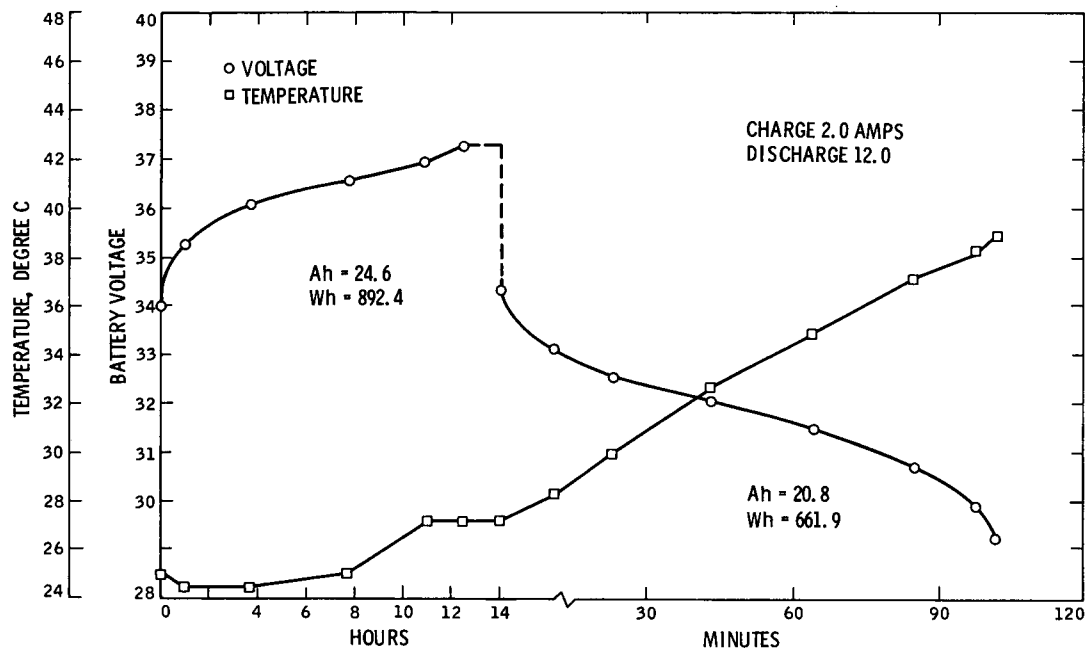


Fig. 102. Charge efficiency test, battery SN 306, charge 2.0 A, discharge 12 A

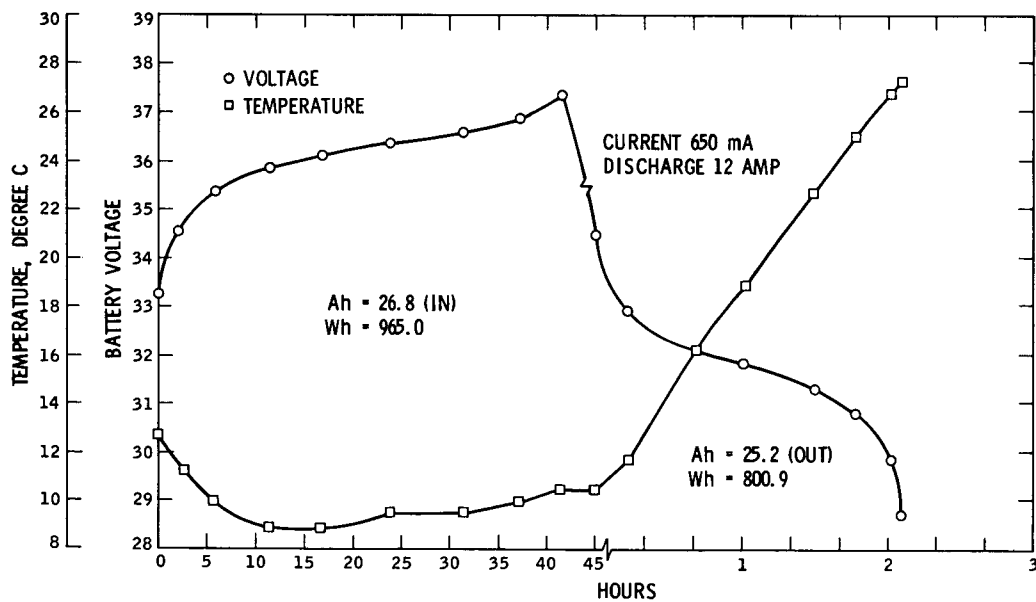


Fig. 103. Charge efficiency test, battery SN 306, charge 650 mA, discharge 12 A

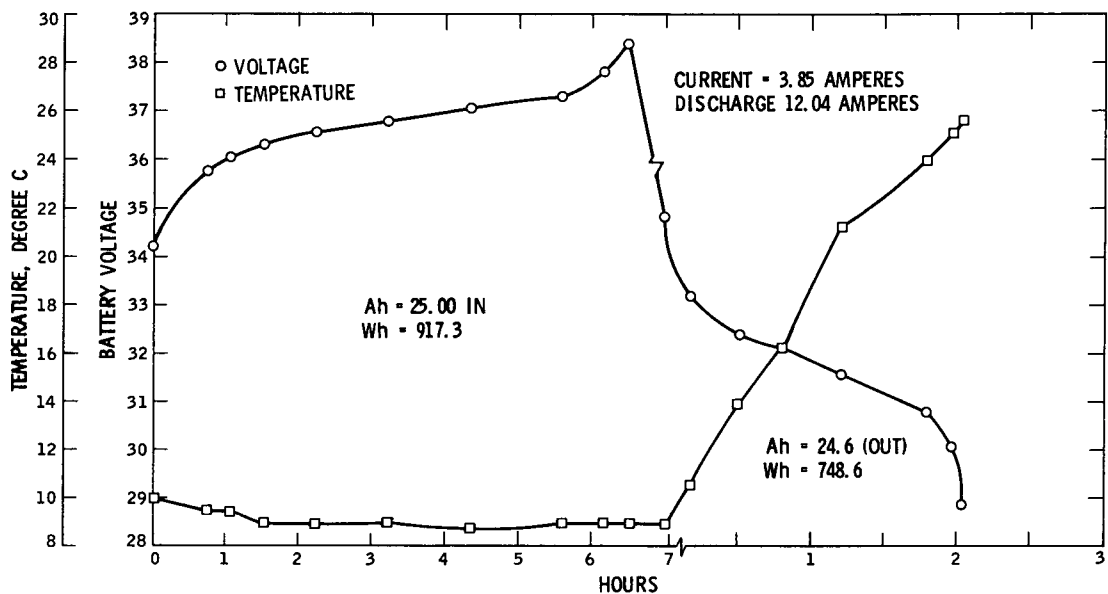


Fig. 104. Charge efficiency test, battery SN 306, charge 3.85 A, discharge 12.04 A

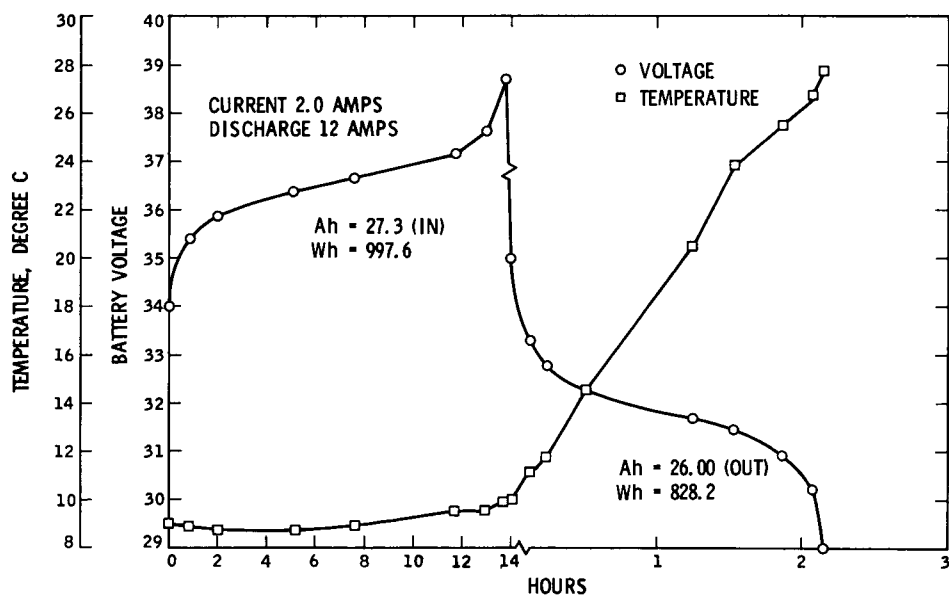


Fig. 105. Charge efficiency test, battery SN 306, charge 2 A, discharge 12 A

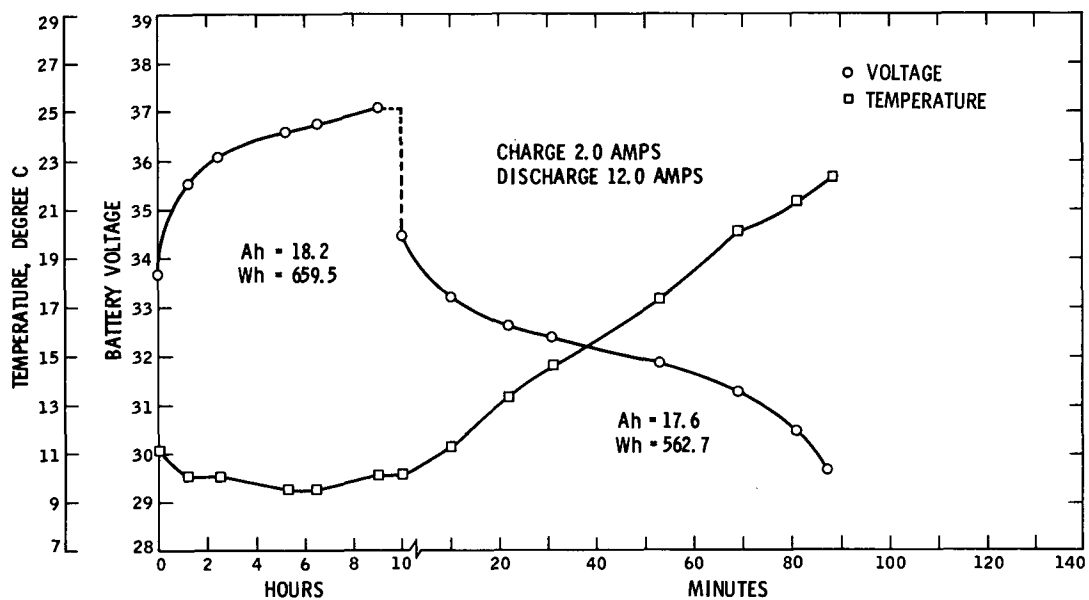


Fig. 106. Charge efficiency test, battery SN 306, charge 2 A, discharge 12 A

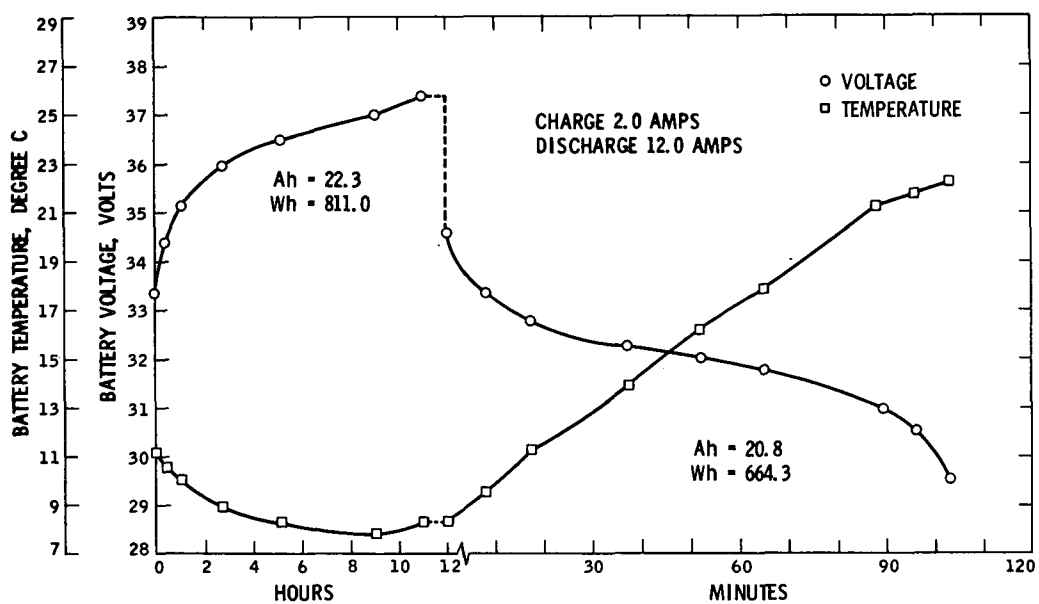


Fig. 107. Charge efficiency test, battery SN 306, charge 2 A, discharge 12 A

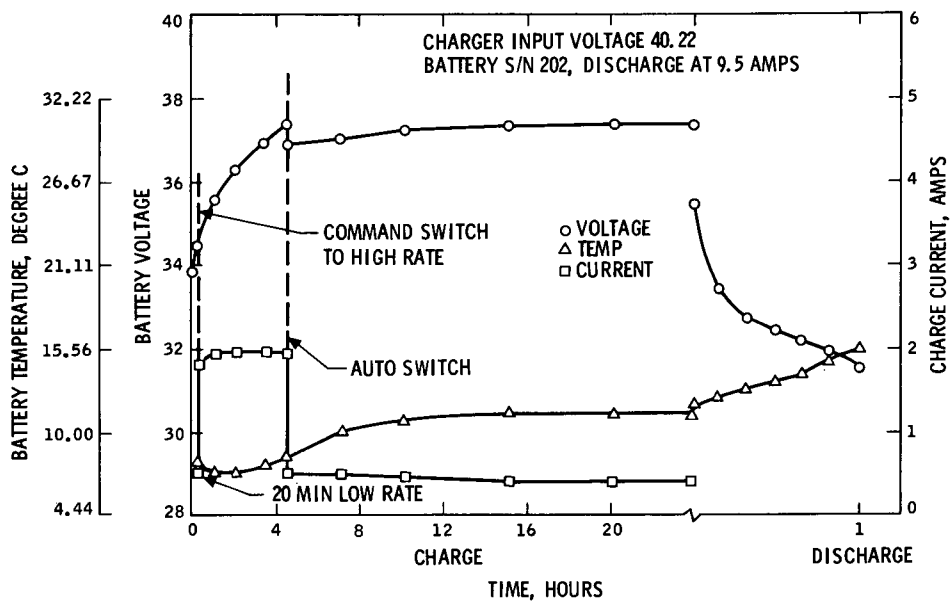


Fig. 108. Battery/charger interface test 9

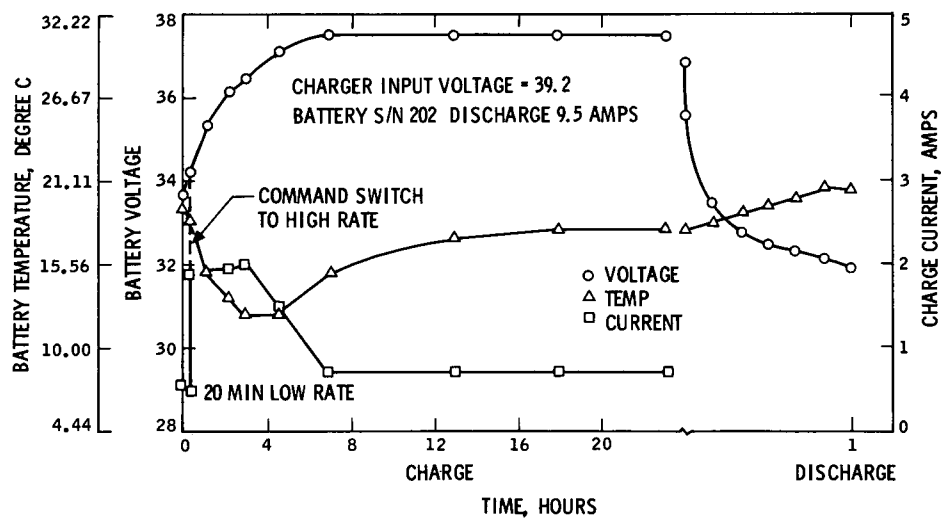


Fig. 109. Battery/charger compatibility test run 3

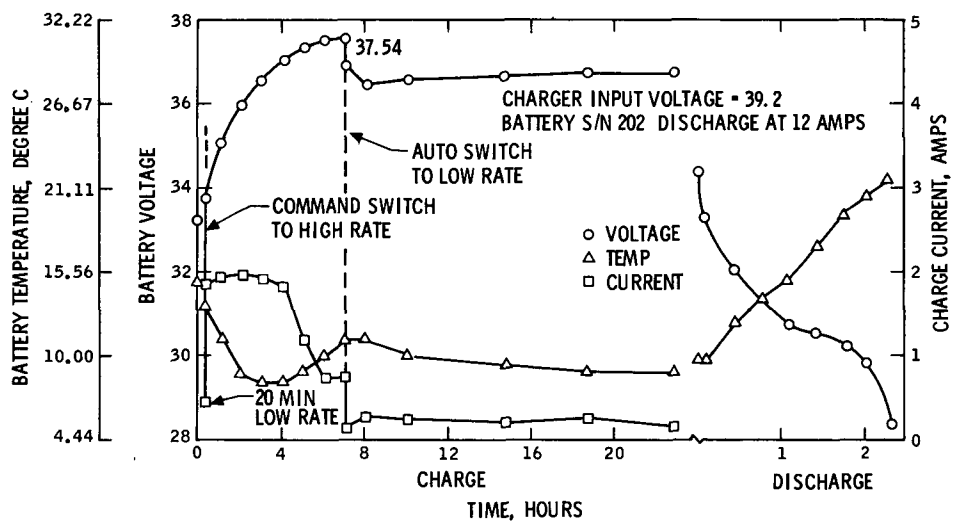


Fig. 110. Battery/charger compatibility test run 11

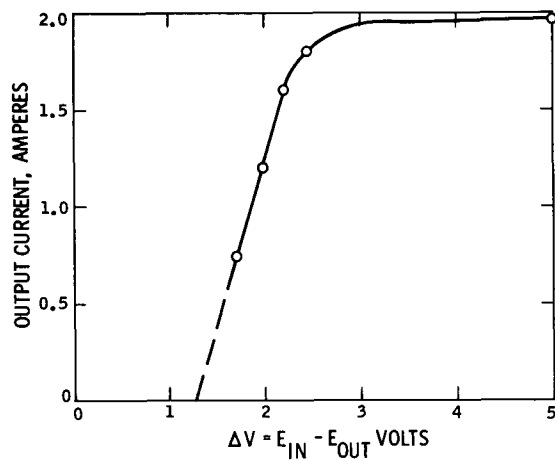


Fig. 111. High-rate charger characteristics

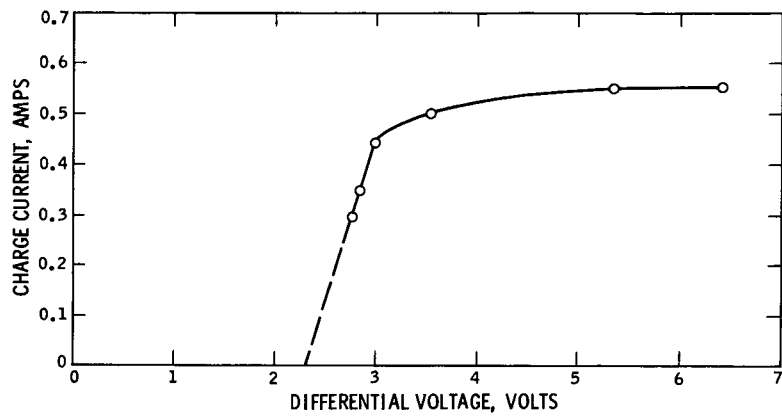


Fig. 112. Low-rate charge current as a function of difference between input voltage and battery voltage

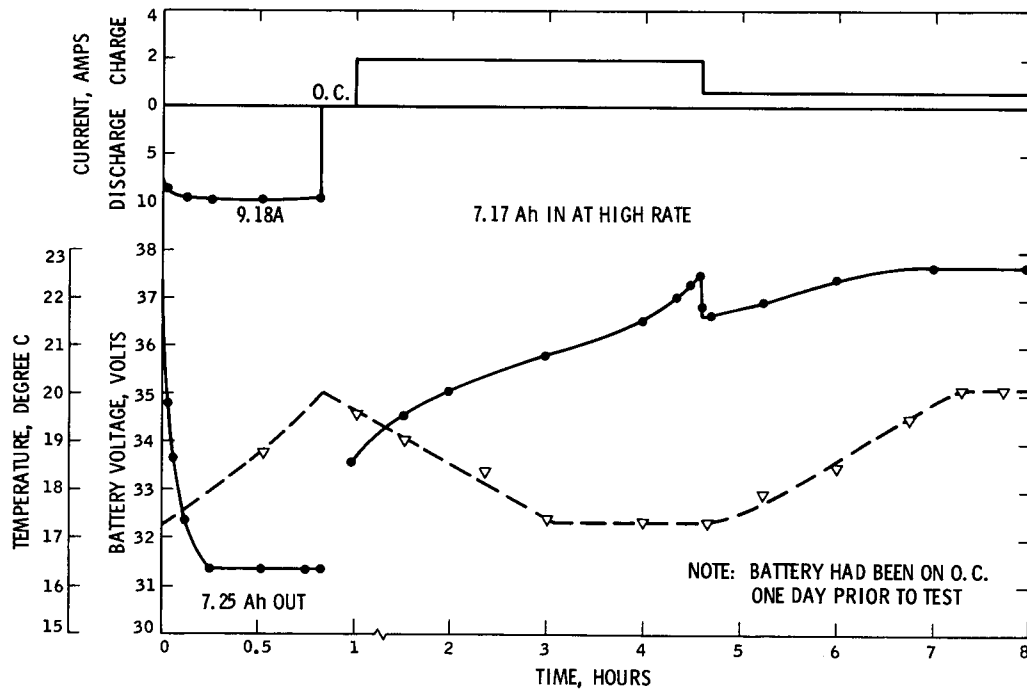


Fig. 113. Results of JFACT discharge, battery SN 304

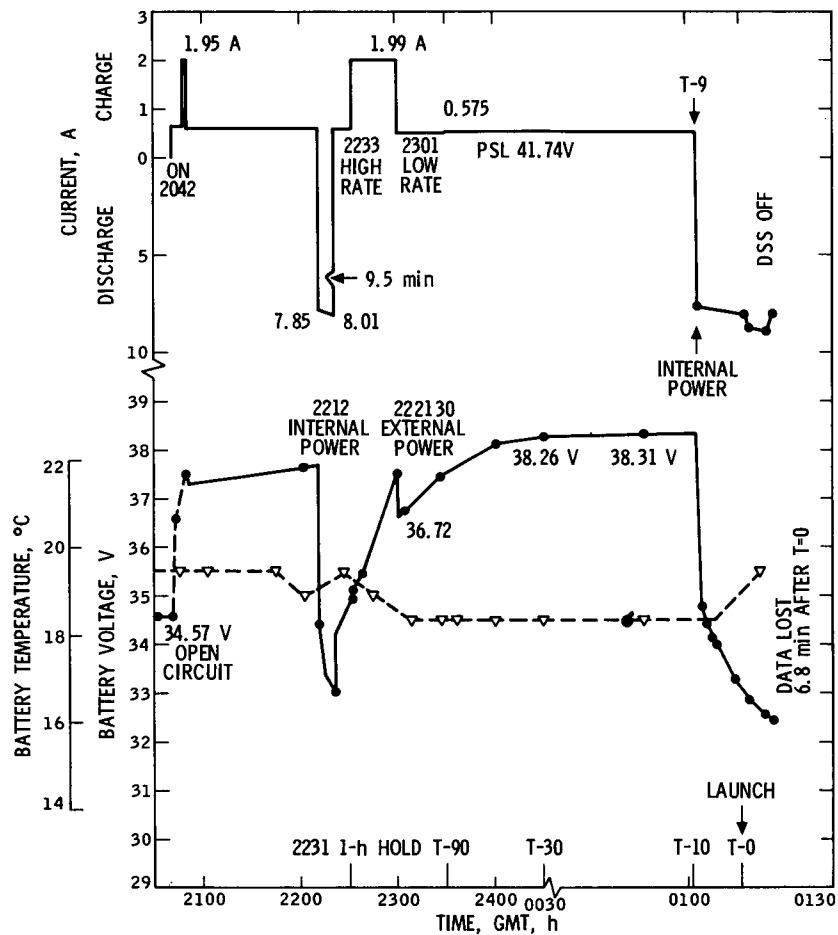


Fig. 114. Battery SN 305 performance data at launch

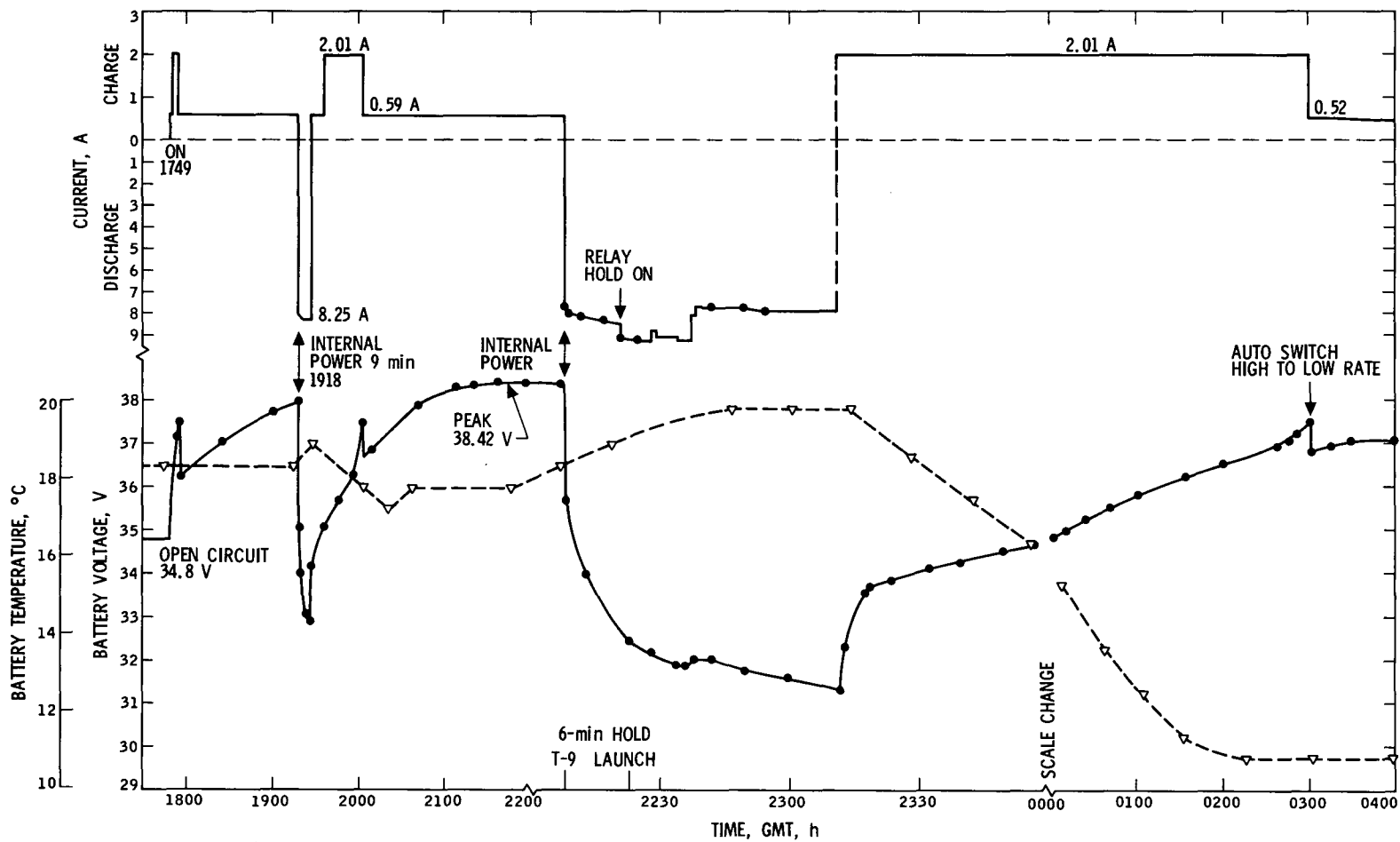


Fig. 115. Battery SN 304 launch performance data during and after launch

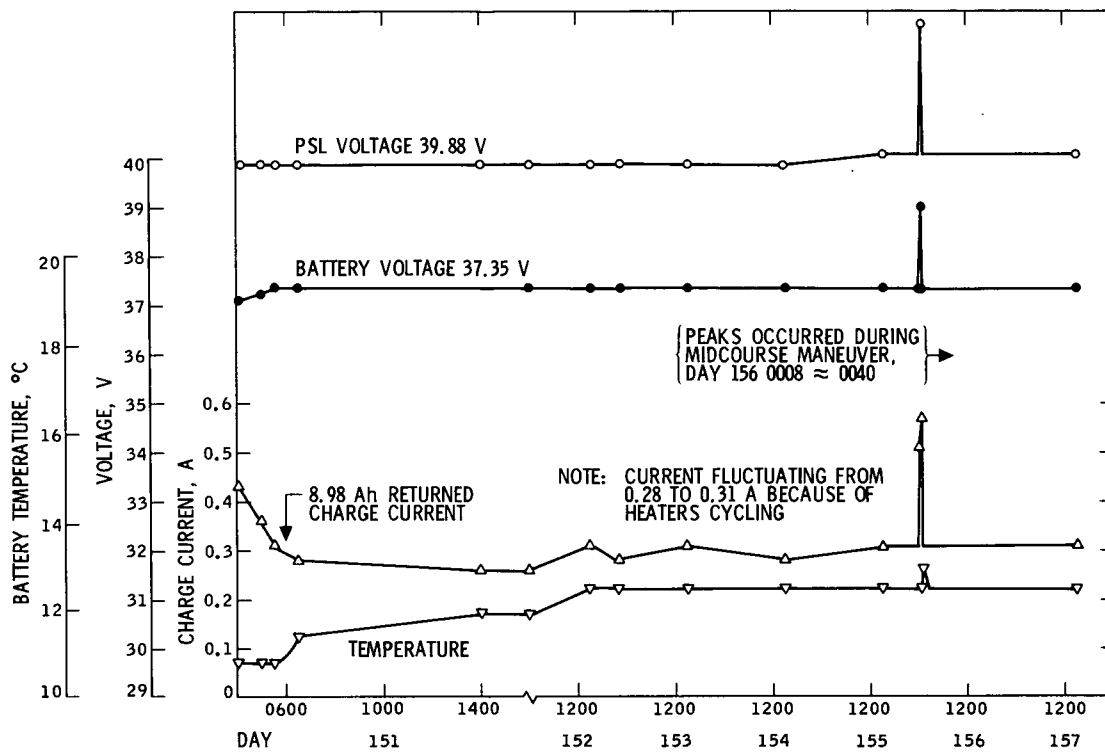


Fig. 115 (contd)

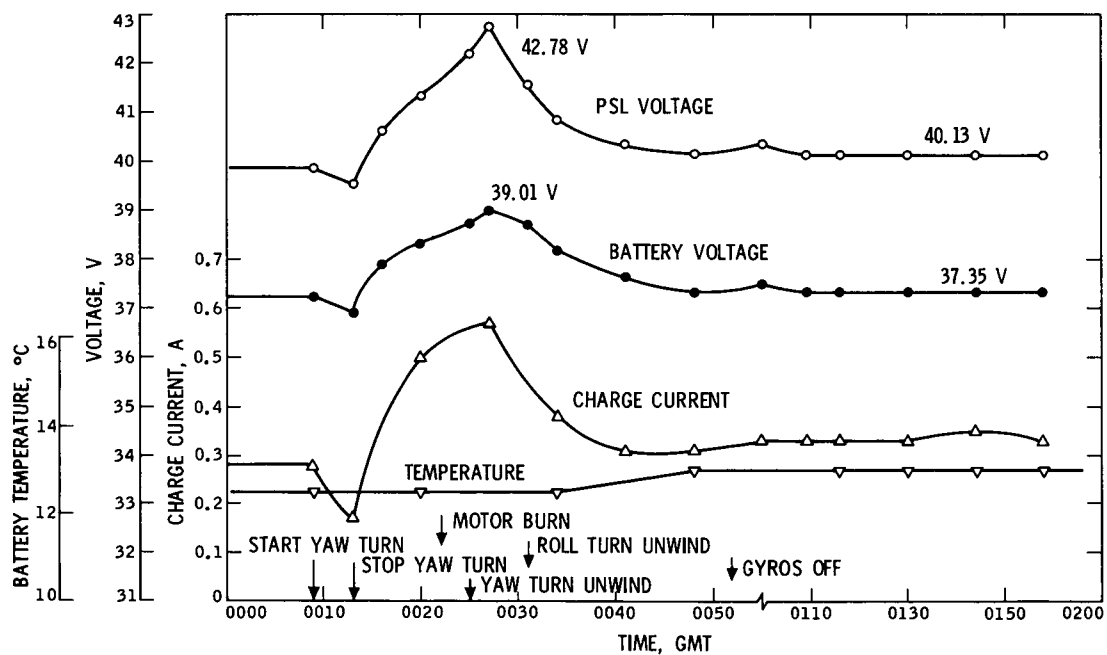


Fig. 116. Effect of first midcourse maneuver on battery

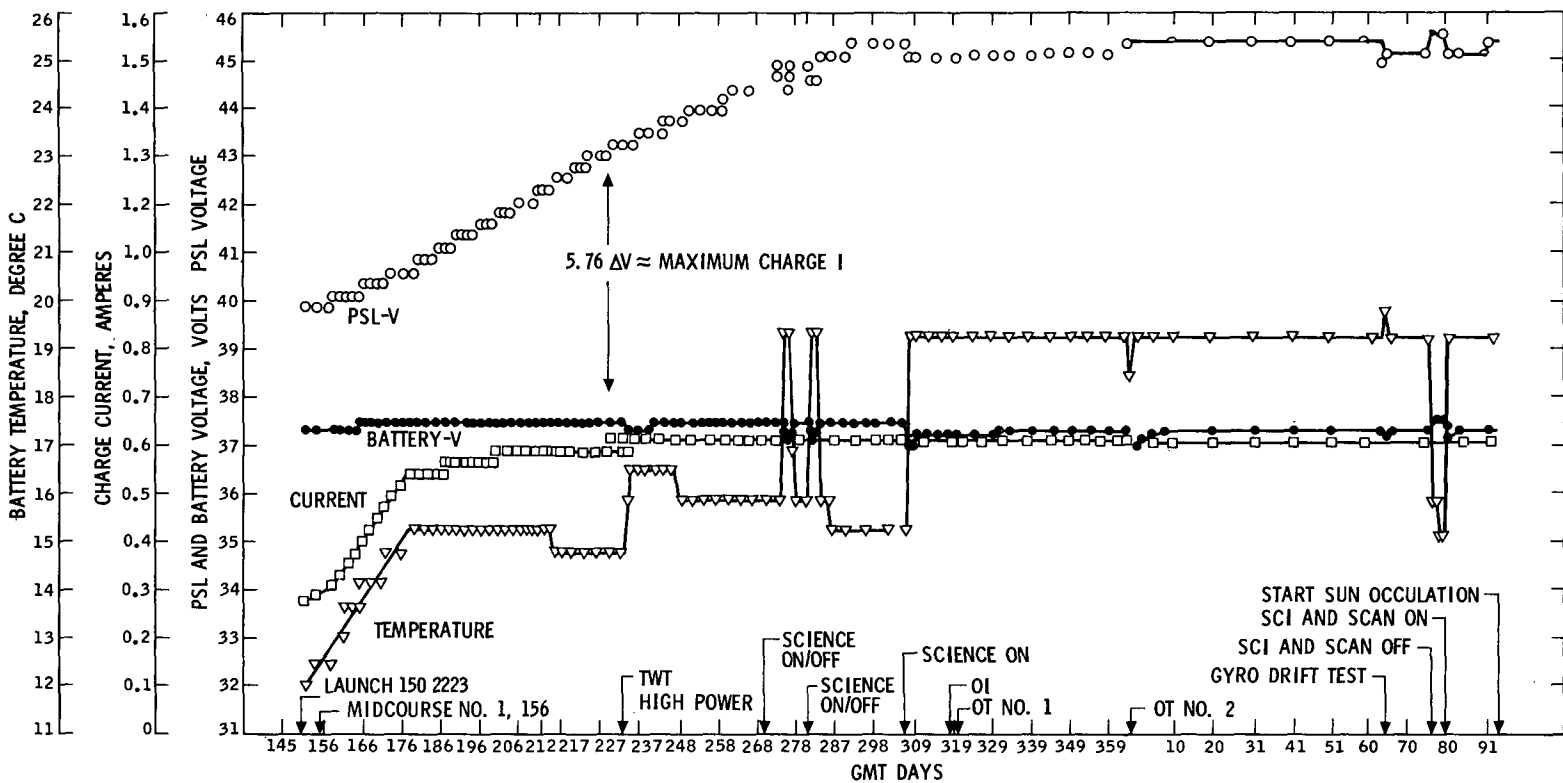


Fig. 117. Battery data, Mariner 9 cruise

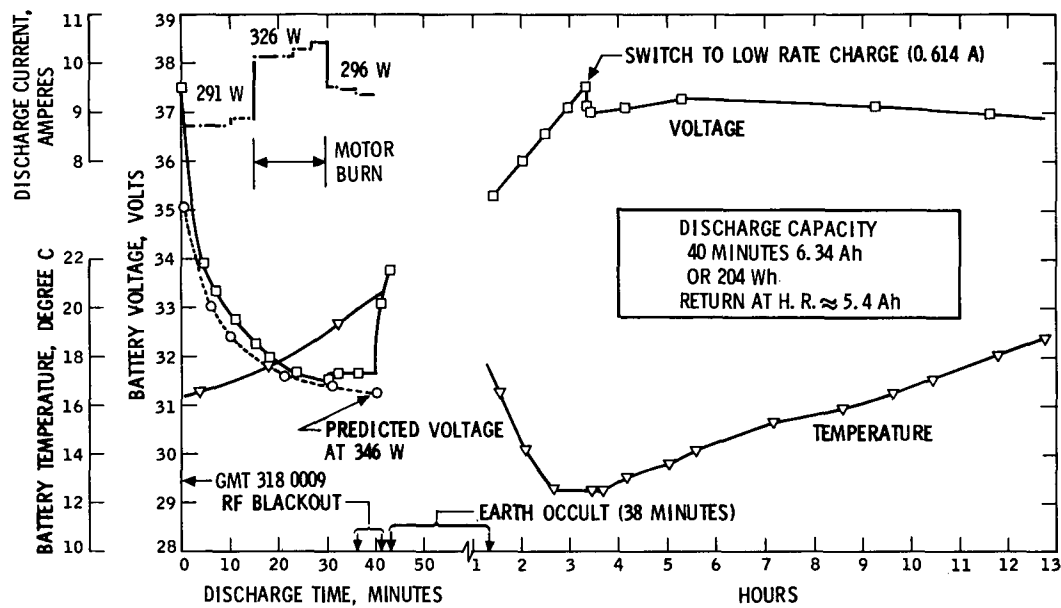


Fig. 118. Battery performance during MOI

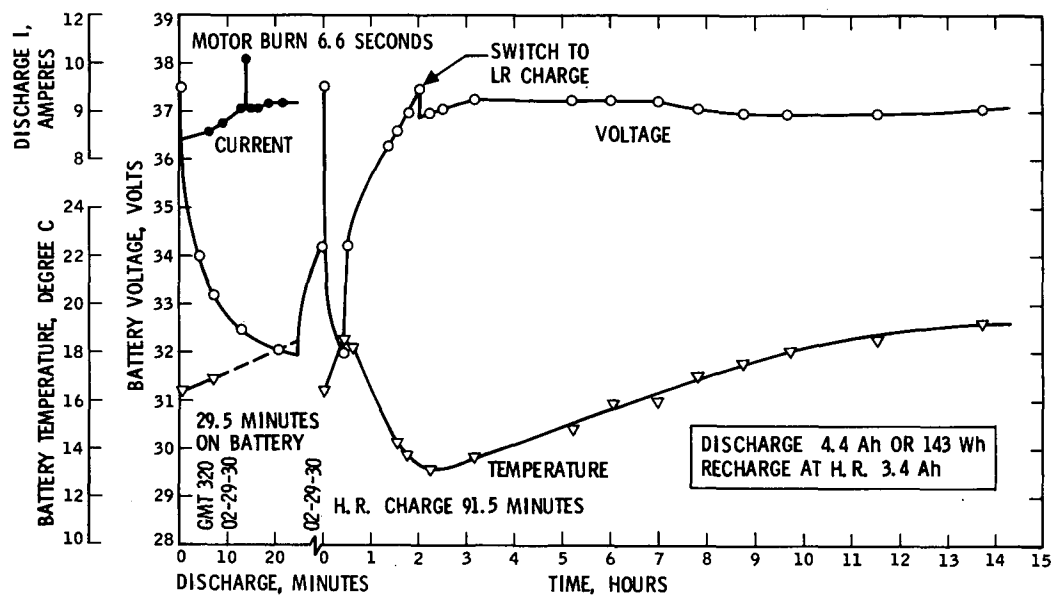


Fig. 119. Battery performance, orbit trim 1

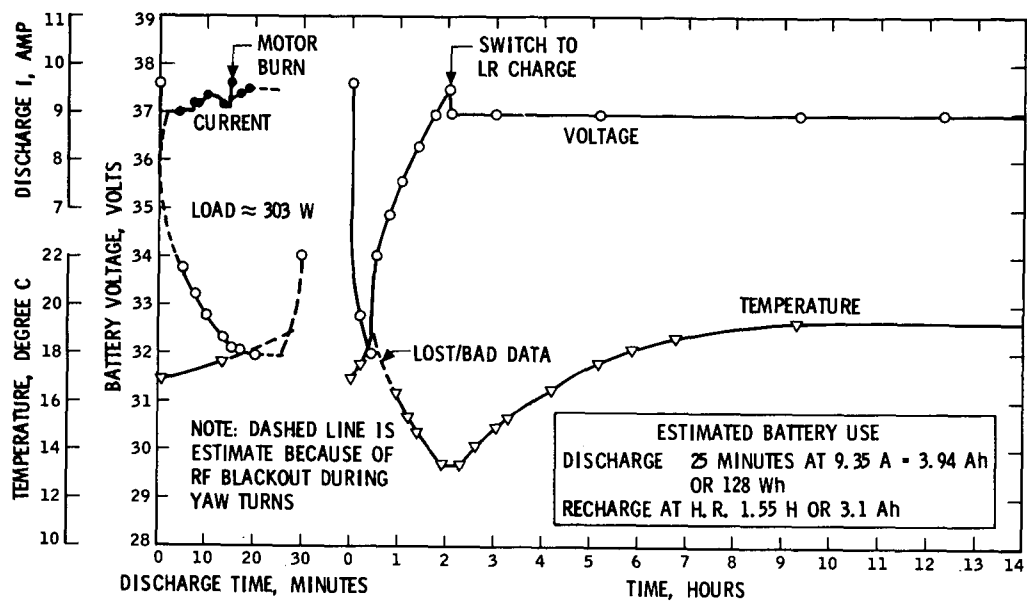


Fig. 120. Battery performance, orbit trim 2

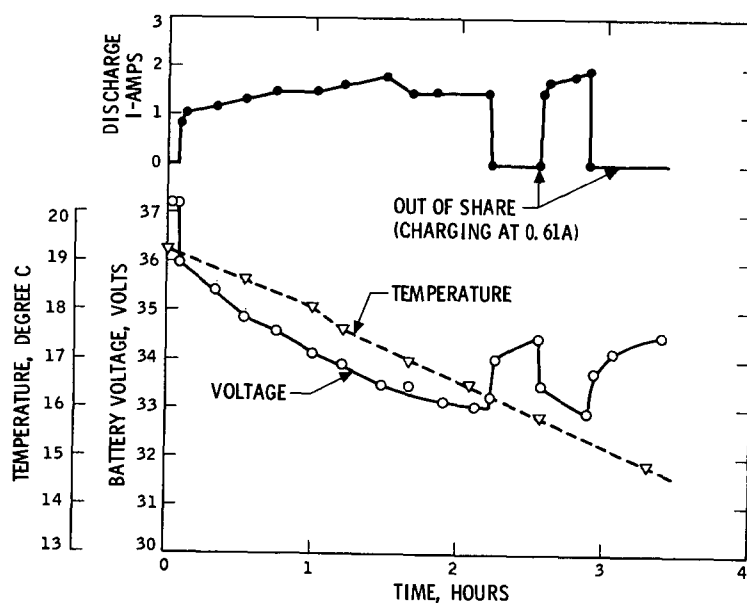


Fig. 121. Battery performance, solar array test 2

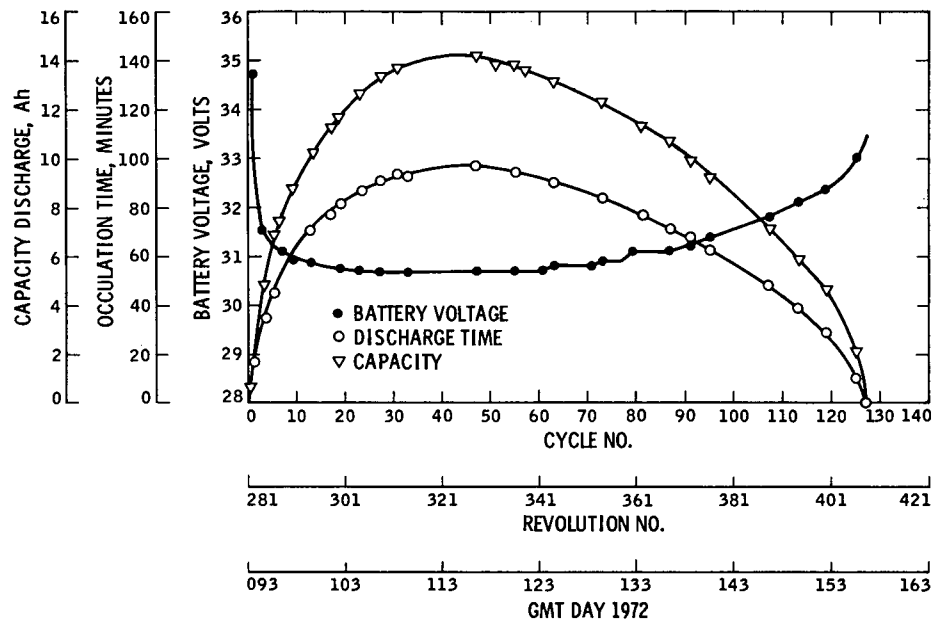


Fig. 122. Battery performance, end of discharge voltage, capacity used, and length of occultation

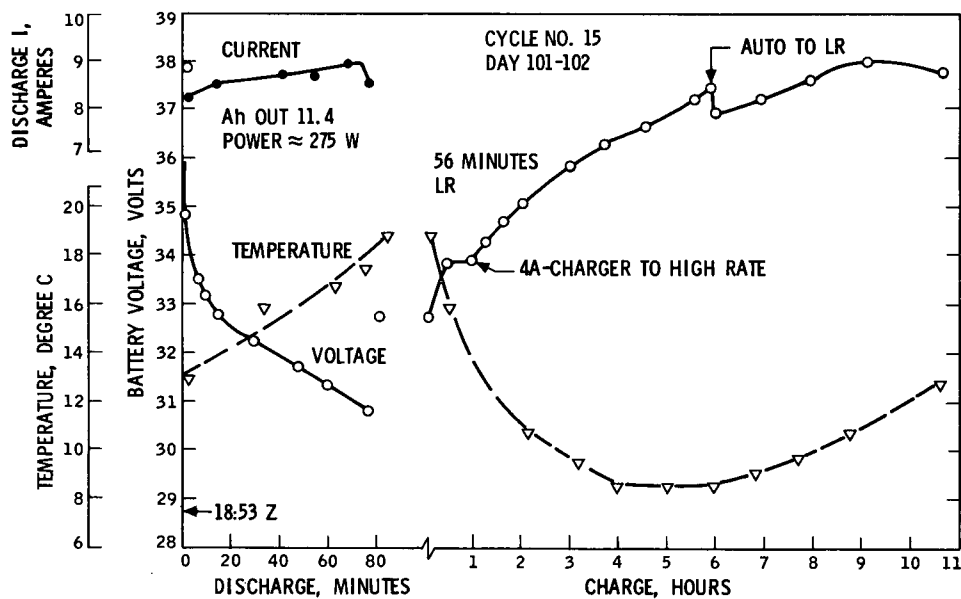


Fig. 123. Battery discharge/recharge, revolution 298

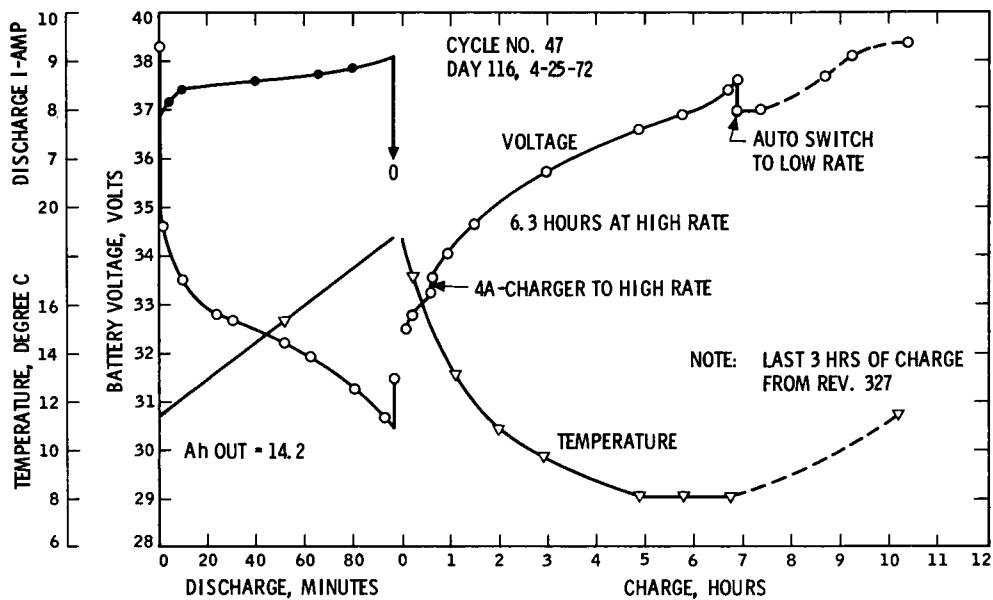


Fig. 124. Battery discharge/recharge, revolution 328

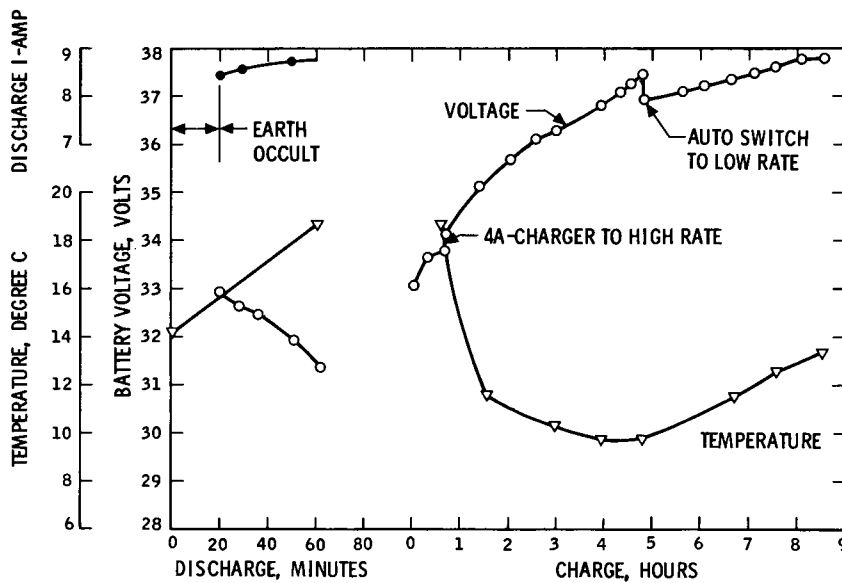


Fig. 125. Battery performance, revolution 375